Mesocosm studies to resolve the fate of polycyclic aromatic hydrocarbons in grass swales as components of Sustainable Drainage System (SuDS) treatment trains.

By

Janine Robinson

The thesis is submitted in partial fulfilment of the requirements for the award of the degree of DOCTOR OF PHILOSOPHY of the University of Portsmouth.

May 2020

Declaration

Whilst registered as a candidate for the above degree, I have not been registered for any other research award. The results and conclusions embodied in this thesis are the work of the named candidate and have not been submitted for any other academic award.

Word count: 57237

Acknowledgements

Firstly I would like to thank my supervisors: John Williams, Fay Couceiro and Joy Watts, who have all taught me so much and offered support and encouragement in my research.

A massive thanks goes to Russell Cole for his help not only in performing the main experiments, but for his help with the GCMS. I couldn't have asked for a better teacher! To all at the ETFS, especially Anita for her help in the lab, and cake!

This journey would not have been the same without my desk mate number 1: Nora, together since the start, friends for life! Desk mate number 2: Lesley! Such a great help, bouncing ideas around and helping me with the lab and GC problems! And of course, thank you to Roshni, always ready with a happy smile, a word of comfort or advice. I would also like to thank everyone from the research office, it's been a journey and a half!

To Nelly, Claire, Tammy, Laura (Dumbledorks forever!) and Sarah, thank you for sharing the journey with me, keeping me sane, laughing and for always being there.

To my family thank you for your support even when you didn't understand quite what it was I was doing!

The biggest thanks of all go to Graham, my rock! His constant support throughout this journey has meant the world to me. Without his encouragement, patience and unquestioning hugs, I wouldn't have been able to achieve any of this work.

Abstract

Urban runoff from impervious surfaces, such as roads, pathways and car parks, causes increases in localised flooding and is a source of pollution entering the aquatic environment. Sustainable Drainage (SuDS) are systems that can mitigate these impacts by mimicking pre-development hydrology, often using swales and detention ponds. Organic pollutants, such a polycyclic aromatic hydrocarbons (PAHs), are particularly found in road runoff and the understanding of their fate in SuDS has been limited due to of a number of factors including the heterogeneity in storm events, site conditions, local traffic, environmental conditions and natural changes in the PAHs themselves.

The aim of this study was to establish a large scale mesocosm to replicate environmental conditions of storm flow through vegetated swales and study the behaviour and fate of particle bound PAHs. A 10 m long physical model of a vegetated swale was constructed in a controlled environment, and a repeatable storm event runoff simulation pattern established. This was to allow observation of the transport and movements of the PAHs along the swale. A method was created for artificially producing road runoff dust, dosed with creosote containing PAH pollutants. Water samples were tested to establish the reduction in PAH aqueous concentrations after passage through the swale soil. Soil samples were collected from locations along the swale, and PAH concentrations established. Results showed that the swale mesocosm provides an effective simulation of storm hydrograph patterns. Aqueous PAH concentrations were significantly reduced after filtration through the swale system. Soil PAH behaviour showed that high molecular weight PAHs, (benzo(a)pyrene, chrysene and pyrene) reduced in concentration with distance along the swale. These PAHs began to accumulate in the 5 – 10 cm soil depth, just below the vegetated root zone. The profiles of the PAHs in the controlled mesocosm environment provide a reference point for field studies and will allow the fates of PAHs to be more precisely predicted for designs on sites where PAH discharges are sensitive. The unique model swale has allowed for the control of variables found in the environment that normally affect field research. This, however, means that results found may not be truly representative of those found in natural environment.

Contents

List of tables

List of figures

List of images

Abbreviations

- ASE – accelerated solvent extraction
- BaP – benzo(a)pyrene
- BMP – Best Management Practices
- C – Carbon
- Cd –cadmium
- CHR – chrysene
- CIRIA – Construction Industry Research and Information Association
- Cu - copper
- DCM – dichloromethane
- EA – Environment Agency
- EC – electrical conductivity
- EPA – Environment Protection Agency
- EQS – Environmental Quality Standards
- EU – European Union
- EUC – European Commission
- FLAN – fluoranthene
- FLU – fluorene
- GCMS – gas chromatography mass spectrometry
- HCl – hydrochloric acid
- IBC – intermediate bulk container
- K_{ow} – partition coefficient
- LID – Low impact development
- LOD – limits of detection
- LOI – loss on ignition
- Na_2SO_4 – sodium sulphate
- NAP – naphthalene
- PAH – polycyclic aromatic hydrocarbons
- Pb – lead
- PSA – particle size analyser
- PYR – pyrene
- RRD – road runoff dust
- SD – standard deviation
- SIM – Selected Ion Monitoring
- SuDS – Sustainable Drainage Systems
- TSS – total suspended solids
- WFD – Water Framework Directive
- WHO – World Health Organisation
- WUSD – Water sensitive urban design

Dissemination

2015

- University of Portsmouth, Technology Faculty Research Conference – poster presentation (1st prize for poster competition).

2016

- University of Portsmouth, SCES – Research Seminar
- University of Portsmouth, Postgraduate poster competition (1st prize)

2017

- International Conference in Urban Drainage (IWA/ICUD, Prague) – Podium presentation, paper in conference proceedings.
- Presentation to Wildflower Turf

2018

- University of Portsmouth Technology Faculty Research Conference- Three Minute Thesis - 1st place
- University of Portsmouth – Three Minute Thesis Competition – 1st place
- SuDSnet international conference (Coventry) – Podium presentation
- CWA annual conference – poster presentation (1st prize for best student poster)

1 Introduction

Pollutants such as metals and polycyclic aromatic hydrocarbons (PAHs) are found in runoff from roads and urban areas. Increasing urbanization, with a dependence on road transport for transport and logistics, means that these releases are increasing. Developments on green field sites can increase flooding and pollution by increasing runoff (Bastien *et al.,* 2012). Over time, especially in dry periods, the pollution will accumulate on surfaces, before being washed off during storms, if the intensity of the storm is strong enough. This is often termed the 'first flush' of a storm. Sansalone & Cristina (2004) described the first flush as a term used to indicate a "disproportionately high delivery of either concentration or mass of a constituent during the initial portions of a rainfall-runoff event". During the 'first flush' of a storm, the pollutant inputs are at their highest (Zhang *et al.,* 2010). It is during this first stage of a storm that the majority of pollutants are washed off impermeable surfaces and are transported into the immediate environment (Clozel *et al.,* 2006).

Different pollutant groups found in storm water runoff consist of suspended solids, heavy metals, nutrients, organic chemicals and bacteria (Kayhanian et al., 2012). Build-up of these pollutants in the receiving waters can result in toxicity to organisms (Camponelli *et al.,* 2010). To help prevent flooding and pollution entering waterbodies, Sustainable Drainage Systems (SuDS) have been developed. SuDS mimic predevelopment hydrology using infiltration and storage (often in wetlands and ponds) as alternatives to sewer-based drainage (Fryd *et al.*, 2012). These systems trap pollutants from roads and other surfaces, where they can be exposed to remediation processes, providing protection for river waters (Leroy e*t al*., 2015).

PAHs are formed by both natural and anthropogenic sources. Natural sources include volcano emissions and forest fires (Manoli & Samara, 1999). Anthropogenic sources include vehicle emissions, coal fires and oil burning. Of these sources, the anthropogenic releases into the atmosphere are the most significant (Wilcke, 2000). PAHs are compounds that contain at least two condensed rings. As a class there are several hundred individual PAHs, made up of carbon and hydrogen molecules. They are formed when there is incomplete

burning of compounds which contain carbon and hydrogen (Wilcke, 2000). PAHs that comprise of up to four benzene rings are termed 'Light PAHs' and those with more than four rings are known as 'Heavy PAHs'. Heavy PAHs are more stable, and have greater toxicity than the light PAHs. Heavier PAHs have increased hydrophobicity, as such are most likely to be found attached to settled or suspended particles in the water column (Simon and Sobieraj, 2006). Light PAHs are more water soluble and as such can also be found in a dissolved state in an aquatic environment (Wenzl *et al.*, 2006). Due to their chemical composition the bonds formed to particulate matter are much weaker and are much more likely to be broken.

In the 1970's, the US Environment Protection Agency (USEPA) identified 16 PAHs as representative of the whole family of PAHs, these are now used as standard, for monitoring purposes (Napier *et al.*, 2008). PAHs are considered key indicators for pollution, but can be difficult to quantify meaning that design guidelines, such as the UK SuDS manual (Woods Ballard *et al.*, 2015), tend to treat pollutant removal as "black box" design components.

Key PAH pollutant removal mechanisms in SuDS are sedimentation, photodegradation, volatilization and adsorption. Quantification of these pollutant removal processes would allow SuDS designs to be refined, and help realise the full potential of such Green Infrastructure. Swales are grassed or vegetated channels, with a slight gradient, normally built to run alongside roads or carparks. Most pollution studies refer to constructed wetlands, with studies focusing on swales or retention ponds (e.g. Leroy *et al*. 2015; Lucke *et al*. 2014) gaining an increased knowledge base. Of those that focus on swales, few consider PAH pollution. Deletic & Fletcher (2006) created a swale for modelling purposes. This swale had no side slopes and focused on the removal of total suspended solids (TSS) in storm water. Leroy *et al.* (2015) developed swale mesocosms to assess the PAH dissipation process. This study returned positive results, but looked at vertical filtration. Swales enable horizontal filtration along the length of the swale, providing increased opportunity for the dissipation of pollutants. In a study of four different swales using simulation experiments, Lucke *et al*. (2014) demonstrated that 50 – 80 % of TSS in runoff is removed in the first 10 m of a swale. Their research further showed that swales were able to attenuate and capture higher pollution levels found in the first flush of storms.

Knowledge of SuDS in new developments is often little understood by the stakeholders involved in the decision process. As such, the importance of the role SuDS play may not currently be taken properly into consideration (Viavattene & Ellis 2013; Hubert *et al.* 2012). While there has been some previous research into the fate and behaviour of pollutants in SuDS (e.g. Wilcke, 2000, Napier *et al*., 2009,Tavera *et al.*, 2018), there are limited studies of PAHs in swale systems.

2 Literature Review

This chapter provides an overview of the development of sustainable drainage to address the challenges arising from the increase in urbanisation, the pollution control measures inherent in such systems. Polycyclic aromatic hydrocarbons, some of the primary pollutants in urban runoff, are discussed along with a review of current literature ascertaining to the difficulty in monitoring organic compounds in the environment.

2.1 Urban runoff

During storm events rain water falling on impervious surfaces flow in the easiest direction, generally this will be following a slope. Recent years have seen a rise in flooding events.

Anthropogenic activities have changed the ecosystem around us, and continue to do so. As populations grow, the need for new housing increases. With an increased need for housing and development, large amounts of greenbelt and the surrounding areas are being dug up and removed to provide space for land developments. Changes to the natural environment by removing layers of soil, and covering with impermeable surfaces, such as tarmac used for roads, can cause significant changes to the environment. This removal decreases the ability of the soil to cope with large amounts of water input during storm events (Bastien *et al.*, 2012). The natural water cycle, driven by energy from the sun, is interrupted by changes in land use. When the land is built upon with impermeable surfaces, there is decreasing ability for infiltration, evapotranspiration and surface roughness, which causes an increase in the velocity and volume of runoff during storm events. Where previously water started in lakes, seas or rivers and ended up back in the same point to begin the cycle again, when

land is built upon using impervious surfaces the cycle is interrupted (CIRIA, 2015). It is predicted that the number of storm events in the UK is likely to increase, and therefore measures must be put in place to cope with this (CIRIA, 2007). Drainage systems have been used to remove wastewater for centuries, with advanced systems being used by the Romans and even earlier in the Mesopotamian Empire (Barbosa *et al.*, 2012). Removal of the natural resources and the ability to cope with increases in water input, have increased the potential for flooding and input of pollutants into water-bodies. As such, systems have been designed to allow for the capacity to deal with storm events and low levels of surface run-off.

During rain events, the rainwater will infiltrate into the soil, following the natural water level. As land is built upon, the ability of the land to absorb water decreases, leaving the accumulating water nowhere to go, giving rise to localised flooding. While occasional flooding is a natural process, in high level storm events the ground can become saturated, when storm water cannot infiltrate the ground regular flooding will become more prevalent. The natural surface runoff hydrograph is altered by urbanisation (Goonetilleke *et al.*, 2005) increasing the levels of runoff. With the changes in the hydrology also comes changes to the quality of the runoff. Pollutants that are deposited on the surfaces of roads influence the quality of the runoff water (Gobel *et al.*, 2007). As the storm water flows over impermeable surfaces, it washes off the deposited pollutants and conveys them into the environment.

In Europe, 70% of the population lives in urban areas, and this figure is expected to rise to 87% by 2050 (United Nations, 2007; Schirmer *et al.*, 2013). To accommodate this more land will be needed, further reducing the ability of the land to cope with rainfall, by increasing the amount of impervious surfaces (Liu *et al.*, 2015). Alongside the elevated urbanisation is the need for more industrial areas, to support the growing population, bringing with it more land use, and the increased likelihood of pollutants being released into the environment. Industrialisation and urbanisation increase the number of cars and other vehicles on the roads. One of the major sources of known pollutants into the environment is vehicular activities. In March 2017 there were 37.5 million vehicles registered to use the roads in the

United Kingdom. Of these, 31.1 million were cars (including low emission cars) (Department for Transport, Vehicle licensing statistics, 2017). In the UK, it has been estimated that in regulated facilities there are up to 11.3 million parking spaces covering 214 Km^2 (Revitt *et al.*, 2014), and this will only have increased in subsequent years.

Pollutants are produced as a by-product of the urban activities. These pollutants can be harmful to organic life, including humans. Pollutants deposited on impervious surfaces find their way into the environment and water bodies such as ponds and rivers, when rain water washes over the surfaces. Once the pollutants are in the water system they affect the quality of the water. Legislation of water quality started in the European Union (EU) in 1975 (ec.europa.eu). Since the initial draft there has been many new policies governing the state of water resources. The EU Water Framework Directive (WFD) requires the water quality of all water bodies to meet a good ecological standard. This is defined in the report as:

> *"The values of the biological quality elements for the surface water body type show low levels of distortion resulting from human activity, but deviate only slightly from those normally associated with the surface water body type under undisturbed conditions."* (European Commission (EC) 2000)

Adopted in 2000 by EU member states, the WFD was issued with the overall aim of protecting ground and surface water bodies and achieving "good ecological status" by 2015, with the final deadline of 2027 for all actions to be realised. Since its inception the report has had many revisions and updates. In the UK the WFD came into effect in 2009, replacing the previously used General Quality Assessment (GQA) which had been used to assess rivers in the UK since 1990. Environmental Quality Standards (EQS) Directive 2008/105/EC set out the standards to be met for chemical pollution. These were revised in the flowing years by an advisory body UK Technical Advisory Group (UK TAG) and updated the levels to be achieved for each rating (high, good, moderate or low). These came into effect in 2014.

Table 2.1 shows some of the levels set for general water quality from the WFD updated standards. Table 2.2 shows the types of river the standards refer to.

Table 2-1 99th percentile standards for Biochemical oxygen demand and ammonia in Rivers (DEFRA, 2014)

Status		99th percentile		
	Types of river	BOD(mg/l)	Total ammonia (mg NH_4-N/l)	Un-ionised ammonia (mgNH_3-N/l)
High	1, 2, 4, 6 and salmonid	7	0.5	0.04
High	3, 5 and 7	9	0.7	0.04
Good	1, 2, 4, 6 and salmonid	9	0.7	0.04
Good	3, 5 and 7	11	1.5	0.04
Moderate	1, 2, 4, 6 and salmonid	14	1.8	0.04
Moderate	3, 5 and 7	14	2.6	0.04
Poor	1, 2, 4, 6 and salmonid	16	2.6	0.04
Poor	3, 5 and 7	19	6	-

Table 2-2 Types of river to which the 99th percentile standards in Table 2.1 apply (DEFRA, 2014).

Alkalinity (as mg/l $CaCO_3$)					
Altitude	Less than 10	10 to 50	50 to 100	100 to 200	over 200
Under 80 metres	Type 1	Type 2	Type 3	Type 5	Type 7
Over 80 metres			Type 4	Type 6	

Current pollution concerns include by-products from human activities and the introduction of pollutants to the environment. Treating water before it is released into the environment is one way of maintaining water quality. This is often done by wastewater treatment works where combined sewers transport the road runoff, along with waste water from properties. Historically, drainage of water off roads using piped networks often flows into combined sewers where the water mixes with sewage. This can put the receiving wastewater treatment works under pressure and in turn cause a release of untreated sewage in times of high flow via the combined sewer overflows. However, these systems can also be overwhelmed in heavy rain or blocked, due to build-up of debris (for example in autumn when leaves are falling) or collapse of pipes. Since the 1960's new build houses have had separate systems for waste and foul water (Ministry of Housing, 2015). This has the benefit for treatment works, in that there is reduced volume requiring treatment, therefore

reduced costs. The surface water is then sent to nearby watercourse, without the benefit of treatment it would have undergone at the treatment works. Drainage systems that mimic natural systems have been integrated into planning guidelines to keep the foul and surface waters separate. Sustainable Drainage Systems (SuDS) form one way in which various countries are working to achieve the targets set out in the WFD. SuDS have been developed over the last few decades and are used to cope with storm surge events before channelling water into local rivers or water bodies. SUDs are part of Welsh and Scottish law, and in the UK DEFRA, and more recently Biodiversity Net Gain (BNG), guidelines support the use of systems such as these.

SuDS can be divided into two distinct types: hard and soft. Hard SuDS are hard standing areas, such as permeable paving (Kazemi, Golzarian, & Myers, 2018). These areas are designed to accept high loads while allowing rain water to filter through to the water table below and can often provide storage. Soft SuDS are more visible and natural looking, made to mimic a natural environment. Invariably, the softer SuDS require a larger area when constructing. As such the harder systems are more attractive in terms of real estate (Kirby, 2005). While the concept of SuDS is widely covered by local councils and government bodies there are many different interpretations of them (Hubert *et al.*, 2012). One of the key issues regarding SuDS is the adoption after the site build has finished. Who is responsible for maintenance of the systems?

2.2 Sustainable Drainage Systems

SuDS is a commonly used term for surface water drainage systems, which have been designed to replicate the natural drainage of an area as it was before development (CIRIA, 2007). They are considered to be a sustainable method of controlling storm water and flood risk (Jackson & Boutle, 2008). Key to the principal of SuDS is prevention or reduction of flooding, by managing the water volume (Zhou, 2014). In the UK the SuDS manual is one of the main reference guides to SuDS design and practices, and the most recent version was issued in 2015. The underlying philosophy of sustainable drainage is to manage surface water in as close to a natural state as possible, maximising the benefits and reducing the

negative impacts caused by urbanisation and industrialisation. When designing SuDS, the systems should be able to provide some of the key aims of sustainability which cover economics, environmental and social aspects. Figure 2-1 shows four areas in which these can be broken into: water quality, water quantity, amenity and diversity (Woods-Ballard *et al.*, 2015). To achieve true sustainable drainage, some of these objectives need to be incorporated in any design.

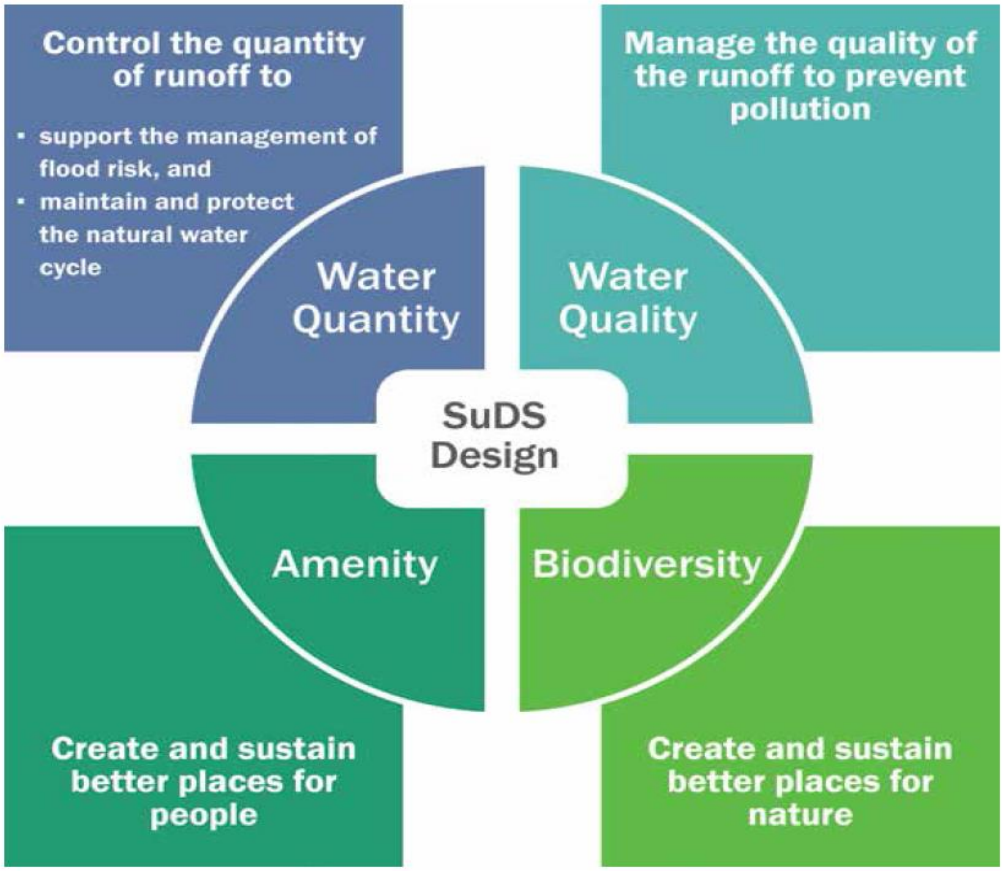

Figure 2-1 Four pillars of a SuDS design (Woods-Ballard et al., 2015).

The concept of sustainable drainage is familiar in many parts of the world. Although these all have similar goals, there is different functionality and focus between each concept (Fletcher *et al*., 2014, Liu *et al*., 2015):

- Best Management Practices (BMP), generally known worldwide.
- Low Impact Development (LID), American and Canada.

- Water Sensitive Urban Design (WSUD), Australia.
- Sustainable Drainage Systems (SuDS), UK.

The above terms constitute some of the more widely recognised systems (Elliott & Trowsdale, 2007, Barbosa *et al*., 2012, Zhou, 2014), all of which are recognised worldwide. Each has a different focus towards the management of storm water (Williams *et al.*, 2019), for example in the UK the emphasis is primarily on flood management, in Australia it focusses on the urban design. Research into sustainable urban drainage has become increasingly important, with a rise in research papers being published. Fletcher *et al*. (2014) compiled a report to try and clarify the differing terms and descriptions used around the world, classifying them according to their primary focus and specificity. They also reported on the rise in interest in storm water management since the early 1980's, showing an exponential increase in the use of urban drainage terminology.

In built up areas, where man-made surfaces are impervious, rainfall has nowhere to drain away to, as such it becomes runoff. Often the sudden build-up of water leads to localised flooding. Apart from losses due to evaporation this runoff needs to be removed efficiently to prevent flooding. Figure 2-2 shows how the rates of infiltration, runoff and evapotranspiration change as the level of impervious surfaces increases. Even a small increase in impervious surfaces can result in stream degradation (US EPA, 2003).

Road runoff is of particular concern due to the pollutants it washes off of the surface and transports into surrounding waterways (Woods-Ballard *et al.*, 2015). These pollutants come from a variety of sources including vehicle emissions.

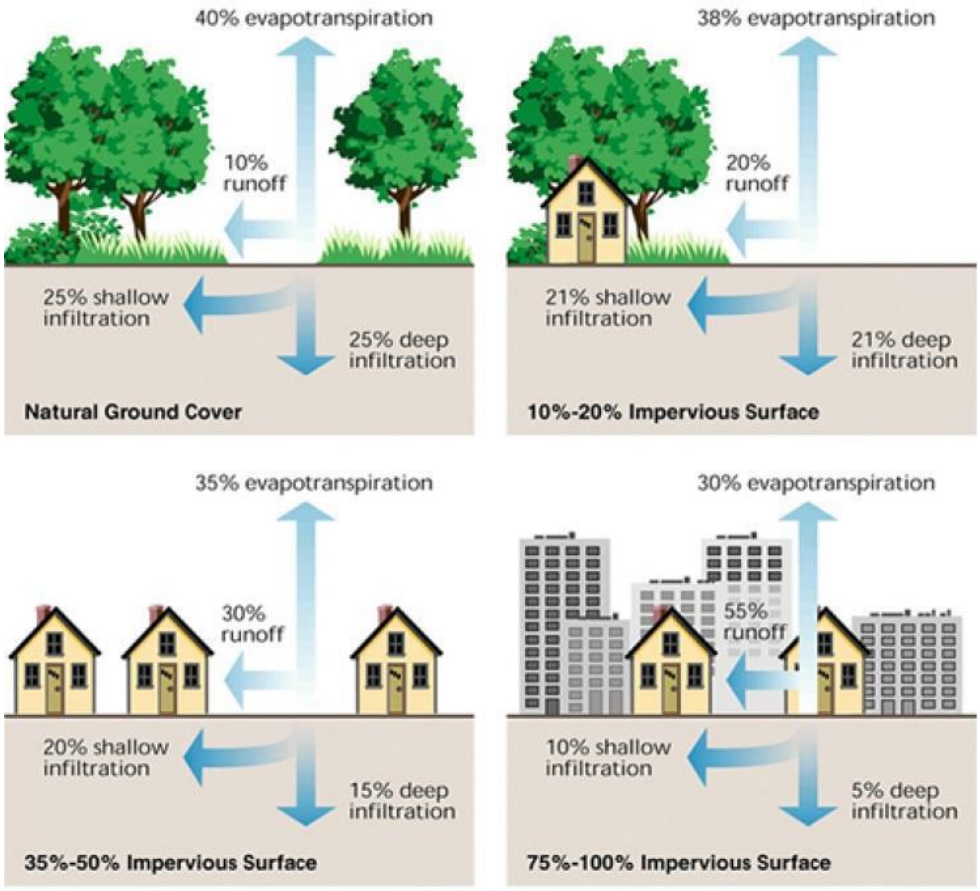

Figure 2-2 Relationship between impervious surface cover and surface runoff (US EPA, 2003).

Knowledge of SuDS in new developments is often little understood by the stakeholders involved in the decision process. As such, the importance of the role SuDS play may not currently be taken properly into consideration (Viavattene & Ellis, 2013). At present, while SuDS are being utilised and incorporated in new builds, they are generally based on 'Black Box' approaches (Roinas *et al.*, 2014). This essentially means that while the value of the system is recognised, the actual processes and mechanisms are little understood. The use of SuDS has added benefits in the local area, not just from the pollutant clean up aspects. The societal and amenity value may be considered to out-weigh the added costs of providing the SuDS area in construction (Hubert *et al*., 2012). There has been uncertainty in the adoption of SUDs systems post construction, and this has implications in the design of areas. In a recent large survey of experts, conducted by Chartered Institution of Water & Environmental Management (CIWEM), a number of key findings were highlighted (Melville-Shreeve *et al*., 2018). Half of the responses showed that one of the biggest barriers to SUDs implementation was the need for a single adoption method. One major concern to come

from the survey was the lack of information available on costs and benefits of implemented systems. The Flood and Water Management Act 2010, contained proposals for national design standards and for SuDS to be adopted by local authorities. This has been followed and implemented by the Welsh government (Williams *et al*., 2019), whereas in the UK this has still to be acted upon (Ellis & Lundy, 2016). In the Sewers for Adoption (8th edition) clarification has been given firmly bringing certain aspects of SUDs under the 'sewers' heading. This gives clear guidance for adoption measures, and the standards that need to be met to be adoptable by water and sewerage companies. This document has been subsumed by the OFWAT Code for Adoption agreements, which call for the water sector to provide guidance on water and sewerage asset adoption. The Code for Adoption is now anticipated to be implemented in 2020 after further consultations with Water agencies and their stakeholders (ofwat.gov.uk).

One concept that is useful in the design of SuDS is the Management Train, also known as the treatment train. This describes the stages of water management in the system and has been defined by the Construction Industry Research and Information Association (CIRIA, 2007) into four stages:

- Prevention
- Source control
- Site control
- Regional control.

A typical SuDS will consist of a number of sections, which when combined make a system which slows down the progression of water before it returns to a local watercourse. Table 2-3 describes some of the components that may be used individually or in combination. Each stage is linked together utilising the various SuDS working together in sequence, rather than standalone units (CIRIA, 2007, Lashford *et al*., 2014). In combination these stages slow down the water flow and aid in the removal of pollutants. Figure 2-3 shows a short treatment train, located in Berewood housing estate in Waterlooville, Hampshire. It comprises of two different examples of swales (B and C) and a wet pond (A). Figure 2-3B is

a vegetated swale with check dams located at intervals down the slope, these aid in slowing water flow down, having a small opening at the base, through which the water has to flow. Check dams are used in swales which have a steeper gradient. Both Figure 2-3 B and C direct water into the wet pond (C). The roadside swale (C) runs parallel to the pond, while the vegetated swale is on a slope running down to the pond.

Table 2-3 Components that may be used to form a SuDS treatment train (CIRIA, 2007b).

System	*Description*
Filter strips	*These are wide, gently sloping areas of grass or other dense vegetation that treat runoff from adjacent impermeable areas.*
Swales	*Swales are broad, shallow channels covered by grass or other suitable vegetation. They are designed to convey and/or store runoff, and can infiltrate the water into the ground (if ground conditions allow).*
Infiltration basins	*Infiltration basins are depressions in the surface that are designed to store runoff and infiltrate the water to the ground.*
Wet ponds	*Wet ponds are basins that have a permanent pool of water for water quality treatment. They provide temporary storage for additional storm runoff above the permanent water level.*
Extended detention ponds	*Extended detention basins are normally dry, though they may have small permanent pools at the inlet and outlet.*
Filter drains and perforated pipes	*Filter drains are trenches that are filled with permeable material. Surface water from the edge of paved areas flows into the trenches, is filtered and conveyed to other parts of the site.*
Infiltration devices	*Infiltration devices temporarily store runoff from a development and allow it to percolate into the ground.*
Pervious surfaces	*Pervious surfaces allow rainwater to infiltrate through the surface into an underlying storage layer, where water is stored before infiltration to the ground, reuse, or release to surface water.*

Figure 2-3 Example of three sections of a SuDS system located in Waterlooville, Hampshire. A: a wet pond. B: a vegetated swale, with check dams at intervals down the slope. C: a roadside swale, shown in the image is one of the drainage channels which directs water from the road onto the swale.

A number of processes take place within the SuDS ecosystem to remove the pollutants. Bastien *et al.,* (2010) showed that by using SuDS treatment train there are significant benefits for removal of pollutants, thus improving water quality. Much of the current literature focussing on SuDS systems concentrates on the water removal efficiency, few studies look at the fate of pollutants, PAHs in particular, in the initial stage of the treatment train.

2.2.1 Swales

Swales are often used in the first elements of a treatment train. They generally fall into one of three main types of swale (Woods-Ballard *et al.*, 2015):

- Standard conveyance swales
- Dry swales
- Wet swales

Of these, wet swales are unlikely to have any impact on groundwater systems. This is due to the design of the system having a liner to contain any water in the system and prevent or inhibit infiltration of the water. Standard conveyance swales generally feature a vegetated channel, often with broad gently sloping sides, and a flat base. Similar on the surface to the standard conveyance swales are the dry swales. These are built with a filter bed and an underdrain to convey the water and prevent waterlogging of the area.

Water will enter the swale and be directed along a channel of vegetation before heading to the next stage. Some systems may have extra drainage under the surface for increased water transport. The primary functions of a swale are for control of the movement of water, added drainage and also cleaning up of the water. Generally swales are quite shallow, with a flat base, so water flows in a narrow layer through vegetation. This allows for sedimentation to occur, cleaning up the water before the next stage. Swales can also be used for some filtration of the water and storage. Typically swales have gently sloping sides with a low gradient, and will not retain water during dry periods, if they need to go around a bend there will be no sharp corners just a gradual curve. In order to allow time for deposition of sediments it is recommended that swales should be at least 35 m in length (Woods-Ballard, 2007). Swales are one feature which has been used in farming and rural practices for a long time, and are now becoming increasingly popular in urban design. These are often found at roadsides to direct storm water runoff (Deletic & Fletcher, 2006).

Several studies have shown that swales are effective in the removal of suspended solids, and that their primary removal function is through sedimentation with some filtration of dissolved particles (Stagge *et al.*, 2012). Lucke *et al*. (2014) showed that most sedimentation occurred during the first 10 m of a swale, between 50% and 80% of Total Suspended Solids (TSS). This study further showed that swales of 30 m in length would remove another 10% - 20% of TSS. The top ten cm of soil has also been shown to be

significant in pollutant retention, with the majority of pollutants being found in this layer (Napier *et al.*, 2009, Tedoldi *et al.*, 2016). This study also recommended that swales be used to filter runoff before it enters a pond or river system. Pollutants were found to move slowly through the soil and as such the top soil be periodically removed to prevent pollutants moving further into the environment.

Guidance on what to plant in SuDS systems is limited, although certain plants are known to aid in the removal of pollutants. Most studies will focus on one specific pollutant, for example in ponds systems various reeds are known to be hyperaccumlators of metals (Ali, Khan, & Sajad, 2013). In a study of *Vetiveria zizanioides* grass it was shown to aid in the uptake of lead (Pb), copper (Cu), zinc (Zn) and cadmium (Cd) (Chen *et al.*, 2004).

As previously stated, SuDS are can be implemented to remove as much pollution from the water that passes through them as possible. With the increase in industrialisation the release of pollutants such as metals into the environment is reaching even greater levels. To tackle this, bioremediation which uses living organisms to manage/remediate polluted soils is becoming increasingly popular (Wenzel, 2009). Phytoremediation is a branch of bioremediation which involves the use of plants for the removal of pollutants from contaminated environments (Haritash & Kaushik, 2009). Phytoremediation uses plants and their associated rhizosphere microorganisms to remove, degrade, contain or transform contaminants (Susarla *et al.*, 2002). The origins of using plants in this manner is not known but has been used for a long time (Padmavathiamma & Li, 2007). Susarla *et al*. (2002) compiled a list of the advantages and constraints associated with phytoremediation, Table 2.4.

Table 2-4 Advantages and constraints of phytoremediation (Susarlaet al., 2002).

Advantage	*Constraint*
In situ	*Limited to shallow ground water, soils and sediments.*
Passive	*High concentrations of hazardous materials can be toxic to plants and animals that consume the plants.*
Solar driven	*Mass transfer limitations associated as with aother biotreatments*
Costs 10-20% of mechanical treatments	*Slower than mechanical treatments.*
Faster than natural attenuation	*Only effective for moderately hydrophobic compounds.*
High public acceptance	*Toxicity and bioavailability of biodegradation products is not known*
Fewer air and water emmissions	*Contaminants may be mobilised into the ground water.*
Conserves natural resources	*Influenced by soil and climate conditions of the site.*

Remediation techniques can be chemical, biological or physical. Phytoremediation is fast becoming a cheap, environmentally friendly method of cleaning up contaminated soils. Once the metals, or other contaminant, have been removed from the environment by the plants the plant tissue can be harvested. The contaminants can then safely be processed by drying, ashing or composting. Some metals are able to be extracted from the waste and recycled, creating a revenue to offset some of the costs of remediation (Raskin *et al.*, 1997). It is this ability of plants that is utilized in SuDS to clean up runoff before it re-enters the local waterbody. Phytoremediation can be sub-divided into a number of processes, shown in Table 2.5.

Table 2-5 Descriptions of the various plant phytoremediation processes for the control of pollutants, information from (Ali et al., 2013).

Process	*Description of process*
Phytoextraction	*Accumulation of pollutants in harvestable biomass i.e., shoots.*
Phytofiltration	*Sequestration of pollutants from contaminated waters by plants.*
Phytostabilization	*Limiting the mobility and bioavailability of pollutants in soil by plant roots.*
Phytovolatilization	*Conversion of pollutants to volatile form and their subsequent release to the atmosphere.*
Phytodegradation	*Degradation of organic xenobiotics by plant enzymes within plant tissues and the associated microbes.*
Rhizodegradation	*Degradation of organic xenobiotics in the rhizosphere by rhizospheric microorganisms.*
Phytodesalination	*Removal of excess salts from saline soils by halophytes.*

Vegetation in the swale can enhance biodegradation and help provide efficient phytoremediation, but it also has another role to play that can aid in remediation. The above ground growth of the plants stabilises the soil, to prevent washing of soil during high water flows and it adds a roughness factor, which will help slow the flow of water down. In flow rates Manning's equation takes into account the roughness of the surface (Woods-Ballard, 2015). The vegetation in the swales can promote removal of organic compounds from road runoff (Jefferies & Napier, 2008). Vegetation has proven to be effective at retaining the particulates in road runoff, and consequentially the attached pollutants (e.g. Bastien *et al.,* 2010a; Bratieres *et al.,* 2008; Stagge *et al*., 2012, Woods Ballard *et al.,* 2015).

The slowing of the water flow aids infiltration, and sedimentation. Clumps of vegetation may act as a dam. As water flows through, over and around the vegetation it is disrupted, suspended particulates may fall out of the water column, or adhere to the vegetation itself.

2.3 Pollutants in the urban environment

Pollutants in the urban environment are generally considered to be (but not limited to) metals, total suspended solids (TSS), organic compounds (such as PAHs), microbial contaminants and nutrients (Gobel *et al.*, 2007).

The UK Government in the Groundwater Regulations (2009) define hazardous substances as:

> '…any substance or group of substances that are toxic, persistent and liable to bio-accumulate'

Metals, PAHs and other pollutants in the environment have become a big concern, because of their persistence in the environment. Effects from runoff pollutants are considered in water quality legislation set out by the EU and in the UK specifically, the Environment Agency (EA). Legislation such as the WFD sets out standards for various water quality parameters.

Previous studies have shown that a number of factors can affect the storm water characteristics, of these season and land use are those often referred to as the most relevant factors (Barbosa *et al.*, 2012). Different pollutant groups found in storm water runoff consist of suspended solids, heavy metals, nutrients, organic chemicals and bacteria (Kayhanian *et al*., 2012). Build-up of these pollutants in the receiving waters can result in toxicity to aquatic organisms (Camponelli *et al*., 2010).

Particularly important is the first flush or storm surge (Kang *et al.*, 2008). The first flush is used to describe the initial higher loading of pollutants in a storm as the flowing water washes built up pollutants off the surface. The first flush effect has been identified in individual storm events, but there is also a seasonal first flush in areas where the weather patterns include extended dry periods (Lee *et al.*, 2004). Studies have shown that pollutant levels are highest immediately after a storm surge due to rainwater washing pollution deposits off of road surfaces etc. (Zhang *et al*., 2010). In a study of storm water runoff into sewers Bertrand-Krajewski *et al.* (1998) suggested that 50% of the pollutant load was transported in the first 38 - 47% of the total volume. It is during the first stage of a storm that the majority of pollutants are washed off of the road surface and make their way into the adjacent environment. However, the levels of pollutants in the first flush is inconsistent due to the variability of individual sites and changes in traffic intensity and the extent of interceding dry periods. Some pollutants are more stable, such as metals, while some pollutants, such as polycyclic aromatic hydrocarbons, are more complex to study as they

can behave differently depending on environmental factors. Due to the stability inherent in metal pollution the effects are easier to study, which is shown by the higher numbers of research papers available (Kuffner *et al.*, 2008, Muthukrishnan, 2010).

During storm events metals and PAHs previously deposited are made mobile and continue to move through the environment. Linked with sedimentation, as water flows through a system, particles are re-suspended and transported further along, taking with them the adhered pollutants (Allen *et al.*, 2015). As previously stated one of the key purposes of SuDS is the removal of pollutants, which helps towards the cleaning up of local receiving water bodies. In SuDS, it has been shown that a large proportion of pollutants are coming from storm water runoff and road runoff (Barbosa *et al.*, 2012). Storm water is diverted from the impervious surfaces into the SuDS, thus reducing the runoff into streams and other water bodies (Camponelli *et al*., 2010).

Many of the pollutants in runoff will be bound to particulate matter, often called dust due to the small sizes. Some of the particulates can be cleaned and removed via regular sweeping of the roads and car parks. In a review of street sweepers/cleaners Amato *et al.* (2010) noted large variation in removal efficiencies of the various machines used, many of which are only efficient at removal of particulates > 15 µm. Table 2-6 gives some examples of quantity of TSS found in road or carpark runoff.

Table 2-6 Weight of total suspended solids found in runoff from roads and carparks.

Study	*Mean TSS (mg/L)*	*Range (mg/L)*	*Notes*
Lee & Bang (2000)	*193*	*15 - 370*	*Highway runoff, Korea.*
Kayhanian et al. (2007)	*112.7*	*1 - 2988*	*Highway runof.*
Camponelli et al. (2010)	*128*	*-*	*Roadway dust and runoff.*
Lundy, Ellis, & Revitt (2012)	*-* *150*	*55 – 1568* *10 - 290*	*High density roads.* *Low density roads.*
Revitt et al. (2014)	*139*	*7.8 - 270*	*Car park runoff review.*
Gobel et al. (2007)	*150*	*-*	*Average from urban car park runoff.*
Leroy et al. (2016)	*290*	*75 - 774*	*Urban highway runoff, France.*

The TSS particulates can be broken down into the fraction sizes, with finer particulates being harder to remove from the environment. Table 2-7 gives examples of particulate fraction sizes found in runoff TSS.

Table 2-7 TSS particulate fraction percentages found in runoff.

Study	*TSS ranges (µm)*	*Notes*
Herngren et al. (2005)	*85% < 75*	*Shopping centre car park.*
Herngren et al. (2006)	*8.6% < 0.45* *58.1% 0.45 – 78* *23.3 % 76 – 150* *5.8 % 151 – 300* *4.2 % > 300*	*Residential area roads.*
Goonetilleke et al. (2009)	*74 % < 150* *91 % < 150* *57 % < 150*	*Car park.* *Lorry Car park.* *Residential road.*
Leroy et al. (2015)	*19.1 % < 2* *68.8 % 2 – 63* *12.1 % 63 - 2000*	*Urban road.*

2.3.1 Polycyclic Aromatic Hydrocarbons

Polycyclic aromatic hydrocarbons (PAHs) are organic compounds that contain at least two condensed (benzene) rings. They can be found in one of three structural arrangements, linear (fluorene), angular (chrysene) and clustered (pyrene). As a class there are several hundred individual PAHs made up of carbon (C) and hydrogen (H) molecules. They are formed when there is incomplete burning of compounds which contain C and H (Wilcke, 2000). PAHs come from both natural and anthropogenic sources, with the incomplete burning of fossil fuels. Natural sources include volcano emissions and forest fires (Manoli & Samara, 1999). Anthropogenic sources include vehicle emissions, coal fires and oil burning. Of these sources the anthropogenic releases into the atmosphere are the most significant (Wilcke, 2000). Some PAHs are made specifically for use in products, for example fluorene (FLU) is used in many chemical processes, and in the manufacturing of dyes (CCME, 2008).

PAHs are known to be toxic, mutagenic and carcinogenic, and as such research into PAHs has been undertaken for many years (Wild & Jones, 1995). They are released into the atmosphere and then deposited on land or water. Due to their potential for bioaccumulation, toxic, carcinogenic and persistent nature PAHs are some of the top pollutants of concern in the environment (Haritash & Kaushik, 2009). In America the Environment Protection Agency (EPA) has identified 16 PAHs as representative of the whole family of PAHs, these are now used as standard for monitoring purposes (Napier *et al*., 2008). These 16 PAHs were identified in 1970's as being targets for study. In 2005 the European Commission (EC) highlighted 15 PAHs as needing monitoring due to food contamination problems (Smith & Lynam, 2010). Of the PAHs listed by the European Commission, eight are found on the EPA list of 15 PAHs. In the UK the Environmental Quality Standards Directive (EQSD; Directive 2008/105/EC amended by Directive 2013/39/EU) a number of PAHs are highlighted as priority substances to be monitored, of these Benzo(a)pyrene is often targeted for monitoring in water bodies as a marker for other PAH levels. In recent years three specific PAHs, benzo(a)pyrene, benzo(k)fluoranthene, and

benzo(g,h,i)perylene, have been designated substances of very high concern under REACH regulation (EC/1907/20006).

Table 2-8 shows the PAHs which are recommended for monitoring. Most industrialised countries have regulations in place concerning PAHs, however in developing countries this is not always true (Rubio-Clemente, Torres-Palma, & Peñuela, 2014). In soils the concentrations are higher in areas of high industrialisation, (Wilcke, 2000). PAHs that comprise of up to three benzene rings are termed 'light PAHs' or low molecular weight. Those PAHs with four or more rings are known as 'heavy PAHs' or high molecular weight. Heavy PAHs are more stable and have greater persistence than the light PAHs. Light PAHs are more water soluble and as such are more likely to be found in an aquatic environment (Wenzl *et al*., 2006).

Table 2-8 PAHs that are recommended for monitoring by the European Commission and the US Environmental Protection Agency.

PAH	*EC*	*USEPA*
5-methylchrysene	✓	
Acenaphthene	✓	✓
Acenaphthylene		✓
Anthracene		✓
benz[a]anthracene	✓	✓
benzo[a]pyrene	✓	✓
benzo[b]fluoranthene	✓	✓
benzo[c]fluorene	✓	
benzo[g,h,i]perylene	✓	✓
benzo[j]fluoranthene	✓	
benzo[k]fluoranthene	✓	✓
chrysene	✓	✓
cyclopenta[c,d]pyrene	✓	
dibenz[a,h]anthracene	✓	✓
dibenzo[a,e]pyrene	✓	
dibenzo[a,h]pyrene	✓	
dibenzo[a,i]pyrene,	✓	
dibenzo[a,l]pyrene	✓	
Fluoranthene		✓
Fluorene		✓
indeno[1,2,3-cd]pyrene	✓	✓
Naphthalene		✓
Phenanthrene		✓
Pyrene		✓

Of these monitored PAHs, six will be analysed in this study: naphthalene (NAP), fluorene (FLU), fluoranthene (FLAN), pyrene (PYR), chrysene (CHR) and benzo(a)pyrene (BaP). Figure 2-4 shows the ring structure of these PAHs.

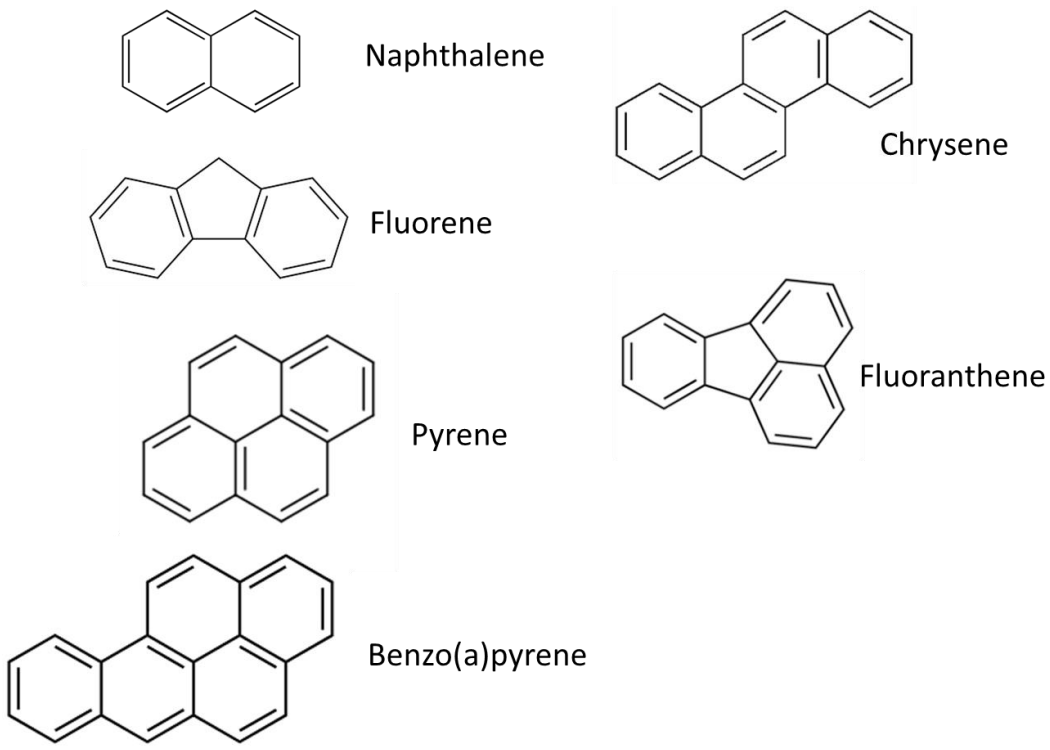

Figure 2-4 Ring structures of PAHs of interest.

These were decided on as a representative range of the two to five ring PAHs, encompassing both light and heavy ranges. Table 2-9 shows some of the physiochemical characteristics of the target PAHs. As shown in Table 2-9 the characteristics are related, for example as the molecular weight increases the solubility decreases. PAHs with low vapour pressure, such as BaP are often found bound with particles, while those PAHs with higher vapour pressure, such as naphthalene, are likely to be found in ambient air. Physio-chemical characteristics of the PAHs will largely determine the behaviour in the environment, for example low weight PAHs will be quicker to transfer than the higher weight ones (Wild & Jones, 1995).

Table 2-10 shows some of the PAH concentrations found in soils around the world. From this sample set it is clear how PAHs vary in concentration. In the UK recent studies have shown that soils near London vary in concentration with combined PAH (n=16) levels having a mean concentration of 18 mg/kg, with a range of 4 to 67 mg/kg (Vane *et al*., 2014).

Table 2-9 Chemical characteristics of the target PAHs (Kim et al., 2016).

PAHs	*Chemical Abstract Registry Number (CAS)*	*Chemical Formula*	*Number of Rings*	*Molecular Weight (g / mol)*	*Melting Point (°C)/ Boiling Point (°C)*	*Water Solubility (mg/l) at 25°C*	*Vapour pressure (mm Hg) at 25°C*	*Henry's Law Constant (atm·m3·mol-1)*	*Log Kow*	*Log K_{oc}*
Naphthalene	*91-20-3*	*C10H8*	*2*	*128.17*	*80 / 218*	*31*	*0.085*	*4.83E-04*	*3.3*	*3.11*
Fluorene	*86-73-7*	*C13H10*	*3*	*166.22*	*115 / 294*	*1.70*	*6×10^{-4}*	*6.34E-05 to 1.00E-04*	*4.18*	*4.14*
Fluoranthene	*206-44-0*	*C16H10*	*4*	*202.26*	*110 / 384*	*0.2 - 0.26*	*9.22×10^{-6}*	*1.3E-05 to 1.6E-05*	*5.16*	*5.03*
Pyrene	*129-00-0*	*C16H10*	*4*	*202.26*	*151 / 394*	*0.135*	*4.5×10^{-6}*	*1.10E-05*	*4.88*	*5.02*
Chrysene	*218-01-9*	*C18H12*	*4*	*228.29*	*255 / 448*	*2×10^{-3}*	*6.23×10^{-9}*	*9.46E-05*	*5.73*	*3.66*
Benzo(a)pyrene	*50-32-8*	*C20H12*	*5*	*252.32*	*179 / 496*	*1.6×10^{-3}*	*5.49×10^{-9}*	*1.13E-06*	*6.13*	*6.01*

Table 2-10 Examples of environmental concentrations of PAHs in soil at various locations around the world. The Waterlooville study results are described in the results section.

PAH	*Field study Waterlooville (ng/g)*	*Smith et al., (1995) (ng/g)*	*Roinas (2014) median for swale inlet (ng/g)*	*Leroy et al., (2015) background levels (ng/g)*	*Jones et al., (1989) (ng/g)*	*Wang et al., (2013) Urban soil (ng/g)*
Location	*Hampshire, UK*	*Birmingham, UK*	*Hampshire, UK*	*France, surface soil.*	*Wales, surface soil*	*Shanghai, 0-20cm depth composites.*
Naphthalene	*2403*	*27.2*	*164*	*4.9*	*35*	*20*
Fluorene	*115*	*28*	*608*	*2.5*	*-*	*14*
Pyrene	*721*	*254*	*729*	*40.6*	*514*	*276*
Chrysene	*501*	*149*	*422*	*38.3*	*406*	*173*
Benzo(a)Pyrene	*668*	*149*	*377*	*32.5*	*138*	*145*

When monitoring water quality there are standards to be met in order to consider the water of good status, as described in the WFD (see section 2.1). Table 2-11 gives the environmental quality standards (EQS) for PAH pollutant levels in surface waters from the original 2008 guidelines and the updated levels from the 2015 revision. For all the PAHs the accepted level has been reduced, an indication of the increased awareness of the potentially damaging effects caused by the presence of PAHs in the surface waters. In the revised levels, no standard was given for the combined benzo groups as the BaP level has been determined as an indicator for all.

Table 2-11 Environmental Quality Standards for PAH pollutant levels in surface waters. AA: Annual average, MAC: maximum allowable concentration, ISW: inland surface waters, OSW: other surface waters. Information from 1: EQS 2008/105/EC and 2: Water framework directive Directions 2015.

PAH	*Ref.*	*AA ISW (ug/l)*	*AA OSW (ug/l)*	*MAC ISW (ug/l)*	*MAC OSW (ug/l)*	*Priority hazardous substance*
Naphthalene	*1*	*2.4*	*1.2*	*-*	*-*	
	2	*2*	*2*	*130*	*130*	
Fluoranthene	*1*	*0.1*	*0.1*	*1*	*1*	
	2	*0.0063*	*0.0063*	*0.12*	*0.12*	
Benzo(a)pyrene	*1*	*0.05*	*0.05*	*0.1*	*0.1*	*X*
	2	*$1.7x10^{-4}$*	*$1.7x10^{-4}$*	*0.027*	*0.27*	
Benzo(b)fluoranthene	*1*	*∑=0.03*	*∑=0.03*	*-*	*-*	*X*
Benzo(k)fluoranthene						*X*
Benzo(g,h,i)perylene	*1*	*∑=0.002*	*∑=0.002*	*-*	*-*	*X*
Indeno(1,2,3-cd)pyrene						*X*

2.3.1.1 Sources of PAHs

As mentioned in section 2.3.1 PAHs are released when there is incomplete combustion of organic materials, such as volcanoes and vehicle emissions. Some PAHs are also manufactured and used commercially, although these tend to be the lighter weight PAHs. Variations in PAH levels occur over the year with changes in seasons, for example in the colder months an increase can be found due to the emissions from domestic heating (Wilcke, 2000).

2.3.1.2 Fate of PAHs

PAHs by their nature are subject to changes over time, due to various processes including volatilisation, degradation, and sorption to particles or release into water (ground water or surface water). The characteristics mentioned in Table 2-9 help determine how each PAH will react. NAP is the most likely of all the PAHs to return to vapour, with a reported volatilisation of 30 % in 48 hours (WHO, 1998a), PAHs with similar structures, two or three rings, may also have similar levels of volatilisation. For the larger four or more ringed PAHs, the loss through volatilisation is likely to be negligible. Ultimately the fate of each PAH is determined by the environment they are exposed to. Each PAH might be subject to chemical or photochemical transformation, with the resultant compounds potentially being more active than the original (Dabestani & Ivanov, 1999). Sorption of PAHs onto soil is often said to be influenced by the types and level of organic matter present and also the sizes of the particles (Wang *et al*., 2014). Sorption to particular particle sizes is a subject that has had varied results with some studies finding that concentrations of PAHs are higher in smaller fraction sizes (Kim *et al.*, 1999) while Rockne *et al*. (2002) found high PAH concentrations in higher fraction sizes.

Half-lives of PAHs, similar to chemical compound half-lives, vary between each PAH depending on the structure and strength (Bertilsson & Widenfalk, 2002). Another factor which plays a large part in determining the half-life is the environment. Roslund *et al.* (2018) showed that half-lives of certain PAHs were increased when organic content of landscaping soil was higher. The study concluded that bacterial community and organic matter content play key roles in the degradation of PAHs. The level and type of contamination may also affect the bacterial community composition.

PAH degradation pathways and products are difficult to trace, with the characteristics of the compounds and the physical, chemical and biological properties of the soil all influencing the degradation processes (Zhang *et al.,* 2006). Degradation products of PAHs are subject to a wide variation depending on the source and route of degradation. For example Figures 2-5 and 2-6 show two different degradation pathways of pyrene by different fungi (Agrawal & Shahi, 2017; Khudhair *et al*., 2015).

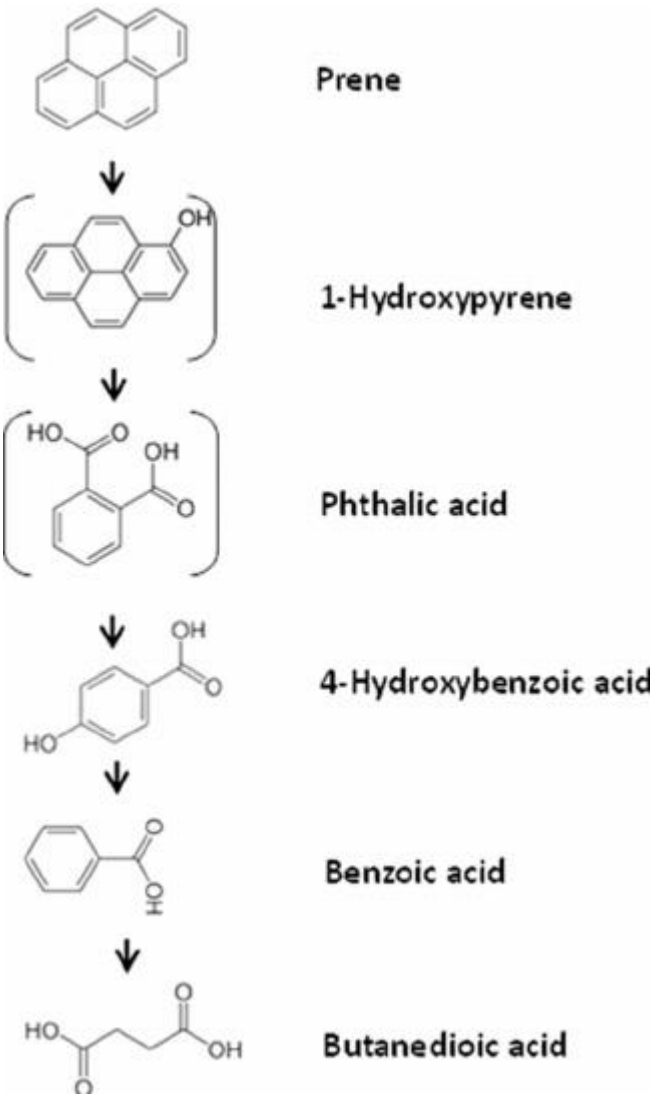

Figure 2-5 Proposed pathway for the degradation of pyrene by Rhizoctonia zeae SOL3. The metabolites in brackets had not been identified during trial. Image from Rehman *et al.*, 1998.

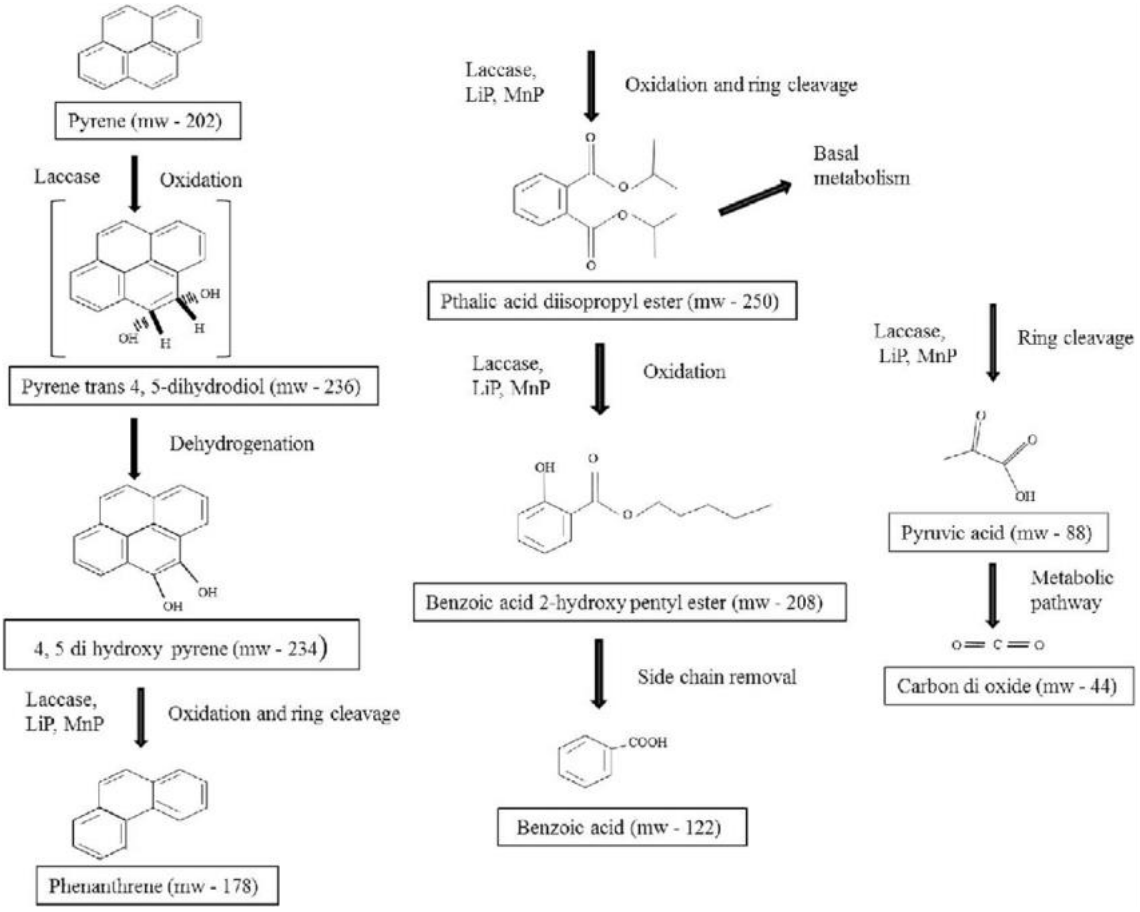

Figure 2-6 Proposed pathway of pyrene degradation by C. byrsina, based on the identified metabolites through GC-MS analysis, pyrene trans 4, 5- dihydrodiol was not identified in the extract. Image from (Agrawal & Shahi, 2017).

2.3.1.3 PAH degradation and behaviour in soils

As mentioned in 2.3.1.2 the fate of PAHs depends on the environment they are in. Different processes are occurring all the time in the soil, each of which could have an impact on the pollutants. Much of the environmental burden of PAHs is contained in the soil. Once deposited to the soil many persistent and strongly sorbed PAHs may reside for many years, but the soil may not be a permanent sink for these compounds (Wild & Jones, 1995). A combination of biological and physiochemical processes occurring in the soil matrix provide a potential for accumulation and degradation of the pollutants (Sposito, 2008). Some of the processes that will be acting on the pollutants include: adsorption, volatilization, photodegradation and biodegradation. PAHs will be subject to sorption and desorption on particulate matter. The sorption/desorption potential of the PAHs determines the potential to be available for transformation/degradation (Cousins *et al.*, 1999).

It is not just bacteria that have been widely studied, fungi have been proven to be efficient at biodegradation of pollutants. One advantage fungi hold over bacteria is that they can grow in a wide variety of substrates, and while growing produce hydrolytic enzymes which penetrate the contaminated soil and aid in removal of hydrocarbons (Messias et al., 2009; Venkatesagowda *et al.*, 2012; Kadri *et al.*, 2017).

Photodegradation is an abiotic process which causes an alteration due to the influence of light, particularly UV light. Each PAH possesses a characteristic UV absorbance spectra. The ring structure of PAHs has a unique UV spectrum, as such, each has a different UV absorbance spectrum (Abdel-Shafy & Mansour, 2015). PAHs absorb the light energy and reach photo-excited states, at which point they are susceptible to change. They can react with other chemicals and oxygen producing reactive oxygen species (ROS) or other oxygenated PAHs (Fu *et al.*, 2012). In a study of photodegradation in view of climate change Marquès *et al*. (2016) showed that LMW PAHs had an increase in volatilization as light and temperature increased. HMW PAHs were also seen to change at different rates, with BaP degrading during the dark indicating a hidden process is also having an effect. This laboratory study was continued in an outdoors trial, using natural light (Marquès *et al.,* 2017). PAHs were degrading at an increased rate compared to artificial light, indicating that solar UV was having a greater effect.

Biodegradation, sometimes referred to as bioremediation, is the breakdown of organic material, such as PAHs, by micro-organisms, such as bacteria or fungi. Biodegradation is a large field with a large number of microorganisms breaking the bonds of organic pollutants (Seo *et al.*, 2009). However, of all the processes that can affect PAHs, biodegradation is perhaps the most important while also being the most difficult, with the persistence of individual PAH species increasing with molecular weight (Haritash & Kaushik, 2009). Not all bacteria have the ability of degrade PAHs, a number of strains have been proven to be effective. Commonly isolated from contaminated sediments for study are *Pseudomonas aeruginosa, Pseudomons fluoresens, Mycobacterium spp., Haemophilus spp., Rhodococcus spp., Paenibacillus spp., Pantoea spp., Sejongia spp* (for example: Yuan *et al.*, 2002; Zeng *et al.*, 2010; Haritash & Kaushik, 2009; Ghosal *et al.*, 2016; Haleyur *et al*., 2018).

In a pot experiment, Agnello *et al.* (2016) used a range of bioremediation techniques in soil co-contaminated with metal and total petroleum hydrocarbons (natural attenuation, phytoremediation, bioaugmentation and bioaugmentation-assisted phytoremediation). Highest levels of removal were gained with the bioaugmentation and bioaugmentation-assisted phytoremediation pots, demonstrating that combining the use of plants and bacteria was the most effective treatment method. Some strains of bacteria are more effective than others in the degradation of PAHs. *Pseudomonas aeruginosa* has been identified as highly effective for both metal and PAH bioremediation as it can produce biosurfactants which enhance the solubility and mobility of hydrophobic HMW PAHs (Mulligan, 2005, Zhang *et al*., 2012, Das & Mukherjee, 2007).

Microbial degradation is one of the main mechanisms for PAH removal from soil, but it is heavily influenced by the bioavailability and the ability of the resident microbial populations. Li *et al*., (2008) used bacterial colonies isolated from aged oil contaminated soil in flask experiments. Their results showed that these colonies were highly successful in degrading 3-5 ringed PAHs. Appropriate implementation of the potential of naturally occurring microorganisms for field bioremediation could be considerably enhanced by optimizing certain factors such as bioavailability, adsorption and mass transfer of PAHs (Ghosal *et al*., 2016).

The process of volatilization involves the transfer of PAHs to the vapour phase, back into the atmosphere. The molecular weight of PAHs, the movement of water and weather conditions affect the rate of volatilization (CCME, 2008). Park *et al.* (1990) showed that volatilization of two ringed compounds were significantly different to three ringed compounds. The study showed that approximately 30% of the naphthalene was lost due to volatilization.

These processes can alter the chemical structure of the PAHs (Serrano *et al.*, 2008). Due to their variation in structure, each PAH will be affected to a different degree by the environment around it. As the PAHs change they form into new compounds, some of which may be more harmful than the original source (Fu *et al.*, 2012). The abiotic factors are most likely to affect the LMW PAHs which have the higher vapour pressures. Biologic

processes will be responsible for the majority of the HMW PAH changes (Leroy *et al.*, 2015).

It is highly unlikely in urban areas that PAHs will be the sole contaminants. How all these processes will work with a range of contaminants still requires much investigation. Recent analytical chemistry and genetic engineering tools might help to improve the efficiency of degradation of PAHs by microorganisms, and minimize uncertainties of successful bioremediation (Haritash & Kaushik, 2009).

2.3.1.4 Impact of PAHs

The toxic, mutagenic and carcinogenic properties of PAHs mean they can have sometimes severe effects. Impacts from PAHs in the environment can be to human health, but also the environment and organisms living in the affected areas. For human health the main exposure pathways are breathing in contaminated air and consumption of food and water (Kim *et al.*, 2013). Most PAHs are easily absorbed in mammals via the intestinal tract, from here they will end up in a variety of tissues, with a strong link to body fat. This is because PAHs are highly lipid soluble (Abdel-Shafy & Mansour, 2015). PAHs can be found in many foods consumed by humans, with smoked fish and meats containing significant amounts. In countries such as Nigeria where traditional smoking practices are still followed, consumption of foods high in PAHs has been highlighted (Akpambang *et al*., 2015).

2.4 Conclusions

While urban runoff has been studied in terms of pollution, some sources of pollution have been more extensively covered. The majority of research has considered the heavy metals or looked at general parameters of water quality such as total suspended solids and total organic carbon. Due to heterogeneity between sites and storms, any field study is open to a number of variables including a variety of removal/degradation mechanisms. This gives rise to questions on the reliability of results being applicable to general understanding of PAH behaviour in SuDS systems. It is this lack in understanding and uncertainty in available information regarding PAHs available to planners and policy makers, which makes their inclusion in development of SuDS systems difficult. This study will focus on the fate of PAHs in a swale mesocosm system, in controlled conditions, to

eliminate some of the variables and provide more evidence on the performance of swales in terms of managing hydrocarbon pollution.

2.4.1 Scope of study

This study aims to further the understanding of PAHs in storm water and their fate and behaviour in a vegetated swale system. Natural heterogeneity between sites, storms and pollution levels leads to uncertainty in general fate and behaviour processes of PAHs. This study offers the opportunity to increase the understanding of PAHs in the environment by building a swale mesocosm in a controlled environment.

2.4.2 Aim/objectives of study.

- Increase understanding of PAH fate and behaviour in vegetated swale systems, to inform design and maintenance codes.

The objectives of the study were the following:

- Characterise the environmental distribution and concentration of PAHs in swale/pond system treating road runoff to provide environmental field concentrations.
- Develop and build a swale mesocosm in a controlled environment, to undertake pollutant fate studies with standardised simulated storm events.
- Develop a recipe for simulating PAH polluted road runoff.
- Undertake a series of storm event simulations and establish patterns of PAH behaviour/accumulation in the swale system.
- Provide further understanding and resolution of the behaviour of PAHs in swale systems to inform design and maintenance codes.

3 Methods

3.1 Field Study – Waterlooville

3.1.1 Site Selection

In Waterlooville, Hampshire UK, a swale/pond SuDS system provided an ideal site for method development and data gathering. The site consists of an 80 m swale (inlet to outlet) and two ponds separated by a narrow berm. Located adjacent to the B2150 (Hambledon Road), the SuDS system receives road runoff from a busy roundabout and short stretch of dual carriageway. Water is directed along the swale, into the first of the two ponds. The outlet from Pond 2 feeds the water into the River Wallington. Figure 3-1 shows the site as viewed when standing by the inlet pipe, Figure 3-2 shows a satellite image of the Waterlooville swale with the soil sampling locations identified along with the inlet and outlet pipes. Figure 3-3 shows a schematic overview of the ponds in the SuDS system. Water flows into the study swale from the road via drains and a swale located on the other side of the roundabout. The swale has a slight slope which directs water towards the pond system before being discharged into the river. The swale was overgrown, showing no signs of maintenance along the swale bed. Maintenance of the grass at the top of the back, on the road side of the swale, was observed on one occasion (June 2015).

This site was chosen due to its use as a previous study site (Roinas *et al., 2014),* with similar water quality data collected, and its proximity to the University of Portsmouth laboratories where analysis was carried out. This allowed water and sediment samples to be collected and conveyed in an insulated box with ice packs to maintain a temperature between 2-8^{o}C. This temperature ensures that minimal activity occurs in the samples which may affect the results. Samples were stored in the insulated box for a maximum of 2 hours before arrival in the laboratory. Access to the site was easy as no permissions were required to be obtained from relevant parties.

Figure 3-1 Waterlooville site swale. Seen on the right of picture is the B2150 commuter road, runoff from this road is received via an inlet pipe into the swale. Water is directed along the swale towards an outlet pipe feeding into the first of two ponds. Water flows between the two ponds before overflow is discharges into the River Wallington. Image authors own, taken from the position of swale inlet pipe.

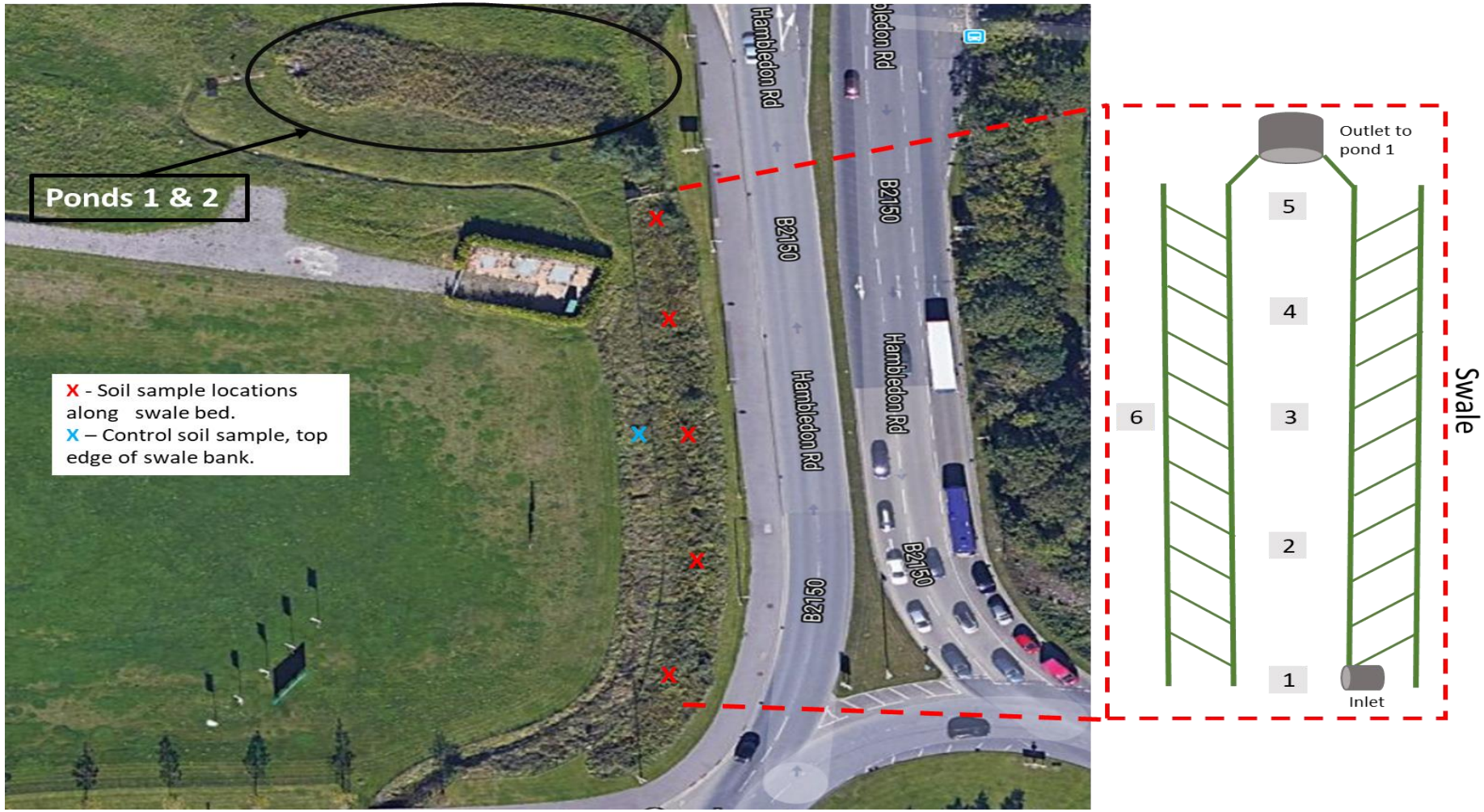

Figure 3-2 Plan view over the swale/pond system in Waterlooville, Hampshire. Sampling locations 1 - inlet, 2 – 20m, 3 – 40m, 4 – 60m, 5 – outlet pipe, 6 – control on top of bank at 40m. Image from Google maps.

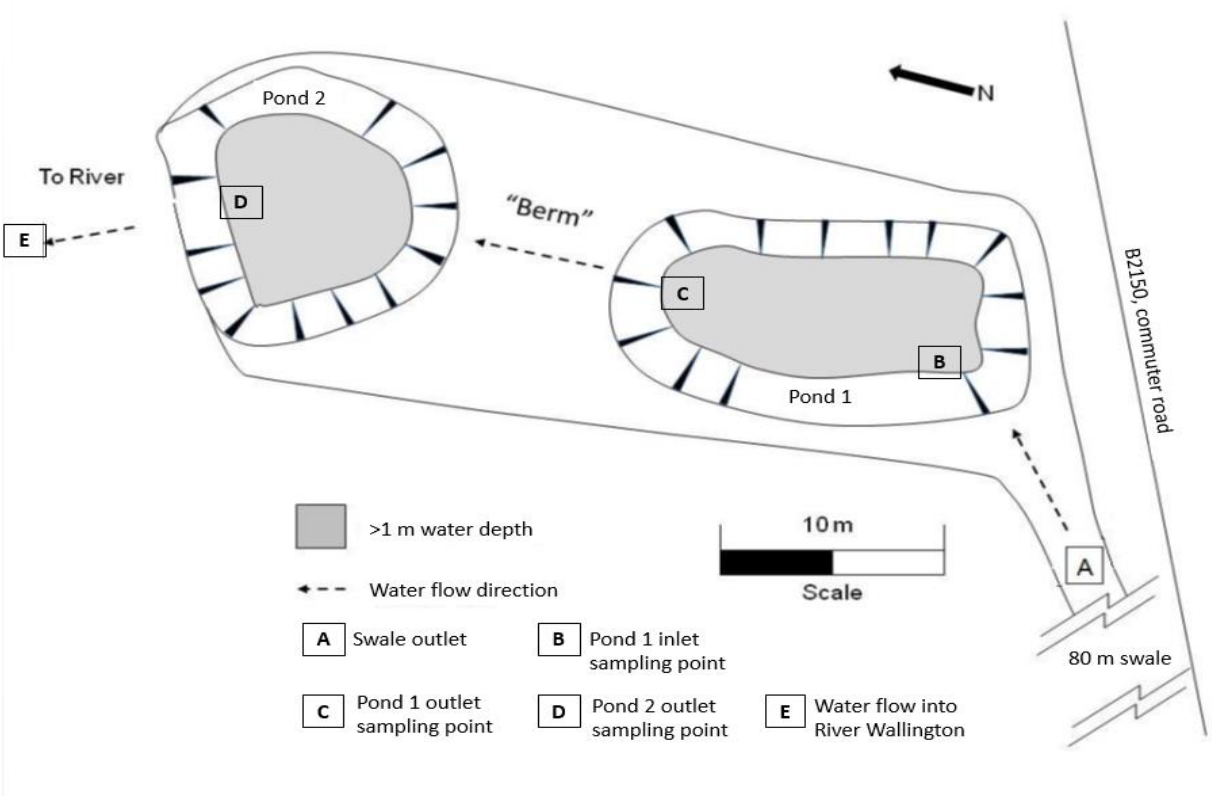

Figure 3-3 Schematic view of the SuDS system in Waterlooville. Water flows along the swale into Pond 1 into Pond 2 before it is discharged into the River Wallington. Water samples taken from Pond 1 inlet [B], Pond 1 outlet [C] and Pond 2 outlet [D]. Sediment samples taken every 20 m along the swale including by the inlet and outlet pipes. Adapted from Roinas et al. *2014, all measurements are approximate.*

3.1.1.1 Field Data Collection- Ponds

Once a month, water quality data was collected from the two ponds (Figure 3-3 P1 and P2). Parameters looked at *in situ* were temperature, pH and conductivity. These measurement were taken in the field using an Oakton PCTestr 35 multi-parameter probe.

Water samples were collected and transported back to the laboratory in a cool box for analysis. Amber 1 L glass bottles were used for the water samples, to prevent any degradation of hydrocarbons by sunlight. Three locations (Figure 3-3) were sampled around the two ponds to give an indication of the changes that occur as water travels through the two ponds.

- P1 inlet (B)
- P1 outlet (C)
- P2 outlet (D)

Whilst onsite water temperature, pH and conductivity readings were taken using Oakton ECRtestr (calibrated as per manufacturers guidelines, and tested for drift before every sampling event).

3.1.1.2 Field Data Collection- Swale

Sediment samples were collected from along the length of the swale at 20 m intervals from the inlet to the outlet (Figure 3-1 and 3-2), a total of six samples will be collected:

- Inlet
- 20 m
- 40 m
- 60 m
- Outlet
- Control (collected at 40 m at top of bank away from roadside).

Samples were collected using a corer modified from a syringe, Image 3-1. The core collector was inserted into the soil surface, deep enough to collect samples with a depth of at least 5 cm for analysis. Once collected samples were stored in a cool box for transport back to the laboratory.

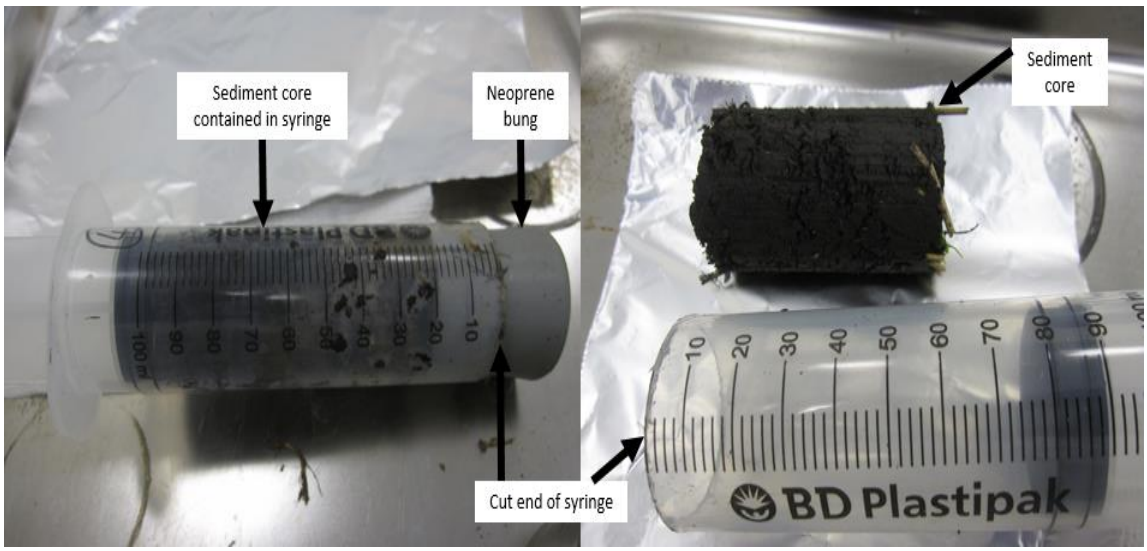

Image 3-1 Sediment corer, adapted from a syringe. Once sample was taken, a neoprene bung was used to create an airtight seal until analysis could be performed.

3.2 Laboratory Analytical Methods

3.2.1 Water hydrocarbon extraction

As stated in 3.1.1.1 in-situ measurements were taken of temperature, conductivity and pH. Once in the laboratory water PAH extraction method followed EPA method 550.1 (2011) using application note 54 from SUPERLCO (Sigma Aldrich) for C18 discs. Summarily this method is the pH of each sample was adjusted to ≤ 2 with 6N hydrochloric acid (HCl), to inhibit any further biological activity. 5ml of methanol was then added to each sample to prevent the hydrocarbons attaching to the surface of the bottle. Dichloromethane (DCM) was used as the extraction solvent. After the final elution stage, the extracted solution was gravity filtered through a 1 g anhydrous sodium sulphate (Na_2SO_4) tube (Bond Elut), to remove any remaining water and collected in clear glass vials. 50 µl of nonane (Fisher Scientific) was added, to act as a barrier and prevent the loss of PAHs through evaporation. The samples were then placed on a heating block set to 40^{o}C and a steady stream on nitrogen (N_2) blown over the surface of the liquid to concentrate the sample down to 1 ml. This final sample was stored in amber GCMS vials in laboratory refrigerators at 2 – 8^{o}C until analysis via Gas Chromatography Mass Spectrometry (GCMS).

3.2.2 Soil hydrocarbon extraction

Soil samples were extracted from the corers and the top 5 cm (surface soil) was used for analysis. The soil was homogenized by hand so the all analysis were representative of this 5 cm surface layer. Each sample was separated for dry weight, organic content (via loss on ignition), and PAH extraction.

3.2.2.1 Soil dry weight and Loss on ignition

Approximately 5 g of sediment (exact weight recorded) was dried in an oven at 105°C overnight and re-weighed, this was to gain the dry weight of the soil. During the drying process, elevated temperatures will cause some PAHs to degrade and be lost from the sample, as such non-dried sediment was used for PAH extraction. The dry weight was then used to allow for moisture weight in the final PAH calculations.

$$\text{Soil water content \%} = \left(\frac{W1-W2}{W1}\right) 100$$

Where
W1 = wet weight of sample.
W2 = dry weight of sample.

The organic content of the soil was also calculated. This was achieved by calculating the loss on ignition (LOI) weight of the soil sample. This was conducted in a muffle furnace (Carbolite). After obtaining the dry weight of the soil samples, they were ground up using a pestle and mortar. Each sample was placed in a pre-weighed ceramic crucible and placed in the muffle furnace and the temperature set to 550°C for four hours (Rocha *et al.*, 2015). Once cooled each sample was reweighed and placed back in the desiccator for twenty minutes and reweighed. If the weight was within 4 % of the initial weight the sample was judged to have stabilized and the weight used. If not the sample was placed in the desiccator for a further 20 minutes and the process repeated until stable. Reduction in weight gives the LOI and indicates the organic content of the sample.

$$\text{\% organic matter} = \left(\frac{W2-W3}{W2-W1}\right) 100$$

Where:
W1 is the weight of the crucible.

W2 is the initial combined crucible + sample weight.

W3 is combined weight after furnace.

3.2.2.2 Soil PAH extraction

An Accelerated Solvent Extractor (ASE200 Dionex), Image 3-2, was used for soil PAH extraction, following Dionex Application note 313 (2011) and EPA Method 3630C. For PAH extraction 3 g of soil was mixed with an equal measure of Hydromatrix (Varian). Hydromatrix was used as a drying agent, removing excess moisture from the soil samples. This was placed in an extraction cell, between two acid washed sand filtration layers. Each layer was separated by cellulose filter papers (Dionex). ASE extraction works by high pressure, high temperature flushing of the samples with solvents following the parameters used for PAH extraction are shown in Table 3-1. The eluted product of the process was stored in amber glass collection vials, and stored in refrigerator at 5 ±3 ^{o}C.

Table 3-1 ASE program parameters used for PAH extraction from sediment samples.

Stage	*Condition*
Solvent used	*Acetone : DCM – 50:50*
Preheat up time	*5 minutes*
Heat time	*5 minutes*
Static time	*5 minutes*
Flush time	*60 %*
Nitrogen purge	*60 seconds*
System pressure	*10.342 MPa*
Oven temperature	*100ºC*
Cycles	*1*
Dionex methods	*Dionex 2011b* *Application note 313*

The eluted solution was then put through a sodium sulphate (Na_2SO_4) drying column, before 50 µl of nonane was added. The sample was then placed in the heating block (40^{o}C) and blown down to 1 ml under a steady stream of nitrogen. A further clean up step was taken by passing the sample through a silica gel column. The column was first conditioned with 4 ml of hexane. Before all the hexane passed onto the gel the 1 ml of sample was added to the column. Just before all the sample filtered onto the gel, 5 ml of hexane:dichloromethane (60:40) was added, this solution eluted the PAH from the silica gel. At this point a clean collection vial was placed under the column to collect the filtered, eluted solution. Once again the solution was blown down to 1ml and transferred to a glass vial suitable for GCMS analysis. PAH levels were determined by the area under the curve to give the PAH in ng/ml this was then converted using the dry soil weight (see 1.2.2.1 for calculation) to gain PAH concentration per dry weight of soil (ng/g).

Image 3-2 Dionex ASE instrument used for PAH extraction from sediment samples. Soil samples were placed in the top carousel, with collection vials on the lower.

3.2.3 Gas Chromatography – Mass Spectrometry

Once the full PAH extraction process was complete the final 1 ml sample, from either water or soil samples, was analysed via GCMS. Each set of samples was run in sequence, using pre-run standards of a PAH mixture from which to set up a calibration curve. Calibration standards were made from PAH Mix 14 (Dr. Ehrenstorfer reference materials). PAHs were quantified by means of a five-point calibration curve using five standards: 100 ng/ml, 250 ng/ml, 500 ng/ml, 750 ng/ml and 1000 ng/ml, along with a blank of hexane. These standards were used as they covered the range of PAH levels expected to be found (Marquès *et al.*, 2017). All analysis was carried out on Agilent Technologies 6890N Network GC system in combination with 5973 Network Mass Selective Detector. Methods determined by a previous PhD student (Roinas, 2015) were used with slight adjustments for timings based on new columns being used in the GCMS. The GC was fitted with a capillary column VF-5ms (30 m x 0.25 mm x 0.25 µm). Limits of Detection (LOD) for the machine were ascertained to determine the lowest level of the PAHs before the results are determined to be background noise. To do this the statistical approach described by Armbruster & Pry (2008) was used. A series of blanks (hexane), were run on the GCMS (n=7). The mean plus 3x the standard deviation give a value below which the results are judged too low to reliably detect. This method was chosen over the empirical approach due to the presence of the target PAHs in the hexane. Table 3-2 shows the LOD used in this study. These levels are within the range determined in method evaluation by Guimarães *et al*. (2013).

Table 3-2 Limit of detection for target PAHs based on a series of blanks (hexane) run to establish the lower detectable limit of said PAHs.

PAH	*Limit of detection (ng/ml)*
Naphthalene	*14.98*
Fluorene	*44.37*
Fluoranthene	*45.23*
Pyrene	*46.31*
Chrysene	*42.41*
Benzo(a)pyrene	*58.33*

GC-MS parameters used for analysis are shown in Table 3-3, and are based on parameters determined by Roinas *et al.,* 2014.

Table 3-3 GC-MS parameters used for PAH analysis of water and sediment samples.

Stage		*Condition*
Ion Trap	*Trap*	*220°C*
	Manifold	*80°C*
	Transfer Line	*300°C*
Column	*Injector*	*280°C*
	Initial temperature 60°C	*Hold for one minute*
	Increase to 150°C	*At 30°C/min*
	Increase to 186°C	*At 6°C/min*
	Increase to 280°C	*At 4°C/min and hold for 20 minutes*

Each target PAH has identifier ions which were used for identification of peaks and retention times. Initial identification was completed using the highest standard (1000 ng/ml), from this a Selected Ion Monitoring (SIM) method was set up to target the selected PAHs for analysis. Table 3-4 shows the identifier ions and retention times of the target PAHs. For each PAH the method was set up to scan a time range that covered the desired time point, which will change slightly after any adjustment or maintenance to the GCMS and integral parts.

Table 3-4 Target PAHs and their characteristic Ion numbers and the retention time.

PAH	*Identifier Ion*	*Retention Time (min)*
Naphthalene	*128*	*5.2*
Fluorene	*165/166*	*9.5*
Fluoranthene	*202*	*17.6*
Pyrene	*202*	*18.7*
Chrysene	*228*	*25.3*
Benzo(a)pyrene	*252*	*32.3*

Results from the GCMS are given in ng/ml. Water samples were converted to ng/L as 1 L of sample was filtered, where less than this was filtered 500 ml was filtered and the results were doubled. For the RRD water, 15 ml was sampled so the results from the

GCMS are equal to ng per 15 ml. For soil PAH levels the following equation was used, to allow for the extra moisture weight to be excluded from the calculation (PAH concentration per dry weigh of soil sample):

$$\frac{x * d}{DW} = S$$

Where:

S is soil PAH concentration (ng /g).

x is value from GCMS (ng / ml).

d is the dilution factor.

DW is the dry weight of soil analysed (g) (see 1.2.2.1 for calculation).

3.3 Swale Mesocosm

3.3.1 Swale Design

In order to accurately assess the potential of swale systems to remove pollutants, a model swale was designed. The swale was built, guided by the dimensions recommended in the CIRIA SuDS manual (Woods-Ballard *et al.,* 2015). Design was based on a hypothetical catchment of a small car park, 4 m x 10 m. Built to these dimensions the swale is 9.8 m in length, 0.6 m wide with a soil depth of 0.3 m after compaction. In cross section the swale has a 0.3 m base and sloping sides of 0.15 m (1 in 3 slope). Longitudinally the slope is 1 in 50, giving a height difference of 0.4 m from inflow to outflow. A base of gravel was spread along the base of the swale structure, to act as a filter and prevent the clogging up of the outflow. Figure 3-4 shows a schematic of the swale dimensions described.

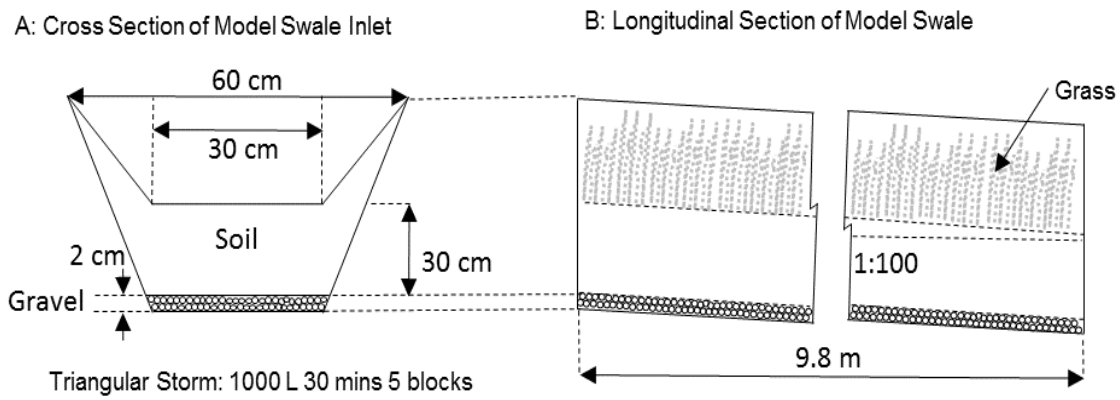

Figure 3-4. Schematic of swale mesocosm dimensions A: cross section, B: longitudinal section showing the slope (1:50) of the swale (not drawn to scale).

3.3.2 Construction of Swale mesocosm

To provide as much control as possible over the inputs onto the swale, it was constructed in a greenhouse located at the University of Portsmouth Environmental Technology Field Station at Petersfield, UK. Unless stated all building materials used were sourced from Wickes UK. The swale was built on 6 support bases, (Image 3-3 A.) made of solid dense blocks (H: 215 mm, L: 440 mm, W: 100 mm). These support columns were used to create the desired elevation change. This was done by reducing the number of blocks in the columns. To support the weight of soil needed to form the swale a strong frame was needed (Image 3-3 B.). Marine plywood sheets were chosen due to their innate strength and resistance to moisture. Panels with a depth of 18 mm, length 2440 mm and width 1220 mm were used. Support beams (2" x 2") of kiln dried wood were used under the base to provide stability and add load bearing strength. Once the frame was constructed it was lined with heavy duty pond liner, before the base was covered with 20 mm gravel pea shingle to create a filter and aid stability of the soil (Image 3-3 C.).

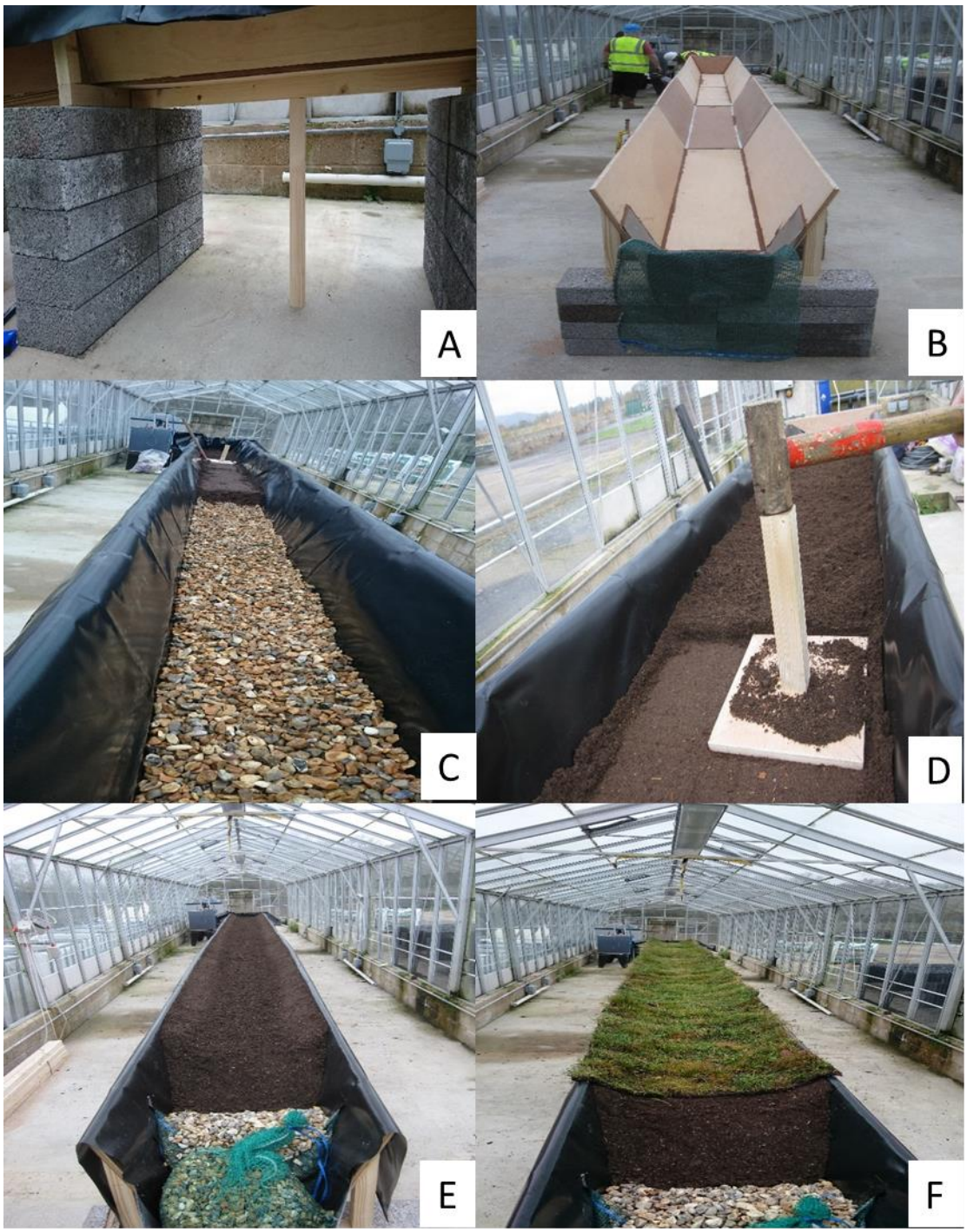

Image 3-3 Swale construction. A. shows the frame support made from marine ply boarding. B. shows the support columns and the external support skeleton around the marine ply. C gravel pea shingle base. D. shows the compaction press and sledgehammer used to compact the soil. E. completed soil profile. F. Wildflower supplied turf along the surface of the compacted soil.

To build the soil up to the required depth, soil was added on top of the gravel layer, to a uniform depth before being compacted down and more soil added, until the desired

depth was reached. For compaction of the soil, a press was made 30 cm x 30cm, and a sledge hammer was used 6 times with equal force, to ensure the compaction was equal along the full length of the swale (Image 3-3 D), this was repeated until the specified depth was achieved. To gain the required profile on the surface a template was constructed from excess marine ply. This profiling tool was then pulled along the surface pushing excess soil down the swale, leaving a smooth profile (Image 3-3 E). Specific SuDS turf was sourced from Wildflower Turf UK, to vegetate the swale (Image 3-3 F). Different species of wildflowers and grasses which make up the turf were chosen specifically because they are shade and drought tolerant, and able to withstand periodic flooding. Cultivated in a unique way, the turf provided is grown up on a mesh base, allowing the turf to be rolled up and shipped soil free. Once on site it is unrolled in the desired location and will quickly establish on the underlying soil.

3.3.2.1 Soil characterisation

Soil used in the swale was top soil sourced from a local supplier (Rolawn Blended Loam Topsoil). The soil was analysed by Particle Size Analyser (PSA) to ascertain the average particle sizes. Table 3-5 shows the percentage of each size particle in the soil, based on average levels in triplicate samples (15 g). Figure 3-5 gives a visual representation of the cumulative particle sizes found in soil samples. Shown on the graph are the 10%, 50% and 90% particle size values. For the swale soil 90% of all the particles were below 1843µm, 50% were below 257µm and 10% were below 10µm.

The soil used to construct the swale is primarily sand based (57%). To establish the organic content of the soil LOI was completed following the method described in section 3.2.2.1, from 28 samples tested, from the length of the swale, an average of 18% organic matter was indicated.

Table 3-5 Particle size analysis of the soil, using Wentworth Scale.

% of each size	*Description*
7.1	*gravel*
22.0	*very coarse sand*
11.5	*coarse sand*
9.0	*medium sand*
14.4	*fine sand*
9.7	*very fine sand*
5.9	*coarse silt*
5.9	*medium silt*
5.4	*fine silt*
4.7	*very fine silt*
3.9	*clay*
99.5	*Total*

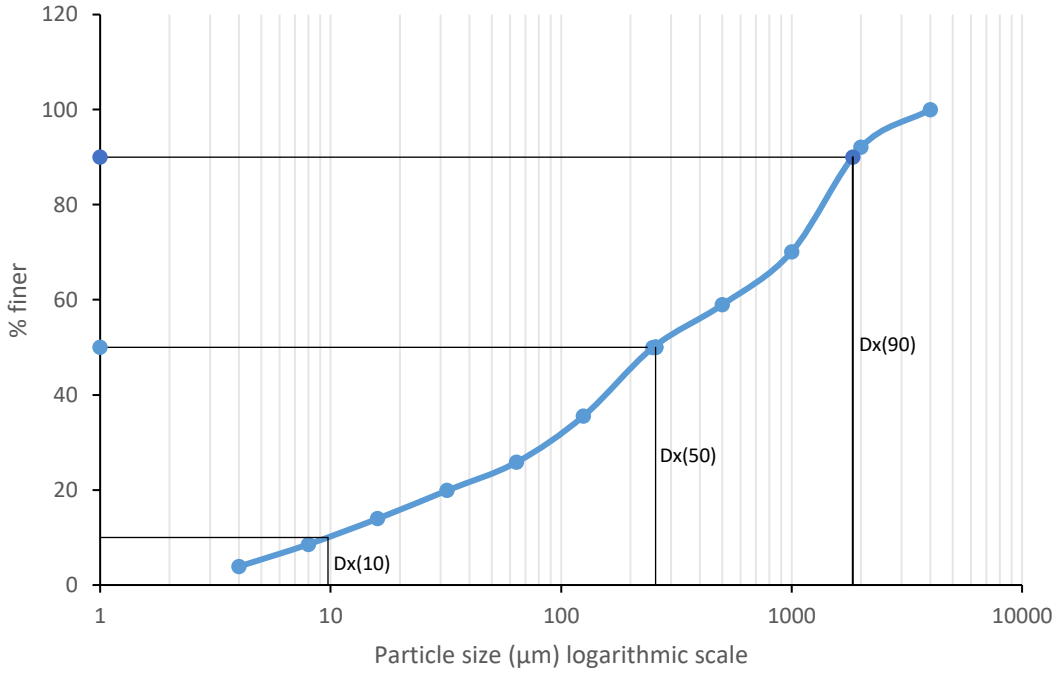

Figure 3-5 Cumulative particle sizes of soil gained via Particle Size analysis. Dx(10), Dx(50) and Dx(90) show the points at which 10, 50 and 90% of particle sizes are smaller.

3.3.3 Hydrological testing of swale mesocosm

UK Building Regulations 2010 Drainage and Waste Disposal (2015 edition) states that for a paved area (including carparks up to 4000 m^2) rainfall intensities of 0.014 L/sec/m^2 may be assumed. For the experiment hypothetical car park this equates to 1008 L in half an hour. To simulate a typical 1 in 5 year storm event that would run off of a 4 m x 10 m car park, 1000 L of tap water was pumped down the model swale over half an hour in a triangular hydrograph. The day before each test run an Intermediate Bulk Container (IBC) was filled with standard tap water. Repeatable storm flows were planned to allow comparisons between events. Although natural storms are highly variable, it was decided to limit the flows to repeatable levels as the actual flow itself was not the concern, the fate of the pollutants in the flow was the primary consideration.

Image 3-4 shows the inlet and outlet arrangement for the swale mesocosm. In A and B the delivery pumps are shown. A shows the IBC connected with a large flexible pipe to the pump, the water then pumped onto the swale at a rate controlled by the pump. B shows the set up for the addition of the pollutant. C shows a side view of the inflow set up. Water and pollutant will mix in the curve of the pipe as it flows through onto the swale. D shows the plan view of the two delivery pipes, the larger is the water pipe and the smaller is the pollutant tubing. The pipes are fixed into the bung at the top of the drainpipe, at a level the means the two stream of liquid mix as the hit the drainpipe. E shows the outflow of the swale mesocosm.

Image 3-4 Inflow and outflow set up on the swale mesocosm. A shows the water storage and pump used to draw water from the IBC and pump it onto the swale. B shows the system set up for keeping the polluted particulates suspended in liquid and the pump used to deliver onto the swale. C and D show the side and plan view of the water inflow. E shows the outflow system, where water drains from the swale.

Flow over the half hour had two increases in flow rate and two decreases, to mimic a storm event, shown in Figure 3-6. The pump from a F1-10 basic hydraulics bench was used to pump the water onto the swale.

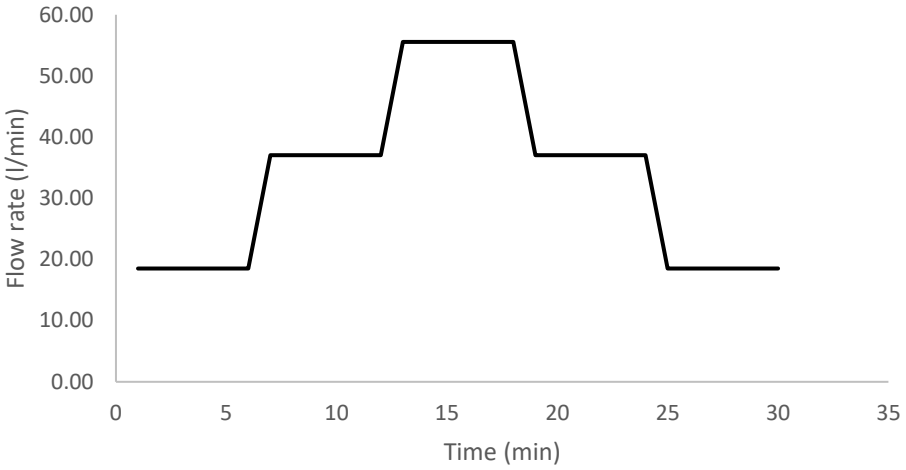

Figure 3-6. Experimental designed flow rates to produce a triangular hydrograph over half an hour.

Therefore the half hour was divided into five sections with the flow increase / decrease every six minutes. At the first increase the flow was double that of the first, the third flow was three times that of the first. By decreasing the flow in reverse, the tailing off of a storm event was created. Essentially this was nine blocks of a set amount of water to be pumped over the half hour.

The theoretical amount of water to be received by the swale for each block was worked out with the following equation:

$$W1 = \frac{T}{9}$$

Where:
W1 is Total water (L) pumped in the first six minutes
T is the total amount of water (L) in the IBC

For the second time step W1 was multiplied by 2, and for the third step W1 was multiplied by three. For the corresponding flow rate per minute, the pumped volume of water was divided by six. Table 3-6 gives the volume of water to be pumped over the swale for each time step and associated flow rate.

Table 3-6 Flow rates and water volume to be pumped over the swale during half hour storm events.

Time step (mins)	*Volume of water (L)*	*Flow rate (L / min)*
0 – 6	*111*	*18.5*
6 -12	*222*	*37*
12 - 18	*333*	*55.5*
18 -24	*222*	*37*
24 - 30	*111*	*18.5*

Trials with the pump gave very close flow rates to this, readings were taken each run to assess the flow for each storm event. This was to allow for the fact that the pump had a screw valve to change the flow which was not 100% accurate and consistent.

Ten test runs were completed to ascertain the reliability of the swale performance hydraulically compared to estimate of flow described above. Testing was done in triplicate at each time point at both the inflow and outflow. During these runs the flow rates were assessed by determining how quickly a set volume of water was collected. For inflow this was always 5 L, for the outflow the measured volume depended on the flow rate and varied from 0.5 L to 5 L. Results of the ten trial runs are shown in Table 5.1 in Chapter 5 Swale mesocosm trial runs – results.

In flow readings were taken every three minutes to ensure that each step point had two sets. Outflow readings were initially taken close together, three minutes apart, but after the flow decreased readings were taken at greater intervals. Flow rate at each time point was calculated as:

$$F = V/A$$

Where
F = flow rate (L/sec)
V = volume of water collected (L)
A = average time to fill set volume (sec)

During every run, the overland / surface flow was also recorded. This was to gain an understanding of how quickly the water could infiltrate the soil. Repeatable storm flows were chosen so that comparisons could be made between the different storm events.

3.3.4 Simulated runoff particulates

Road runoff dust (RRD) was simulated based on research findings of average particulate amounts and sizes (Table 2-6 and 2-7). Based on the average TSS in previous research there is variation in quantity, for this study an average of those papers cited in Table 2-6 was used. This gave an average of 166.1 mg/L of particulates in road runoff (Table 2-6). During each storm event the pollutant dosed RRD was added during the first 15 minutes. Adding pollutant to first 500 L of water equates to 83,050 mg of RRD to be added (166.1 mg x 500 L), this is 83.05 g added over 15 minutes.

Fresh RRD was created for each storm run, 120 g consisting of the appropriate particle ratios was weighed out. The extra weight was to allow for testing to be carried out for each run to determine the levels of pollutant added to the swale. Fraction size ratios taken from average levels documented in literature review (Table 2-6) are shown in Table 3-7. Average levels were chosen due to the variation in levels indicated in previous research.

Table 3-7 Road runoff particulate fraction size ratios and amount of each fraction for 120 g of RRD.

Fraction size	*% of particulates*	*g per 120 g RRD*
< 63 µm	*80*	*96*
63 – 150 µm	*14*	*16.8*
150 – 425 µm	*6*	*7.2*

To achieve the desired fraction size ratios, soil from the same source as the swale base was dried and ground down to its constituent particles. This dried soil was then separated into the various fraction sizes using sieves of appropriate sizes (Endecotts stainless steel sieves). Soil was chosen as opposed to street dust as it was less likely to have pollutant loading which may affect the experimental data.

3.3.5 Creating Simulated Road Runoff Dust dosed with PAH pollutants.

To create the simulated RRD tests small jar tests were carried out initial using diesel fuel as the polluting agent. Test results showed low levels of only some of the target PAHs in the soil samples, so extra tests using creosote were carried out (Bartoline 100% Coal Tar Creosote). On testing, this contained all the PAHs being assessed at higher concentrations than the diesel. This enabled a lower volume to be used when dosing the RRD. Soil contaminated with coal tar, has previously been shown to have high PAH levels (Lors *et al.*, 2012). Previous studies have used a variety of dosing agents from isolated individual PAH standards (e.g. Agrawal & Shahi, 2017; Chen *et al.*, 2015; Leroy *et al*., 2015) to diesel fuel (e.g. Serrano *et al*., 2008).

The PAH levels needed to be detectable, so an increase on average background environmental levels was used. The background level was determined via a study on a local swale receiving runoff from a commuter road, Waterlooville, Hampshire, and averages reported by previous studies, including a previous study of the Waterlooville site (Table 3-8). As one of the PAHs of most concern, B(a)P is often found in the lowest concentration, pollution levels used on the swale needed to be high enough to detect, so as to enable assessment of the reduction along the length.

Table 3-8 PAH levels from previous research used to determine experimental levels.

PAH	*Field study Waterlooville (ng/g)*	*Kim & Young 2009 (ng/g)*	*Smith et al. 1995 (ng/g)*	*Water-looville (ng/g)*	*Dobbins et al. 2006 (ng/g)*	*Leroy et al. 2015 background levels (ng/g)*	*Mean Levels (ng/g)*	*Standard Deviation (ng/g)*
NAP	*2403*	*22*	*27*	*66*	*600*	*5*	*521*	*950*
FLU	*115*	*2*	*28*	*60*	*52*	*3*	*43*	*43*
PYR	*721*	*61*	*254*	*62*	*64*	*41*	*201*	*267*
CHR	*501*	*46*	*149*	*63*	*-*	*38*	*159*	*196*
BaP	*668*	*37*	*149*	*170*	*-*	*33*	*211*	*263*

Test runs of 1 ml creosote with 3 g of soil, using both water and acetone as the mixing liquid were completed to determine the best delivery. Table 3-9 shows the results of the target PAH's for the test runs. Shown in the table is the ng /g PAH from creosote and also the percent of the PAH that adhered to the soil (from readings from the beaker liquid before mixing). Based on these results it was determined that acetone is the best mixing solution. Acetone also evaporates quickly, which will leave dry soil to be added onto the swale in the pollution phase.

Table 3-9 Results of test runs to determine the most effective solution to ensure maximum pollution on soil particles.

PAH	*Water*		*Acetone*	
	soil ng / g	*% on soil*	*soil ng / g*	*% on soil*
NAP	*15,528*	*4*	*132,277*	*24*
Fluorene	*90,577*	*6*	*1,048,333*	*24*
PYR	*154,637*	*5*	*2,070,527*	*23*
CHR	*27,566*	*2*	*274,010*	*9*
B(a)P	*56*	*2*	*3,597*	*17*

Using the values from Table 3-10, the level of creosote needed to dose the swale and achieve a detectable level of pollution in 1/3 of the soil. First the target concentration needed to be established:

$$T = (RRD/\left(\frac{(l * w * d)b}{3}\right))P$$

Where
T is the target concentration (ng / g)
L is the length of the swale (cm)
W is the width of the swale base (cm)
D is the depth of the soil (cm)
B is the bulk density of soil (sandy soil) to get the weight of soil in the volume)
RRD is the amount of RRD added in the storm run (g)
P is the pollution level on 1 g of soil (ng / g)

Example calculation:

$$T = \left(83/\left(\frac{(976 * 20 * 30)1.3}{3}\right)\right)1048333$$

- The volume of soil is 585600 cm^3.
- There is 761280 g of soil in the swale, therefore 253760 g in 1/3 of the swale.
- In each run 83 g of contaminated soil (RRD) will be added (based on average levels in road runoff).
- 83 g over 253760 g of clean soil = 83/195200 = 3.3 x 10^{-4}
- There was 1048333 ng/g fluorene in contaminated sediment.
- Therefore (3.3 x 10^{-4}) x 1048333 = 343 ng/g target concentration

Using 1 ml of creosote to dose 3 g of soil, a target of 343 ng / g of fluorene visible in 1/3 of the swale is returned. This value is 3.5 x environmental levels found in the Waterlooville swale study conducted in 2015-2016. As realistic background levels, this was used to ensure detectable levels from the first experiment.

Tests to determine the levels needed were conducted using 1 ml of creosote on 3 g of soil. For the full experimental run 120 g of RRD will be dosed, therefore 40 ml of creosote was be used to dose the RRD, using acetone to suspend the particles to ensure maximum adhesion. Tests showed that with this volume of RRD, it was difficult to keep the particulates in suspension, so the RRD was divided into four beakers, 30 g in each. Table

3-7 gives the volumes of each fraction size used. Once the synthetic RRD was created, the desired weights were placed into a glass beaker and 200 ml of acetone added. Using a magnetic stirrer the particles were fully suspended in the liquid and 10 ml of creosote added. For one minute this mixture was stirred at high speed before reducing to a lower speed that kept the particulates in full suspension for twenty minutes. This allowed the creosote time to adhere to the surface of the particulates. After the twenty minutes, the beaker was removed from the stirrer and completely covered with tin foil to prevent photodegradation of the PAH in the creosote. Air holes were pierced on the top cover to allow for the acetone to evaporate. Four beakers were dosed and left for 72 hours, in a fume cupboard to allow complete evaporation of the acetone, leaving the required amount of RRD ready for use. A sample from each beaker was collected for analysis of PAH levels, and placed in the freezer until extraction and analysis could be undertaken. After this the RRD from all four beakers was combined, mixed by hand, wrapped in foil and stored in a refrigerator overnight until the trial run. Fresh RRD was created for each trial run.

Table 3-10 shows the PAH values gained from RRD before being put in the beakers for the experimental runs. By their very nature PAHs are volatile and will breakdown over time. These values are from the RRD before it was mixed in water for sending down the swale. Results from each run (Table 3-10) show that there was variation in pollutant concentrations. RRD from trial run 3 had some very high levels, including some extremely high outliers. There were a number of areas in which an error could occur: equipment, materials, time between dosing and analysis and human error. Investigations of equipment and rerunning samples on the GCMS showed that the results here were consistent. This suggests the error most likely occurred via human error and adding of the creosote to the acetone. A reasonable explanation is that an extra dose of creosote was added in error. While for some PAHs there is good correlation in pollutant levels on the particulates between runs (e.g. NAP and BaP) for others there was variation across the ten trial runs. However, this was not detected at the time due to delays in sample analysis. Once the RRD samples had been collected they were frozen due to equipment failures, initially the ASE for the extraction and then the GCMS which meant that the samples were initially frozen for 3 – 6 months before analysis could

begin. Samples were also moved between laboratories during the extraction process due to necessary equipment being in different buildings. The extraction process for each sample took a minimum of two days due to the cycle time of the ASE and the clean-up steps necessary. The clean-up steps used gravity filtration which took longer for some samples than others. A maximum of 12 samples could go through the extraction process at a time due to space constraints. While every effort to maintain dosing techniques between each run, it is apparent from these results that it was not as effective as hoped. This is discussed in Chapter 4.

Table 3-10 Soil dosing PAH levels µg/g for each experimental run. Samples taken from dosed soil before suspension in water for transport onto swale.

Run	*Total NAP (µg/g)*	*Total FLU (µg/g)*	*Total FLAN (µg/g)*	*Total PYR (µg/g)*	*Total CHR (µg/g)*	*Total BaP (µg/g)*
1	*44*	*243*	*823*	*484*	*12*	*2*
2	*314*	*2,909*	*11,506*	*6,642*	*681*	*9*
3	*243*	*5,694*	*34,266*	*61,531*	*28,489*	*37*
4	*260*	*5,437*	*23,534*	*14,839*	*1,977*	*38*
5	*311*	*5,803*	*17,515*	*10,650*	*8,788*	*16*
6	*251*	*5,163*	*13,375*	*7,852*	*1,062*	*16*
7	*189*	*3,609*	*9,471*	*5,539*	*483*	*18*
8	*162*	*1,217*	*2,909*	*2,028*	*170*	*32*
9	*150*	*1,376*	*384*	*1,486*	*799*	*22*
10	*203*	*197*	*493*	*320*	*316*	*35*

3.3.6 Simulated storm run pollutant addition

Over 15 minutes, 83 g of polluted RRD suspended in 2.4 L of tap water to be pumped onto the swale. Using a peristaltic pump (Millipore Easy-load Masterflex) a set flow rate of 140 ml/min was set up (Figure 3-7), which assuming even dispersal of particles in the water column would pump 5.6 g of RRD in a minute. Tygon tubing was used as to deliver the polluted RRD. This provided a gradually diluting level of pollutants over 15 minutes as the water flow was increased to simulate the first flush effect, seen in the natural environment (Roinas *et al.,* 2014). Due to the construction of the inflow pipe the water and polluted water mixed as it flowed through the pipe and onto the swale.

To prevent clogging of the tubing before it reached the inlet pipe, the polluted RRD was separated into smaller quantities. Three beakers had 32 g of RRD added to 800 ml of tap water. A buffer of 100 ml and 4 g of RRD was included in each beaker to allow for full suspension of particles and allow for the full 700 ml with 83 g of RRD to be pumped onto the swale. Each beaker was run for five minutes, and then switched for the next beaker. A magnetic stirrer in each beaker was used to keep the RRD in complete suspension.

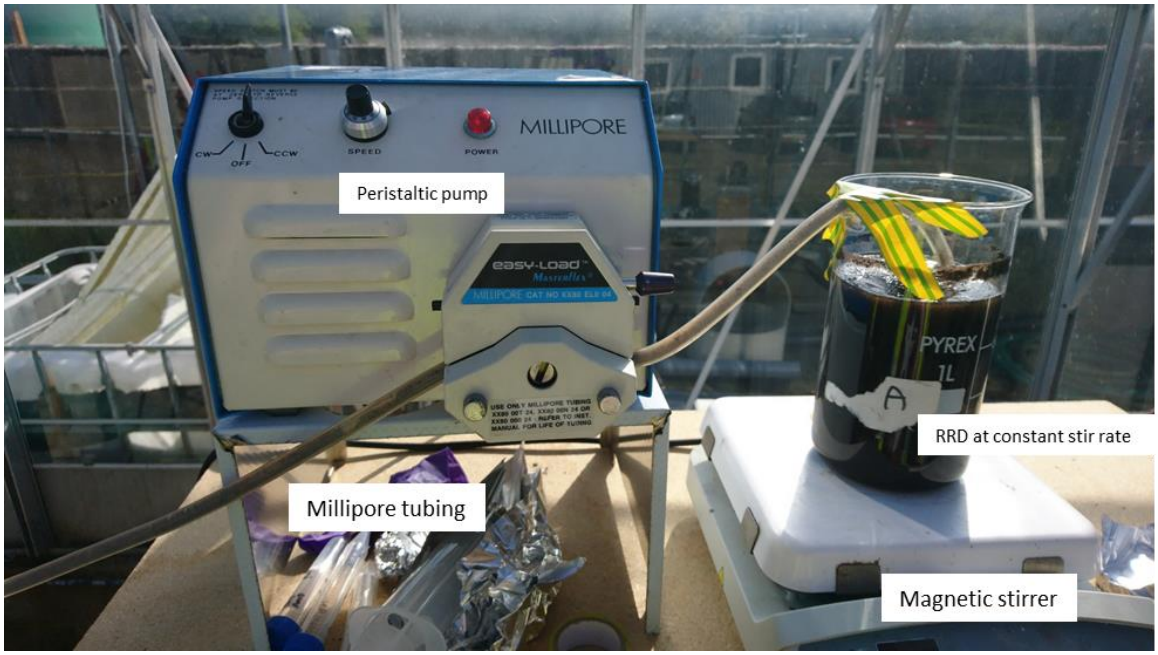

Figure 3-7 Equipment set up for adding polluted simulated road runoff dust to the inflowing water.

3.3.7 Swale experiment sampling

3.3.7.1 Water

Samples of the RRD water was taken, while the RRD was in full suspension. This was to give an indication of the pollution added in the storm event. Three samples of 1 L were also collected from the IBC to measure the ambient PAHs in the tap water. Water samples were also taken from the inflow, directly as the water came out of the pipe, and from the outflow. All samples from the inflow and out flow were taken at the same time points each run, except the first flush sample which was expected to vary depending on the water residence time in the swale.

In total, fourteen samples were taken during each storm run:

- 3 x RRD beakers .

- 3 x IBC.
- Inflow samples at 2, 9 and 17 minutes after experiment start.
- Outflow samples at first outflow, 23, 30, 60 and 90 minutes after experiment start.

Due to the nature of the sampling at specific time points it was not possible to take these samples in triplicate except for the IBC. Inflow sampling time points were set after the pump flow rate changes, to allow study of the dilution effect of the pollutants in the water. The first two outflow sampling time points were selected based on the very first out flow time (this varied slightly each run, but was always within a short time frame) and the average peak outflow rate from pre-trial testing. The 30, 60 and 90 minute samples were chosen based on the slowing flow rates determined in pre-trial testing. Thirty minutes was the end of the inflowing water, and 90 minutes was when there was very low volume of water exiting the swale. After this point there was low volume of water exiting the swale. These were informed from the original hydrology tests, which showed the distinct step levels for the inflow, and for the out flow when to expect outflow to start and when to expect peak outflow and how quickly it would tail off.

3.3.7.2 Soil

Twenty four hours after the experiment run, soil samples were collected from the swale. This allowed for full infiltration any excess water to filter through the swale. Samples were collected from five locations along the swale: 1 m, 2 m, 3 m, 5 m and 8 m. To achieve random sampling, a 40 cm x 40 cm quadrat, Image 3-5, was constructed with two cm square grid lines, and a random coordinate generator was used to select the coordinates the core sample would be taken (Appendix shows the locations used). For every run, new coordinates were generated for each

The quadrat was placed at each sampling point so that the potential collection zone was +/- 20 cm around the meter mark. Cores were taken using 2 cm tubing, with the side partially cut out to allow for sample removal (Image 3-6). With the quadrat in place the corer was pushed vertically down through the soil until the drainage gravel was felt. The corer was then removed and taken into the laboratory to extract the soil core. The holes in the swale were refilled with soil from the original source stockpile.

Once extracted the core was separated into layers for analysis:

- 0 – 5 cm,
- 5 – 10 cm,
- 10 – 15 cm,

Each sample was wrapped in tin foil, labelled and once all samples collected placed in the freezer until PAH extraction could be performed.

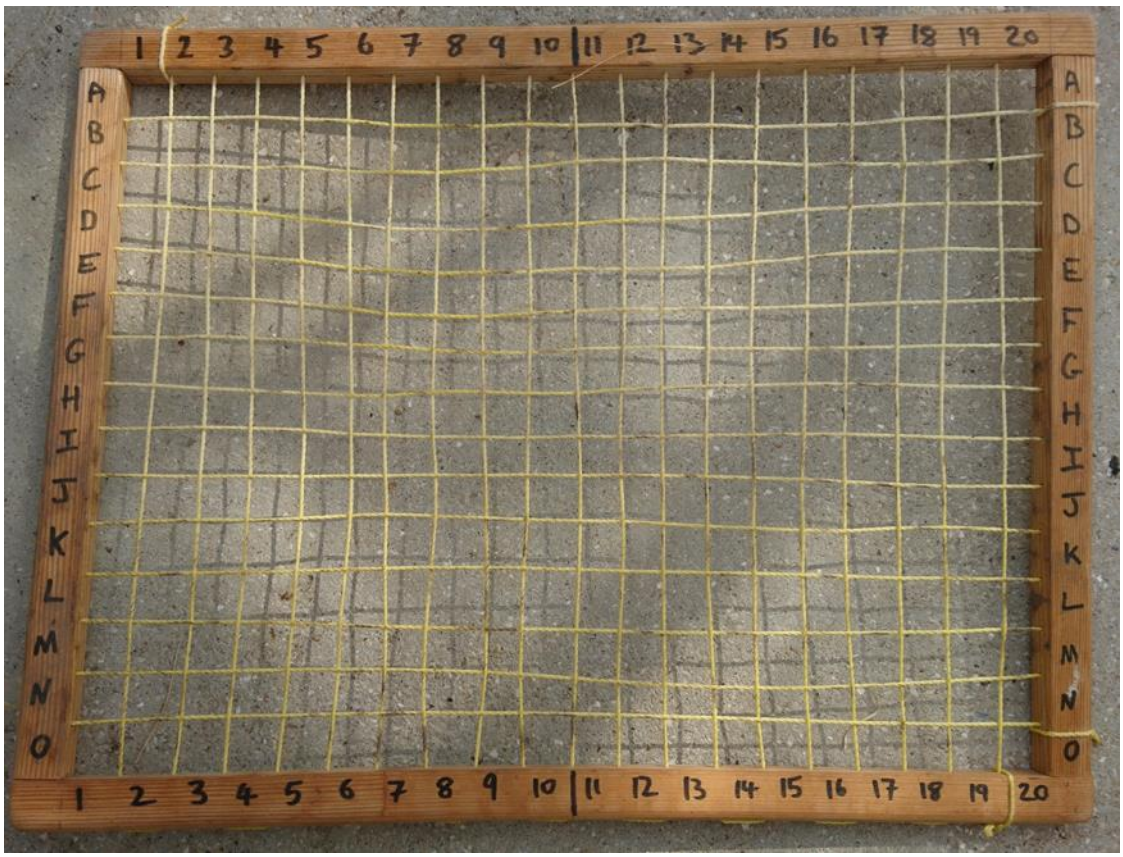

Image 3-5 Quadrat constructed to position on swale for core extraction locations.

Image 3-6 Example of extracted cores from swale.

Once collected samples were analysed following the methods described in section 1.2. Soil samples were kept frozen until analysis could be performed to reduce the degradation of the PAHs present. Soil moisture content for all samples was ascertained as described in above. Figure 3-8 shows the average moisture content (%) of soil samples from both the 0 – 5 cm layer and the 5 – 10 cm layer, taken from all ten trial runs. For the majority of cases there was no significant difference in moisture content between the layers (Table 0.3 in Appendix shows the full analysis). However for six of the ten runs there was a significant decrease in moisture content at the 1 m sampling location (trial runs 2, 3, 4, 5, 8 and 10). Figure 3-9 shows soil moisture levels from Trial run 5. This potentially indicates that the storm water is not filtering vertically down through the soil. Other significant decreases were seen at 2 m for trial run 1, 5 m for trial run 5 and at 8 m for trial runs 7, 8 and 10. For the 8 m sampling location, this decrease might have been expected due to the surface flow only reaching past the 8 m mark for a very short period of time, before it receded back towards the beginning of the swale, as shown in Results Figure 5-5. When comparing locations on each individual run, there were no significant changes in moisture level.

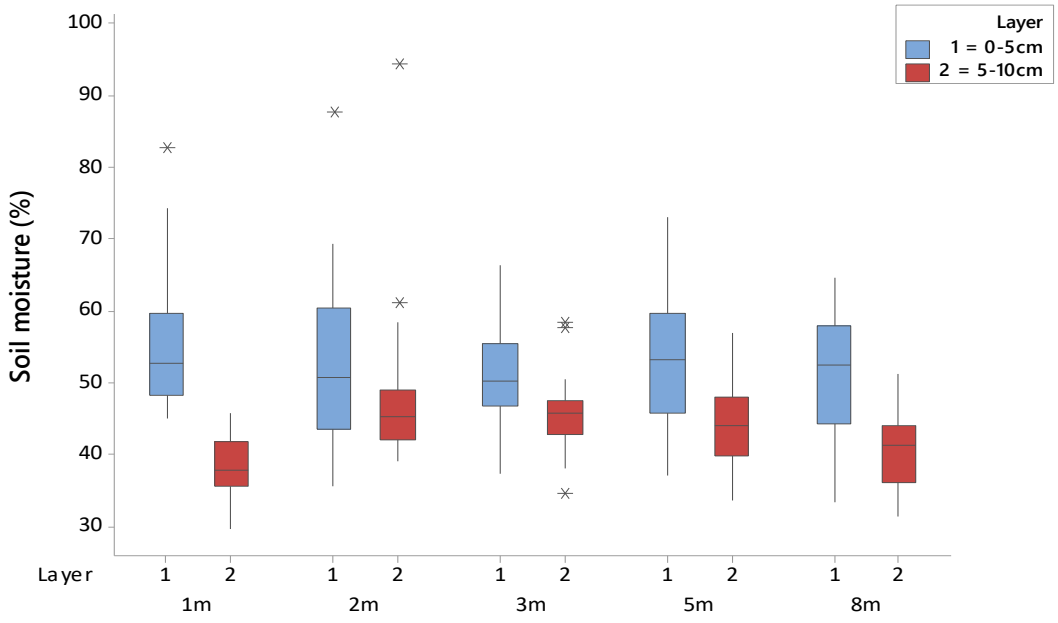

*Figure 3-8 Soil moisture levels (%) taken from results of all ten trial runs. Boxes show the median and 75 percentile and the whiskers show the 95 % confidence limits, * denote the outliers.*

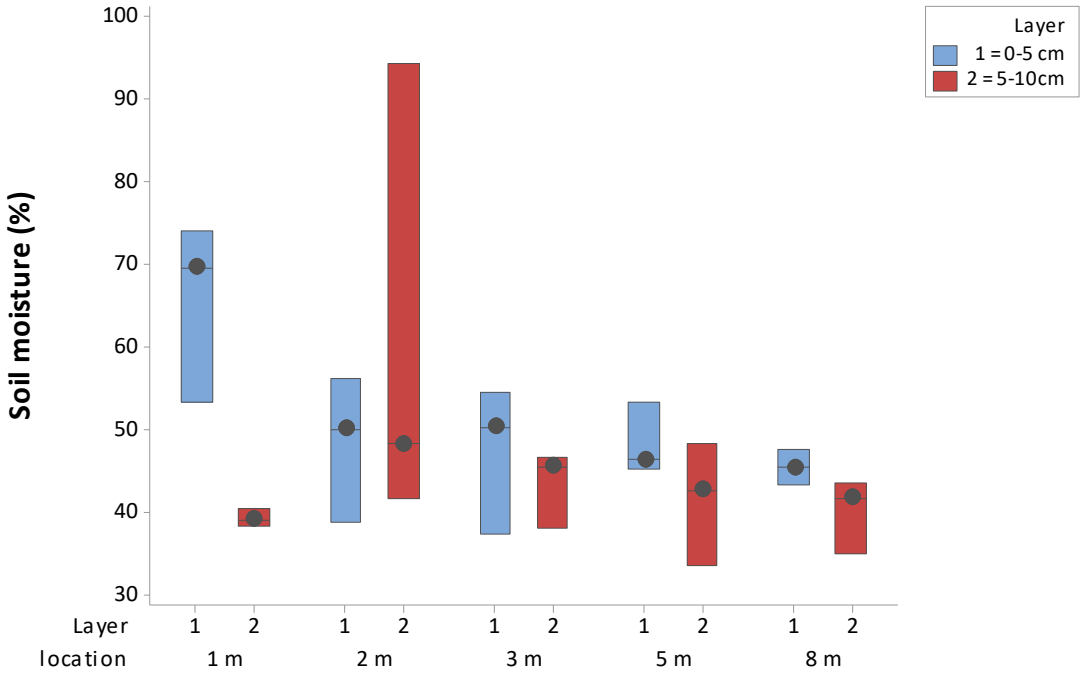

Figure 3-9 soil moisture levels (%) taken after Trial Run 5.soil layers 0-5 cm and 5-10 cm are shown. Boxes show the median and 75 percentile limits.

3.4 Statistical analysis

Data analysis for such a large data set was complex, requiring a number of analysis to be performed. The software that was chosen for the analysis was Minitab. Minitab enables the identification of p values and rejecting the null hypothesis when it is true. The p values are given for hypothesis testing at 0.05 significance level (Minitab, 2009). Microsoft Excel was also utilised for data collation and some graphical representations. Data was tested for normality (Anderson-Darling summary) and where data was of normal distribution the standard analysis of variance, ANOVA tests, were performed to test relationships between groups of data, with Tukey analysis to show where differences occurred in the data sets. Where data was not normally distributed if feasible it was transformed to Log_{10} to determine if this gave a better approximation of normality. Environment studies, such as those with storm water runoff, cannot always be normalised and so analysis should be performed taking this into account. In these

instances non-parametric testing, such as Kruskal-Wallis tests was performed. To assess the relationship between PAHs Minitab cluster observations were utilised. Data was analysed for significant differences in PAH concentrations between sampling locations and soil depth for the same runs, and also differences between runs. Correlations were completed to determine relationships between different variables (Spearman Rho correlations) such as. Outliers in the data were investigated using graphical summary plots to identify those which may introduce errors into the analysis (Barnett, 2004). Due to the nature of the study, the outliers were included in analysis as they are based on environmental data and therefore expected to be demonstrated. However there were some extreme outliers where concentrations were so high that they were excluded for clarity in the graphical interpretations. These are detailed in the results section.

4 Results and Discussion: Waterlooville Field study

This chapter will report and discuss the results gained from a 15 month study of the swale/pond SuDS system in Waterlooville. Peaks in pollutant levels were seen during the winter months, especially January. In a study of the same swale system, previous findings showed similar seasonal patterns (Roinas *et al.*, 2014). Levels gained from the swale were used to inform levels of PAHs to dose the model swale system.

4.1 Swale analysis

4.1.1 Soil organic content

Figure 4-1 shows the organic content of samples taken from the swale over five consecutive months. The swale had a variety of vegetation along the base and side slopes of the swale, leading up to short grass at the top of the slopes. The control sample was taken in this grassed area. June, July and August could be considered the growing season in the UK, when temperatures are generally conducive to plant growth. As seen in Figure 4-1 the lowest organic content was in the control samples, this is consistent with the local vegetation levels. The highest level was seen in the outlet sample for July. Samples from 20 m and 60 m were most consistent with little variation.

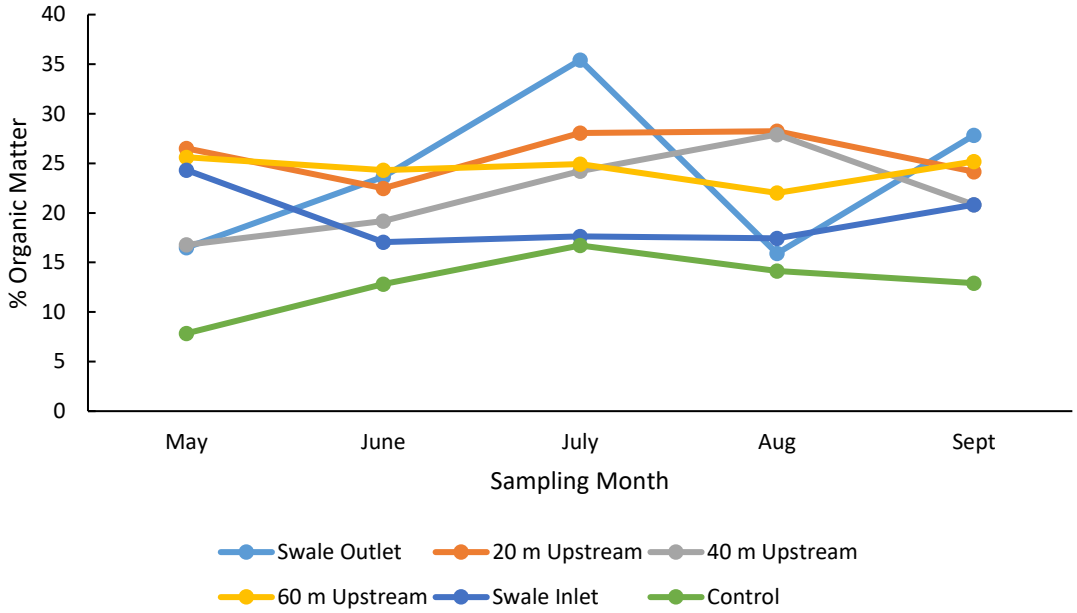

Figure 4-1 Organic matter content of soil samples taken along the length of Waterlooville swale.

4.1.2 Soil PAH

Results from the swale analysis show that over the 14 months samples an increase in Nap and FLU concentrations was seen. These increases were seen over the over the course of the observation time, when comparing the first samples to the last taken. NAP is present in the environment in high levels which may explain why it is present in higher levels to the other PAHs (de Boer & Wagelmans, 2016).

Figure 4-2 shows the concentrations for the PAHs, transformed to Log_{10}, at each sampling location for the cumulative 15 month trial period. Levels of PAHs in the swale over the 15 months showed a pattern of increase between inlet and 20m sample site, then a decrease in concentration with distance towards the outlet. Samples at the 20 m location were on average the highest, with levels at the outlet the lowest. Appendix table 8.1 has full data set for all samples. Nap had the largest concentrations, which corroborates previous research (Roinas *et al,* 2014) at the site.

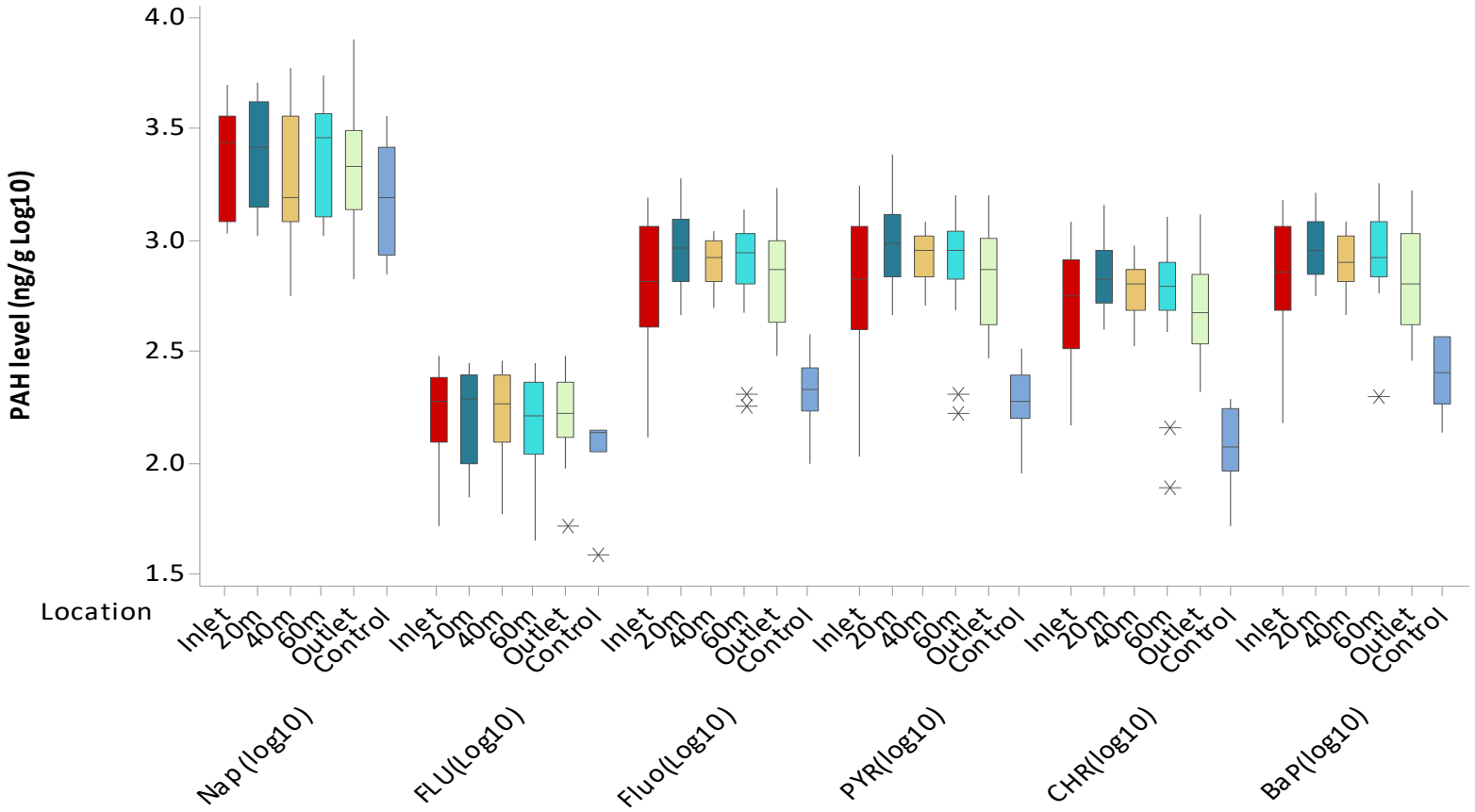

*Figure 4-2 PAH concentrations from 15 monthly samples from Waterlooville swale study site. Data converted to Log_{10} to provide clarity between the high levels seen for NAP and the lower values for other PAHs. Boxes show the median and 75 percentile and the whiskers show the 95 % confidence limits, * denote outliers.*

Naphthalene in all locations showed a general increase in concentration accumulation over the fifteen months of sampling, Figure 4-3. On average the control sample had the lowest concentration, and the 60 m sampling location had the highest. The inlet and outlet samples had very similar levels to each other, both being lower on average than the mid swale samples. ANOVA analysis showed that there was no significant difference in NAP concentration between locations (f = 0.85, P = 0.516). When comparing the levels between the monthly samples a significant difference was gained (F = 11.32, P = 0.000). Tukey analysis showed this to be from big peaks in October 2015 and January 2016. January average NAP concentration was higher than all other months. September 2015 through to May 2016, with the exception of November 2015, were all similar to each other. Figure 4-3 shows the NAP concentrations over the period of study.

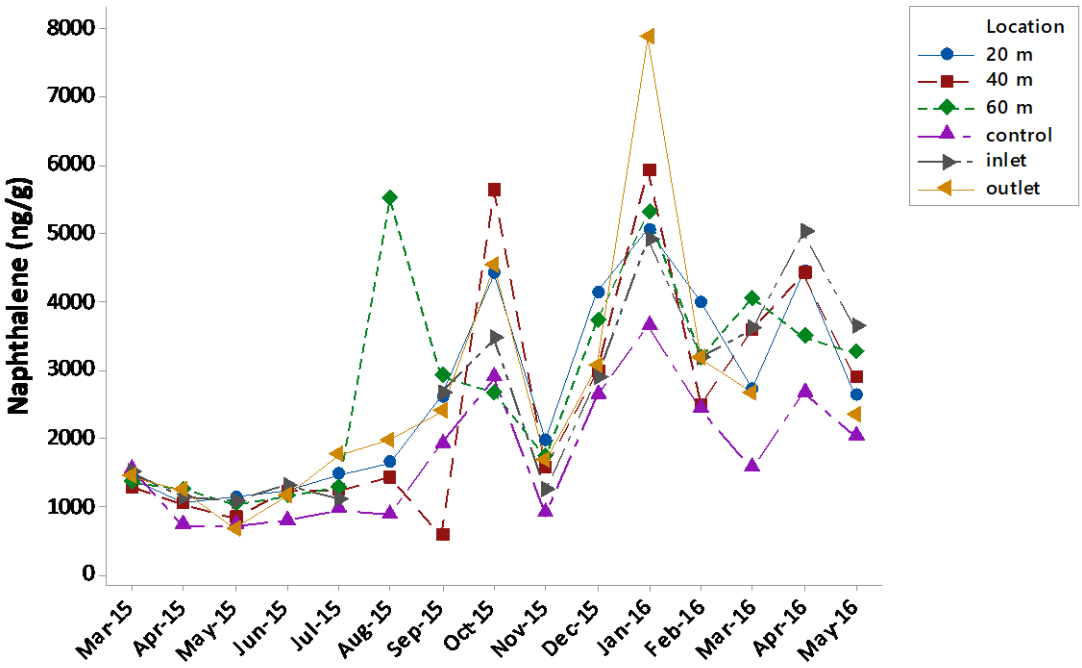

Figure 4-3 Naphthalene concentrations (ng/g) in Waterlooville swale over a 15 month period.

NAP had the highest concentrations in all locations, including the control (Figure 4-2 and 4-3), which indicates that a high influx of this PAH could be from air deposition rather than movement through the swale. Zehetner *et al.* (2009) showed that roadside PAH

levels were often influenced by airborne particulates. The physio-chemical composition of NAP means it is one of the most prevalent in the atmosphere, its low temperature of condensation (volatility) means it is more likely to return to its gaseous state (Sims *et al.*, 1990). Smith *et al.*, (1995) suggested that the atmospheric deposition was the dominant source of PAHs in soils. Given the proximity to the busy commuter road, and the levels of NAP in the control samples being similar to those found in the swale bed, it is possible that atmospheric deposition is responsible for the majority of the NAP in the samples. In a previous study of the site, similar patterns of NAP consistency throughout the swale were reported (Roinas *et al.*, 2014). While NAP is the weakest of all the PAHs, and the one most likely to pass between phases, it is also the highest produced (Jia & Batterman, 2010). In a study of pollution in agricultural land, Zerrouki *et al*. (2017) showed that the NAP was of road surface origin. Zerrouki *et al*. (2017) suggest that the high levels of NAP in the fuel of road vehicles give a rise of 10% of secondary organic aerosols (SOAs).

When a correlation matrix was performed NAP and FLU showed high association (Spearman rho 0.737, P-value 0.000) and also a positive correlation with time (Spearman rho 0.654, P-value 0.000, and Spearman rho 0.562, p-value 0.000 respectively). These two PAHs showed similar patterns of accumulation and loss over the study period. The other PAHs had similar pattern of a slight decrease in concentration over time when comparing the first monthly samples to the final samples, evidenced by negative spearman rho correlations, see Appendix table 8.2 for full results.

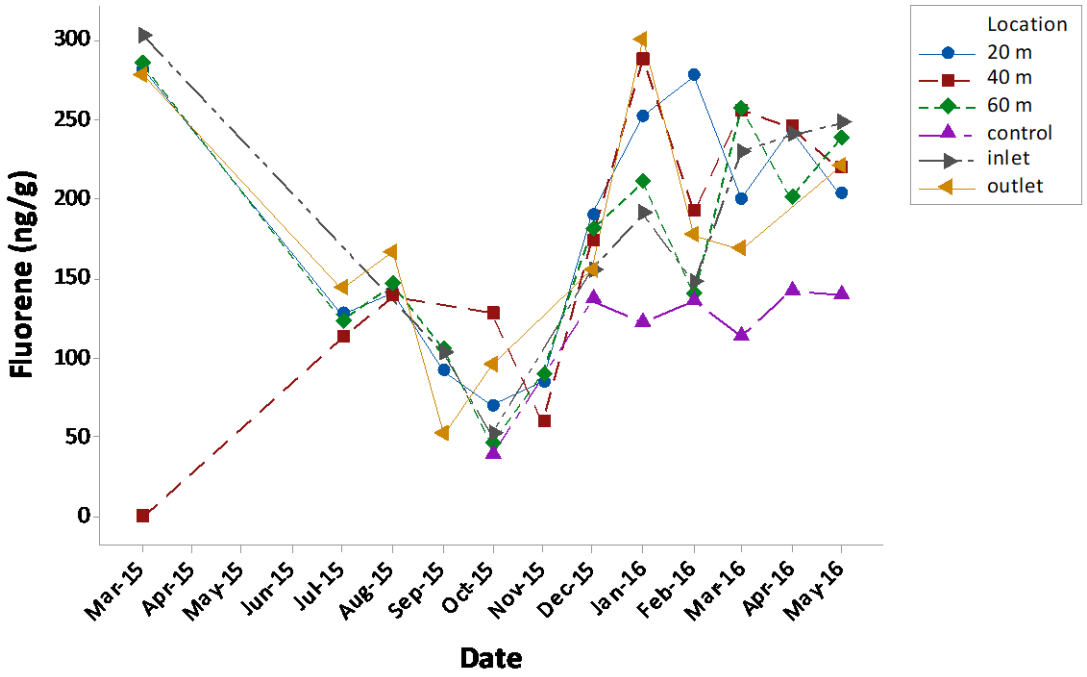

Figure 4-4 Fluorene concentrations (ng/g) in Waterlooville swale over a 15 month period.

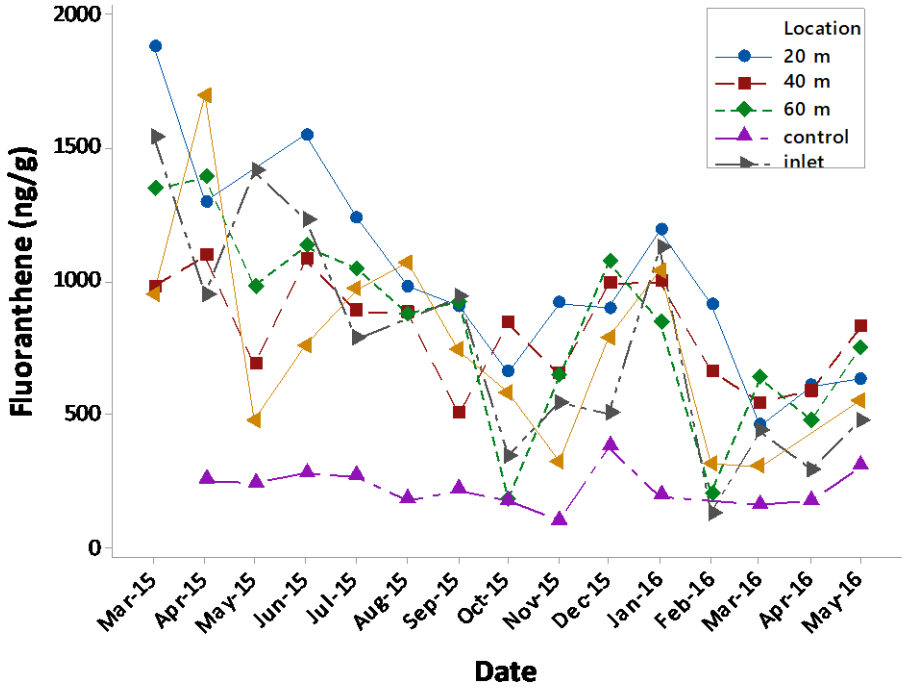

Figure 4-5 Fluoranthene concentrations (ng/g) in Waterlooville swale over a 15 month period.

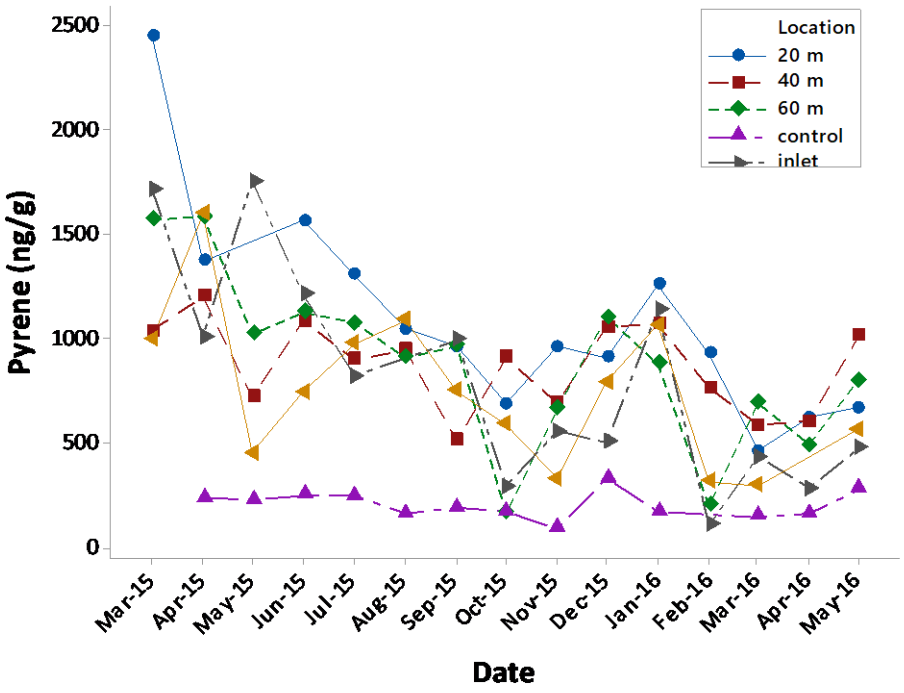

Figure 4-6 Pyrene concentrations (ng/g) in Waterlooville swale over a 15 month period.

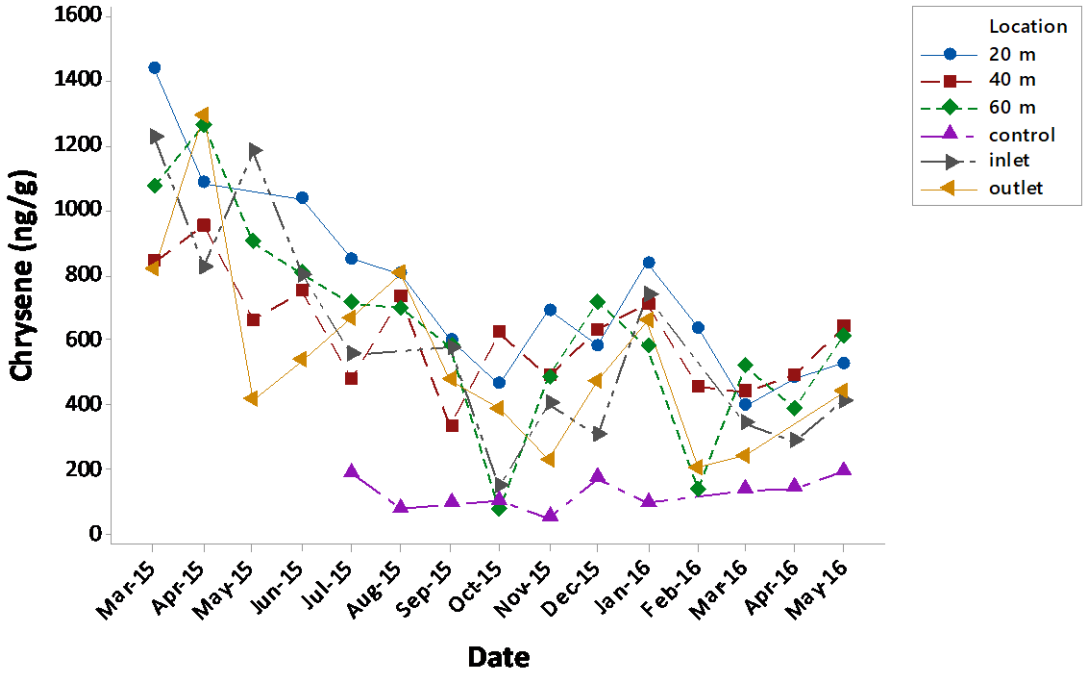

Figure 4-7 Chrysene concentrations (ng/g) in Waterlooville swale over a 15 month period.

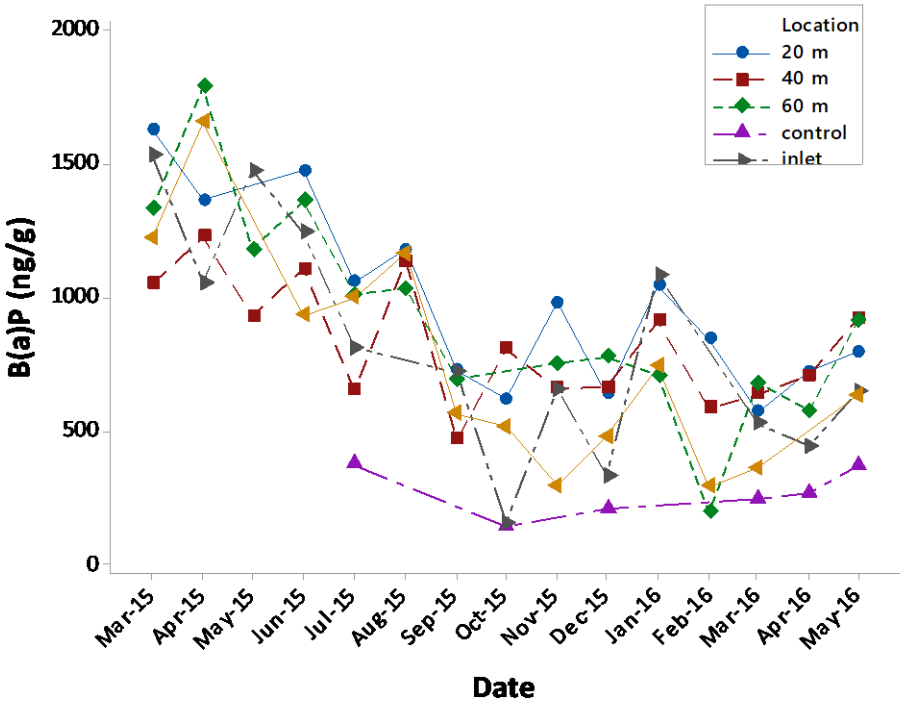

Figure 4-8 Benzo(a)pyrene concentrations (ng/g) in Waterlooville swale over a 15 month period.

Levels of FLAN, PYR, CHR and BaP showed a general decrease over the 15 month study, Figure 4-4 to 4-8, between the first and last sample sets. All these PAHs showed increases and decreases in the same sampling locations. As shown in Figures 4-4 to 4-8 there were monthly increases seen, with the largest spike being in January 2016, which was also shown in NAP results (Figure 4-3). FLU, Figure 4-4 was similar to NAP in that the levels stayed fairly consistent over the trial period, with start and end concentrations not being significantly different. Summaries by the MetOffice (metoffice.gov.uk) show that the winter of 2015/16 was warmer than average, with few periods of frost or cold. As such there was no added gritting salt on the roads adding to the pollutant build up in runoff. During the monitoring time there was also lower than average rainfall, this also would have affected the pollutant levels entering the system. The reduction in input of pollutants via road runoff may offer insight into the lack of heavier PAH accumulation, and only the lighter PAHs appearing to accumulate. Levels in the PAHs showed decreases in concentrations in the months up to October 2015 from the start of the sampling process. Levels then started increasing again, when temperatures were lower, and heavier rainfalls were experienced. It has been shown that during the warmer summer months PAHs are more likely to volatise, and lower levels found in soil. During colder

winter months the high molecular weight PAHs are more readily deposited in the soil (Wang *et al.,* 2008). This same study suggested that it is during the summer months that PAHs are more likely to move between the soil and air. Levels are higher than other environmental reports (Table 2-10), potentially due to the area behind the swale being an active housing development works, with large vehicles regularly passing by, and dust being produced in the building works. Chang *et al.* (2002) showed that the degradation of PAH was affected by SOM. A peak in organic matter was seen in January 2016 and a rise in PAH levels was seen at the same time, this shows the same effect shown by Chang *et al.* (2002).

Averages of the environmental levels of each PAH, shown in Table 4-1, were calculated for reference use in determining pollution levels to dose the simulated artificial road runoff dust. As seen from these results NAP was found with large variation in concentrations, with a high standard deviation. Similar variability in concentrations were found in a study of roadside pollution entering agricultural land (Zerrouki *et al*., 2017).

Table 4-1 Mean environmental concentrations of PAHs from Waterlooville swale.

PAH	*Mean concentration (ng/g)*	*Standard deviation*	*Median concentration (ng/g)*
Naphthalene	*2403*	*180.0*	*2484.0*
Fluorene	*115*	*10.3*	*175.8*
Pyrene	*721*	*42.9*	*861.4*
Chrysene	*501*	*49.3*	*911.6*
Benzo(a)Pyrene	*668*	*33.6*	*603.6*

4.2 Pond system

4.2.1 Water PAHs

Conducted on a monthly basis over fourteen months, March 2015 to May 2016, water quality parameters were tested in the pond system at Waterlooville. The sample taken at the inlet to the pond was fed directly from the swale. PAH analysis of the water was conducted between July 2015 and May 2016, due to limitations in equipment. GCMS

analysis of the target PAHs only returned concentrations for NAP in water samples, Figure 4-9, all other PAHs were below detection limit. NAP concentrations were all low, but above detection limits, except for April 2016 where limits were too low to be detected. Across the full sample run there was no pattern of decrease between the ponds, however levels detected were all below those set out in the EQS and WFD standards for surface water pollutant levels (see table 2-10, Chapter 2). Similar results were reported by Roinas *et al.* (2014), however this study detected levels of other low range PAHs FLAN and PYR which were not detected during this period of monitoring.

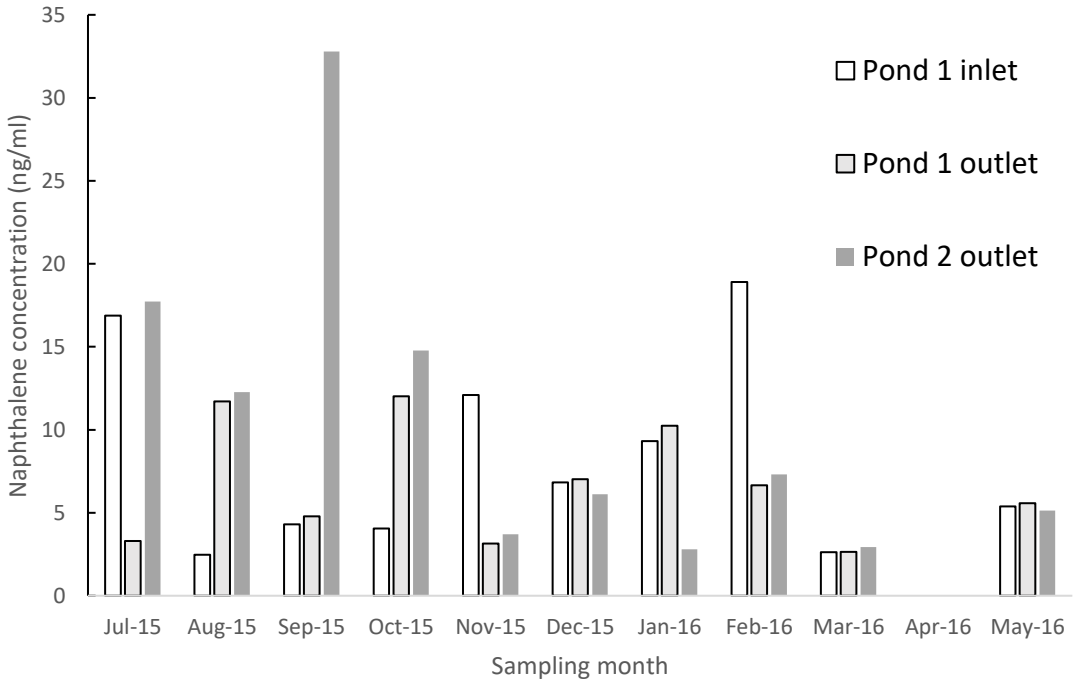

Figure 4-9 Monthly naphthalene concentrations from the Waterlooville pond system, samples from three locations, Pond 1 inlet and outlet and Pond 2 outlet.

One potential reason for lack of detectable PAHs in the pond is the retention factor of the swale. Vegetation has proven to be effective at retaining the particulates in road runoff, and consequentially the attached pollutants (e.g. Bastien *et al.,* 2010a; Bratieres *et al.,* 2008; Stagge *et al*., 2012, Woods Ballard *et al.,* 2015). Larger ponds show increased biodiversity due to dilution effect of pollutants in the increased water volume (Sun *et al*., 2018), this may also offer explanation to the lack of heavier PAHs in the pond system. The swale that directs runoff into the pond system may also have had a role to

play in the reduction of PAHs. This has been shown in previous studies of roadside swales in France, where removal of a number of PAHs in runoff was found to be consistently high (Leroy *et al*., 2015). In both the swale and the ponds vegetation was dense, no maintenance was observed throughout the period of study. This level of vegetation may have captured the majority of TSS and with it the particulate attached pollutants (Stagge *et al*., 2012). As shown NAP was detected in low concentrations in the pond water samples, its presence may be attributed to its physio-chemical properties. It is possible that NAP, which has a much higher solubility factor than other PAHs, attached to particulates was leached back into the water column as water flowed through the swale and into the pond system (Sims *et al.*, 1990, de Boer & Wagelmans, 2016). The lack of other PAHs in the water samples does not mean they were not present in the pond system. Water in the pond system was slow moving and in most months had no visible outflow, this then allows time for particulates to settle out. In a review of BMP performance, Barrett (2008) showed that the longer water remained in a system the lower the effluent concentrations. Sediment and suspended solids were not assessed in this study, a sediment trap set up in a previous study of the pond system (Roinas *et al*. 2014) was checked on each visit, but no sediment could be collected from the trap. It is therefore possible that had this been analysed levels may have been detected. This pattern of LMWPAH in the water column and HMWPAH in the sediment was found in a study of the Kor River in Iran (Adeniji *et al.*, 2018). Here it was shown that a 3 ring PAH (acenaphthene) had the highest concentration in the water and Fluoranthene was the highest in the sediment.

4.2.2 Water Quality

Throughout the monitoring period the temperature varied as expected with the change of seasons. Temperature of the pond water samples stayed consistent during each month's samples across each of the three sampling locations. Statistically there was no significant differences in temperature between the pond sampling locations (ANOVA F = 0.03, P = 0.967). EC in Pond 1 stayed consistent between the inlet and outlet sampling points and for the majority of sampling months Pond 2 EC was lower than Pond 1, Figure 4-10. A decrease in EC could indicate that as the water flows through the system particulate matter is settling out of the water column, thus reducing the ion

concentration in the water. March 2016 showed a big spike in EC in Pond 1, this corresponds with a low temperature. If the road had been gritted due to cold weather, the added salt content may be responsible for the sharp rise seen in Pond 1.

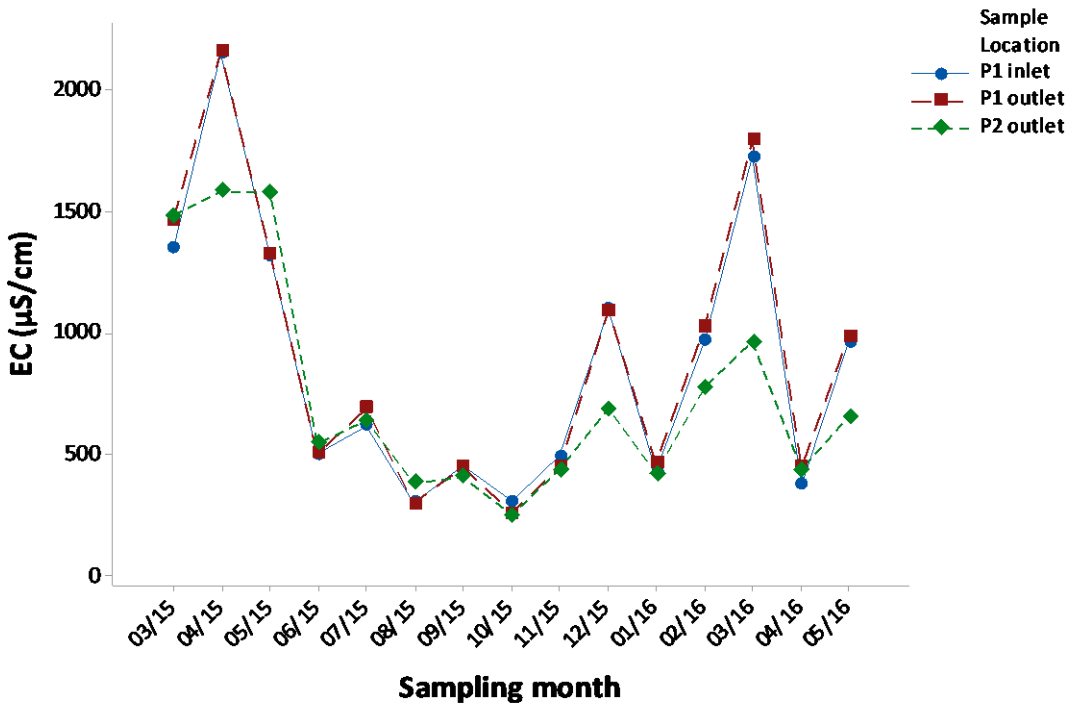

Figure 4-10 Electrical conductivity across a two pond SuDS system in Waterlooville. Samples were taken from three locations Pond 1 inlet and outlet, and Pond 2 outlet.

Overall, the results reported for the SuDS system in Waterlooville, show similar patterns to those reported by Roinas *et al.*, (2014).

5 Swale mesocosm trial runs – results

5.1 Hydrology

5.1.1 Storm Events – Clean Water

To assess if the swale mesocosm was hydraulically comparable to environmental swale systems, a series of ten test storm simulations were undertaken, measuring outflow to produce a hydrograph. Six of these also assessed the inflow rates, to allow for testing of the retention capacity of the swale. The tests were also used to determine the

repeatability of the pump to produce consistent flows and to assess the reproducibility of the hydrological performance of the swale. The inflow and outflow hydrographs were also compared to other field studies to evaluate the mesocosm in terms of performance in retaining water and delaying peak flow.

Preliminary testing of the pump to ensure repeatability showed that there was consistent inflow water pumped over the half hour testing (Table 5-1). All runs fell within two standard deviations of the mean (1124 ± 50 L). The experimental design was for 1000 L to be pumped down the swale over 30 minutes. Ensuring an accurate volume of water was difficult due to equipment available. The IBC used for water storage had an outlet pipe close to the base of the container. However, towards the end of the run when water was low, if it fell lower that the outlet pipe air mixed with the water and a steady flow was not achievable. In order to prevent this, the IBC had to be filled over the 1000 L mark so that the outlet pipe was submerged at all times of the storm event. However, due to the variability in water being sent onto the swale, flow level readings were taken during each of the main trial runs. Further, because flow rates were calculated for each individual trial, specific data can be used.

Table 5-1 Results of preliminary flow tests of the pump set up for each 6 minute flow block. An estimate of the total volume pumped over half an hour is also shown. Time steps are as described in Chapter 3.

Time step (mins)	*Test 1 (L)*	*Test 2 (L)*	*Test 3 (L)*	*Test 4 (L)*	*Test 5 (L)*	*Test 6 (L)*
0 – 6	*106*	*126*	*108*	*107*	*106*	*98*
6 – 12	*230*	*252*	*260*	*223*	*242*	*241*
12 -18	*356*	*358*	*369*	*353*	*398*	*393*
18 – 24	*247*	*261*	*264*	*284*	*261*	*284*
24 – 30	*139*	*137*	*147*	*151*	*113*	*129*
Total (L)	*1078*	*1133*	*1149*	*1119*	*1121*	*1144*

Figure 5.1 shows a representative hydrograph for both inflow and outflow water in the swale. Shown is this figure is also the two time points between which the lag time is gained. These points are the peak inflow time and the time at which the peak volume of outflow water was determined.

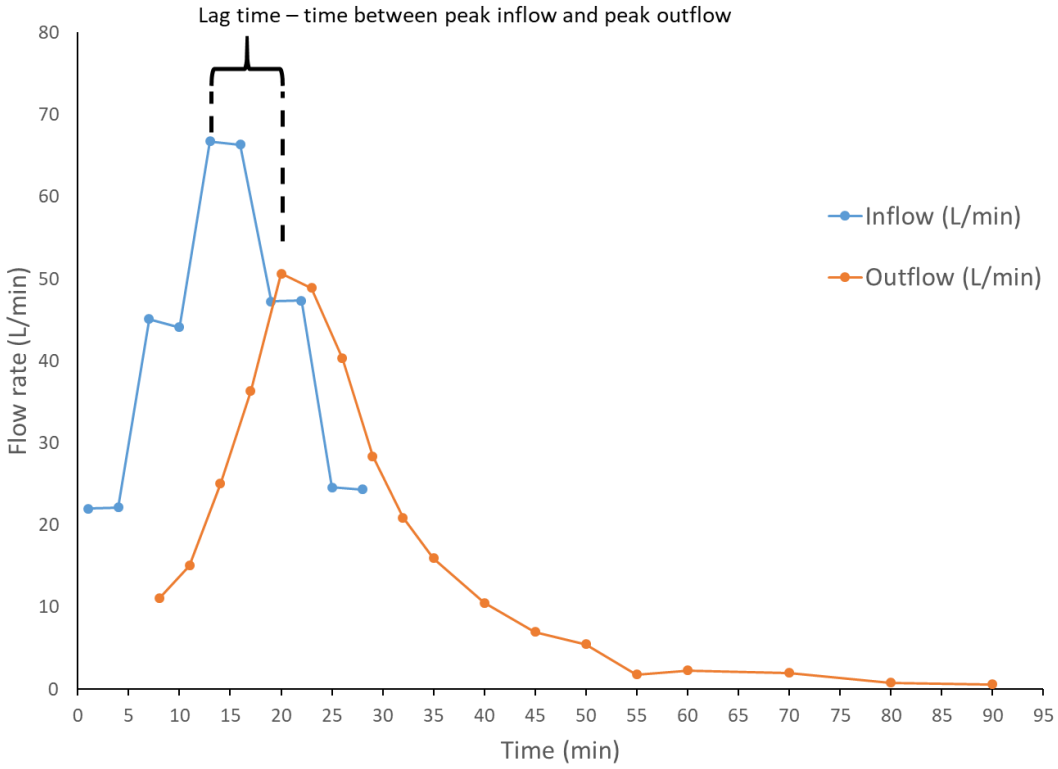

Figure 5-1 Inflow and outflow hydrographs showing the lag time between peak inflow onto the swale and the peak outflow from the swale.

Table 5-2 shows the time of first outflow, peak outflow and the lag time (retention time) for each trial run, generated by the difference between inflow and outflow. For the test runs with no inflow measured, assumptions based on inflow average rates are taken from the recorded results. For the peak inflow time the start of the 12 – 18 minutes time step is used as this was the point at which the highest flow rate entered the swale. These initial test runs of the swale to assess performance were performed in pairs, with a second full run performed one or two days after the first. This was to determine any changes caused by the recent soil saturation.

Table 5-2 Flow descriptors: time of first outflow from the swale, peak outflow, lag time and reduction in flow water outflow rate for ten test runs on the model swale. Lag time determined using a peak inflow time of 12 minutes. Runs 5 – 8 show no reduction level as no inflow readings were taken during the run.

Test run date	*Test run*	*Time of first outflow (mins)*	*Time of peak outflow (mins)*	*Peak flow lag time (mins)*	*% reduction of flow volume*
19/04/2016	*1*	*11*	*22*	*10*	*34*
22/04/2016	*2*	*7*	*19*	*7*	*6*
28/04/2016	*3*	*13*	*22*	*10*	*26*
29/04/2016	*4*	*7*	*22*	*10*	*18*
12/05/2016	*5*	*11*	*22*	*10*	*-*
13/05/2016	*6*	*8*	*19*	*7*	*-*
02/06/2016	*7*	*9*	*19*	*7*	*-*
03/06/2016	*8*	*6*	*19*	*7*	*-*
15/07/2016	*9*	*10*	*19*	*7*	*36*
17/10/2016	*10*	*8*	*22*	*10*	*34*

Based on the results of the test runs an average lag time of 9 minutes for water to flow out of the swale, and 8.5 minutes between peak inflow and the peak outflow. While there is no set recommendations for the lag time of water in a swale, various studies have calculated the performance of swales abilities to retain water. Deletic & Fletcher (2006) performed a study of an improvised swale on a grassed slope in Aberdeen, Scotland with an average outflow rate of between 33 and 87 % of the inflow rate. For the test runs performed, those completed when the swale was dry showed levels of reduction seen in this study. When the swale was already saturated the water reduction was outside of the range found by Deletic and Fletcher (2006). Haga *et al*. (2005) described the changes in lag time due to soil saturation, which was demonstrated in the trial runs of the model swale. If the swale was longer the retention time would increase due to the increased infiltration and holding capacity (Tedoldi *et al.*, 2016).

The final column of Table 5-2 shows the percentage reduction in outflow rate compared to the inflow rate. An average of 26% reduction across the five runs where inflow was measured. These results, 74 % of the inflow water being calculated in the outflow, fall

within the range described by Deletic and Fletcher (2006). Revitt *et al*. (2017) showed that across a range of available data the typical mean volume reduction was 42% (SD ±7.3%) in swales. The test swale results were below this level, however this may be influenced by the limited scale of the swale and volume of soil for water retention.

The test runs were performed in pairs, with a second run performed one or two days after the first. This was to determine any changes caused by recent soil saturation. Table 5-2 shows that the outflow was seen earlier during these second runs, suggesting that the soil in the swale was less able to retain the water. Test runs completed while soil was still damp from the previous run, were on average having outflow 3.5 minutes earlier than the tests with dry soil. This has been shown in previous studies (for example: Deletic, 2001, Davis *et al.*, 2012 & Shafique *et al.*, 2018) where in heavy storms a swale is more likely to be of use as conveyance of water rather than for attenuation. It is worth noting that at no point in any of the runs did water surface flow reach the end of the swale, all water eventually filtered into the soil.

Figure 5-2 shows the outflow hydrographs produced from two of the initial trials of the swale and pumping system (Tests 9 and 10). In the test runs, all water infiltrated the soil with some being retained in the soil and the remainder reaching the outflow via filtering through the swale bed.

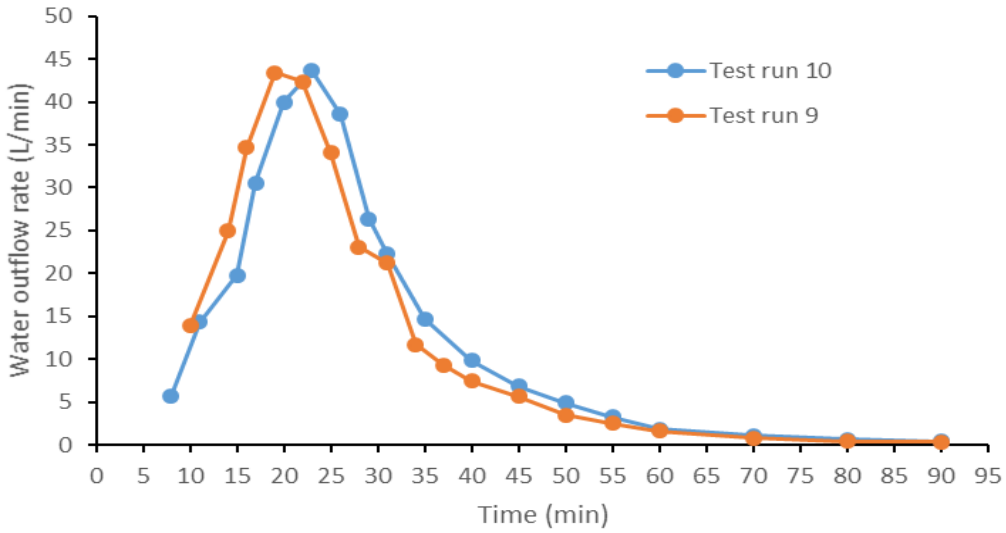

Figure 5-2 Outflows from two test runs to determine performance of grassed swale.

For the six test runs where both inflow and outflow were measured it was possible to determine the volume of water lost between the two points. Table 5-3 shows a simple mass balance of the inflow and outflow volumes and the volume of water unaccounted for. This volume of water will either have been retained in the swale soil, taken up by plants or lost via evapotranspiration. Further understanding of what processes are involved with the water loss for these trials was not possible as no moisture content analysis of the sediment was completed. Grass cover, such as that used in the swale mesocosm, provides ideal vegetative cover to encourage high infiltration rates (Deletic, 2000). In a laboratory study of how a slope can effect infiltration, Morbidelli *et al*. (2016) showed that a vegetated slope will reduce the variability of saturation for different flows, thought to be due to the variation of roughness, rather than the grass itself.

Across the six test runs which had both inflow and outflow measured, a mean inflow of 1124 L, mean outflow of 902 L and mean retained volume of 222 L. The reduction in outflow water volume was significantly different to the volume of water being sent onto the swale (paired T-test $P < 0.001$).

Table 5-3 Water mass balance of inflow, outflow and unaccounted volumes of water during test runs on the swale mesocosm in 2016. The final column shows the percentage reduction in the water volume leaving the swale.

run date	*inflow (L)*	*Outflow (L)*	*Amount unaccounted for (L)*	*Water loss (%)*
19 April	*1078*	*749*	*329*	*30*
22 April	*1133*	*993*	*140*	*12*
28 April	*1149*	*877*	*272*	*24*
29 April	*1119*	*1020*	*100*	*9*
15 Jul	*1121*	*859*	*263*	*23*
17 Oct	*1144*	*918*	*226*	*20*

Overall the initial testing of the pump capacity and swale performance showed that the volume of water pumped down the swale it was within a reasonable margin of error. The swale itself performed as it was designed to do, successfully simulating the

hydrology expected in the field. As such the main trials were run in the same manner, and measurements of inflow and outflow recorded at set time points.

Due to the decrease in retention ability in the tests performed soon after a first test, the main trials were scheduled to run two weeks apart, this allowed the soil time to dry out.

5.1.2 Storm Events: Polluted Water

The ten trial pollution runs were performed as described in the methods chapter (Section 3.3.3). For these trials the same monitoring as the test runs was used, with both inflow and outflow measured. Table 5-4 shows a simple mass balance for the levels of water entering and leaving the swale, the unaccounted volume losses (inflow volume – outflow volume) and percentage reduction. By subtracting the volume of water leaving the system from the volume sent onto the swale, the volume remaining in the swale can be calculated (Gocht *et al.*, 2007). The volume unaccounted for will make up the mass balance. This volume will be somewhere in the swale system, either in the soil or lost due to evaporation. The mean inflow of 1244 L was higher compared to the initial tests. However all runs fell within two standard deviations (112 L) except the first run (22/11/16). The reduction in volume of water exiting the swale was consistent, with an average outflow volume of 1030 L (standard deviation 73 L). A one-way ANOVA showed that there was a significant difference between average inflowing and outflowing water volume (n=10, F-value = 37.19, P-value = 0.00). Run 10 showed the greatest reduction in volume, with a reduction of 28 % of the inflowing water. Figure 5-3 shows the changes in temperature of the water over the trial period. The runs with the lower volumes of water exiting the swale were also runs where the water temperature was higher (Figure 5-3). This could have been due to higher moisture deficit in the soil, the higher temperatures would also have caused moisture loss through increased evapotranspiration.

Variations in flow rate were observed, and also increased volumes of water. As previously discussed, the pump used for the trial runs had a screw valve, which meant precise control was not possible. By performing flow readings for each trial run, an accurate account of water input was created. The results of both the test and trial runs

were consistent and within an acceptable margin of error. As shown in the test runs, the trial runs showed similar delay in initial outflow time.

Table 5-4 Mass balance for flow from trial runs, showing approximate amount of water unaccounted for in the swale and the percentage reduction in water volume. Water volumes are approximate based on area under the curve calculations.

	Trial run date	*Inflow (L)*	*Outflow (L)*	*Amount unaccounted for (L)*	*Water loss (%)*
1	*22/11/2016*	*1,113*	*979*	*134*	*12*
2	*05/12/2016*	*1,254*	*1,085*	*170*	*13*
3	*20/12/2016*	*1,257*	*1,054*	*203*	*16*
4	*10/01/2016*	*1,284*	*1,057*	*227*	*18*
5	*23/01/2017*	*1,273*	*1,127*	*146*	*11*
6	*06/02/2017*	*1,316*	*1,103*	*213*	*16*
7	*20/02/2017*	*1,230*	*1,049*	*181*	*15*
8	*06/03/2017*	*1,202*	*918*	*284*	*24*
9	*20/03/2017*	*1,234*	*1,016*	*218*	*18*
10	*03/04/2017*	*1,278*	*915*	*363*	*28*

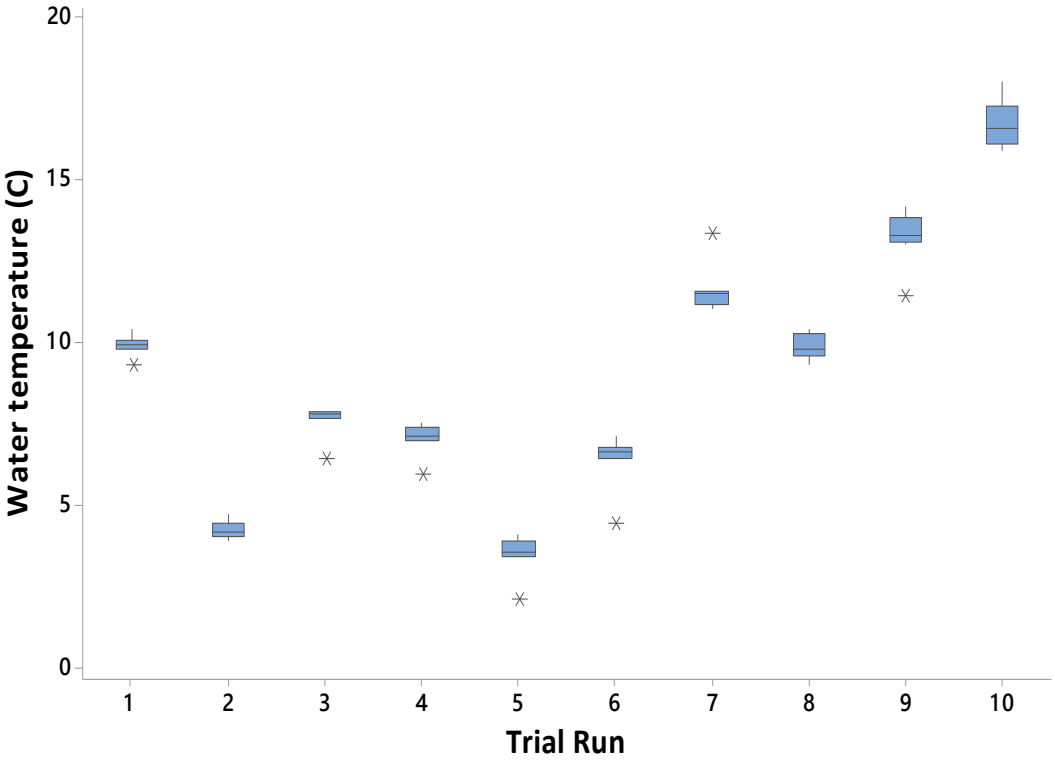

*Figure 5-3 Average water temperatures (°C) for the ten swale trials. Each run had eight samples taken comprising of both inflow and outflow water. Outliers are marked by **

Hydraulically the swale performed consistently over the test runs, under the designed experimental inflow conditions. Figure 5-4 is a hydrograph from trial run 7, showing an example of both the inflow with the stepped flow rate, and the lag time of the outflow. This gives an indication of the swales performance of delaying storm flows.

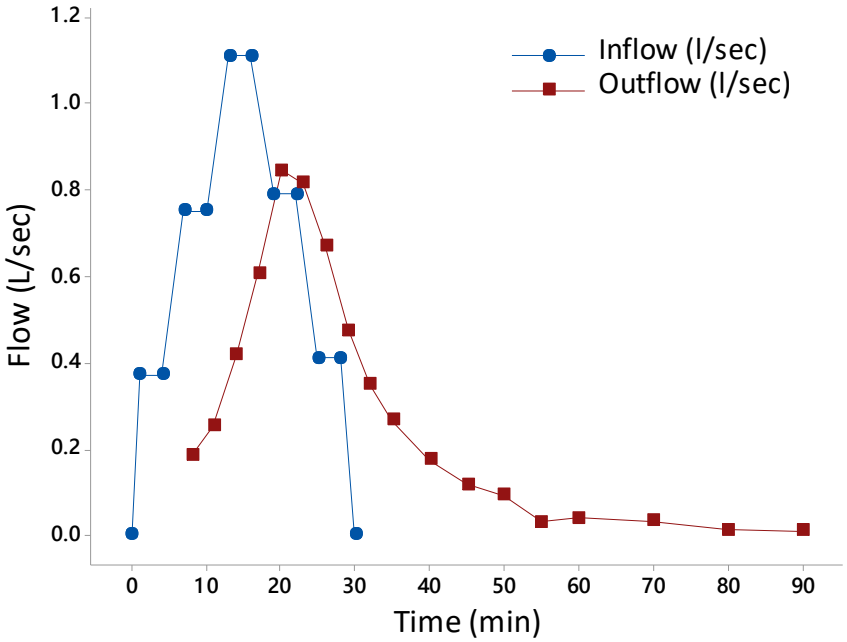

Figure 5-4 Example of inflow and outflow hydrographs (from run 7) showing the delay in outflow and the reduction in peak water discharge.

Table 5-5 shows the outflow times for each individual trial run, along with the peak flow time and the lag time of the peak flow compared to the peak inflow. Peak outflow rate was reduced compared to the peak inflow rate, demonstrating the attenuation of flow by swale systems (Woods-Ballard *et al.*, 2015). Similar levels of delay in hydrograph lag times were also demonstrated by Rujner *et al.*, (2018), with higher lag times corresponding with low soil water content.

Table 5-5 Outflow from the polluted water storm simulations. Outflow time is calculated from the trial start time as 0 minutes. Peak outflow is the time point when flow rate was highest, and peak flow lag time is calculated using the start of the peak inflow rate at 12 minutes.

Trial run	*Outflow time (mins)*	*Peak outflow (mins)*	*Peak flow lag time (mins)*
1	*7.0*	*21*	*14.0*
2	*7.5*	*23*	*15.5*
3	*7.0*	*23*	*16.0*
4	*7.5*	*21*	*13.5*
5	*7.0*	*20*	*13.0*
6	*7.0*	*20*	*13.0*
7	*7.5*	*20*	*12.5*
8	*8.0*	*20*	*12.0*
9	*8.0*	*23*	*15.0*
10	*8.0*	*20*	*12.0*
Average	*7.5*	*21*	*13.7*

During each run the the overland surface flow distance was measured at set time points. To measure this, the water visible on the surface soil was measured from the start of the swale to the furthest point water was visible before infiltration into the soil. Table 5-6 shows the results of these recordings. Figure 5-5 shows the average surface flow from all ten runs. The longest distance of surface flow was seen at 21 minutes on average, this corresponds with the peak outflow, which was also on average 21 minutes (see table 5.5). In a study of infiltration in established vegetated swales with varying flow rates, Rujner *et al.* (2018) showed that for higher flow rates the water was less able to filter into the soil. As the water flowed over the surface it would have transported the particulates (and pollutant) with it. Surface PAH pollution could be expected to be seen to this point. When looking at the timings of the peak overland flow, they correspond to the highest inflow rates. At this point the water does not have time to filter into the soil and so flows further from the inflow point before it has slowed and the volume spread over a larger area to ease filtration into the soil (Morbidelli *et al*., 2016). As the water flows over the surface the vegetation acts as buffers and slows the flow (Vargas-Luna *et al.*, 2015). At the peak flow, approximately 55 L/min was flowing onto the swale, even at this rate the water infiltrated into the soil before reaching the end of the system.

However the system was close to reaching capacity at the higher flow rate, which would lead to the system turning to a conveyance swale in higher storms (Davis *et al*., 2012). Resuspension of polluted particulates deposited in previous flows will also be a factor for consideration. It is during the peak flow that particulates, and the adsorped pollutants, will be transported further down the swale. Surface flow was not correlated to inflow rate (Spearman rho analysis, p-value >0.05), but this may be due to the differing times of sample taking, the infiltration capacity of the soil being progressively exceeded as the storm progressed, or the slow of flow by the vegetation causing a slight offset.

Table 5-6 Distance of surface flow (m) along swale for each of 10 experimental runs. Average surface flow is shown in the final row.

Time (mins)	*3*	*6*	*9*	*12*	*15*	*19*	*21*	*24*	*27*	*30*
Run	*Surface Flow Distance (m) before infiltration*									
1	*0.7*	*-*	*-*	*3.0*	*5.1*	*-*	*8.0*	*8.7*	*1.7*	*1.2*
2	*0.8*	*1.2*	*2.8*	*3.9*	*5.3*	*8.2*	*8.9*	*8.6*	*8.3*	*1.6*
3	*0.8*	*1.0*	*2.7*	*3.4*	*5.5*	*8.2*	*9.1*	*9.1*	*2.1*	*0.5*
4	*0.9*	*1.4*	*2.9*	*4.2*	*5.9*	*8.2*	*9.0*	*9.0*	*2.7*	*0.7*
5	*1.2*	*1.7*	*3.0*	*4.2*	*6.4*	*8.0*	*9.0*	*8.9*	*8.5*	*0.0*
6	*1.1*	*1.4*	*3.2*	*4.5*	*6.5*	*8.9*	*9.0*	*8.9*	*8.6*	*0.0*
7	*1.3*	*1.7*	*3.2*	*4.2*	*5.7*	*8.2*	*9.0*	*8.7*	*2.2*	*1.8*
8	*1.0*	*1.6*	*3.1*	*3.8*	*5.7*	*7.9*	*9.0*	*8.6*	*2.2*	*2.1*
9	*1.3*	*1.5*	*3.2*	*3.8*	*6.2*	*7.5*	*8.7*	*8.8*	*2.8*	*2.1*
10	*2.2*	*2.2*	*3.5*	*3.8*	*5.3*	*5.8*	*5.2*	*5.0*	*0.7*	*0.2*
Average (m)	*1.1*	*1.6*	*3.1*	*3.9*	*5.8*	*7.9*	*8.5*	*8.4*	*4.0*	*1.0*

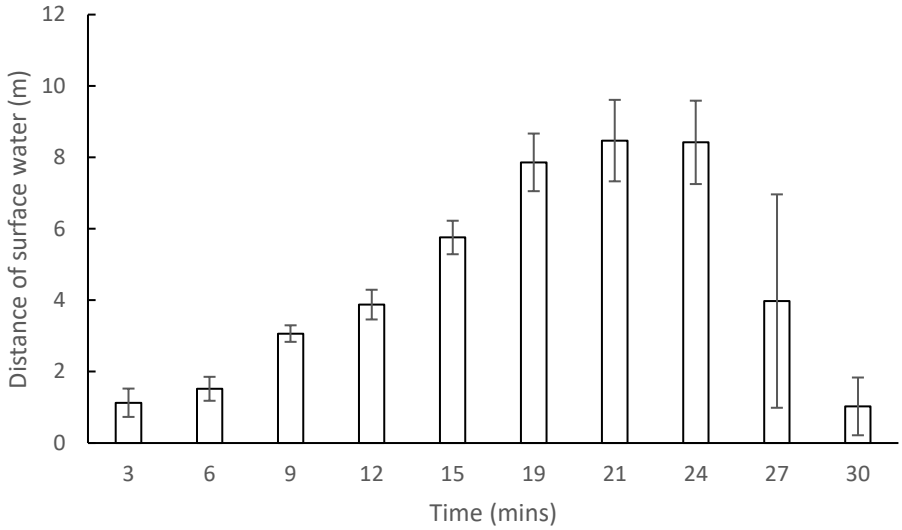

Figure 5-5 Surface flow distance before complete infiltration with experiment run time.

5.2 Trial runs – Water quality

The inflow was tested to assess the effect adding the pollutant had on the tap water used. Water from the IBC was tested each run to ascertain base levels before the RRD was mixed in as water was pumped onto the swale (Table 5-7). Over the course of the ten polluted trial runs, the temperature showed some variation in line with the ambient temperature inside the greenhouse. The addition of RRD did not affect the storm water as it was pumped onto the swale (ANOVA F-value = 0.0, P-value = 1.0). The water temperature was also not altered significantly as it passed through the swale. Table 5-7 shows the water quality parameters measured over the ten trial runs for the IBC and inflow samples.

Table 5-7 Water quality parameters measured over ten trial runs. Intermediate Bulk Container (IBC) is an average taken from 30 samples, all other values are averages from 10 samples.

Variable	*Sample location*		*Statistics*		
		Mean	*SD*	*min*	*max*
EC (µS/cm)	*IBC*	*460*	*18*	*425*	*459*
	Inflow – 2 mins	*462*	*15*	*435*	*478*
	Inflow – 9mins	*464*	*13*	*442*	*482*
	Inflow – 17mins	*460*	*10*	*441*	*471*
pH	*IBC*	*9.02*	*0.27*	*8.6*	*9.4*
	Inflow – 2 mins	*8.83*	*0.40*	*8.2*	*9.3*
	Inflow – 9mins	*8.80*	*0.18*	*8.5*	*9.1*
	Inflow – 17mins	*8.82*	*0.23*	*8.4*	*9.1*
COD (mg/L)	*IBC*	*9.3*	*8.2*	*0*	*26*
	Inflow – 2 mins	*56.1*	*23.1*	*27*	*98*
	Inflow – 9mins	*38.2*	*24.9*	*18*	*82*
	Inflow – 17mins	*19.1*	*12.6*	*5*	*39*

The PAH dosing had no major influence on the EC and pH of the water being applied to the system, which was typically about 461 µS/cm and 8.8 respectively. The tap water used for the storm water fell well below the maximum allowable levels as set out in the EU Drinking Water Directive, 98/83/EC (The Council of the European Union, 1998) which gives a maximum EC of 2500 µS/cm and pH range of 6.5 – 9.5. Figure 5-6 shows the change in EC from the source water IBC and over the first 17 minutes of the storm trial run. The median value collected from the 2 minute samples was 466 µS/cm, showing an increase occurred in the water after it was mixed with the RRD. The addition of the polluted RRD into the water flow served as a source of ions, thus increasing the EC in the water. As flow onto the swale increased and the RRD particles were diluted, water EC did decrease, giving further evidence of the RRD being the source of the increased EC potential in the water. The changes of EC in inflow samples was not statistically significant. This slight increase and gradual decline in value follow patterns discussed by Gobel *et al.* (2007) in a review of storm water runoff. This study collated data from over

100 trials and concluded that on average in the first 2 mm of a storm the pH and EC will increase, before decreasing gradually over time.

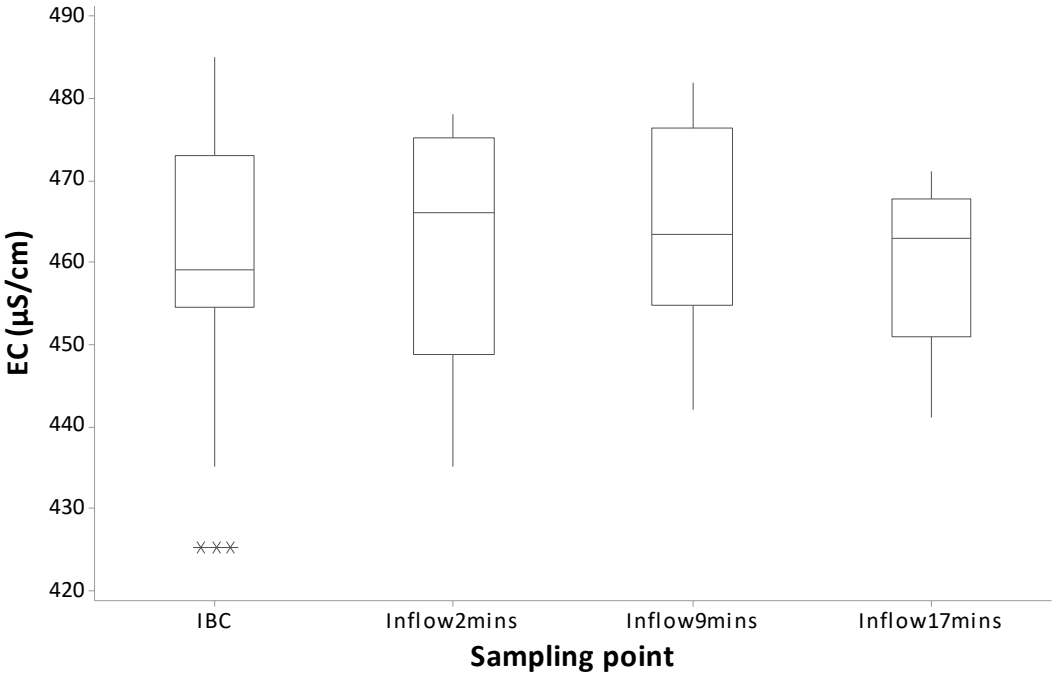

*Figure 5-6 Electrical conductivity (µS/cm) from IBC and inflow samples for ten trial runs. Boxes show the median and 75 percentile and the whiskers show the 95 % confidence limits, * denote outliers.*

Figure 5-7 shows the pH values taken in the inflow, as stated there was no significant changes in the water pH levels. Addition of RRD into the water did show some pH decreases over time, with a median value of 8.9 at 2 minutes and 8.75 at 9 minutes. An increase was then seen in the sample taken two minutes after the RRD was ceased. This would imply that the RRD was affecting the alkalinity slightly, but not significantly enough to say that it was having an adverse effect on the water.

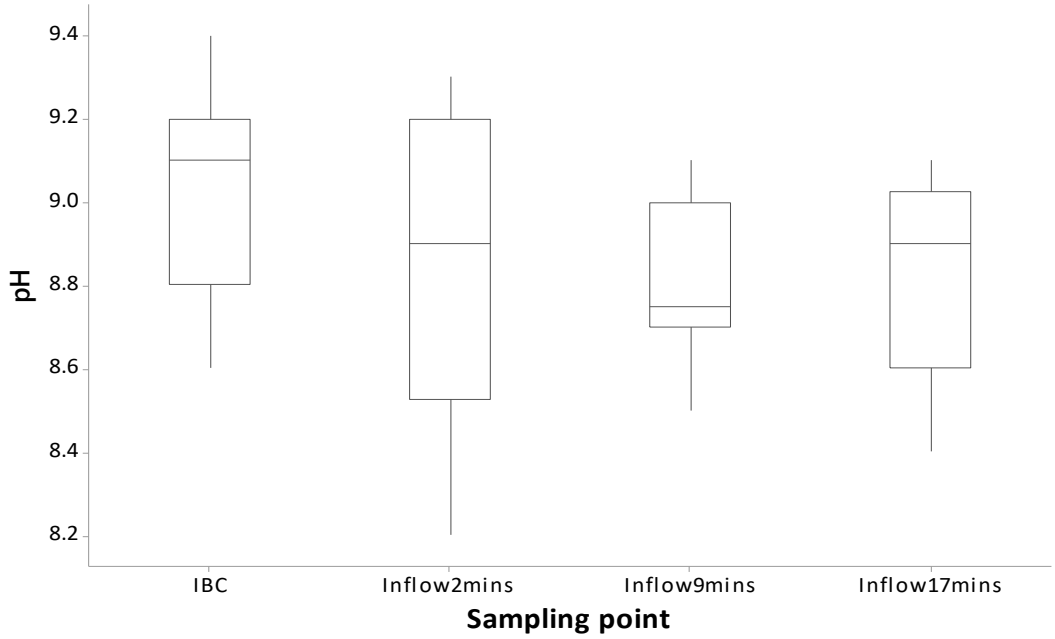

Figure 5-7 pH from IBC and inflow samples for ten trial runs. Boxes show the median and 75 percentile and the whiskers show the 95 % confidence limits.

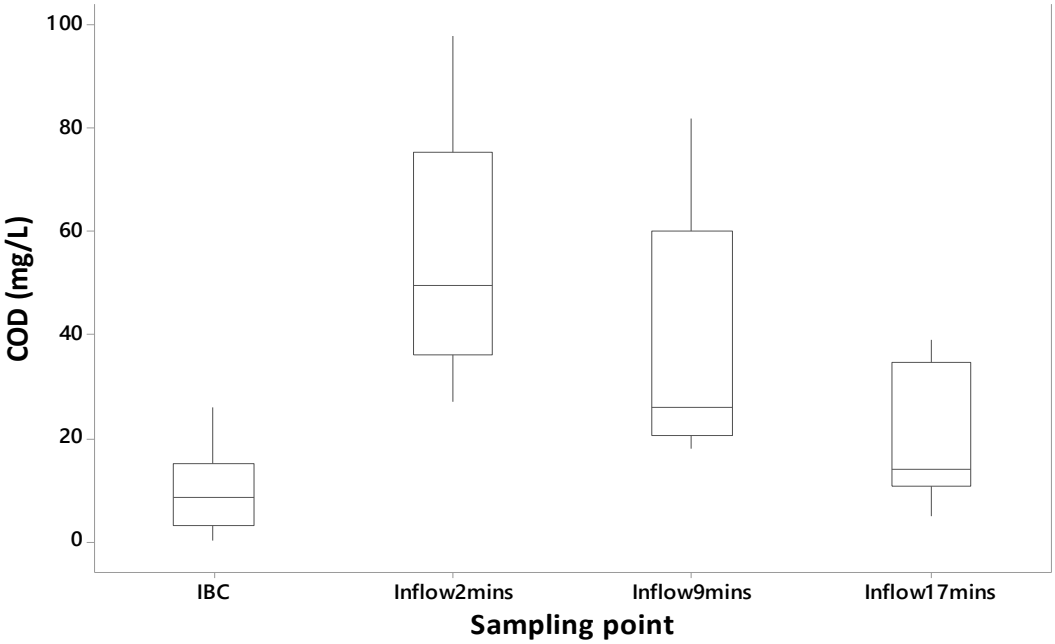

Figure 5-8 COD (µS/cm) from IBC and inflow samples over ten trial runs. Boxes show the median and 75 percentile and the whiskers show the 95 % confidence limits.

During the first stages of the pollutant dosing the COD rose to about 45 mg/l, this then fell due to dilution of the organic pollutant levels over the next stages of the inflow hydrograph. Figure 5-8 shows the COD averages from over the ten runs. A significant increase was seen compared to the IBC COD level in all the outflow samples. The 2 minute sample had the greatest increase (Kruskal-Wallis H = 21.95, DF = 1, P = 0.000), 9 minute sample (Kruskal-Wallis H = 16.74, DF = 1, P = 0.000), and the 17 minute sample the least (Kruskal-Wallis H = 5.64, DF = 1, P = 0.018). When comparing the inflow samples there was a decrease in COD over time, as the increased flow diluted the RRD. The samples from 17 minutes were significantly lower when compared to the 2 and 9 minute inflow samples, H = 10.57, DF = 1, P = 0.01 and H = 4.81, DF = 1, P = 0.028 respectively. Samples from 9 minutes were lower compared to the 2 minutes, but this was not significant (Kruskal-Wallis H = 3.57, DF = 1, P = 0.059). These results suggest that the addition of RRD was causing a rise in COD. This has been shown in studies of runoff, where COD increased in the initial stages of storms, gradually decreasing as the storms continued (e.g. Lee & Bang, 2000, Wang *et al.,* 2013). As COD is an indication of the organic matter in the water, it could be considered as a linked process in the pollution cycle and the addition of the RRD, with the organic pollutants, could be expected to increase this value. Roinas *et al. (*2014) showed evidence of COD being influenced in the first flush effect, showing a trend of COD decreasing with time during storms. As COD can be linked to an increase in organic matter, monitoring of COD in the environment could help to indicate when intensive remediation and clean-up of an area should be considered.

Water quality in the outflow showed evidence of passage through the swale affecting certain parameters, Table 5-8 and Figure 5-9 show the results for all outflow samples. As seen with the inflow, temperature was not affected in any way and stayed consistent throughout each run. Temperature can affect PAH behaviour, higher temperatures see an increase in degradation (Coover & Sims, 1987, Chunhui *et al.*, 2017; Jia & Batterman, 2010). As mentioned previously, physiochemical properties of each PAH are slightly different, lower weight PAHs will start to volatise at lower temperatures than the higher weight PAHs. There was however a significant decrease in the pH when the inflow and outflow were compared (Kruskal-Wallis, H = 16.89, DF = 1, P = 0.000). While there was

some variation in outflow pH over time (Figure 5-9), the overall value stayed relatively stable in all the runs. Even with outliers included in analysis, there were no significant changes in pH levels in the outflow, and the water remained alkaline through all samples. When comparing the pH of each run there was no significant difference (Kruskal-Wallis H = 8.53, DF = 9, P = 0.482).

Table 5-8 Water quality parameters from outflow of ten trial runs.

Variable	*Sample location*	*Statistics*			
		Mean	*SD*	*min*	*max*
Temperature (°C)	*1st outflow*	*8.07*	*1.34*	*4.23*	*2.1*
	out 23 min	*9.00*	*1.28*	*4.06*	*3.9*
	out 30 min	*9.08*	*1.29*	*4.08*	*3.5*
	out 60 min	*9.26*	*1.37*	*4.32*	*3.4*
	out 90 min	*9.61*	*1.44*	*4.57*	*3.8*
EC (µS/cm)	*1st outflow*	*545*	*14.5*	*484*	*621*
	out 23 min	*510*	*22.5*	*444*	*685*
	out 30 min	*487*	*7.7*	*449*	*516*
	out 60 min	*544*	*11.2*	*471*	*587*
	out 90 min	*574*	*12.4*	*494*	*618*
pH	*1st outflow*	*8.61*	*0.05*	*8.4*	*8.9*
	out 23 min	*8.57*	*0.04*	*8.2*	*8.7*
	out 30 min	*8.58*	*0.04*	*8.4*	*8.8*
	out 60 min	*8.57*	*0.05*	*8.3*	*8.9*
	out 90 min	*8.59*	*0.04*	*8.4*	*8.8*
COD (mg/L)	*1st outflow*	*69*	*9.47*	*26*	*127*
	out 23 min	*39*	*5.18*	*13*	*61*
	out 30 min	*38*	*4.98*	*18*	*71*
	out 60 min	*70*	*6.4*	*38*	*101*
	out 90 min	*78*	*8.98*	*33*	*123*

Outflow EC (median 547 µS/cm) was significantly higher compared to the combined inflow values (median 461 µS/cm) (Kruskal-Wallis H = 24.85, D = 1, P = 0.000). EC had an initial drop from a mean of 545 µS/cm in the initial first flush sample, to 510 µS/cm in the 23 minute sample, but this was not significant (Kruskal-Wallis H = 3.16, DF = 1, P

=0.076). Peak outflow rate was at 21 minutes, it was during this time that the residence time of water in the swale would have been at its lowest, and meaning there was less opportunity for the water to be affected by ion-transfer. Outflow samples at 23 and 30 minutes, the time points where residence time was lowest, did not have significant difference to the inflow samples, or each other, giving further indication that the swale was the cause of the change in EC. There was a gradual rise in EC values from the 30 minute mark as water was slower to leave the swale. The highest EC was in the 90 minute sample, mean 574 µS/cm, at this point water would have been in the swale for at least one hour. Samples at 23 and 30 minutes were significantly lower than the 60 and 90 minute samples:

- 23 vs 60 min: H = 3.86, DF = 1, P = 0.049
- 30 vs 60 min: H = 9.14, DF = 1, P = 0.002
- 23 vs 90 min: H = 6.61, DF = 1, P = 0.010
- 30 vs 90 min: H = 12.62, DF = 1, P = 0.000

There was a significant difference in EC when comparing the trial runs (Kruskal-Wallis H = 18.3, DF = 9, P = 0.032). The highest EC, 685 µS/cm was seen during trial run 6 at the 23 minute sample point, this is shown as an outlier in Figure 5-9. The lowest EC, 444 µS/cm, was also at the 23 minute sample point during trial run 10 (Table 5-8). Outflow EC levels were well within limits (<2,500 µS/cm) set by the EU WFD, (Table 2.1). The elevated EC levels in the outflow are an indication of an increase in dissolved ions, this is most likely be due to leaching from the soil and evapotranspiration which can cause a concentrating of solutions and thus higher levels of the ions. Water quality testing of EC in both inflows and out flows of the system can show how passage through the soil can affect the water.

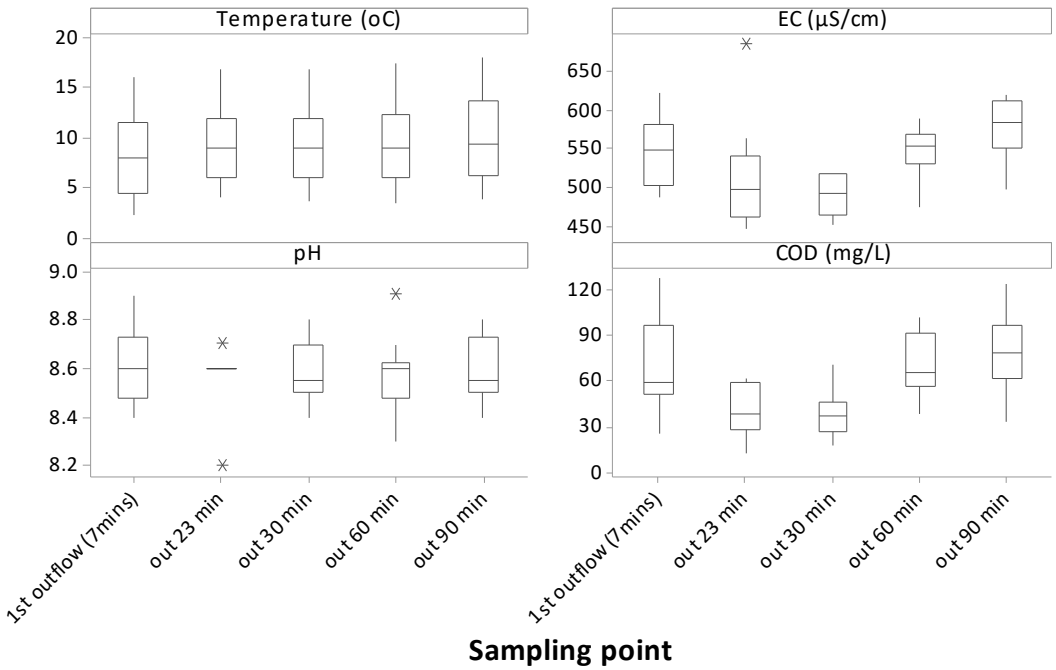

Figure 5-9 Outflow quality parameters from ten trial runs. Sample time points are from the start of the trial run.

Outflow COD concentrations decreased over the first thirty minutes of monitoring, this can be seen clearly in Figure 5-9. COD levels between each trial run had a significant change (Kruskal-Wallis H = 18.81, DF = 9, P = 0.027) Inflow COD was significantly lower than the first outflow (Kruskal-Wallis H= 16.29, DF = 1, P = 0.000). Samples from the 23 and 30 minute samples showed no difference to inflow levels or each other, but were significantly lower than the other outflow samples:

- 23 vs 30 min: H = 0.04, DF = 1, P = 0.850
- 23 vs 60 min: H = 8.04, DF = 1, P = 0.005
- 23 vs 90 min: H = 8.04, DF = 1, P = 0.005
- 30 vs 60 min: H = 0.04, DF = 1, P = 0.850
- 30 vs 90 min: H = 0.04, DF = 1, P = 0.850

COD levels of release into the environment are governed by the EU, with an emission range of 30 – 100 mg/L (European Commission, 2016). Overall, the addition of the RRD to the tap water caused an increase in COD and EC inflow samples. This successfully

imitates the first flush phenomena shown in road runoff around the world. Chow & Yusop (2014) when investigating storms in residential, commercial and industrial sites suggest that COD might be more closely linked with runoff volume and peak flow rather than antecedent dry days. This study demonstrated high COD in the first flush of the storms. A similar rise in COD was seen in the trial runs when comparing the first inflow water (at 2mins sampling time) and the first out flow samples (average 56 mg/L and 69mg/L respectively). This difference was not significant (ANOVA p= 0.078), and both levels are within the EU range. These results show similar behaviour to that shown in a study of roadside swales in France (Leroy *et al*., 2016).

5.3 Trial runs - Water PAH Pollution

Over the ten trial runs samples showed reduction in dissolved pollutant concentrations the outflow samples for all target PAHs. Only one outlier was excluded from the result data set, Run 8 inflow sample at 17 minutes had a concentration of 81,441 ng/ml (Grubbs test determined). Based on the anaysis, this one sample fell so far out of the range of the rest of the data set it was determined to be an anomolous result, possibly caused by contamination in the extraction process. To prevent overall skewing of the results this data point was excluded in any further analysis. Figure 5-10 shows the PAH concentrations in the inflowing water and the first flush outflow samples. This was done to see the effect that passage through the swale had on the water and pollutants. NAP, FLU, FLAN and PYR all show a decrease between the inflow and outflow samples. CHR also showed this pattern in concentration reduction, except for trial run 8 where the first outflow had an increase compared to the inflow 9 and 17 minute samples. When compared to the inflow 2 minute sample all outflowing samples had significantly lower PAH concentrations, with the only exception being BaP in the first flush samples (Kruskal-Wallis H = 1.12, P = 0.290). BaP was much more varied in concentration, however all values were lower in the first outflow than the 2 minute inflow. The 2 minute inflow had significantly higher concentrations of NAP, FLU, FLAN and PYR than the 17 minute inflow samples (H/P values = 5.33/0.021, 5.61/0.018, 5.23/0.022 and 6.22/0.013 respectively). The two minute samples were not significantly different when compared to the 9 minute samples, although as can be seen in Figure 5-10 the majority of samples had lower concentrations. Trial run 3 had not only elevated concentrations,

but the sample from 9 minutes inflow was higher than the 2 minutes sample for all PAHs except NAP. Trial run 3 had the highest recorded concentrations, which after investigation, are believed to be an operator error when dosing the RRD with the creosote, potentially a double dose was added in error. Table 5-9 shows the average PAH concentrations for the inflow samples. The timings given for sampling are to show the difference in pollutant level with the amount of water flowing into the system. Inflow samples across the ten trial runs, showed the dilution effect arising from the increased water flow mixing the constant rate flowing RRD pollutant and successfully simulated the first flush effect. Schiff, et al. (2016) demonstrated that the peak pollutant concentrations occurred in runoff during the first ten minutes of the storm, this was seen in these results. As shown by the minimum and miximum values recorded in Table 5-9 there was wide vairation in the concentrations recovered druing the ten trial runs. Of the targeted PAHs only BaP showed small range in concentrations. As a highly hydrophobic substance, this is likely to have adsorbed to the particulates and removed from the simulated storm (Xing *et al.,*2006)

Table 5-9 Descriptive statistics for inflow samples taken over ten trial runs. Where a value was below the detectable level of PAH this is represented by x.

Variable	*Inflow sample time (mins)*	*Concentration (ng/L)*			
		Mean	*SD*	*min*	*max*
NAP	*2*	*28819*	*26599*	*7496*	*88975*
	9	*17704*	*24593*	*1447*	*74162*
	17	*8748*	*13530*	*228*	*32089*
FLU	*2*	*96693*	*77374*	*33717*	*274610*
	9	*77640*	*98508*	*3564*	*319390*
	17	*36593*	*49441*	*x*	*150951*
FLAN	*2*	*117507*	*73981*	*45393*	*294650*
	9	*110738*	*154153*	*21519*	*502010*
	17	*53767*	*50109*	*2310*	*137150*
PYR	*2*	*59633*	*44367*	*24534*	*167314*
	9	*57478*	*87034*	*x*	*293024*
	17	*26670*	*28295*	*x*	*80164*
CHR	*2*	*8614*	*6501*	*1725*	*18934*
	9	*13323*	*18890*	*1503*	*44156*
	17	*2903*	*3114*	*164*	*7682*
BaP	*2*	*84*	*59*	*x*	*166*
	9	*68*	*106*	*x*	*307*
	17	*52*	*60*	*x*	*139*

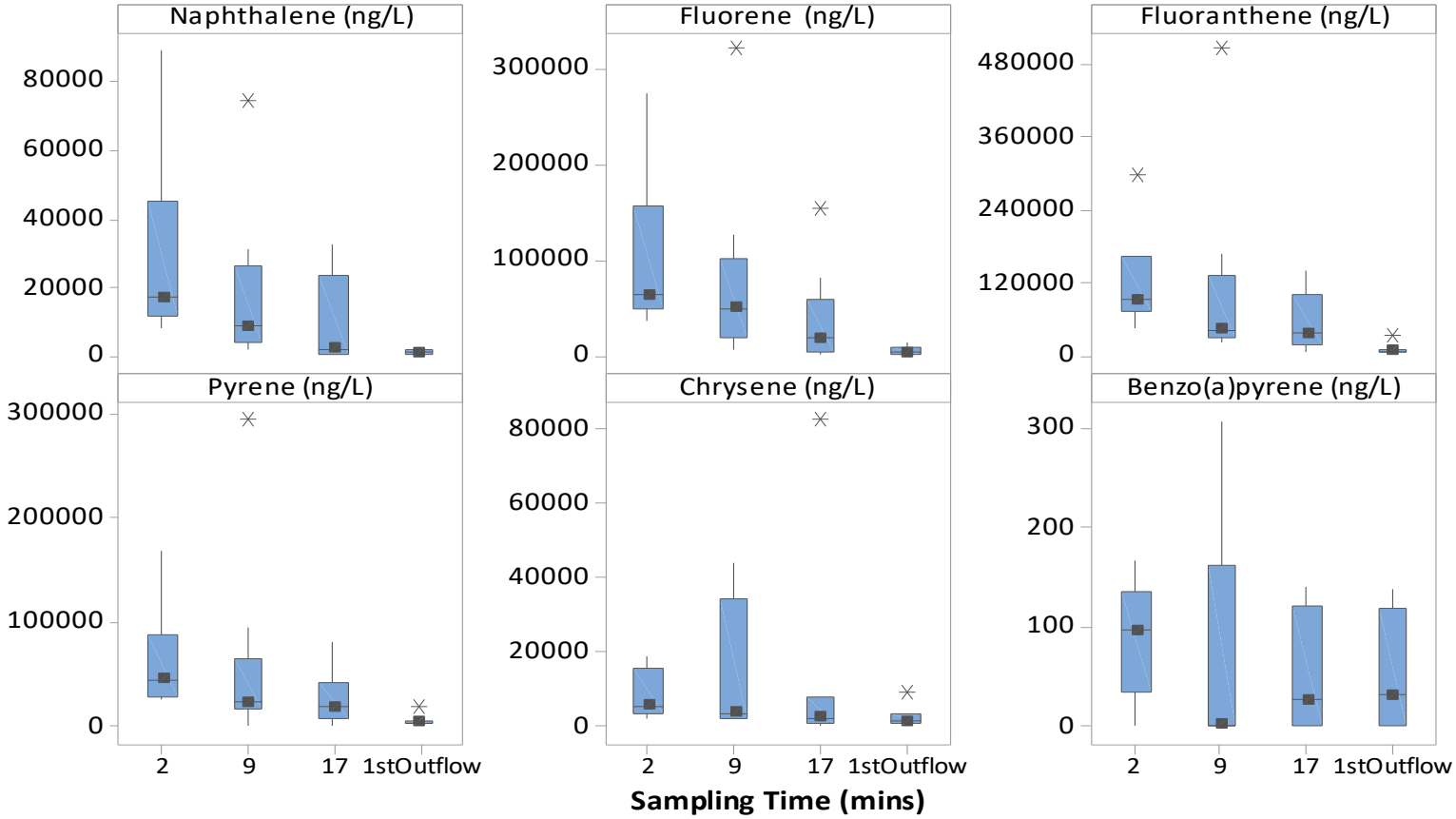

Figure 5-10 PAH concentrations from ten experimental runs. Inflow samples taken at 2, 9 and 17 minutes, shown with the first outflow PAH concentrations. First outflow samples were collected from the first water flowing out the swale, on average 7.45 mins after the start of the trial runs.

Table 5-10 Descriptive statistics for outflow samples taken over ten trial runs.

PAH	Outflow sample (mins)	PAH concentration (ng/L)			
		Mean	SD	min	max
NAP	1st outflow	796	662	125	2137
	out 23 min	862	624	237	2298
	out 30 min	561	359	6	1167
	out 60 min	400	215	167	729
	out 90 min	307	161	89	534
FLU	1st outflow	3551	4639	17	12451
	out 23 min	2563	2193	33	6714
	out 30 min	2240	2465	37	8392
	out 60 min	1044	1361	61	4604
	out 90 min	1190	1952	19	6432
FLAN	1st outflow	6413	8594	466	30075
	out 23 min	4101	2484	932	8313
	out 30 min	2814	1323	875	5300
	out 60 min	1195	600	511	2165
	out 90 min	1987	1570	341	5240
PYR	1st outflow	3908	4919	263	17510
	out 23 min	1988	1269	322	4244
	out 30 min	1038	606	92	2098
	out 60 min	375	349	X	905
	out 90 min	509	576	X	1965
CHR	1st outflow	2064	2662	X	8480
	out 23 min	1083	1533	X	3659
	out 30 min	1196	1855	X	5290
	out 60 min	2087	3167	X	9324
	out 90 min	1443	1789	X	5402
BaP	1st outflow	53	60	X	138
	out 23 min	28	48	X	136
	out 30 min	12	25	X	61
	out 60 min	20	45	X	136
	out 90 min	20	46	x	138

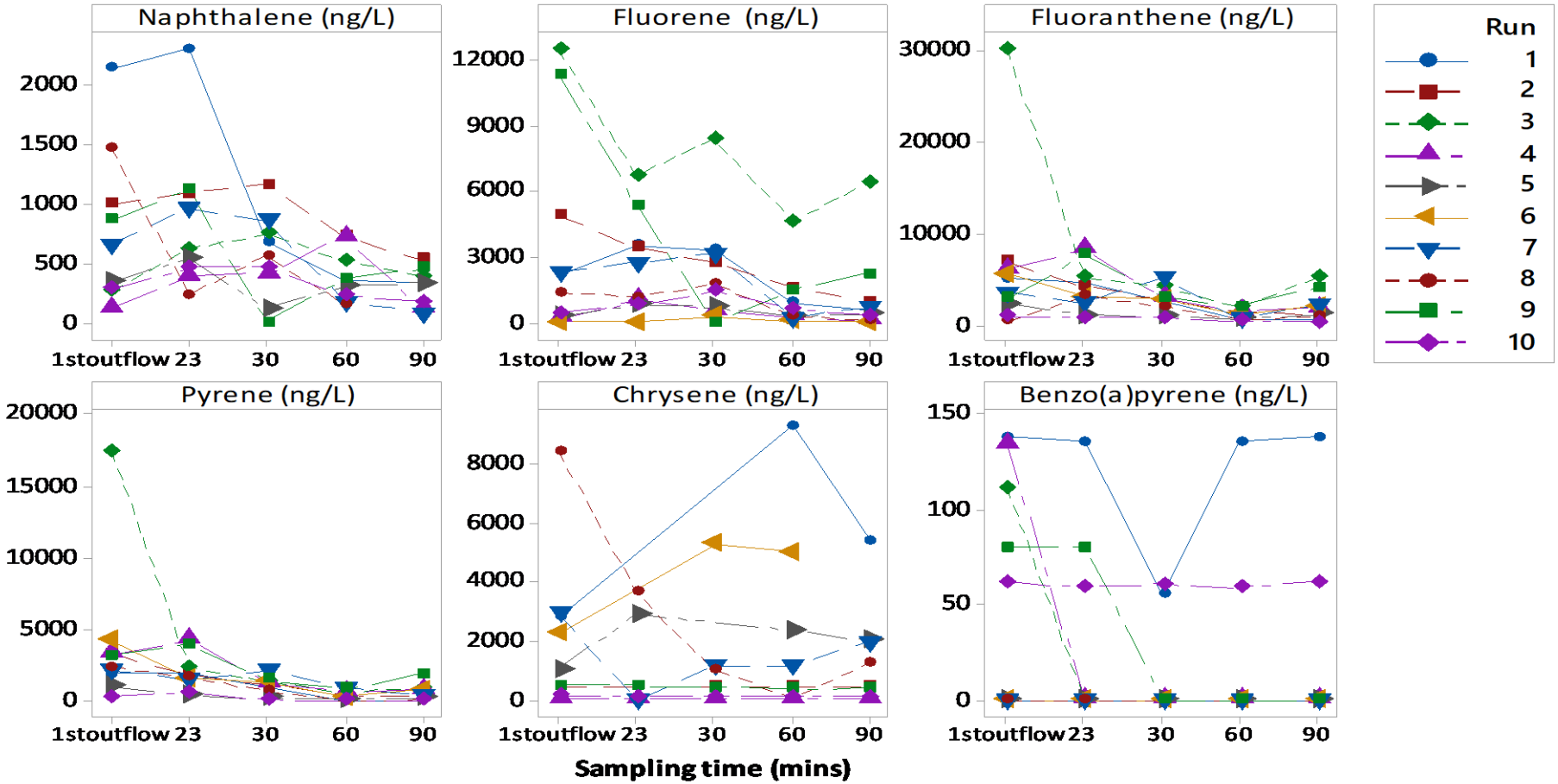

Figure 5-11 Outflow PAH concentrations from ten trial runs. Reduction in concentration is seen over time for majority of pollutants. First outflow was on average at 7.45mins

Outflow samples showed a pattern of reduction in PAH concentration over time, Table 5-10 gives the mean concentration from ten trial runs. The first outflow concentrations were generally higher than later samples, a trend that for the majority of samples continued with time. Figure 5-11 shows the concentrations with time for each individual run. From this graph it can be observed that while trial run 3 had higher than average pollutant input, this is largely reduced in the outflow to similar levels of the other runs. Figure 5-12 shows concentrations of FLU and FLAN from trial run 6 as an example of the decrease in the water over time.

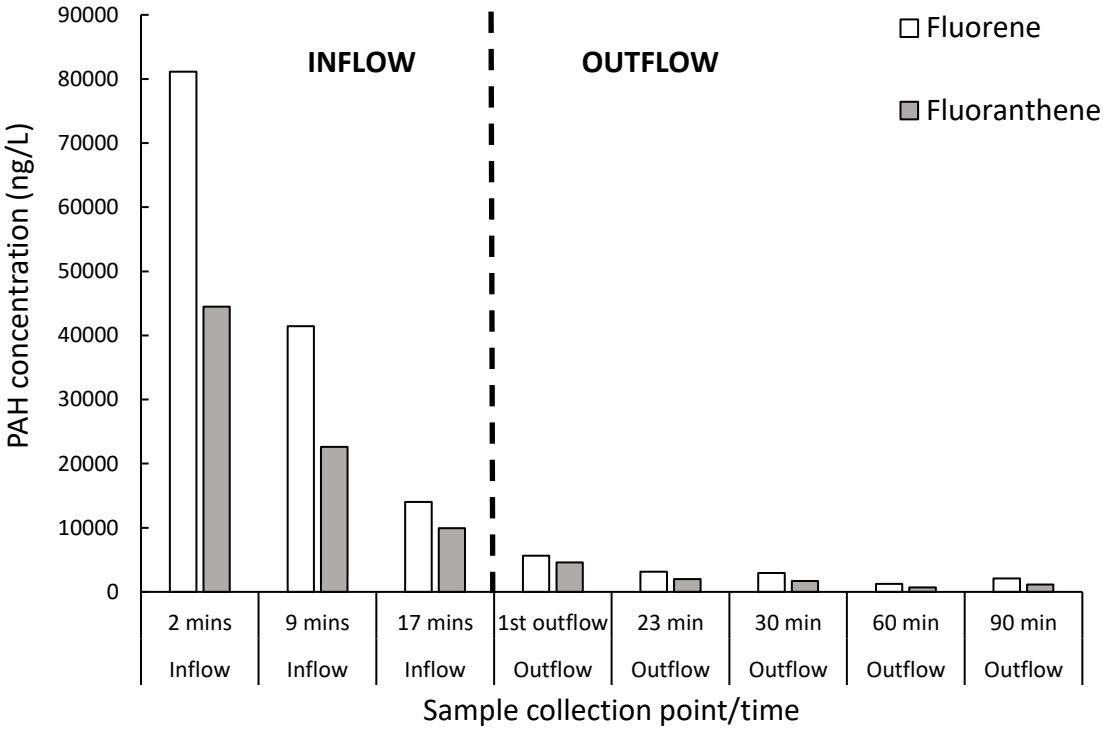

Figure 5-12 Fluorene and Fluoranthene concentrations from inflow and outflow samples at specified time points. Example shows trial run 6 results.

As an indication of the pollutant removal efficiency of the swale, the first inflow sample and the first flush were compared. Table 5-11 shows the mean PAH concentrations gathered from all ten of the trial runs for inflow and first outflow and the difference between the two values. This gives an indication of the reduction in PAH concentration during passage through the swale in a simple mass balance calculation. The pollution

reduction in the system will have been lost due to a number of processes in the soil of the swale, these processes are discussed in greater detail in section 5.5.1.

Table 5-11 Simple mass balance equation showing amount of PAHs lost as water flowed through the swale.

PAH	*Inflow (ng/L)*	*First outflow (ng/L)*	*Difference (ng/L)*
NAP	*28819*	*796*	*28023*
FLU	*96693*	*3551*	*93142*
FLAN	*117507*	*6413*	*111094*
PYR	*59633*	*3908*	*55725*
CHR	*8614*	*2064*	*6550*
BaP	*84*	*53*	*31*

For NAP, FLU, FLAN and PYR removal efficiency on average over the ten trial runs was 94 %, 96 %, 95 % and 94% respectively. CHR and BaP both had instances of increases in concentration. For CHR this occurred in trial run 8 where the concentration was nearly doubled in the outflow sample compared to the 2 minute inflow (96 % increase). Overall there was an average of 54 % removal of CHR. The elevated BaP concentration was detected in first outflow sample of trial run 3, with an increase of 27 %. On average there was a 51 % removal of BaP in the water. Table 5-12 gives the % reduction in PAH concentration in the first outflow samples compared to the 2 minute inflow. An average reduction is given for each PAH in the final row.

Table 5-12 Reduction in dissolved PAH concentration (%) between 2 minute inflow sample and first outflow. Total PAH is shown in the first column, individual PAHs are also shown. Where value is missing, concentrations detected in both inflow and outflow samples were below limit of detection, so comparisons could not be made.

Trial run	*Concentration reduction (%)*						
	$\sum_6$PAH	*NAP*	*FLU*	*FLAN*	*PYR*	*CHR*	*BaP*
1	*93*	*77*	*96*	*94*	*96*	*~*	*79*
2	*91*	*91*	*91*	*92*	*88*	*95*	*~*
3	*93*	*100*	*95*	*90*	*90*	*100*	*-27*
4	*96*	*99*	*100*	*93*	*93*	*~*	*19*
5	*96*	*94*	*99*	*95*	*96*	*62*	*100*
6	*92*	*~*	*100*	*93*	*90*	*18*	*100*
7	*97*	*99*	*98*	*98*	*98*	*74*	*~*
8	*97*	*96*	*99*	*100*	*97*	*96*	*100*
9	*92*	*93*	*80*	*97*	*91*	*89*	*38*
10	*99*	*98*	*99*	*98*	*99*	*89*	*41*
Average	*95*	*94*	*96*	*95*	*94*	*54*	*56*

Results of the original testing of the swale hydrology and during the trial runs showed that the swale performed consistently, and in line with hydraulic properties demonstrated in the field (Davis *et al*., 2012, Lucke *et al.*, 2014). The swale also performs to guidelines set out in the CIRIA SuDS manual (Woods-Ballard *et al.*, 2015). The retention time shown in the trials and initial test runs was eight and a half minutes, this falls above the minimum of eight minutes recommended by the San Mateo pollution prevention program. This document states that if 90 % of the flow enters the swale at one location, a minimum retention time of 8 minutes should be seen in the longest flow path (cityofsanmateo.org).

Spearman rho correlation analysis indicates that there are some significant relationships, especially between the PAHs, Table 5-13. NAP, FLU FLAN and PYR all show to be strongly correlated with each other. This was shown in the outflow waters as all concentrations reduced over time (Figure 5-11). NAP and BaP were not correlated (p-value 0.075)

Table 5-13 Spearman rho correlation analysis of Swale inflow and outflow variables. Strong correlations are seen between PAHs

		Air temp	EC	COD	NAP	FLU	FLAN	PYR	CHR
EC	rho	-0.384							
	P-value	0.000							
COD	rho	0.078	0.417						
	P-value	0.494	0.000						
NAP	rho	-0.053	-0.455	-0.216					
	P-value	0.664	0.000	0.074					
FLU	rho	0.080	-0.546	-0.19	0.845				
	P-value	0.485	0.000	0.095	0.000				
FLAN	rho	-0.105	-0.513	-0.303	0.721	0.801			
	P-value	0.359	0.000	0.007	0.000	0.000			
PYR	rho	-0.114	-0.46	-0.246	0.748	0.792	0.96		
	P-value	0.312	0.000	0.028	0.000	0.000	0.000		
CHR	rho	-0.145	-0.197	0.024	0.591	0.555	0.523	0.556	
	P-value	0.250	0.115	0.852	0.000	0.000	0.000	0.000	
BaP	rho	0.308	-0.317	0.188	0.216	0.381	0.268	0.300	0.264
	P-value	0.005	0.004	0.095	0.075	0.001	0.018	0.007	0.033

The longer the water resides in the swale soil, the slower it flows, giving particles greater chance to be filtered out in the soil. This will lead to a reduction in PAH levels in the water, especially of the more hydrophobic PAHs. These removal results are similar to those mentioned by Leroy *et al.* (2015), which showed consistently high removal rates by a roadside swale over a 12 month period. The results shown in the current research are lower than those of Leroy *et al.* (2015), however consideration should be given to the timescale, 12 months to 2 years for the Leroy *et al.* and 20 weeks for the present study. There was also negative correlation between EC and all PAHs except CHR, indicating that as COD levels rise the PAH levels are decreasing. For CHR a negative relationship was shown, just not large enough to be significantly correlated.

Over the ten runs, the water PAH concentrations were significantly reduced from the initial inflow, showing a high performance of the swale.

5.4 Trial runs – soil

PAH concentrations were analysed for every run, at all sampling locations. Samples were collected in triplicate. Due to the heterogeneity of environmental samples, and the PAH propensity for adhesion to soil particulates, this section will look at concentrations for each run individually, before considering the effect of the PAHs together. Descriptive statistics for PAHs in each run are presented in Appendix 8.4 tables 8-6 to 8-28. The following sections will discuss the results with regards to distribution of the PAHs along the length of the swale, infiltration below the surface and build-up over time.

5.4.1 Trial runs – PAH fate.

To assess the movement of PAHs along the length of the swale samples were taken at the specified sampling locations. When looking at distribution of the PAHs along the swale in the surface layer, there was much variation and no clear patterns across all ten trial runs. Kruskal-Wallis analysis of the surface layer, across the ten trial runs showed that there were significant differences for all PAHs, Table 5-14. Due to the nature of the data, triplicates for each locations and non-normal distribution, identification of where the difference occurred was not possible. However, graphs of the data give visual indications of where such differences might be occurring. These will be discussed for each PAH individually.

Table 5-14 Kruskal-Wallis results of comparison of PAH concentrations between the ten trial runs for the 0 – 5 cm and 5 – 10 cm soil layers.

PAH	*0 – 5 cm layer*			*5 – 10 cm layer*		
	H	*DF*	*P*	*H*	*DF*	*P*
NAP	*79.78*	*9*	*0.000*	*89.7*	*9*	*0.000*
FLU	*69.28*	*9*	*0.000*	*5.7*	*9*	*0.770*
FLAN	*68.34*	*9*	*0.000*	*61.75*	*9*	*0.000*
PYR	*99.63*	*9*	*0.000*	*99.07*	*9*	*0.000*
CHR	*110.85*	*9*	*0.000*	*93.44*	*9*	*0.000*
BaP	*100.55*	*9*	*0.000*	*107.53*	*9*	*0.000*

5.4.1.1 Naphthalene

Naphthalene has high potential to become dissolved and therefore highly mobile in storm water, and this was demonstrated by the results collected in this study. NAP was seen in all sample locations in the 0 – 5 cm layer, for all trial runs, except for trial runs 2, 4 and 5 where it was not detected at the 1 m location for run 2, 3 m location for run 4 and locations 1 and 2 m for run 5. Figure 5-13 shows the mean concentrations for all runs in the surface 0 – 5 cm layer. There was no emerging pattern of surface PAH concentration distribution over the ten trial runs. NAP showed consistent levels along the swale throughout the ten trial runs, with higher concentrations towards the beginning of the swale. When looking at the standard deviation in samples, the values show lots of overlap, as demonstrated with no significant difference in concentration between locations (Kruskal-Wallis H =0.75, DF = 4, P = 0.946). This could be due to the solubility of NAP meaning that it was transported in the water and deposited as the water filtered through the vegetation. This vegetation may have provided greater potential for adsorbing to particulate surface areas. Vegetation cover in swales and other SuDS systems has been shown to promote particulate capture as water flows though (Tsavdaris, 2014). Sedimentation and filtration in the vegetated layer have been reported as two key PAH removal processes in swales (Stagge et al., 2012).

When considering just the surface soil level, it would appear that very low concentrations will be detectable, and very little accumulation over time (Table 5-15). This lack of accumulation is evident in the quick reduction of concentration in the soils after the high dosing during trial run 3 (Figure 5-13). By trial run 4 the levels of NAP had reduced significantly compared to levels in the previous run (Kruskal-Wallis H = 21.77, DF = 1, P = 0.000). Between trial runs 4 and 10 there is no sign of levels increasing, indicating that in the intervening days between trial runs, the NAP is being lost. Of the many pathways that PAHs can be lost, volatilisation is perhaps a likely cause. Volatilisation of NAP happens very easily, and with a high vapour pressure (Henry's Constant) the PAH is readily desorbs from soil particles and goes into the gaseous phase (Trapido, 1999; Allan *et al*., 2016).

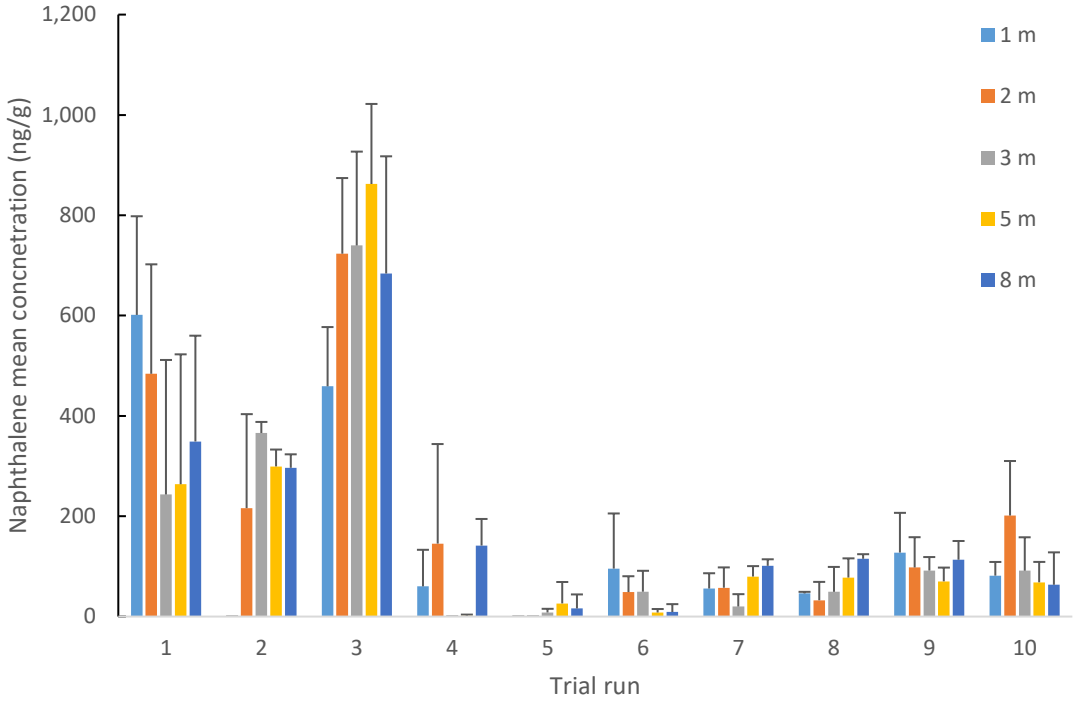

Figure 5-13 Mean naphthalene concentrations for each trial run in the 0 – 5 cm layer. Error bars are standard deviation of the mean.

Table 5-15 Mean concentration and standard deviation of naphthalene values found in the 0 5 cm layer for all trial runs.

Location	Variable	Trial run Nap concentration (ng/g)										$\sum_{10}$ Mean (ng/g)
		1	2	3	4	5	6	7	8	9	10	
1m	Mean	601	0	459	60	0	96	56	46	128	82	153
	SD	197	0	118	73	0	110	31	321	79	27	96
2m	Mean	484	216	723	145	0	49	58	33	98	210	202
	SD	218	187	151	198	0	32	41	37	60	109	103
3m	Mean	243	366	740	0	8	50	20	49	92	91	166
	SD	268	22	187	0	7	42	25	49	27	67	69
5m	Mean	264	299	862	144	26	8	80	78	70	68	190
	SD	259	34	160	25	43	7	21	38	27	41	66
8m	Mean	349	297	684	142	16	9	101	115	113	63	189
	SD	211	27	234	53	28	16	13	9	37	65	69

Figure 5-14 shows the 5 – 10 cm NAP concentrations for all ten trial runs. As seen in this figure it was only in the first five trial runs that NAP was detected in the 5 – 10 cm layer. NAP was the only PAH that was detected in the 5 – 10 cm layer in the first trial run. The concentration of NAP in trial run 1 was significantly lower in the second layer for the 1 m and 2 m sampling locations (ANOVA: f=16.61, P = 0.015 and F=7.88, P=0.048 respectively). There was a reduction in concentration at the 3 and 5 m locations, but due to variation in samples the reduction was not significant. These results for trial run 1 show that the majority of the NAP was being retained in the upper layer. The infiltration through to the second layer is likely due to transportation of NAP in its dissolved form in the water as it filtered through the soil. In trial runs 2 and 3 the NAP concentration was higher in the 5 – 10 cm layer for all locations. Figures 5-15 and 5-16 show the NAP concentration across the 0 – 5 cm and 5 – 10 cm layers. Trial run 1, Figure 5-15, NAP concentrations were higher in the top layer. For trial run 2 the higher levels in the mid layer were significantly higher than the upper layer (Figure 5-16) except for the 5 m location (ANOVA f = 6.61, P = 0.098). There was no significant difference in concentration between the sampling points (ANOVA F = 0.29, P = 0.883). Many studies have shown that NAP is one of the most abundant PAHs in storm and rain water (e.g Brown & Peake, 2006 , Kim & Young, 2009, Prabhukumar & Program, 2011, Leroy *et al.*, 2015). NAP has the highest solubility of the PAHs studied (Table 2-9), so it is the most likely to be the

last to sorb to particulates (Yang *et al.*, 2011a). This property also make it highly likely to get re-suspended in subsequent storm flows (Allen *et al.*, 2015). The increase in concentration in the 5 – 10cm layer in runs 2 and 3 may have been due to this factor. Another influence to the high values is if a sample was taken and had a concentrated dose, this would raise the average concentration level, this can be seen in the size of the error bars. It does not, however, explain why the same trends were not seen again in later runs.

Some of the variation seen over the ten trial runs in NAP concentration may be attributed to the variation in levels in the inflow water. As shown previously there was a wide range of concentration levels recovered in the inflow water samples.

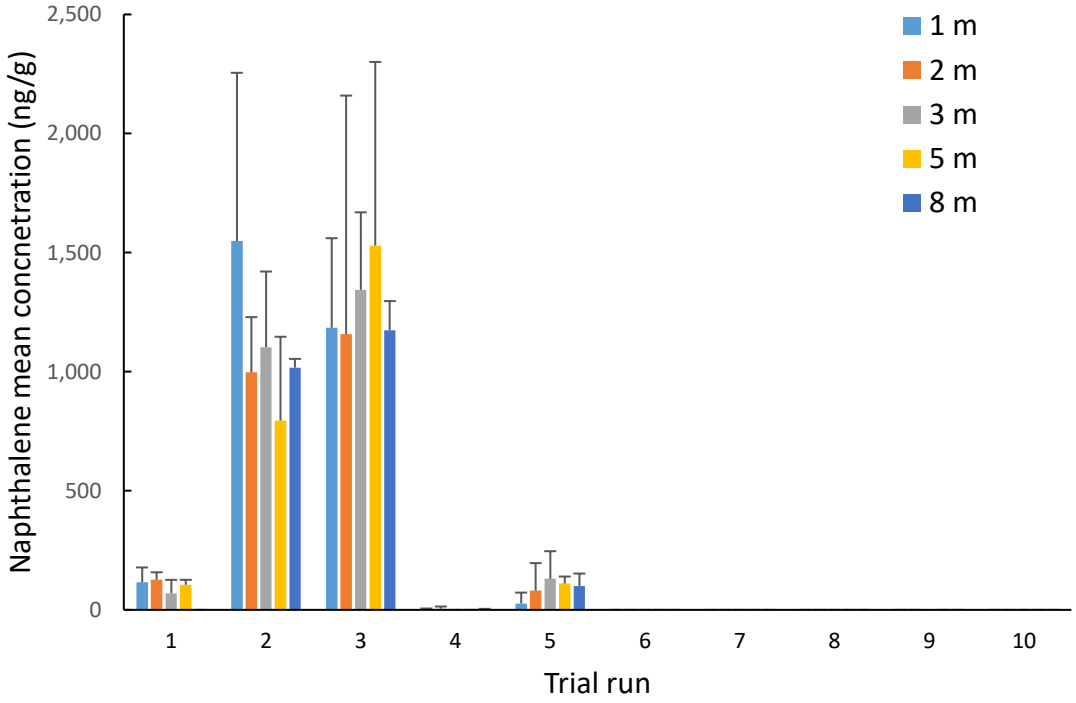

Figure 5-14 Mean naphthalene concentrations for each trial run in the 5 – 10 cm layer. Error bars are standard deviation of the mean.

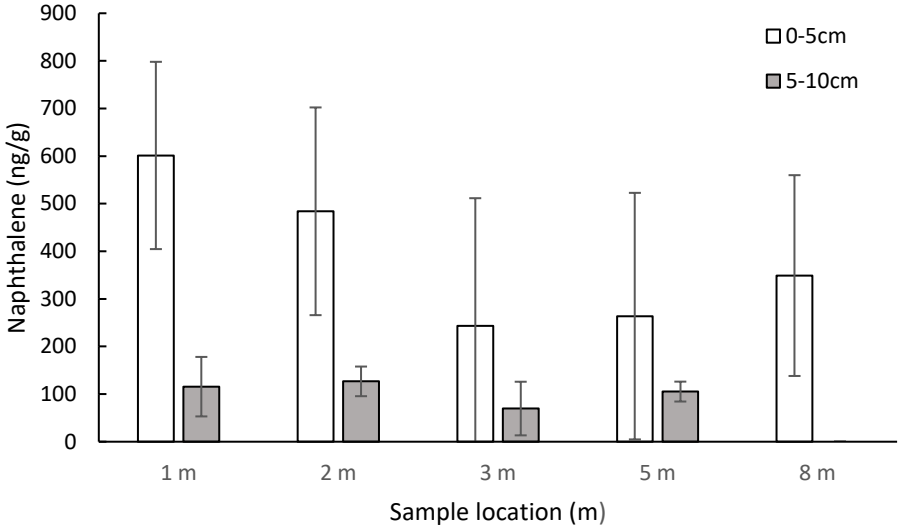

Figure 5-15 Naphthalene concentrations in each soil layer from trial run 1.

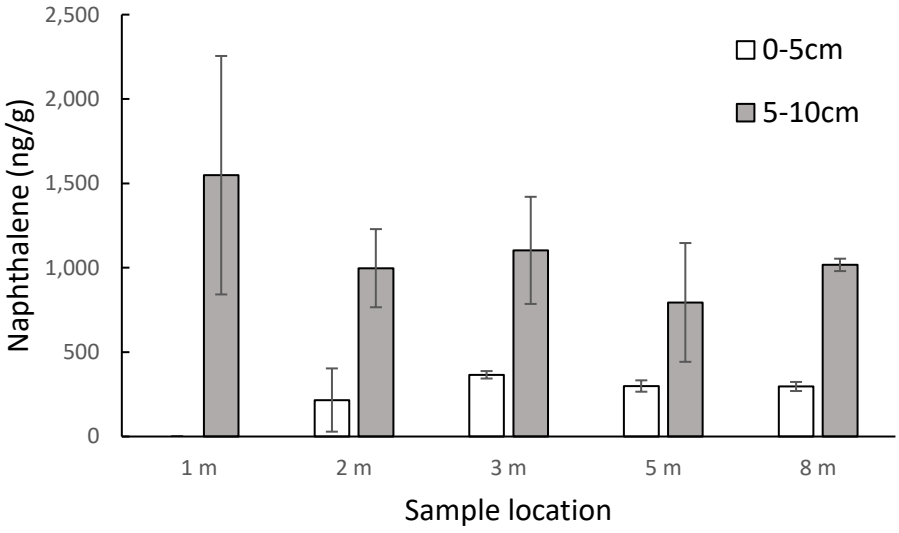

Figure 5-16 Naphthalene concentrations in each soil layer from trial run 2.

Figure 5-17 shows two contour plots, trial runs 1 and 10, generated in Minitab of distribution of NAP along the length of the swale and depth. Contour plots are generated by connecting points with the same response value, producing contour lines (support.minitab.com). From these two plots it is easier to visualise the distribution of the PAH over the distance and depth variables of the experiment. Due to its chemical composition and structure, NAP is the PAH with the highest solubility and easy

volatilization out of all the studied PAHs (Liu *et al.*, 2014). Behaviour seen in the controlled study varied to that found in the study of the Waterlooville swale. In the exposed environment NAP was present at constant levels, including in the control samples. These findings suggest that in the field for NAP the predominant route to the swales is from atmospheric deposition rather than via storm water runoff. The reduction in NAP concentration after the third trial run in the presented results could suggest that some degradation is occurring between storm events. There was a period of one month between runs 3 and 4 due to logistics or running the trials, this allowed a longer period between sampling than in all other trial runs which were separated by only two weeks. The most likely routes for this decrease are as mentioned volatilisation or microbial degradation. In a study of the biodegradation of NAP Andersen *et al.* (2008) showed that more than 90% of NAP vapours were biodegraded aerobically within the 5 – 10 cm above the water table in the natural environment. The same study showed that in laboratory column experiments had a mean biodegradation rate of 11 days. These results might offer explanation of the drop in NAP after the third trial run. Volatilisation is also increased with temperature, which given the higher temperatures seen in the final few trial runs (Figure 5-3) may explain the lack of NAP in these runs.

For the purposes of SuDS maintenance if considering only NAP the surface layer is the area of most concern, however given the likelihood of volatilisation it is unlikely that NAP will need to be a target for intense remediation.

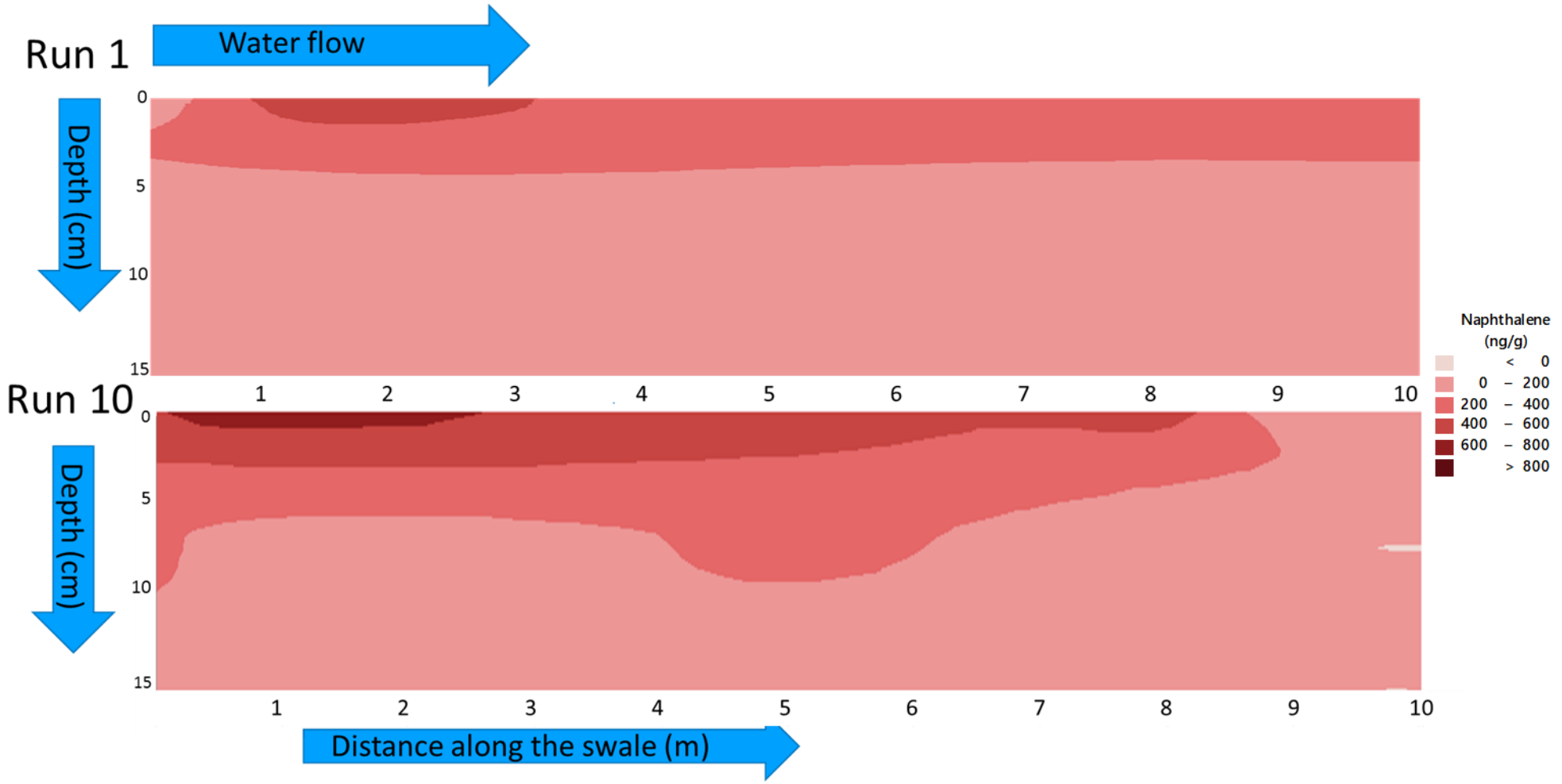

Figure 5-17 Contour plots showing concentrations of NAP along the swale from trial run 1 and trial run 10.

5.4.1.2 Fluorene

FLU was present in the surface samples (0 – 5 cm) for all ten trial runs. However, towards the end of the testing run lower concentrations were determined, with trial run 10 only having FLU presence detected in the 1 and 2 m samples. Figure 5-18 shows the 0 – 5cm layer concentrations (converted to Log_{10}) from all trial runs. Trial run 6 showed increased levels in the first three sampling locations, and very low levels in the final two locations. For the majority of samples the interquartile ranges are large, further showing the variability of environmental sampling.

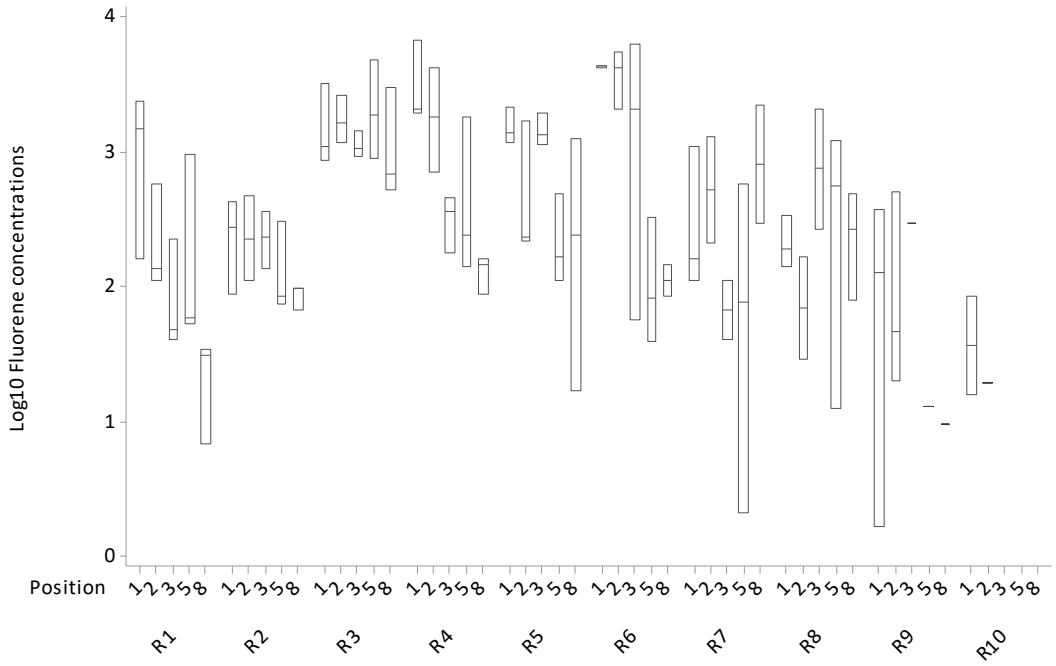

Figure 5-18 Box plot showing Fluorene concentrations in the 0 - 5 cm layer for each trial run.

Table 5-16 shows the mean concentrations and standard deviation for samples at each location for each run. Statistically there was a difference in concentration between locations (Kruskal-Wallis H = 12.24, P = 0.016). For the majority of runs the highest concentrations were found in the first 3 m of the swale. Two runs had higher concentrations further down the swale, runs 3 and 7 which skews the total mean for all ten runs to show that concentrations were high all along the swale. The most notable exception was in trial run 7 where the final sample location had the highest mean concentration for the run (mean 1263 ng/g). Concentrations in run 3 were high in all locations with the 5m location having the highest levels.

Table 5-16 Mean concentration and standard deviation of fluorene values found in the 0 5 cm layer for all trial runs.

Location	*Variable*	*Trial run (ng/g)*										*$\sum_{10}$Mean (ng/g)*
		1	*2*	*3*	*4*	*5*	*6*	*7*	*8*	*9*	*10*	
1m	*Mean*	*1344*	*265*	*1718*	*3585*	*1583*	*4327*	*462*	*221*	*170*	*33*	*153*
	SD	*1114*	*173*	*1304*	*2740*	*530*	*4283*	*563*	*99*	*192*	*45*	*96*
2m	*Mean*	*276*	*193*	*1813*	*2235*	*715*	*3907*	*501*	*66*	*191*	*6*	*202*
	SD	*266*	*244*	*753*	*1789*	*846*	*1737*	*694*	*90*	*274*	*11*	*103*
3m	*Mean*	*105*	*243*	*1149*	*329*	*1485*	*2852*	*50*	*793*	*97*	*0*	*166*
	SD	*106*	*115*	*271*	*140*	*440*	*3240*	*56*	*1150*	*167*	*0*	*69*
5m	*Mean*	*351*	*152*	*2536*	*731*	*253*	*148*	*220*	*590*	*4*	*0*	*190*
	SD	*512*	*128*	*2034*	*941*	*204*	*151*	*315*	*593*	*7*	*0*	*66*
8m	*Mean*	*24*	*86*	*1414*	*131*	*512*	*77*	*1263*	*279*	*3*	*0*	*189*
	SD	*15*	*18*	*1419*	*38*	*671*	*74*	*1366*	*205*	*6*	*0*	*69*

The mean FLU concentrations for all ten runs (final column of Table 5-15) shows that the levels were high in locations 5m and 8m, but this result is skewed slightly by the higher levels seen in runs 3 and 7. When comparing with surface flow the highest dosed water reached a distance of 3.1m by 9 minutes into the trial. During this time the more intensely polluted water will have been filtering through the soil level with the particulates settling out into the soil layer. As flow increased, the water travelled further over the surface before infiltration, this would have transported the polluted particulates to the further end of the swale (Tedoldi *et al*., 2016). When the water was flowing faster there is less time for particulate to settle out of the water column (Bach *et al.*, 2014).

Levels of FLU were rarely detected in the 5 – 10 cm layer samples (Figure 5-19) and showed no signs of accumulation, statistically there was no difference in the concentration between each trial run (Kruskal-Wallis H = 5.7, P = 0.770). In trial runs 1 and 9 there was no FLU detected below the 0 – 5 cm layer (Figure 5-18). Where there was penetration into the 5 – 10 cm layer, the concentration was lower than the concentration in the 0 5 cm layer. Trial run 10 was the only exception to this, with a mean concentration of 33 ng/g in the 0 – 5 cm layer and 209 ng/g in the 5 – 10 cm layer at the 1 m sampling location. Individual run analysis (ANOVA) of FLU between the layers, showed that in trial run ten the increase in the second layer at 1 m was significantly higher (f = 12.19, P = 0.008). Fluctuations seen in the 5 – 10cm layer will most likely be through movements of the particulates through the soil as the flow water dislodges and re-suspends particulates back into the water column. Degradation may also be occurring due to the presence of bacteria, this is not an anoxic layer so microbial degradation may still be taking place (Glick, 2010). In this layer photodegradation will not be playing a part in the losses.

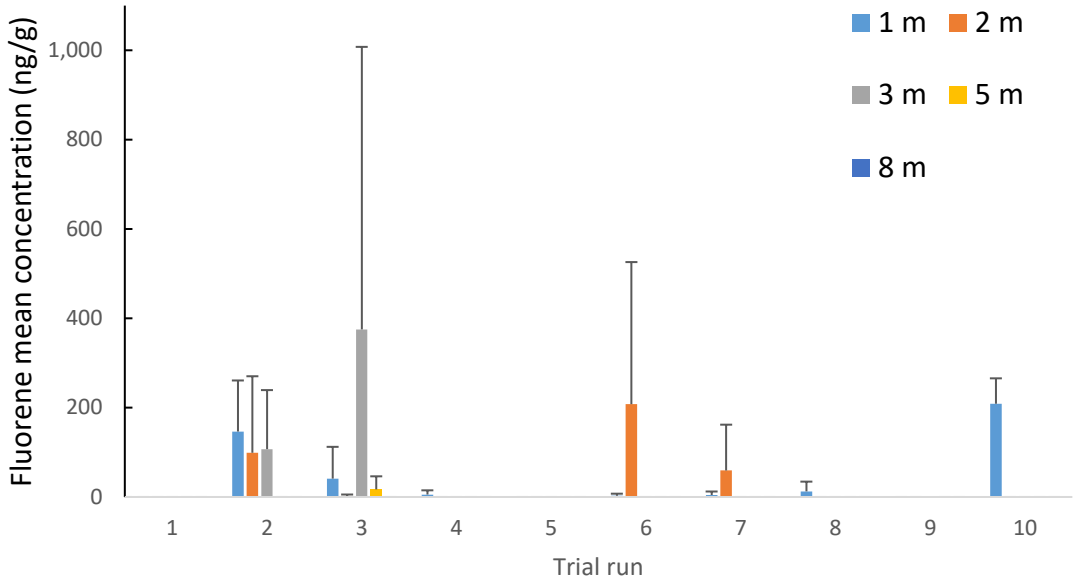

Figure 5-19 Mean fluorene concentrations (ng/g) in the 5 – 10 cm layer for each trial run. Error bars are standard deviation of the mean.

5.4.1.3 Fluoranthene

In the surface layer of the swale, Figure 5-20, FLAN showed a general pattern of increasing concentration over time, until the 6th and 7th trial runs. Thereafter levels decreased, with no levels found in sampling location 8 m for the final trial. Trial run 7 was an exception to this, having the highest mean concentration in the 8 m location over all ten trial runs (32,127 ng/g). The changes in concentration between the trial runs was significant (Kruskal-Wallis H = 68.34, P = 0.000) which highlights the heterogeneity of the samples. In the study at Waterlooville a gradual decline in FLAN concentration over time was also seen (Roinas *et al.*, 2014a).

When comparing the individual locations along the swale there is, in general, higher concentrations at the start of the swale. Table 5-17 shows the means and standard deviation for the trial runs, the overall combined mean values show that there was a higher concentration for 8 m samples, compared to the mid swale samples (3 and 5 m). These results also show a great deal of variety in the data set, with large range in concentrations. This is led by the high level in the 7th trial run, otherwise the trend was for a lower level at 8 m compared to those at the beginning of the swale. In contrast to all the other PAHs, FLAN did not show the same elevated levels in run 3 when a

suspected dosing error occurred. Checks were made on the programming of the settings on the GC-MS and no error detected. It is difficult to determine why this was the case, one possible reason would be that an error was made in the analysis or extraction process, however this seems unlikely due to the presence of the other PAHs in high concentrations.

No microbial testing was completed on the swale, however there may have been microbial degradation of the PAHs, specific species of bacterial have been identified that utilise certain PAHs (Kanaly & Harayama, 2000; Kuiper *et al.*, 2004; Mueller & Shann, 2006) so it is possible that FLAN was being microbially degraded. A study of a bacterial strain found in a Chinese oil refinery showed association with FLAN degradation (Jin *et al.*, 2017). However considering the elevated levels seen in the other PAHs, and lack of reduction in later runs of FLAN this seems to be unlikely. If the bacteria was present and degrading at a high level, this should have been seen in the later runs.

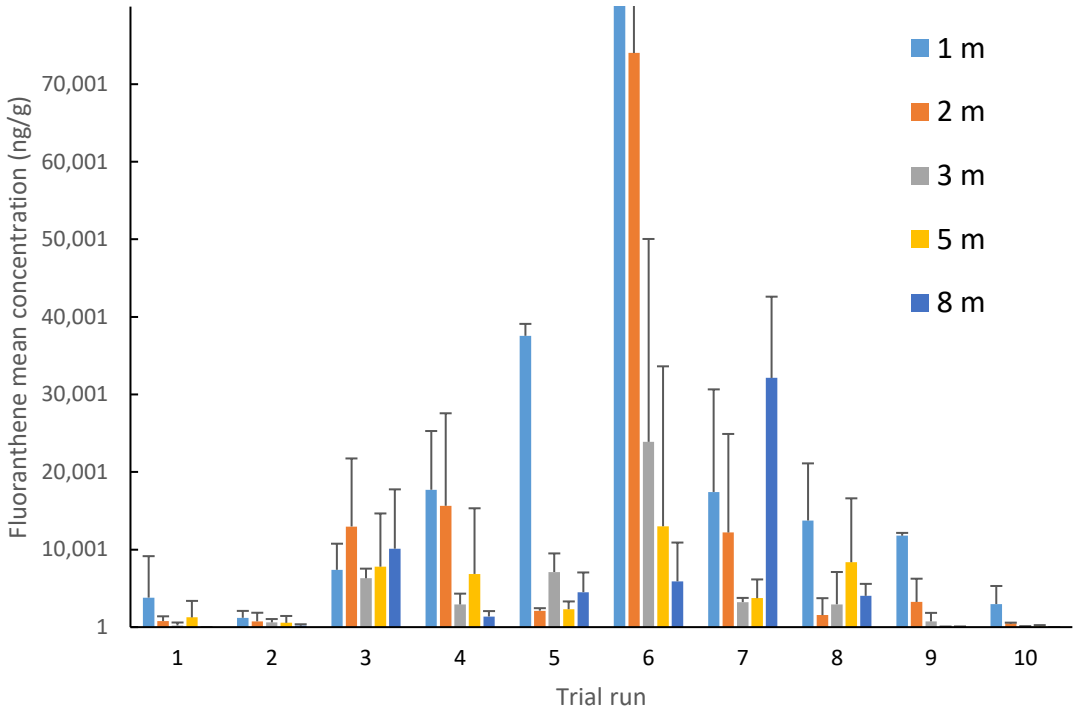

Figure 5-20 Mean Fluoranthene concentrations (ng/g) for 0 – 5 cm layer. Error bars are standard deviation of the mean. (Graph capped at 80,000ng/g for clarity, trial run 6 0-5cm mean = 148,157 ng/g).

Table 5-17 Mean concentration and standard deviation of fluoranthene values found in the 0 5 cm layer for all trial runs.

Location	Variable	Trial run (ng/g)										$\sum_{10}$ Mean (ng/g)
		1	2	3	4	5	6	7	8	9	10	
1m	Mean	3807	1205	7391	17713	37560	148157	17429	13745	11789	2976	26177
	SD	5344	888	3367	7570	1538	142354	13226	7369	362	2330	18434
2m	Mean	781	752	12974	15644	218	74018	12201	1547	3250	488	12187
	SD	612	1101	8776	11928	326	28308	12704	2187	2992	90	6902
3m	Mean	218	614	6297	2926	7107	23893	3228	2944	740	48	4801
	SD	378	429	1242	1392	2398	26150	540	4164	1098	83	3787
5m	Mean	1256	553	7795	6861	2314	13005	3733	8368	34	94	4401
	SD	2126	886	6862	8462	1000	20620	2419	8237	43	164	5081
8m	Mean	-	203	10113	1373	4512	5902	32127	4034	32	-	5829
	SD	-	167	7649	695	2538	5003	10477	1543	55	-	2812

From the second trial run, infiltration into the 5 - 10 cm layer was seen, Figure 5-21. Concentrations of the ten trial runs were significantly different both between runs (Kruskal-Wallis H = 61.75. P = 0.000), and sampling locations (Kruskal-Walls H = 28.32, P = 0.000).

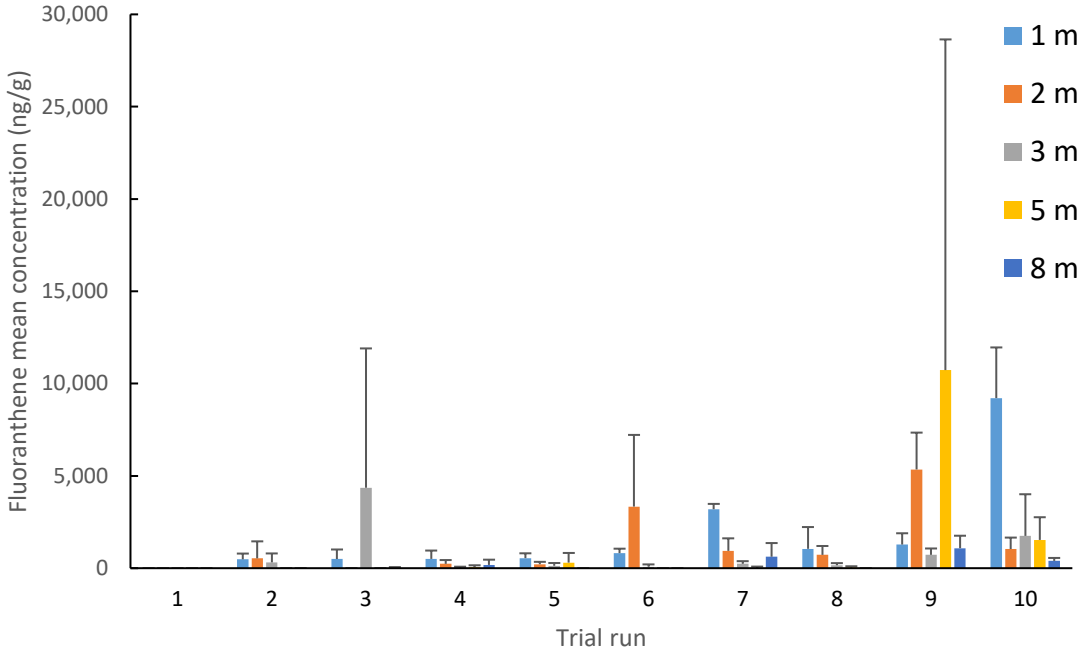

Figure 5-21 Mean fluoranthene concentrations (ng/g) for 5 – 10 cm layer for each trial run. Error bars are standard deviation of the mean.

Up until the 8th trial run, the levels were lower in the mid layer compared to the surface layer. Kruskal-Wallis analysis shows that there were significant differences in concentration levels between the layers (H = 18.67, P = 0.000). In the 9th run the samples at 2 and 5 m were increased compared to the surface layer (2 m: 0 -5 cm = 3250 ng/g, 5 – 10 cm = 5348, 5 m: 0 – 5 cm = 33 ng/g, 5 – 10 cm = 10732). The 5 m concentration was the highest detected in the mid layer throughout all ten trial runs. In the final run the mid layer had higher levels of FLAN at all sampling locations compared to the 0 -5 cm layer, indicating that water bound FLAN, and any particulates with FLAN already attached are filtering through the soil pore holes, and not being retained in the upper layer.

5.4.1.4 Pyrene

PYR samples returned some very high concentrations in the surface layer, not just in the third trial run, but runs 6 and 8 also had elevated levels, Figure 5-22. Trial run 7 was unusual in that no PYR was detected in any samples However, as other PAHs were detected in these samples and the parameters of the GCMS had not changed, the lack of PYR presence is accepted as an indication of the true levels in these particular samples.

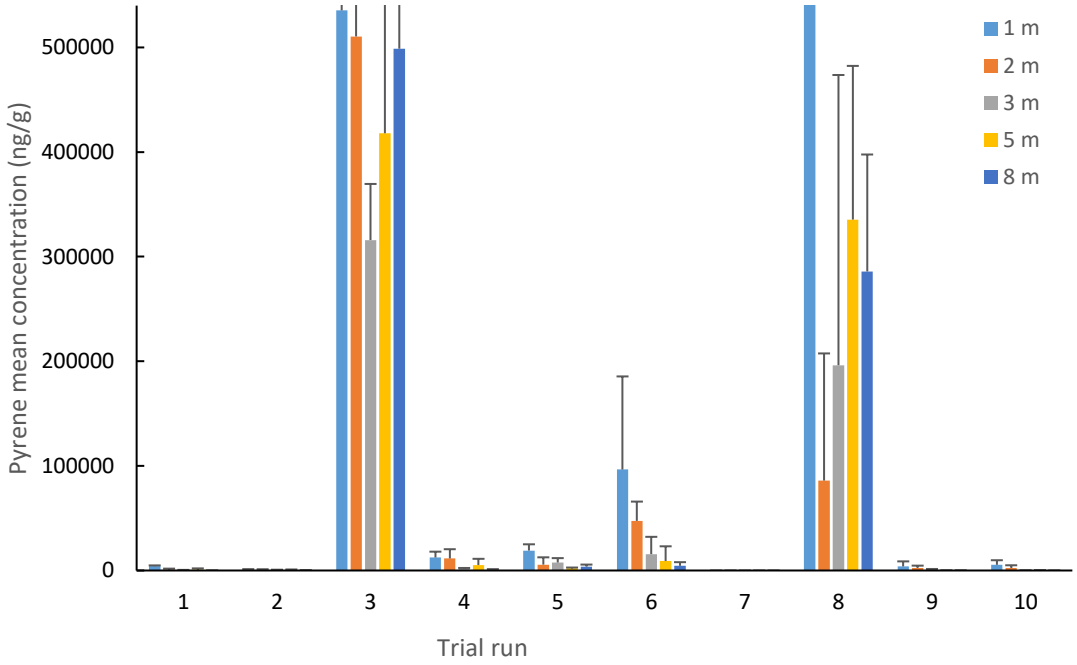

Figure 5-22 Mean pyrene concentrations (ng/g) for 0 – 5 cm layer. Error bars are standard deviation of the mean. (Graph capped at 5000,000 ng/g for clarity in the lower concentrations, missing values can be found in table 5-17).

Figure 5-23 shows the same data as Figure 5-22 converted to a log scale, to show with greater clarity the lower concentrations. Here the changes in concentration along the length of the swale is clearer. There is a statistical significance between sampling locations over the ten trial runs (Kruskal-Wallis H =108.37, P = 0.000), however given the large range in concentrations between runs this might not give a true indication as the large values returned in a number of runs may be skewing the result. Table 5-18 gives the 0 – 5 cm mean PYR concentrations and SD for all trial runs. The final column gives

the mean for the combined trial runs. With the elevated levels it is difficult to detect any patterns occurring in the data, with no consistent trends observed in deposition. The only exception to this was the 1m sampling location always returned the highest concentration level. The variety see in the levels of concentration may be attributable to the resuspension of particulates, moving the adsorbed PAHs through the swale. A number of studies have shown that particulates drop out if the water column in the first section of a swale (Lucke et al., 2014). As the swale mesocosm in this study is fairly short it is likely that particulates are not having time to settle out, and so pollution is detected all along the swale. For example Barrett *et al.* (1998) showed that a grass strip of at least 8m would be effective at removing storm water pollutant loads. To get a true indication of settlement patterns, in future a longer swale mesocosm would give better indications.

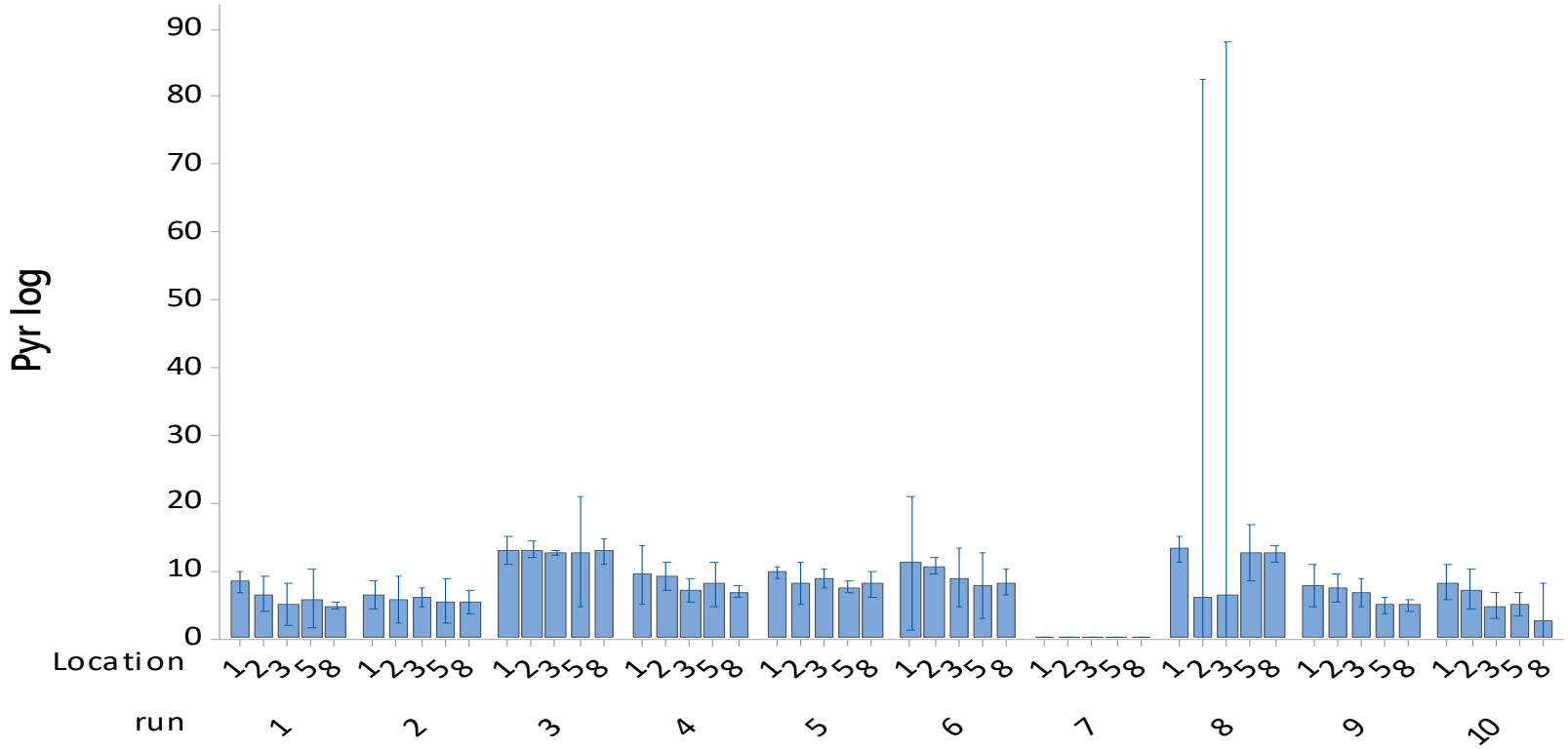

Figure 5-23 Pyrene concentrations converted to Log scale for greater understanding of the lower concentrations. Error bars show 95% confidence interval for the mean.

Table 5-18 Mean concentration and standard deviation of pyrene values found in the 0 5 cm layer for all trial runs.

Location	*Variable*	*Trial run (ng/g)*										*$\sum_{10}$Mean (ng/g)*
		1	*2*	*3*	*4*	*5*	*6*	*7*	*8*	*9*	*10*	
1m	*Mean*	*4150*	*766*	*535388*	*12402*	*19012*	*96504*	*-*	*624484*	*3874*	*5417*	*130200*
	SD	*720*	*521*	*403472*	*5596*	*6031*	*89022*	*-*	*343515*	*4848*	*4380*	*85811*
2m	*Mean*	*945*	*545*	*510488*	*11515*	*5566*	*47421*	*-*	*85954*	*2421*	*2246*	*66710*
	SD	*829*	*651*	*254155*	*8821*	*7021*	*18432*	*-*	*121557*	*2218*	*2745*	*41643*
3m	*Mean*	*271*	*486*	*315878*	*1437*	*7605*	*15652*	*-*	*196195*	*902*	*150*	*53858*
	SD	*305*	*268*	*53625*	*970*	*4209*	*16510*	*-*	*277461*	*541*	*103*	*35399*
5m	*Mean*	*814*	*427*	*417939*	*5175*	*2033*	*9040*	*-*	*335477*	*142*	*192*	*77124*
	SD	*1189*	*459*	*333747*	*5973*	*783*	*14073*	*-*	*146889*	*56*	*147*	*50332*
8m	*Mean*	*112*	*236*	*498796*	*956*	*3626*	*4489*	*-*	*285852*	*134*	*35*	*79424*
	SD	*22*	*130*	*412317*	*330*	*2015*	*3466*	*-*	*111822*	*43*	*40*	*53019*

After the first trial run there is consistently penetration of PYR into the mid layer of soil. This follows a general pattern of decreasing with distance, for each run. Despite very high concentrations in the surface layer, levels in the 5 – 10 cm layer were much more consistent between the runs, Figure 5-24. Over the ten trial runs there is a slow build-up of concentration, a significant difference between runs was returned (Kruskal-Wallis H = 99.07, P = 0.000). There were also significant changes in concentration between sampling locations across all ten runs (Kruskal-Wallis H = 11.32, P = 0.023).

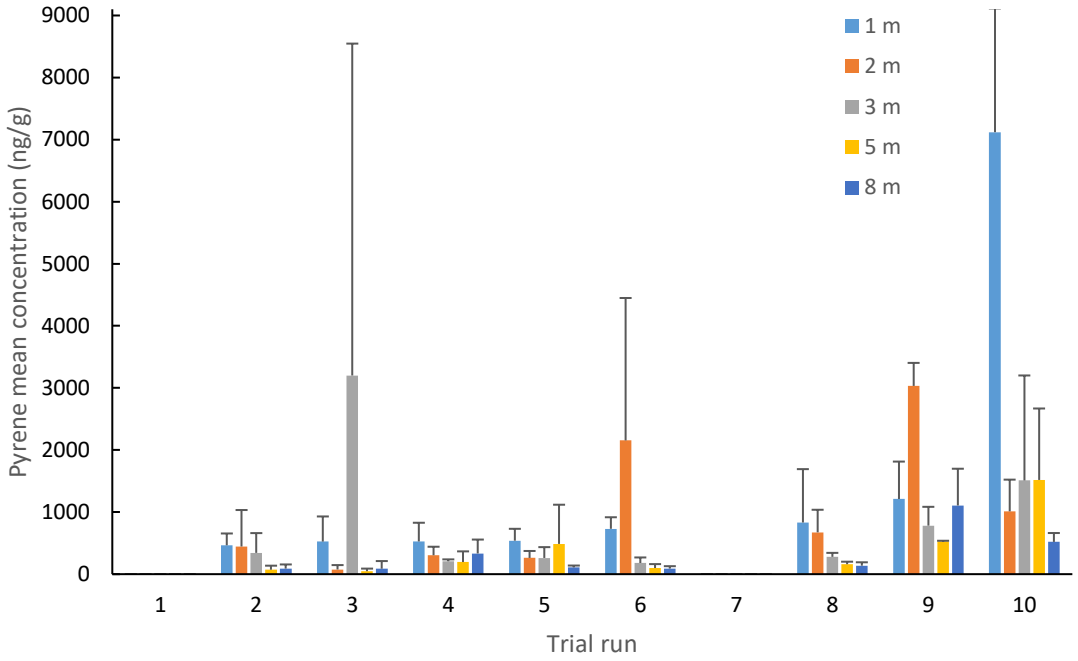

Figure 5-24 Mean pyrene concentrations (ng/g) for 5 – 10 cm layer. Error bars are standard deviation of the mean.

Similar to FLAN, in trial run 9 concentrations in the mid layer were starting to exceed the surface layer. Trial run 10 had higher levels in the all sampling locations for the 5 – 10 cm samples, except 2 m, when compared to the surface layer.

In the runs analysed for the presence to PAHs in the 10 -15 cm layer, PYR was present in all. In trial run 8 the levels were higher than the mid layer, however in the final two runs this was not the case, with mean concentrations being lower. Over the ten trial runs there was no clear pattern of accumulation in the surface, this is likely to have been obscured by the elevated levels detected during the mid runs. When considering the 5

– 10 cm layer over the course of the ten trials, it would appear that a gradual increase in the concentrations is beginning to be indicated.

5.4.1.5 Chrysene

In the first trial run CHR was only detected at sampling locations 1 m and 5 m, it was not detected in the 5 – 10 cm layer at any location. Figure 5-25 shows the mean concentrations at each location for all ten trial runs. In the 0 – 5 cm layer, CHR had some of the highest concentrations recorded. A mean concentration of 3096 µg/g was detected from the 1 m samples in trial run 4. These elevated levels in trial run 4 follow the increased pollutant input from run 3, showing an accumulation at 1, 2 and 5 m locations.

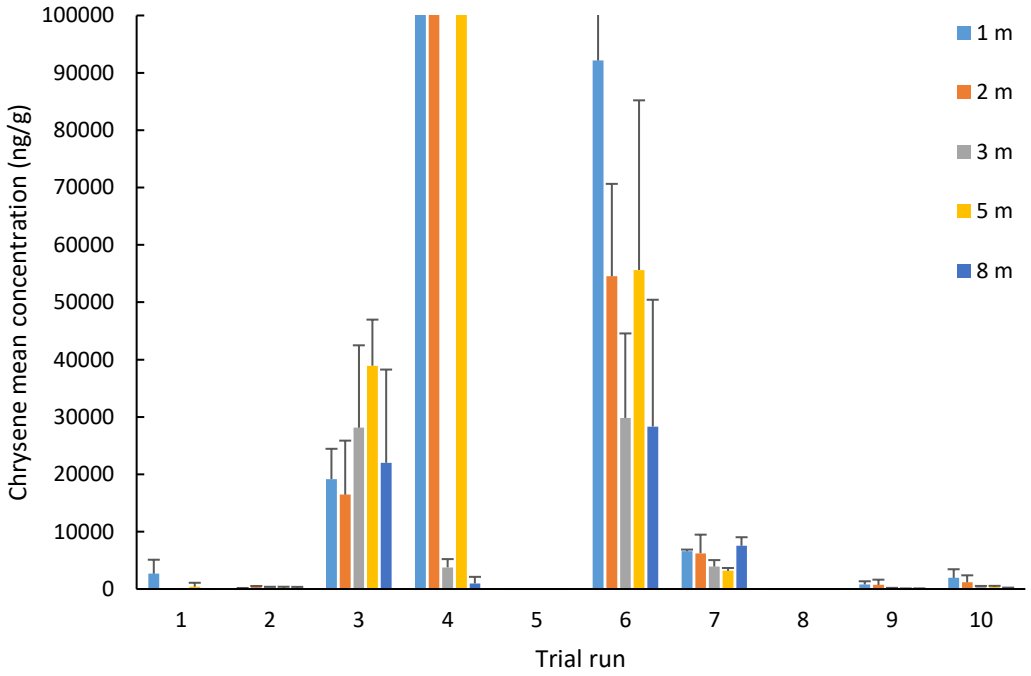

Figure 5-25 Mean chrysene concentrations (ng/g) for 0 – 5 cm layer. Error bars are standard deviation of the mean. (Graph capped at 100,000 ng/g for clarity in the lower concentrations, missing mean and SD values can be found in table 5-17).

Table 5-19 Mean concentration and standard deviation of chrysene values found in the 0 5 cm layer for all trial runs.

Location	*Variable*	*Trial run (ng/g)*										*$\sum_{10}$Mean (ng/g)*
		1	*2*	*3*	*4*	*5*	*6*	*7*	*8*	*9*	*10*	
1m	*Mean*	*2669*	*107*	*19168*	*3096366*	*-*	*92143*	*6580*	*-*	*789*	*618*	*321844*
	SD	*2441*	*74*	*5282*	*1985170*	*-*	*45465*	*294*	*-*	*563*	*147*	*203944*
2m	*Mean*	*0*	*323*	*16451*	*368769*	*-*	*54531*	*6234*	*-*	*913*	*757*	*44798*
	SD	*0*	*203*	*9420*	*521518*	*-*	*16110*	*3248*	*-*	*917*	*282*	*55170*
3m	*Mean*	*0*	*369*	*28122*	*3778*	*-*	*29826*	*3909*	*-*	*150*	*578*	*6673*
	SD	*0*	*23*	*14370*	*1435*	*-*	*14737*	*1134*	*-*	*54*	*229*	*3198*
5m	*Mean*	*398*	*272*	*38937*	*899958*	*-*	*55630*	*3168*	*-*	*71*	*682*	*99912*
	SD	*689*	*127*	*8033*	*80329*	*-*	*29574*	*499*	*-*	*32*	*234*	*11952*
8m	*Mean*	*0*	*259*	*22017*	*967*	*-*	*28330*	*7540*	*-*	*85*	*280*	*5948*
	SD	*0*	*113*	*16244*	*1156*	*-*	*22105*	*1490*	*-*	*23*	*201*	*4133*

Table 5-19 gives all mean concentrations for CHR surface layer, from the standard deviation figures large variations in the data is clear. These means, however are noticeably high, mainly due to the high figures returned during a number of runs. While some outliers could be expected, in environmental data they cannot be discounted, and so included in the analysis.

Using the mean from all ten trial runs there was a pattern of a reduction in concentration between the 1 and 3 m sampling locations, before a rise in the 5 m samples and a reduction again in the 8 m samples. Overall the samples from the 8 m point were the lowest for each trial run. Due to the high concentrations recorded in the mid experiment trials it is unclear if there was any accumulation over time in the surface layer. Trial runs 5 and 8 had no detected concentration in the surface layer samples, while investigation did not show up any errors this could be attributed to, it is possible an operator error occurred. The high levels returned, particularly in Run 4 may have been an anomaly when the low levels returned in the 3 m and 8 m samples are taken into consideration. Or there was possibly a number of other explanations, such as pockets of polluted RRD may have accumulated in dams created by vegetation which caused a higher than expected level of pollution. Another possible explanation would be that RRD from previous runs was dislodged from previous resting spots by the flow of water. Resuspension of particulates, and movement further along the swale is a key method of pollutant movement (Allen *et al.*, 2015; Guittonny-Philippe *et al.*, 2014; Gunawardana *et al.*, 2012; Revitt *et al.*, 2017; Weiss *et al.*, 2010). Although the concentrations returned were high, giving a very large confidence interval, all data points were included as with all environmental data the outliers should not necessarily be discounted.

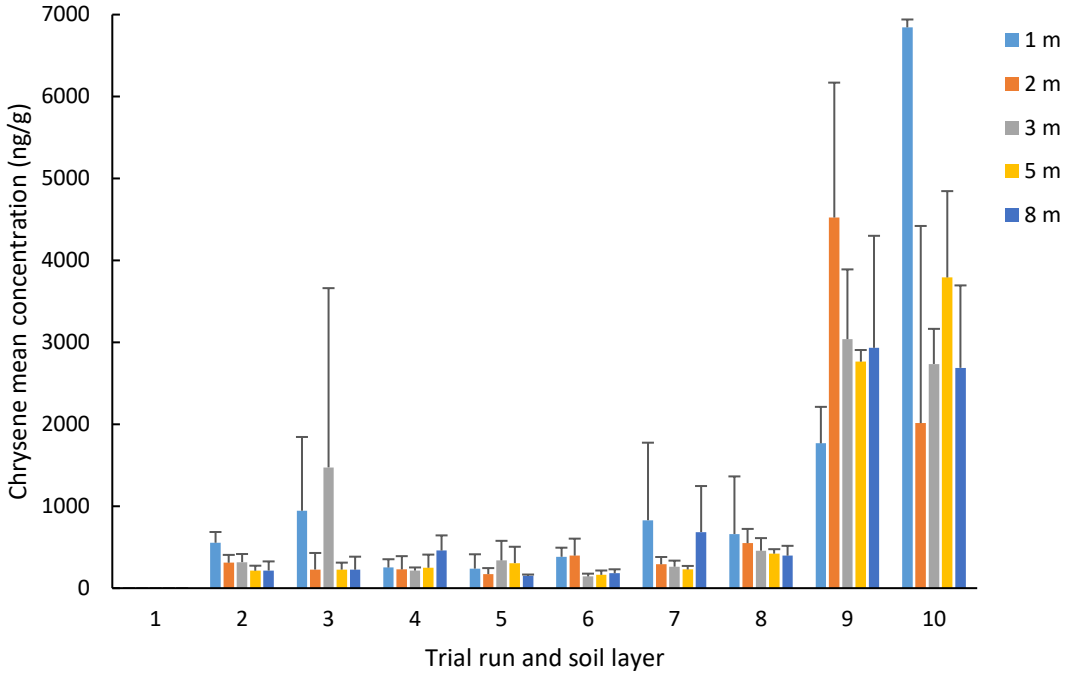

Figure 5-26 Mean chrysene concentrations (ng/g) for 5 – 10 cm layer. Error bars are standard deviation of the mean.

From the second trial there was detectable levels of CHR in the 5 – 10 cm layer (Figure 5-26). For the first eight runs the levels in the mid layer were consistent, with no real increase. Trial run 9 had a large increase in the mean concentrations at all sampling locations compared to run 8. These higher levels were seen again in trial run 10. Statistically, comparison between the runs of the 5 – 10 cm layer showed a significant difference (Kruskal-Wallis H = 93.44, P = 0.000), visually (Figure 5-26) trial runs 9 and 10 are showing a large increase in concentration. Analysis of the 10 – 15 cm layer showed CHR to be present. The levels were consistent across all sampling locations, with little variation.

Figure 5-27 is a contour plot of CHR along the swale form trial runs 1 (top image) and 10 (bottom image), from this image combined with the data used to generate it, it shows that the pollutant is beginning to accumulate in the 5 – 10 cm layer. From this image, the intense pocket of concentration is seen at 1 m sampling point, indicating the vertical flow with little transport of pollutant along the surface of the swale. This agrees with findings that have shown that preferentially heavier PAHs will adsorb to coarser particulates (Aryal *et al.*, 2005). Heavier particles will settle out of the water column much quicker than the lighter particles. This was seen with NAP, which was found along

the surface of the system in Run 1 and Run 10 contour plots (Figure 5-17). Similar patterns of accumulation are shown for BaP (Figure 5-30) in Run 10, however in Run 1 here accumulation was detected further along the swale surface compared to the pattern seen for CHR. Also shown is a zone of pollution further down the swale, this indicates that lateral flow through the swale is occurring. These figures demonstrate the transportation of PYR and accumulation points along the swale.

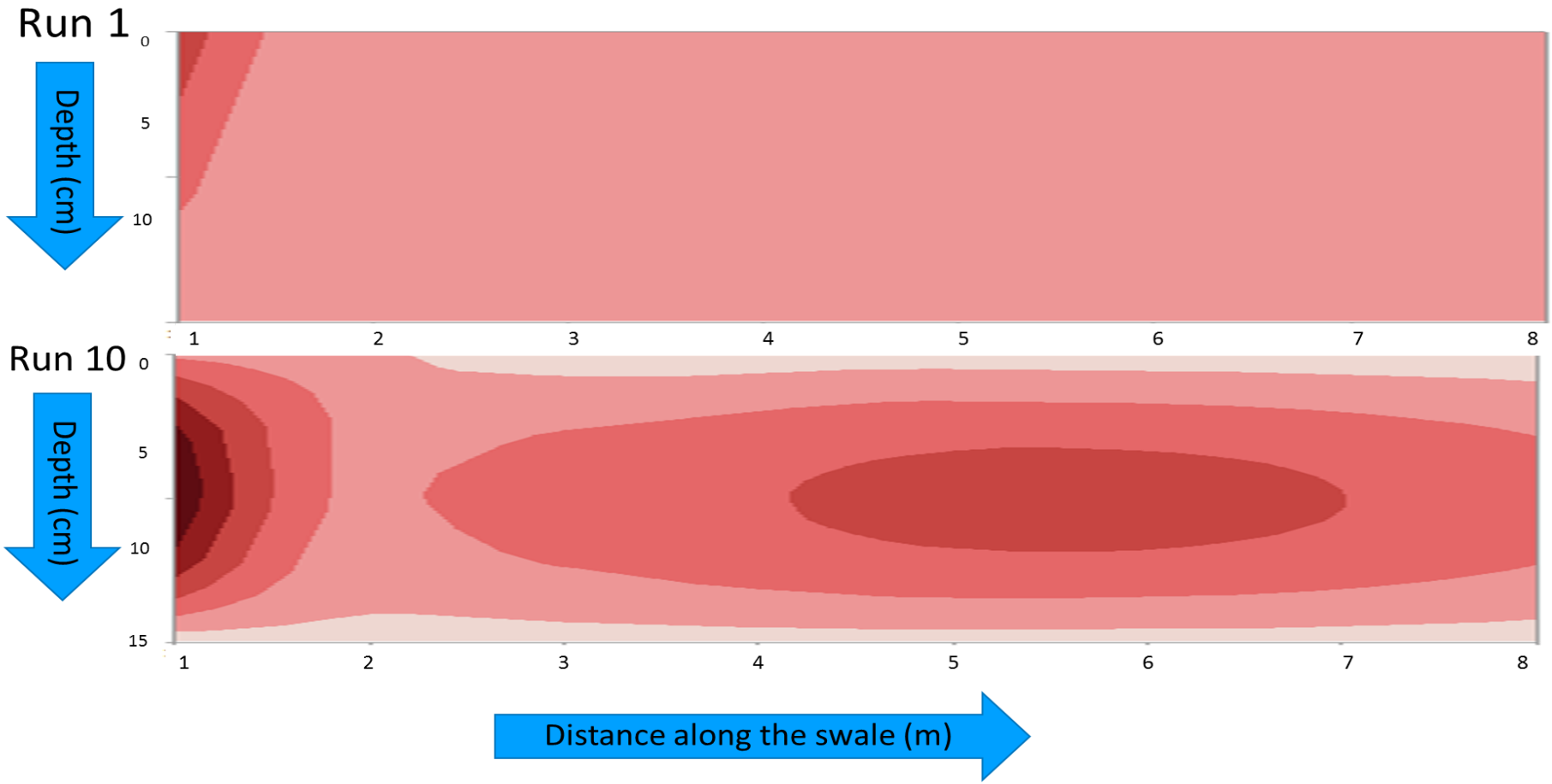

Figure 5-27 Contour plots of chrysene concentrations along the length and depth of the swale. The top plot is from trial run 1, the bottom plot is trial run 10. Darker colours indicate greater concentration pollution.

5.4.1.6 Benzo(a)pyrene

BaP levels were the most consistent throughout all the trial runs, with much lower variation in the triplicate samples. Figure 5-28 shows the 0 – 5 cm layer mean concentrations at each sampling location. After low concentration levels in the first two trial runs, the added input in trial run 3 caused a jump in BaP levels along the swale. In run 4 levels stayed relatively stable when compared to run 3, with slight increases in sample locations 2 and 8 m and decreases at the other locations. When comparing concentration in the surface layer across the ten trial runs there was a significant difference (Kruskal-Wallis H = 100.5, P = 0.000). This might be explained due to the variation in RRD concentration across all the runs. There is however on average, when all ten runs are combined, a decrease in mean concentration along the length of the swale, Table 5-20. This suggests that similarly to previous studies BaP is attached to larger fraction sized particles, which settle out of the water column (Wang *et al*., 2013)

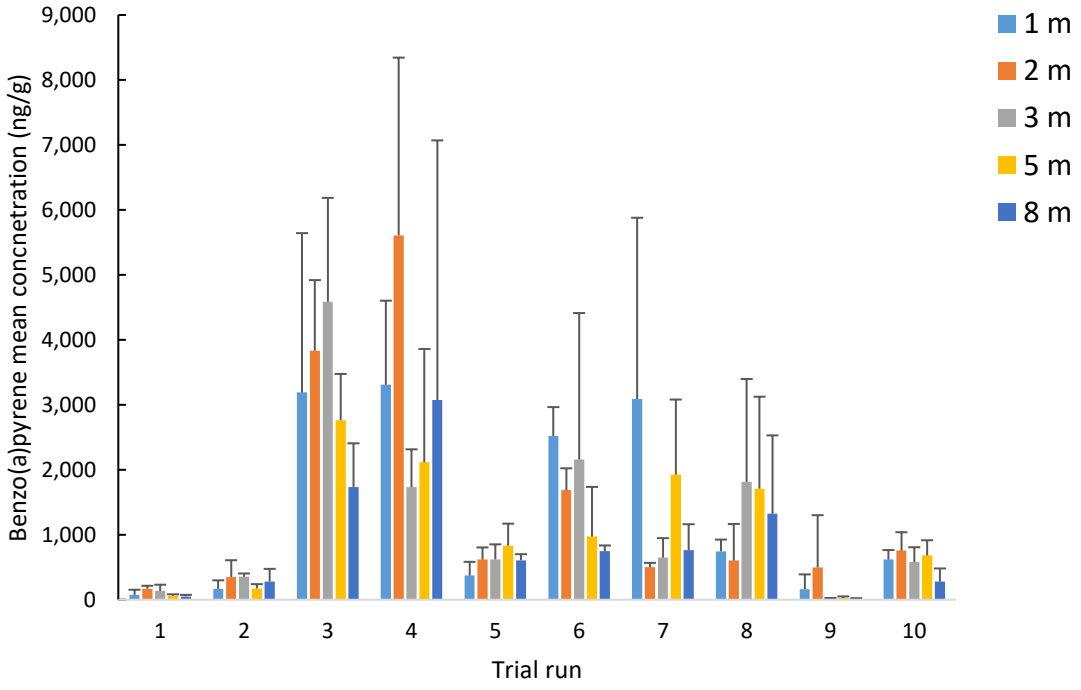

Figure 5-28 Mean BaP concentrations (ng/g) for 0 – 5 cm layer. Error bars are standard deviation of the mean.

Table 5-20 Mean concentration and standard deviation of BaP values found in the 0 5 cm layer for all trial runs.

location	Variable	Trial run (ng/g)										$\sum_{10}$Mean (ng/g)
		1	2	3	4	5	6	7	8	9	10	
1	Mean	74	168	3190	3309	372	2522	3090	744	163	618	1425
	SD	80	131	2452	1293	211	443	2790	182	227	147	796
2	Mean	167	350	3832	5607	618	1687	502	605	497	757	1462
	SD	48	258	1088	2736	187	336	66	561	804	282	637
3	Mean	135	353	4586	1735	621	2158	648	1813	10	578	1264
	SD	96	51	1599	581	232	2254	300	1584	17	229	694
5	Mean	65	173	2762	2116	833	973	1925	1710	27	682	1127
	SD	18	67	713	1744	338	763	1157	1415	24	234	647
8	Mean	50	282	1731	3074	608	749	761	1323	9	280	887
	SD	24	193	676	3995	93	86	401	1207	15	201	689

As observed with most other PAHs there was no BaP in the 5 -10 cm layer in the first trial run, Figure 5-29. Levels in the mid layer remained similar from run to run, with an increase showing in the final few runs. In the final two trial runs the concentrations in the mid layer were higher than those in the surface layer and the 10 -15 cm layer. Sampling locations 1 and 5 m in trial run 10 had equal mean concentrations, 7056 ng/g, which was the highest value over the ten trial runs for BaP across all layers sampled.

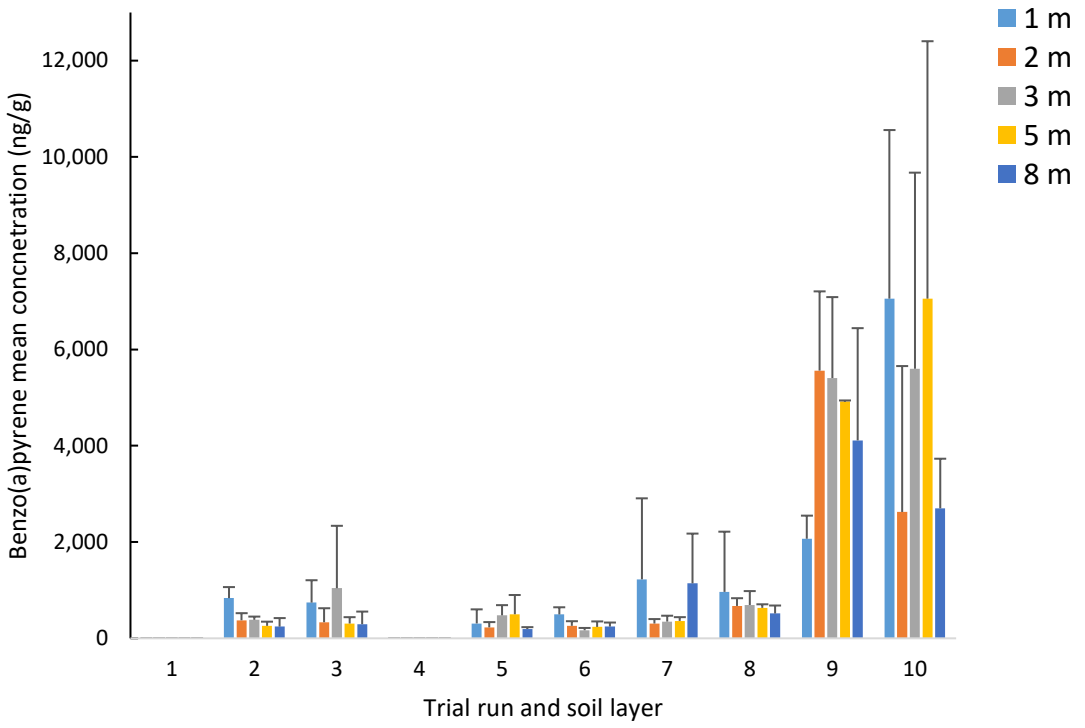

Figure 5-29 Mean BaP concentrations (ng/g) for 5 - 10 cm layer. Error bars are standard deviation of the mean.

Run 4 was unusual in that no BaP was detected in the 5 – 10cm layer (Figure 5-29). Other pollutants were detected on the soil samples, and settings checked on the GC-MS to make sure no changes had occurred. No alterations had happened, so these results were taken as indicator of the true level. Levels of BaP were high on the 0-5cm layer in run 4, so it is possible that the BaP from this run did not filter through, and remained on the surface. Flow through the system is lateral and vertical, as such not detecting pollutant on the mid layer in these samples does not mean it had not flowed through in other locations.

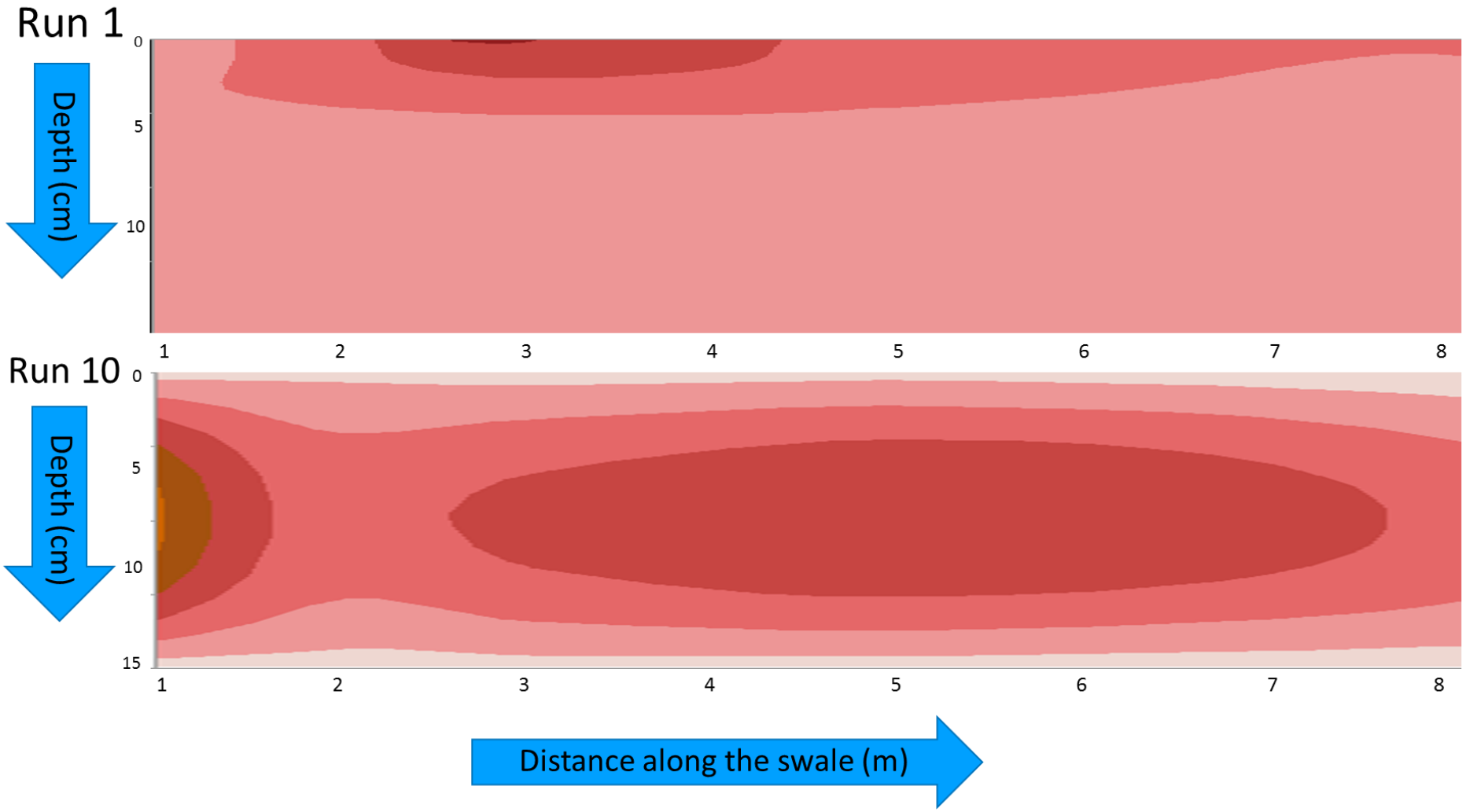

Figure 5-30 Contour plots of benzo(a)pyrene concentrations along the length and depth of the swale.

Levels detected in previous runs (1, 2 and 3) may have been degraded in the time between Run 3 and 4, five weeks compared to two weeks between all other runs, this may have allowed the mid-level BaP time to degrade below detectable levels. As mentioned previously some strains of bacteria are able to degrade PAHs, Ping *et al*. (2017) found that with the presence of PL7 strain (*Raoultella planticola*) the half life of BaP was 9.46 days. If BaP degrading bacteria were present in the soil, this is a possible explanation for the loss of concentration in run 4. This is further backed up by the similarities in levels in Run 2 and 5, both two weeks after a run where no detectable level was seen in the mid layers.

Contour plots generated for trial runs 1 and 10 are shown in figure 5-30. Trial run 1 shown in the top plot, shows a concentration of BaP accumulating in the surface layer. By the final trial there was increased levels accumulating in the mid layer, especially in the 1 m location and between the 3 and 5 m locations. Resuspension of particulates in the storm water may be responsible for the movement of the PAHs through the system. Vertical and lateral flow and filtration by the soil is shown by the accumulation of PAHs in the mid layer, this was also seen for CHR (Figure 5-27) but not in NAP (Figure 5-17).

These changes in accumulation may be due to the PAH weight, as heavier PAHs both BaP and CHR are more hydrophobic and will preferentially attach to particulates, NAP is much less hydrophobic and will stay unbound in the water column. If the flow is slow enough particulates will fall out of the water column at the beginning of the swale, whereas NAP may be transported further in the water flow.

However these results do show that there are many factors to take into account when looking at pollutant mitigation in the environment. Mass balances can be a key method to determine the fate of pollutants, giving indications of losses and gains in a system. Given the difficulties in the analysis experience during this study, full mass balance analysis could not be completed for the soil. Water PAH mass balances show that there was removal of the pollutants when looking at the inflow compared to the outflow

Gocht *et al. (*2007) used mass balance analysis in rural soils, and estimated that 90% of incoming PAHs would be retained in the top-soils, in particular the heavier of the PAHs.

5.5 General discussion

As shown in the results above there is complex behaviour occurring in every trial run. There was overall a build-up in concentrations of the 4 and 5 ring PAHs, the 2 and 3 ring PAHs showed the opposite. This change in dominant PAHs requires further investigation. Van Den Heuvel & Van Noort, (2003) speculated that individual PAHs had specific adsorption sites, therefore there would be less competition between PAHs. They speculate that each PAH has a specific shape that aids in sorption to particulates, this was also mentioned in an study of sorption mechanisms (Yang *et al.*, 2011b). Studies have also shown that heavier PAHs are more likely to be associated with coarser fractions (Aryal et al., 2005)

Concentrations of NAP were consistent in the first four trial runs, by trial run 5 the levels detected via GCMS analysis was barely ever over 100 ng/g in any layer or location. Due to their physiochemical properties, low molecular weight PAHs, such as NAP, are more soluble in water compared to the high molecular weight compounds (Stogiannidis & Laane, 2015). The high molecular weight PAHs, such as BaP, are more likely to rapidly adsorb to particulates, such as the soil particles, rather than dissolving in the water column (Bertilsson & Widenfalk, 2002). There are a number of PAHs that appear to have behaviour that correlates across the trial runs. Tables 4-24, 4-25, 4-26 and 4-27 in appendix show the results of a correlation analysis between the PAHs for the full swale, 0 – 5 and 5 – 10 cm layers respectively. These results show that several PAHs appear to have a strong positive correlation with each other, while others an association at a weaker level, Figure 5-31, based on all results from all ten trial runs. In general the associations are stronger on the surface layer. The dendrogram is a tree diagram that displays the groups that are formed by clustering observations at each step and their similarity levels. The similarity level is measured along the vertical axis (alternately, you can display the distance level), and the different observations are listed along the horizontal axis (Minitab 18). The data displayed here show that NAP is more closely related to CHR than the other light weight PAHs, this is contrary to expectation, especially FLU which it has very similar physiochemical properties. It is unclear why this is so, and may be due to vagaries of environmental sampling.

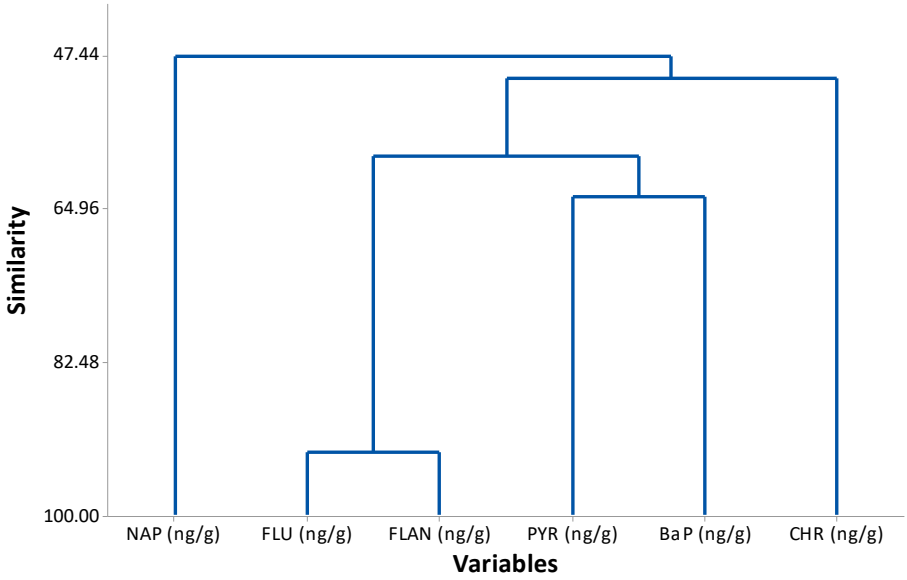

Figure 5-31 Dendrogram showing the relationship between PAHs in the swale from ten trial runs.

Relationships in the water samples were much closer to those that could be expected based on physiochemical properties when analysed in Minitab (Figure 5-32), with the lighter NAP and FLU, and FLAN and PYR all being closely related. This also gives an indication that pH and temperature may be linked to concentration levels. Changes in temperature have been shown to affect BaP degradation (Ping e*t al*., 2017) where a change of 10^{o}C significantly decreased degradation rates. Levels of pH are known to affect microbial health, and different pH levels were show to be key for bacteria colony forming units (CFU ≈500 at pH7 and ≈1000 at pH 5.2).

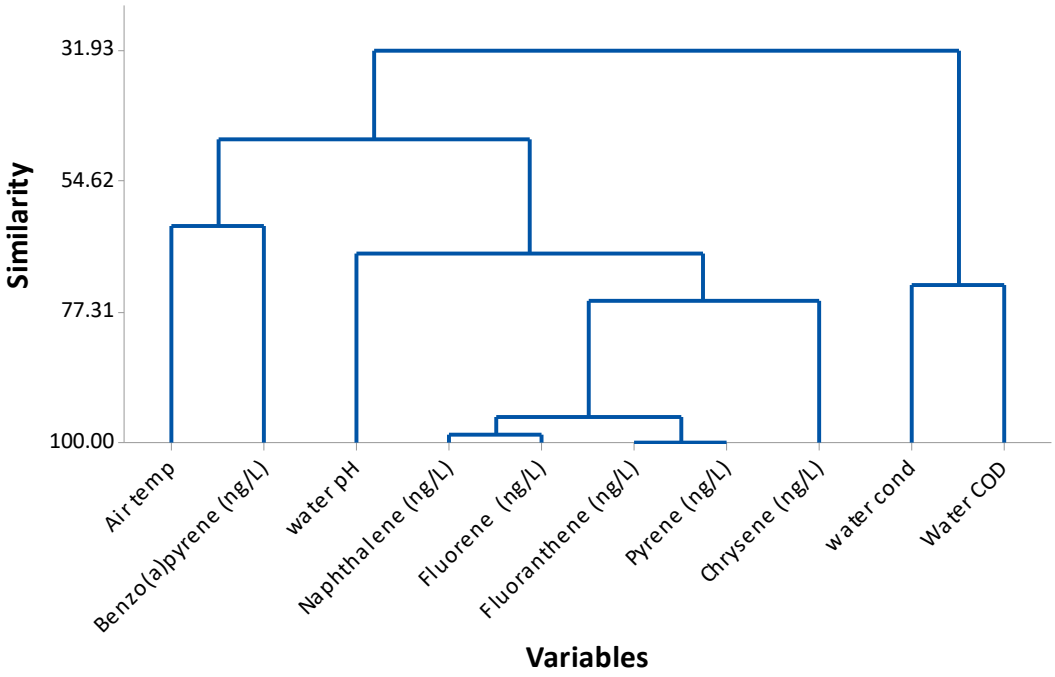

Figure 5-32 Relationships for pollutant and chemical variables in inflow and outflow water samples.

FLU and FLAN have a strong positive association in the full data set, Figure 5-33 (spearman rho 0.716, P-value 0.000). This association reflects their similar physiochemical properties. The association is strongest in the 0 – 5 cm layer (spearman rho 0.794, P-value 0.000). FLU and FLAN both had increases in concentration up until the 6th trial run, after which levels started decreasing. This change in concentration is clearly seen in Figure 5-33, the association still holds for the greater concentrations. There was nothing obvious to explain why the levels were elevated in run 6, potential explanations may be that the temperature was colder, causing a lack of degradation between Run 5 and 6. Colder temperatures have been shown to limit degradation (Eriksson *et al*., 2003) During February temperatures were staying fairly cold, with an average of 5^{o}C daily average during the experiments in the greenhouse (personal record of temperatures). This may be a reason for higher levels accumulating between runs rather than being degraded.

They were both generally found in the beginning of the swale decreasing in concentration with distance from the inflow. Figure 5-33 shows the strong positive

relationship between the two compounds. These two compounds have similar physio-chemical matrices (Chapter 2, table 2-8).

Of the other PAHs BaP and PYR are the other closely related compounds in the complete data set (spearman rho 0.552, p=value 0.000). The similarity in behaviour is stronger when the 0 – 5 cm layer is considered in isolation (spearman rho 0.655, p-value 0.000). Moisture content of the soil has been reported as a major factor that can affect the behaviour of PAHs in soils (Baker *et al.*, 2009). However in the results presented in this study there was only weak correlation between PAHs and moisture content (Appendix table 4-27).

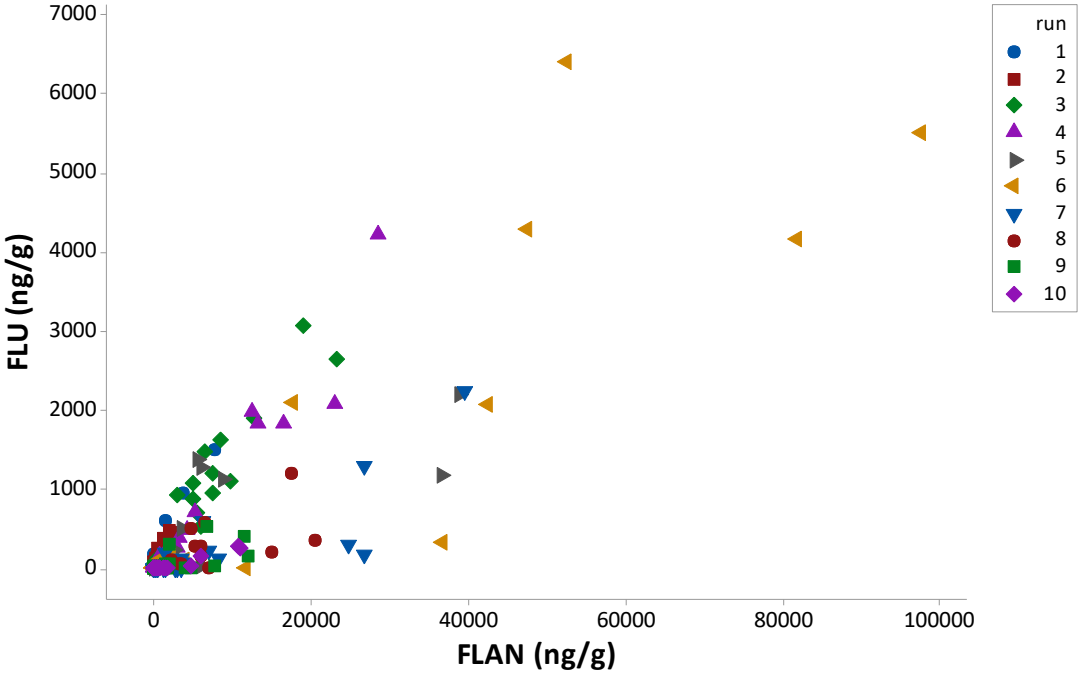

Figure 5-33 Scatterplot showing relationship between Fluorene and Fluoranthene in swale soil, data taken from ten trial runs.

5.5.1 Mechanisms at work in the swale.

SuDS systems, not just swales, provide ideal environment for a number of pollutant removal and removal processes. This section will discuss some of the possible mechanisms that played a key role in the results gained from the model swale experimental trials. The different processes can be separated into two key groups removal of the particulates by means of settling out, for example sedimentation with the pollutants attached, and the second group which involves the dissolved pollutants

which will involve processes such as microbial degradation, adsorption and chemical precipitation (Gavrić *et al.*, 2019). The main mechanisms that were suggested by the distribution patterns seen in this study were sedimentation and degradation. The degradation, or loss, of PAH concentration may have occurred through a number of different pathways: photodegradation, volatilisation, biodegradation. Image 5-1 shows a simple pictorial representation of mechanisms involved in the transport, degradation and accumulation of PAHs in the swale. As the water flows horizontally along the surface, vegetation acts as a buffer dam, slowing the flow and particulates will start to settle out on the surface (Vargas-Luna *et al.*, 2015). Mass balances can be a key method to determine the fate of pollutants, giving indications of losses and gains in a system. Table 5-11 shows the influent and effluent PAH concentrations, along with the missing concentration to make up the mass balance of the system. The missing levels of PAH will have undergone a number of processes through which the pollutants will be retained, degraded or returned to their gaseous state in the atmosphere. Gocht *et al. (*2007) used mass balance analysis in rural soils, and estimated that 90% of incoming PAHs would be retained in the top-soils, in particular the heavier of the PAHs. Table 5-11 shows the % reduction of PAH concentrations in the water samples at the 2 minute inflow, and the first effluent to leave the swale during each run. The results seen fall between 91 and 97 % reduction for ∑6 PAH in individual runs, and an average of 95% across all ten trial runs, which corresponds with the estimate of Gocht *et al.* (2007).

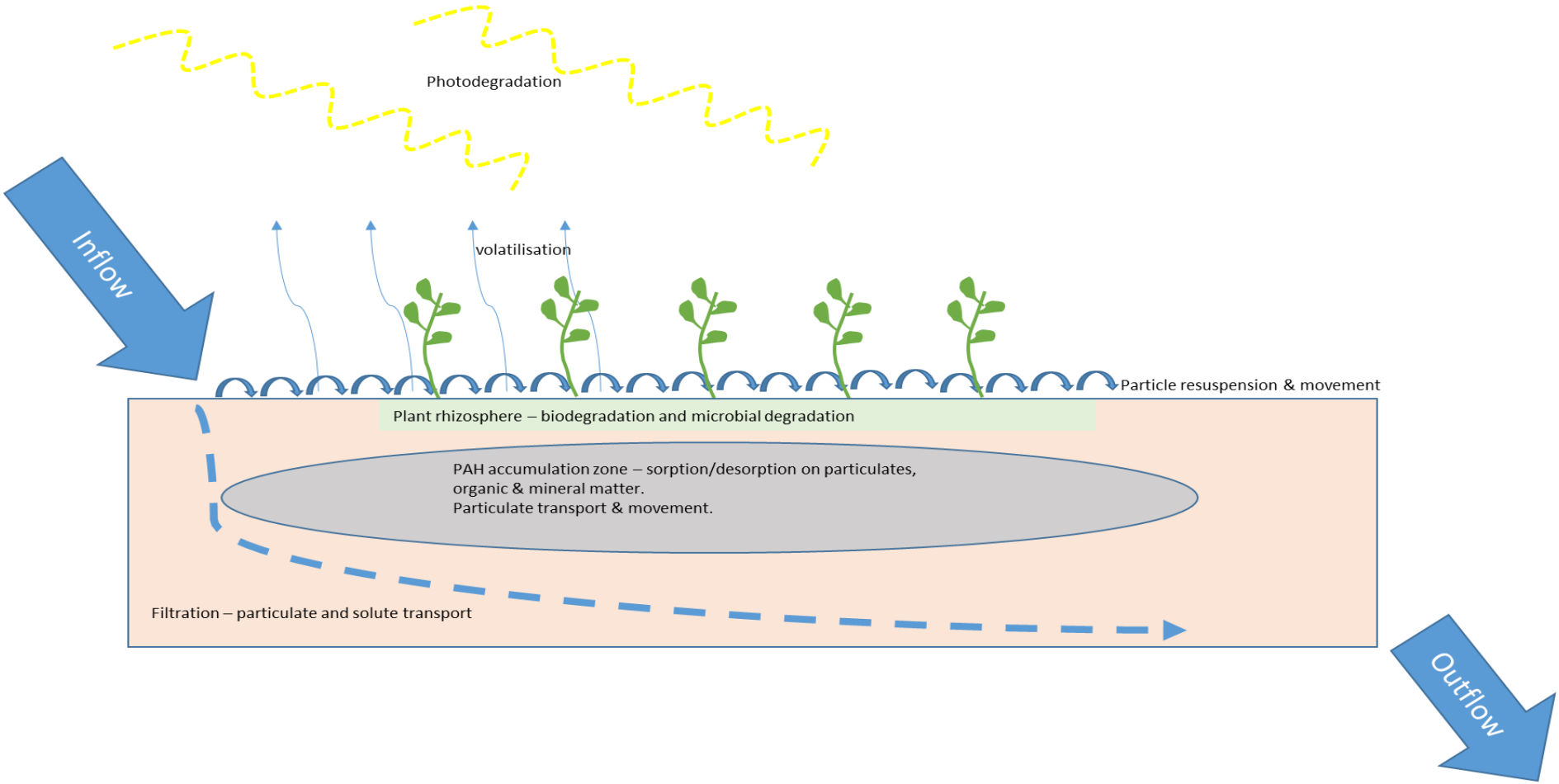

Image 5-1 Pictorial representation of mechanisms of PAH transport, degradation and retention in a swale.

On entering a SuDS system pollutants will be carried along by the flow of water, as the water flows it infiltrates through the pore holes into the soil and can filter laterally and horizontally down the slope, encouraged by the gradient. Pore holes may become clogged with particulates in the water column, causing alternative pathways to be used by the water. Where pore holes are clogged, any attached pollutant will accumulate. The fluctuations in levels seen in this study may be due to this effect in the soil. If the pollutants built up in a large concentration in a small area, it may not have been detected by the random sampling procedure set up. Water flow will follow the easiest path, so the pollutant will not have an even distribution throughout the swale. Some of the variation in accumulation seen may be due to where the samples were taken from, and missing possible hot spots of pollution build up.

A key mechanism of high molecular weight PAH accumulation in swale systems is adsorption and sedimentation, with 90 % of PAHs accumulating in soils (Gocht *et al.*, 2007). This can be attributable to the adsorption onto particulates which then get deposited, or filtered out as water flows through vegetation and the soil (Stagge *et al.*, 2012, Yu *et al.*, 2001). Modelling of surface sedimentation has shown that levels of sediment decreases along the length of a swale, with the smaller, lighter particles travelling further compared to the coarser particles (Deletic, 2005). The heavier weight PAHs, such as BaP, are more likely to rapidly adsorb to particulates in the environment, such as the soil particles, rather than dissolving in the water column (Bertilsson & Widenfalk, 2002). As the molecular weight of PAHs increases, as does the hydrophobic nature. This is due to the K_{ow} properties of each individual PAH, as mentioned higher weight PAHs have a greater K_{ow} making them adsorb to particulate surfaces, lower weight PAHs are more likely to desorb and become available in the water column (Kumata *et al.,* 2000). Previous research has demonstrated this when looking at inlet water compared to outlet water (e.g. Revitt *et al.*, 2004, Roinas *et al.*, 2014). Sorption to particulates is influenced by the range of particle sizes and organic composition (Wang *et al*., 2014), however there is confusion over this with varying reports of size association. Kim *et al*., (1999) presented research showing that PAH concentrations were higher in smaller fraction particulates, while Rockne *et al.*, (2002) showed the opposite. Competition between PAHs for adsorption sites on particulates requires

greater understanding, (Van Den Heuvel & Van Noort, 2003). In the storm events discussed in this research artificial runoff dust provided particulates for the PAHs in the creosote to attach to.

Filtration of the water through the vegetation and soil pores will also provide opportunities for the suspended particulates to be removed. As water flowed along the swale, the velocity of the flow was slowed due to the roughness of the vegetated swale surface. The vegetation provided barriers to the flow, causing pooling along the length. Image 5-2 shows evidence of this, along with visual of darker deposits being left being on the vegetation. This was caused by the creosote polluted simulated runoff dust, Image 5-3 shows a closer look at this deposition. Image 5-3 was taken shortly after the end of a half hour storm event, once all remaining water had filtered into the soil. This image clearly shows the darker deposits left in the vegetation, this shows evidence of the particulates in the storm water settling out of the water column onto the soil surface.

Once retained in the swale system, other degradation processes start to affect the PAH concentration. Vegetation in the swale serves not just as barriers to slow water flow, but for the purpose of phytoremediation, the use of plants to remove, degrade or contain pollutants (Zhou *et al*., 2013). Studies have shown some plant cell cultures are able to degrade PAHs (Kucerová *et al.*, 2001). Leroy *et al.* (2015) demonstrated that grasses were the best filter for suspended solids, and macrophyte plants used (*Juncus effusus, Iris pseudacorus and Phalaris arunsinacea*) all reduced target PAHs in the soil by up to 99.4 % (pyrene). This study also showed that degradation of BaP varied between 75.5 – 91 %, depending on which plant was used. Plants used in the turf provided by Wildflower Turf, are specialised SuDS plants chosen for their ability to withstand periods of drought and also submersion (wildflowerturf.co.uk). Their phytoremediation properties have not yet been assessed. The plants in the turf produced a dense mat of roots, which in the model swale was mainly centred in the surface layer, 0 – 5 cm. It was in this layer that the reduction of PAHs was seen clearly. Accumulations of PAHs were beginning to be seen in the 5 – 10 cm layer. Root systems provide an environment for microbes, such as bacteria and fungus. These microorganisms' abilities to degrade pollutants, including PAHs, are widely reported (e.g. Griffiths *et al.*, 1999, Zhang *et al.,*

2006, Kawasaki *et al.*, 2015). Over time microbes will be subject to self-selectivity, and species suited to the environment will become dominant (Griffiths *et al.*, 1999). Microbial activity was not studied as part of this research, and so any changes that may have occurred are not accounted for.

Image 5-2 Pooling of water after the flow had ceased. Darker deposits show evidence of polluted sediment being retained on the surface.

Image 5-3 surface of the swale shortly after the half hour storm event ceased, all water had infiltrated the soil, particulates left behind on the surface show the pollution.

Above ground accumulation will be susceptible to volatilisation and photodegradation, both of these processes will result in the removal of PAHs from the system. Volatilisation will result in the pollutants passing into the gaseous phase and subsequent atmospheric dispersion, and is highly dependent on environmental conditions (Lin, 2018). Temperatures in the greenhouse may have caused losses due to volatilisation in the 24 hours between the storm run and the collection of samples. As mentioned previously, as the PAH molecular weight increases the tendency to volatise decreases (Ghosal *et al*., 2016) as such this is potentially a more important process for the lighter PAHs such as NAP. Photolysis and volatilisation potential is highest in SuDS features such as swales, due to the extended exposure time and large surface area (Scholes *et al.*, 2008). BaP was found to degrade when light was not present, in an unidentified process when the effects of global warming were studied (Marquès *et al*., 2016). Concentrations of BaP in the swale was found to be highly variable between runs, indeed in run 4 it was not detected.

In a study of soil properties Marquès *et al*. (2017) demonstrated that the different textures found in different soils can have an effect on PAH sorption, degradation and volatilisation. Their results indicated that the lower weight compounds were associated with the finer textured soils, while the heavier PAHs with the coarser particles. Resuspension of particulates, while not a removal function, has the potential to move pollutants further through the system (Sprovieri *et al*., 2007, Allen *et al.*, 2015). This was seen in the later trials with increases in pollution in the 5 m and 8 m locations. Suspension of particulates in the water column as it filters through the system, and removal in the soil was evidenced by the accumulation of pyrene, chrysene and benzo(a)pyrene in the 5 – 10 cm layer.

Despite the attempts of this project to reduce the variability affecting the swale system, it was evident that some of these were not eliminated. Two of the main processes of pollutant input to swales, atmospheric deposition and runoff were able to be separated by constructing the swale mesocosm in the greenhouse. The greenhouse could stop atmospheric deposition, by stopping wind blowing particulates into the surface. However, light and temperature were not able to be controlled in the greenhouse. There was no way to control the exposure to sunlight as the greenhouse did not have blinds.

Due to the protection provided by the greenhouse the internal temperature was generally elevated to external temperatures. As mentioned previously, self-selectivity in the microbial population may bring uncertainty in degradation potential, especially in areas of acute PAH pollution, for example heavy goods yards, lorry car parks and building sites. The swale was also subject to soil movement and settling with each storm run, these effects will be seen in environmental swales, especially newly built systems. It had been the storm design intention to have influent levels consistent, but ultimately these showed high variability of pollutant concentrations. There are still degradation pathways not yet fully understood which will in future need to be studied further. While some of the processes discussed here are less significant for the heavier weighted PAHs they will have had some influence, and it is possible that sections tested were uninfluenced by the pollutant in the storm water. The suggested alternative degradation pathway suggest by Marquès *et al*. (2016) may be a factor that needs to be considered. Degradation pathways will ultimately interact with and influence one another, understanding of how this happens, and what the outputs are will of necessity need future studies (Lin, 2018).

Overall this study has shown that the swale mesocosm was efficient in reducing flow rates, and attenuating the storm flow. As such, it successfully simulated behaviour in the field in terms of hydraulic properties and pollution attenuation. Sedimentation has previously been identified as a key mechanism of reducing the pollutant flow into waterbodies (e.g. Bäckström, 2002; Deletic, 2001; Deletic & Fletcher, 2006). This was seen on the surface of the swale, including on the vegetation (Image 5-2 and 5-3). This sedimentation causes the retention of pollutants in the swale system, which facilitates the other removal mechanisms. Vertical and lateral flow and filtration through the system resulted in reduction of PAHs in storm water. Gradual build-up of concentrations in the surface soil layer over time, and the penetration into the lower layers indicate that future remediation plans must be considered by planners and developers when establishing swale systems.

6 Future for SuDS

In a recent published draft of Sewers for Adoption 8th edition, Water UK (2018) have made clearer definitions of SuDS and their inclusion in drainage systems, giving clearer information for water companies to consider adopting in future. It was prepared by the Water Companies, developers, and other stakeholders, and has been approved by Ofwat. Currently one of the major barriers for general acceptance of SuDS systems in the post development stage adoption of the systems and the maintenance schedules needed to maintain efficiency. Proposals in the latest draft, due to be implemented in 2019 set out more detailed guidance for developers of the standards that the SuDS components must meet to be adopted into the sewerage and wastewater systems once the building works are completed. The new guidelines have published in draft form to enable policies and procedures to be adapted to comply with the new regulations. One of the key new features is the guidance on SuDS design to enable them to fall under the heading of sewage systems and therefore available for adoption by water companies. In clarifying the guidelines for including SuDS, and providing reference information regarding their advantages, it is likely that SuDS may become a more viable option for developers in England when planning new builds.

While there are various guidance documents to aid SuDS design and understanding (e.g. Woods-Ballard *et al*, 2015 in the UK) they do not offer much understanding of the performance of the systems. The SuDS manual does suggest simple pollution removal indices, with values for pollution hazard level and mitigation level for SuDS components developed from the method set out by Ellis *et al.* (2012). To be effective in pollutant removal the chosen SuDS component (or components if a treatment train is being set up) must have a pollution mitigation index that equals or exceeds the hazard index:

Total SuDS mitigation index ≥ pollution hazard index
(for each contaminant type) (for each contaminant type)

Using these indices in the SuDS manual the swale system for hydrocarbons is scored:

- **Total SuDS mitigation index – 0.6**
- **Pollution hazard index – 0.4**

The reduction in PAH levels in the water leaving the test swale indicate agreement with this index method, showing positive removal rates of hydrocarbons.

There are a number of modelling systems which take the processes into consideration, and are continually adding to current understanding of the complex systems (Gavrić *et al*., 2019). Early work on models are being used to develop further understanding and new models: sediment transport and runoff generation model TRAVA (Deletic, 2001 & 2005) and the Australian developed MUSIC model which looked at pollutant mitigation performance to inform SuDS selection process (Wong *et al.*, 2001). Recent models using a number of parameters are being used to further understanding of how SuDS should be designed to exploit the full potential of SuDS systems. The development of impact assessment models, which considers the potential pollutant impact of storm water after passage through a SuDS system, shows that long term monitoring and maintenance of the systems will be essential for continued effectiveness (Ellis *et al.*, 2012; Revitt *et al*., 2017).

With the new guidelines providing the extra clarity and encouraging the adoption of SuDS, the findings in the presented research may aid in the decision making to determine which conveyance devices to use. The PAHs in the current study were accumulating just below the vegetated zone, as such increased maintenance may be needed to remove the contaminated soil layer, and replacing it. A combined system, using both hard and soft SuDS, might include a method of capturing the majority of suspended solids, such as a sediment trap, before the water flows through the swale. However, this method will also present maintenance issues, such as monitoring of the trap and removal and disposal/remediation of the trapped sediment. The knowledge gained from this study can help inform these decisions. In areas of high sediment production, such as motorways, a combined system will prolong the life of the swale. In areas of low pollution production, a simple vegetated swale may provide the necessary removal without becoming overloaded.

The findings presented in this thesis serve to increase the current knowledge base on PAHs, and the swale mesocosm provides a unique insight into pollutant movement through the system, and areas of concentration. The swale mesocosm also provides a

proven template that can be built quickly and easily to study the environmental effects, without putting undue pollutants into the environment.

7 Conclusions

This study provides in important contribution to the understanding of PAHs in SuDS systems via a unique swale mesocosm design. The extended swale mesocosm, has built upon simplified models used in previous research. The 10 m long physical model of a swale was able to include lateral and vertical flow properties and mimic environmental processes in the lab, which is often lost in jar experiments (Leroy *et al.*, 2015). The controlled environment allowed for the separating of two major transport processes of pollutants – road runoff and atmospheric deposition by only considering aqueous inputs. The swale mesocosm successfully simulated the hydrology and storm water attenuation observed in operational swales. The swale mesocosm provides a template for future studies to develop a standardised mesocosm for use in pollutant fate and behaviour.

PAH behaviour in the swale was in line with their physio-chemical properties, showing mobility in the low molecular weight compounds and accumulation of the higher weight ones. Over the course of the trials, heavier PAHs started to translocate from the surface vegetated area and started to accumulate just below the dense vegetated in the 5 – 10 cm layer. Providing visual representation, such as contour plots, of pollutant loading in the swale with depth may provide clearer information to interested parties, who may not fully understand the complexities of pollutant interactions. The results show further evidence that PAHs washed off of roads will undergo a number of processes which may delay, or even prevent, their input into local waterbodies. The movement of pollutants through the system will be determined ultimately by water flow and resuspension of particulates. The results presented in this study show that pockets of pollutants can build up over time, generally below the surface level root zone. This study demonstrates that understanding the complex patterns that take place in each individual system will need to be considered in the design phase. Understanding of this will provide key details of how best to implement swale design to best treat the pollutants.

Results presented in this study provided evidence for, and offers information of PAH fate and behaviour in vegetated swale systems. Future design codes and maintenance schedules should be set up with future need of land remediation, such as surface skimming to remove contaminated soil. Plant choice will also need to be addressed during the planning stage, species used in the turf on this study showed a key ability to withstand and recover from high pollutant dosing. Healthy vegetation is fundamental to the microorganisms continued presence in the subsurface layers of the SuDS systems, and the degradation processes they can effect. Having specific plant species that can cope with both submersion and periods of drought will benefit SuDS performance. Further studies into the benefits of wildflowers will give further indication of the best mixes to be used.

However, it is also clear from the presented results that the many factors involved will each have an influence on the fate of PAHs. It should be noted that every site will have its own requirements, and influences that will play a part in how a SuDS system performs, and key features including soil type will affect how the vegetation and microbiota perform. It is clear that while attempts were made to reduce the variability, the nature of the materials used, and equipment failures, gave rise to unforeseen variances that were not accounted for. Future SuDS and similar installations should consider the need for long term periodic monitoring for pollution build-up in the soil profile. This would require there to be monitoring set up before the system is in place to gain initial readings.

8 Future work

There are still many challenges in the acceptance of SuDS as a useful tool in meeting the demands of industrialisation. Future work should look at increasing knowledge and understanding of the benefits they can bring to an environment, particularly in the removal and clean-up of pollutants. Using models such as the swale developed in this research studies of deposition and resuspension of particulates would provide valuable understanding of these processes and the residence time of polluted particulates before they move further down the treatment train. In this study analysis of total suspended solids was not completed in the water, this could provide increased understanding of

the degradation patterns in swale systems. Seasonal variations should also be considered in any future work, as factors such as temperature, pH and soil nutrient levels can all affect the degradation process.

In completing the research many lessons were learnt, of which future work should take into account. While it is unknown if the delay experienced in sample analysis affected the results, future work should ensure that analysis is completed as quickly as possible after sampling. A number of equipment failures and delays in finding parts for repair, meant that extraction and analysis was delayed in most cases by at least 6 months. Another factor to consider would be the environment the extraction process was completed in. Due to the nature of the large equipment it was not possible to complete extraction within one laboratory. Samples had to go through various processes using equipment stored across four laboratories. These spaces were multi use areas, and although every effort was taken to thoroughly clean each space there is potential that cross contamination affected the samples.

Potential contamination could have come from the trial site itself. This was on a working sewage treatment works, with arctic lorries and sludge tanks moving by the greenhouse regularly. As the greenhouse was not a fully sealed, airtight unit dust raised by the passage of the lorries could have made its way into the greenhouse. RRD samples also had to be moved from the onsite laboratory into the greenhouse, and soil samples carried back into the laboratory. This study added pollutants in a much higher level than would normally be expected to be seen in the environment in order to have levels present that were detectable from the beginning. This may have overloaded the system, and provided uncertain results. Future studies should take this into account, and potentially reduce the levels of pollutant added.

Rhizosphere and microbial studies, assessing the rate of species shifting in response to seasonal changes, and pollutant loading over time would provide beneficial understanding of this key process in the degradation of PAHs. Pollutant interactions, and how they all combine will also benefit understanding of the mitigation systems. Given the complex nature of environmental studies an overall understanding of how

pollutants interact and affect the uptake, degradation and remediation of each other may be difficult to fully understand.

These recommendations added to the current level of knowledge and understanding of SuDS, help to optimise future design and maintenance codes, and help planners and developers in utilising SuDS in a beneficial way for the environment and stakeholders.

9 References

Abdel-Shafy, H. I., & Mansour, M. S. M. (2015). A review on polycyclic aromatic hydrocarbons: Source, environmental impact, effect on human health and remediation. *Egyptian Journal of Petroleum*, *25*(1), 107–123. https://doi.org/10.1016/j.ejpe.2015.03.011

Adeniji, A. O., Okoh, O. O., & Okoh, A. I. (2018). Analytical Methods for Polycyclic Aromatic Hydrocarbons and their Global Trend of Distribution in Water and Sediment: A Review. *Recent Insights in Petroleum Science and Engineering*. https://doi.org/10.5772/intechopen.71163

Agnello, A. C., Bagard, M., van Hullebusch, E. D., Esposito, G., & Huguenot, D. (2016). Comparative bioremediation of heavy metals and petroleum hydrocarbons co-contaminated soil by natural attenuation, phytoremediation, bioaugmentation and bioaugmentation-assisted phytoremediation. *Science of the Total Environment*, *563–564*, 693–703. https://doi.org/10.1016/j.scitotenv.2015.10.061

Agrawal, N., & Shahi, S. K. (2017). Degradation of polycyclic aromatic hydrocarbon (pyrene) using novel fungal strain Coriolopsis byrsina strain APC5. *International Biodeterioration and Biodegradation*, *122*(May), 69–81. https://doi.org/10.1016/j.ibiod.2017.04.024

Akpambang, V. O. E., Purcaro, G., Lajide, L., Amoo, I. A., Conte, L. S., & Moret, S. (2015). Polycyclic Aromatic Hydrocarbons in Some Nigerian Roasted Plant Foods. *Frontiers in Food & Nutrition Research*, *1*(1), 1–5.

Ali, H., Khan, E., & Sajad, M. A. (2013). Phytoremediation of heavy metals--concepts and

applications. *Chemosphere*, *91*(7), 869–881. https://doi.org/10.1016/j.chemosphere.2013.01.075

Allan, I. J., O'Connell, S. G., Meland, S., Bæk, K., Grung, M., Anderson, K. A., & Ranneklev, S. B. (2016). PAH Accessibility in Particulate Matter from Road-Impacted Environments. *Environmental Science and Technology*, *50*(15), 7964–7972. https://doi.org/10.1021/acs.est.6b00504

Allen, D., Olive, V., Arthur, S., & Haynes, H. (2015). Urban sediment transport through an established vegetated swale: Long term treatment efficiencies and deposition. *Water (Switzerland)*, *7*(3), 1046–1067. https://doi.org/10.3390/w7031046

Allen, D., Olive, V., Arthur, S., Haynes, H., Universities, S., & Avenue, R. (2015). *Urban Sediment Transport through an Established Vegetated Swale: Long Term Treatment Efficiencies and Deposition*. 1046–1067. https://doi.org/10.3390/w7031046

Amato, F., Querol, X., Johansson, C., Nagl, C., & Alastuey, A. (2010). A review on the effectiveness of street sweeping, washing and dust suppressants as urban PM control methods. *Science of the Total Environment*, *408*(16), 3070–3084. https://doi.org/10.1016/j.scitotenv.2010.04.025

Andersen, R. G., Booth, E. C., Marr, L. C., Widdowson, M. A., & Novak, J. T. (2008). Volatilization and biodegradation of naphthalene in the vadose zone impacted by phytoremediation. *Environmental Science and Technology*, *42*(7), 2575–2581. https://doi.org/10.1021/es0714336

Armbruster, D. A., & Pry, T. (2008). Limit of blank, limit of detection and limit of quantitation. *The Clinical Biochemist. Reviews / Australian Association of Clinical Biochemists*, *29 Suppl 1*(August), S49-52. https://doi.org/citeulike-article-id:3416410

Aryal, R. K., Furumai, H., Nakajima, F., & Boller, M. (2005). Dynamic behavior of fractional suspended solids and particle-bound polycyclic aromatic hydrocarbons in highway runoff. *Water Research*, *39*, 5126–5134. https://doi.org/10.1016/j.watres.2005.09.045

Bach, P. M., Rauch, W., Mikkelsen, P. S., McCarthy, D. T., & Deletic, A. (2014). A critical review of integrated urban water modelling – Urban drainage and beyond. *Environmental Modelling & Software*, *54*, 88–107. https://doi.org/10.1016/j.envsoft.2013.12.018

Bäckström, M. (2002). Sediment transport in grassed swales during simulated runoff events. *Water Science and Technology*, *45*(7), 41–49. https://doi.org/10.2166/wst.2002.0115

Baker, K. L., Langenheder, S., Nicol, G. W., Ricketts, D., Killham, K., Campbell, C. D., & Prosser, J. I. (2009). Environmental and spatial characterisation of bacterial community composition in soil to inform sampling strategies. *Soil Biology and Biochemistry*, *41*(11), 2292–2298. https://doi.org/10.1016/j.soilbio.2009.08.010

Barbosa, a E., Fernandes, J. N., & David, L. M. (2012). Key issues for sustainable urban stormwater management. *Water Research*, *46*(20), 6787–6798. https://doi.org/10.1016/j.watres.2012.05.029

Barnett, V. (2004). *Environmental Statistics: Methods and Applications.* Chichester, UK: John Wiley & Sons Ltd.

Barrett, M. E. (2008). Comparison of BMP Performance Using the International BMP Database. *Journal of Irrigation and Drainage Engineering*, *134*(October), 556–561. https://doi.org/10.1061/(ASCE)0733-9437(2008)134:5(556)

Barrett, M. E., Walsh, P. M., Jr., J. F. M., & Charbeneau, R. J. (1998). Performance of Vegetative Controls for Treating Highway Runoff. *Journal of Environmental Engineering*, Vol. 124, pp. 1121–1128. https://doi.org/10.1061/(ASCE)0733-9372(1998)124:11(1121)

Bastien, N., Arthur, S., Wallis, S., & Scholz, M. (2010a). Optimising regional sustainable drainage systems pond performance using treatment trains. *Desalination and Water Treatment*, *19*(1–3), 2–11. https://doi.org/10.5004/dwt.2010.1881

Bastien, N., Arthur, S., Wallis, S., & Scholz, M. (2010b). The best management of SuDS

treatment trains: a holistic approach. *Water Science and Technology : A Journal of the International Association on Water Pollution Research*, *61*(1), 263–272. https://doi.org/10.2166/wst.2010.806

Bastien, N. R. P., Arthur, S., & McLoughlin, M. J. (2012). Valuing amenity: public perceptions of sustainable drainage systems ponds. *Water and Environment Journal*, *26*(1), 19–29. https://doi.org/10.1111/j.1747-6593.2011.00259.x

Bertilsson, S., & Widenfalk, A. (2002). Photochemical degradation of PAHs in freshwaters and their impact on bacterial growth - Influence of water chemistry. *Hydrobiologia*, *469*, 23–32. https://doi.org/10.1023/A:1015579628189

Bertrand-Krajewski, J. L., Chebbo, G., & Saget, A. (1998). Distribution of pollutant mass vs volume in stormwater discharges and the first flush phenomenon. *Water Research*, *32*(8), 2341–2356. https://doi.org/10.1016/S0043-1354(97)00420-X

Bratieres, K., Fletcher, T. D., Deletic, a, & Zinger, Y. (2008). Nutrient and sediment removal by stormwater biofilters: a large-scale design optimisation study. *Water Research*, *42*(14), 3930–3940. https://doi.org/10.1016/j.watres.2008.06.009

Brown, J. N., & Peake, B. M. (2006). Sources of heavy metals and polycyclic aromatic hydrocarbons in urban stormwater runoff. *The Science of the Total Environment*, *359*(1–3), 145–155. https://doi.org/10.1016/j.scitotenv.2005.05.016

Camponelli, K. M., Lev, S. M., Snodgrass, J. W., Landa, E. R., & Casey, R. E. (2010). Chemical fractionation of Cu and Zn in stormwater, roadway dust and stormwater pond sediments. *Environmental Pollution (Barking, Essex : 1987)*, *158*(6), 2143–2149. https://doi.org/10.1016/j.envpol.2010.02.024

Canadian Council of Ministers of the Environment. (2008). *Canadian Soil Quality Guidelines Carcinogenic and Other Polycyclic Aromatic Hydrocarbons (PAHs)*.

Chang, B. V., Shiung, L. C., & Yuan, S. Y. (2002). Anaerobic biodegradation of polycyclic aromatic hydrocarbon in soil. *Chemosphere*, *48*(7), 717–724. https://doi.org/10.1016/S0045-6535(02)00151-0

Chen, F., Tan, M., Ma, J., Zhang, S., Li, G., & Qu, J. (2015). Efficient remediation of PAH-metal co-contaminated soil using microbial-plant combination: a greenhouse study. *Journal of Hazardous Materials*. https://doi.org/10.1016/j.jhazmat.2015.09.068

Chen, Y., Shen, Z., & Li, X. (2004). The use of vetiver grass (Vetiveria zizanioides) in the phytoremediation of soils contaminated with heavy metals. *Applied Geochemistry*, *19*(852), 1553–1565. https://doi.org/10.1016/j.apgeochem.2004.02.003

Chow, M. F., & Yusop, Z. (2014). Sizing first flush pollutant loading of stormwater runoff in tropical urban catchments. *Environmental Earth Sciences*, *72*(10), 4047–4058. https://doi.org/10.1007/s12665-014-3294-6

Chunhui, W., Shaohua, W. U., Shenglu, Z., Yaxing, S. H. I., & Jing, S. (2017). Characteristics and Source Identification of Polycyclic Aromatic Hydrocarbons (PAHs) in Urban Soils : A Review. *Pedosphere: An International Journal*, *27*(1), 17–26. https://doi.org/10.1016/S1002-0160(17)60293-5

CIRIA. (2007). *The SUDS manual*. Retrieved from http://www.persona.uk.com/A47postwick/deposit-docs/DD-181.pdf

CIRIA. (2015). *The SuDS manual*. https://doi.org/London C697

Clozel, B., Ruban, V., Durand, C., & Conil, P. (2006). Origin and mobility of heavy metals in contaminated sediments from retention and infiltration ponds. *Applied Geochemistry*, *21*(10), 1781–1798. https://doi.org/10.1016/j.apgeochem.2006.06.017

Coover, M. P., & Sims, R. C. (1987). The effect of temperature on polycyclic aromatic hydrocarbon persistence in an unacclimated agricultural soil. *Hazardous Waste and Hazardous Materials*, *4*(1), 69–82. https://doi.org/10.1089/hwm.1987.4.69

Cousins, I. T., Beck, A. J., & Jones, K. C. (1999). A review of the processes involved in the exchange of semi-volatile organic compounds (SVOC) across the air-soil interface. *Science of the Total Environment*, *228*(1), 5–24. https://doi.org/10.1016/S0048-

9697(99)00015-7

Dabestani, R., & Ivanov, I. N. (1999). A compilation of physical, spectroscopic and photophysical properties of polycyclic aromatic hydrocarbons. *Photochemistry and Photobiology*, *70*(1), 10–34. https://doi.org/10.1111/j.1751-1097.1999.tb01945.x

Das, K., & Mukherjee, A. K. (2007). Crude petroleum-oil biodegradation efficiency of Bacillus subtilis and Pseudomonas aeruginosa strains isolated from a petroleum-oil contaminated soil from North-East India. *Bioresource Technology*. https://doi.org/10.1016/j.biortech.2006.05.032

Davis, A. P., Stagge, J. H., Jamil, E., & Kim, H. (2012). Hydraulic performance of grass swales for managing highway runoff. *Water Research*, *46*(20), 6775–6786. https://doi.org/10.1016/j.watres.2011.10.017

de Boer, J., & Wagelmans, M. (2016). Polycyclic Aromatic Hydrocarbons in Soil - Practical Options for Remediation. *Clean - Soil, Air, Water*, *44*(6). https://doi.org/10.1002/clen.201500199

DEFRA. (2014). Water Framework Directive implementation in England and Wales: new and updated standards to protect the water environment. *Department for Environment Food and Rural Affairs*, (May), Date Accessed 2017-04-06. https://doi.org/10.1016/j.jengtecman.2009.06.008

Deletic, A. (2000). Sediment behaviour in overland flow over grassed areas. Retrieved from http://sfx.scholarsportal.info/guelph/docview/1469135689?accountid=11233%5Cnhttp://sfx.scholarsportal.info/guelph?url_ver=Z39.88-2004&rft_val_fmt=info:ofi/fmt:kev:mtx:dissertation&genre=dissertations+%26+theses&sid=ProQ:ProQuest+Dissertations+%26+Theses+A

Deletic, A. (2001). *Modelling of water and sediment transport over grassed areas*. *248*, 168–182.

Deletic, A. (2005). Sediment transport in urban runoff over grassed areas. *Journal of*

Hydrology, *301*(1–4), 108–122. https://doi.org/10.1016/j.jhydrol.2004.06.023

Deletic, A., & Fletcher, T. D. (2006). Performance of grass filters used for stormwater treatment—a field and modelling study. *Journal of Hydrology*, *317*(3–4), 261–275. https://doi.org/10.1016/j.jhydrol.2005.05.021

DIRECTIVE 2000/60/EC OF THE EUROPEAN PARLIAMENT AND OF THE COUNCIL of 23 October 2000. (2014). *Water Framework Directive*.

Dobbins, R. A., Fletcher, R. A., Benner, B. A., & Hoeft, S. (2006). Polycyclic aromatic hydrocarbons in flames, in diesel fuels, and in diesel emissions. *Combustion and Flame*, *144*(4), 773–781. https://doi.org/10.1016/j.combustflame.2005.09.008

Elliott, a, & Trowsdale, S. (2007). A review of models for low impact urban stormwater drainage. *Environmental Modelling & Software*, *22*(3), 394–405. https://doi.org/10.1016/j.envsoft.2005.12.005

Ellis, J. B., & Lundy, L. (2016). Implementing sustainable drainage systems for urban surface water management within the regulatory framework in England and Wales. *Journal of Environmental Management*, *183*, 630–636. https://doi.org/10.1016/j.jenvman.2016.09.022

Ellis, J. B., Revitt, D. M., & Lundy, L. (2012). An impact assessment methodology for urban surface runoff quality following best practice treatment. *The Science of the Total Environment*, *416*, 172–179. https://doi.org/10.1016/j.scitotenv.2011.12.003

Environmental Protection, E. and W. (2009). *Groundwater (England and Wales) Regulations 2009*. Retrieved from http://www.legislation.gov.uk/uksi/2009/2902/pdfs/uksi_20092902_en.pdf

Eriksson, M., Sodersten, E., Yu, Z., Dalhammar, G., & Mohn, W. W. (2003). Degradation of polycyclic aromatic hydrocarbons at low temperature under aerobic and nitrate-reducing conditions in enrichment cultures from northern soils. *Applied and Environmental Microbiology*, *69*(1), 275–284. https://doi.org/10.1128/AEM.69.1.275-284.2003

European Commission. (2016). Commission Implementing Decision (EU) 2016/902 for common waste water and waste gas treatment/management systems in the chemical sector. In *Euratom* (Vol. 75). https://doi.org/http://eur-lex.europa.eu/pri/en/oj/dat/2003/l_285/l_28520031101en00330037.pdf

Fletcher, T. D., Shuster, W., Hunt, W. F., Ashley, R., Butler, D., Arthur, S., … Viklander, M. (2014). SUDS, LID, BMPs, WSUD and more – The evolution and application of terminology surrounding urban drainage. *Urban Water Journal*, (December), 1–18. https://doi.org/10.1080/1573062X.2014.916314

Fryd, O., Dam, T., & Jensen, M. B. (2012). A planning framework for sustainable urban drainage systems. *Water Policy*, *14*(5), 865. https://doi.org/10.2166/wp.2012.025

Fu, P. P., Xia, Q., Sun, X., & Yu, H. (2012). Phototoxicity and environmental transformation of polycyclic aromatic hydrocarbons (PAHs)-light-induced reactive oxygen species, lipid peroxidation, and DNA damage. *Journal of Environmental Science and Health - Part C Environmental Carcinogenesis and Ecotoxicology Reviews*, *30*(1), 1–41. https://doi.org/10.1080/10590501.2012.653887

Gavrić, S., Leonhardt, G., Marsalek, J., & Viklander, M. (2019). Processes improving urban stormwater quality in grass swales and filter strips: A review of research findings. *Science of the Total Environment*. https://doi.org/10.1016/j.scitotenv.2019.03.072

Ghosal, D., Ghosh, S., Dutta, T. K., & Ahn, Y. (2016). Current state of knowledge in microbial degradation of polycyclic aromatic hydrocarbons (PAHs): A review. *Frontiers in Microbiology*, *7*(AUG). https://doi.org/10.3389/fmicb.2016.01369

Glick, B. R. (2010). Using soil bacteria to facilitate phytoremediation. *Biotechnology Advances*, *28*(3), 367–374. https://doi.org/10.1016/j.biotechadv.2010.02.001

Gobel, P., Dierkes, C., & Coldewey, W. G. (2007). Storm water runoff concentration matrix for urban areas. *Journal of Contaminant Hydrology*, *91*(1–2), 26–42. https://doi.org/10.1016/j.jconhyd.2006.08.008

Gocht, T., Ligouis, B., Hinderer, M., & Grathwohl, P. (2007). Accumulation of polycyclic aromatic hydrocarbons in rural soils based on mass balances at the catchment scale. *Environmental Toxicology and Chemistry*, *26*(4), 591–600. https://doi.org/10.1897/06-287R.1

Goonetilleke, A., Egodawatta, P., & Kitchen, B. (2009). Evaluation of pollutant build-up and wash-off from selected land uses at the Port of Brisbane, Australia. *Marine Pollution Bulletin*, *58*(2), 213–221. https://doi.org/10.1016/j.marpolbul.2008.09.025

Goonetilleke, A., Thomas, E., Ginn, S., & Gilbert, D. (2005). Understanding the role of land use in urban stormwater quality management. *Journal of Environmental Management*, *74*(1), 31–42. https://doi.org/10.1016/j.jenvman.2004.08.006

Griffiths, B., Ritz, K., Ebblewhite, N., & Dobson, G. (1999). Soil microbial community structure - Effects of substrate loading rates. *Soil Biology & Biochemistry*, *31*, 145–153. https://doi.org/10.1016/S0038-0717(98)00117-5

Guimarães, E. D. F., Rodrigues, J. M., De La Cruz, M. H. C., Sartori, A. V., De Souza, V., & Figueroa-Villar, J. D. (2013). Determination of PAHs: A practical example of validation and uncertainty assessment. *Journal of Chromatographic Science*, *51*(9), 845–855. https://doi.org/10.1093/chromsci/bms185

Guittonny-Philippe, A., Masotti, V., Höhener, P., Boudenne, J.-L., Viglione, J., & Laffont-Schwob, I. (2014). Constructed wetlands to reduce metal pollution from industrial catchments in aquatic Mediterranean ecosystems: a review to overcome obstacles and suggest potential solutions. *Environment International*, *64*, 1–16. https://doi.org/10.1016/j.envint.2013.11.016

Gunawardana, C., Goonetilleke, A., Egodawatta, P., Dawes, L., & Kokot, S. (2012). Source characterisation of road dust based on chemical and mineralogical composition. *Chemosphere*, *87*(2), 163–170. https://doi.org/10.1016/j.chemosphere.2011.12.012

Haga, H., Matsumoto, Y., Matsutani, J., Fujita, M., Nishida, K., & Sakamoto, Y. (2005).

Flow paths, rainfall properties, and antecedent soil moisture controlling lags to peak discharge in a granitic unchanneled catchment. *Water Resources Research*, *41*(12), 1–14. https://doi.org/10.1029/2005WR004236

Haleyur, N., Shahsavari, E., Taha, M., Khudur, L. S., Koshlaf, E., Osborn, A. M., & Ball, A. S. (2018). Assessing the degradation efficacy of native PAH-degrading bacteria from aged, weathered soils in an Australian former gasworks site. *Geoderma*, *321*(February), 110–117. https://doi.org/10.1016/j.geoderma.2018.02.004

Haritash, a K., & Kaushik, C. P. (2009). Biodegradation aspects of polycyclic aromatic hydrocarbons (PAHs): a review. *Journal of Hazardous Materials*, *169*(1–3), 1–15. https://doi.org/10.1016/j.jhazmat.2009.03.137

Herngren, L., Goonetilleke, A., & Ayoko, G. A. (2005). Understanding heavy metal and suspended solids relationships in urban stormwater using simulated rainfall. *Journal of Environmental Management*, *76*(2), 149–158. https://doi.org/10.1016/j.jenvman.2005.01.013

Herngren, L., Goonetilleke, A., & Ayoko, G. A. (2006). Analysis of heavy metals in road-deposited sediments. *Analytica Chimica Acta*, *571*(2), 270–278. https://doi.org/10.1016/j.aca.2006.04.064

Hubert, J., Edwards, T., & Jahromi, A. (2012). Comparative study of sustainable drainage systems. *Proceedings of the ICE- …*, *166*(3), 138–149. Retrieved from http://www.icevirtuallibrary.com/content/article/10.1680/ensu.11.00029

Jackson, J., & Boutle, R. (2008). Ecological functions within a sustainable urban drainage system. *11th International Conference on Urban …*, 1–10. Retrieved from http://web.sbe.hw.ac.uk/staffprofiles/bdgsa/11th_International_Conference_on_Urban_Drainage_CD/ICUD08/pdfs/309.pdf

Jefferies, C., & Napier, F. (2008). *SOURCE CONTROL POLLUTION IN SUSTAINABLE DRAINAGE Supplementary Report (Draft)*.

Jia, C., & Batterman, S. (2010). A critical review of naphthalene sources and exposures

relevant to indoor and outdoor air. *International Journal of Environmental Research and Public Health*, *7*(7), 2903–2939. https://doi.org/10.3390/ijerph7072903

Jin, J., Yao, J., Liu, W., Zhang, Q., & Liu, J. (2017). Fluoranthene degradation and binding mechanism study based on the active-site structure of ring-hydroxylating dioxygenase in Microbacterium paraoxydans JPM1. *Environmental Science and Pollution Research*, *24*(1), 363–371. https://doi.org/10.1007/s11356-016-7809-4

Jones, K. C., Stratford, J. A., Waterhouse, K. S., & Vogt, N. B. (1989). Organic Contaminants in Welsh Soils: Polynuclear Aromatic Hydrocarbons. *Environmental Science and Technology*, *23*(5), 540–550. https://doi.org/10.1021/es00063a005

Kadri, T., Rouissi, T., Kaur Brar, S., Cledon, M., Sarma, S., & Verma, M. (2017). Biodegradation of polycyclic aromatic hydrocarbons (PAHs) by fungal enzymes: A review. *Journal of Environmental Sciences (China)*, *51*, 52–74. https://doi.org/10.1016/j.jes.2016.08.023

Kanaly, R. A., & Harayama, S. (2000). *MINIREVIEW Biodegradation of High-Molecular-Weight Polycyclic Aromatic Hydrocarbons by Bacteria*. *182*(8), 2059–2067.

Kang, J.-H., Kayhanian, M., & Stenstrom, M. K. (2008). Predicting the existence of stormwater first flush from the time of concentration. *Water Research*, *42*(1–2), 220–228. https://doi.org/10.1016/j.watres.2007.07.001

Kawasaki, A., Warren, C. R., & Kertesz, M. A. (2015). Specific influence of white clover on the rhizosphere microbial community in response to polycyclic aromatic hydrocarbon (PAH) contamination. *Plant and Soil*, 1–15. https://doi.org/10.1007/s11104-015-2756-2

Kayhanian, M, Suverkropp, C., Ruby, a, & Tsay, K. (2007). Characterization and prediction of highway runoff constituent event mean concentration. *Journal of Environmental Management*, *85*(2), 279–295. https://doi.org/10.1016/j.jenvman.2006.09.024

Kayhanian, Masoud, Fruchtman, B. D., Gulliver, J. S., Montanaro, C., Ranieri, E., &

Wuertz, S. (2012). Review of highway runoff characteristics: comparative analysis and universal implications. *Water Research*, *46*(20), 6609–6624. https://doi.org/10.1016/j.watres.2012.07.026

Kazemi, F., Golzarian, M. R., & Myers, B. (2018). Potential of combined Water Sensitive Urban Design systems for salinity treatment in urban environments. *Journal of Environmental Management*, *209*, 169–175. https://doi.org/10.1016/j.jenvman.2017.12.046

Khudhair, A. B., Hadibarata, T., Yusoff, A. R. M., Teh, Z. C., Adnan, L. A., & Kamyab, H. (2015). Pyrene metabolism by new species isolated from soil Rhizoctonia zeae SOL3. *Water, Air, and Soil Pollution*, *226*(6). https://doi.org/10.1007/s11270-015-2432-4

Kim, D., & Young, T. M. (2009). Significance of Indirect Deposition on Wintertime PAH Concentrations in an Urban Northern California Creek. *Environmental Engineering Science*, *26*(2), 269–278. https://doi.org/10.1089/ees.2007.0277

Kim, G. B., Maruya, K. A., Lee, R. F., Lee, J. H., Koh, C. H., & Tanabe, S. (1999). Distribution and sources of polycyclic aromatic hydrocarbons in sediments from Kyeonggi Bay, Korea. *Marine Pollution Bulletin*, *38*(1), 7–15. https://doi.org/10.1016/S0025-326X(98)00077-0

Kim, K.-H., Jahan, S. A., Kabir, E., & Brown, R. J. C. (2013). A review of airborne polycyclic aromatic hydrocarbons (PAHs) and their human health effects. *Environment International*, *60*, 71–80. https://doi.org/10.1016/j.envint.2013.07.019

Kirby, A. (2005). SuDS—innovation or a tried and tested practice? *Proceedings of the ICE - Municipal Engineer*, *158*(2), 115–122. https://doi.org/10.1680/muen.2005.158.2.115

Kucerová, P., In Der Wiesche, C., Wolter, M., Macek, T., Zadrazil, F., & Macková, M. (2001). The ability of different plant species to remove polycyclic aromatic hydrocarbons and polychlorinated biphenyls from incubation media. *Biotechnology Letters*, *23*(6), 1355–1359.

https://doi.org/10.1023/A:1010502023311

Kuffner, M., Puschenreiter, M., Wieshammer, G., Gorfer, M., & Sessitsch, A. (2008). Rhizosphere bacteria affect growth and metal uptake of heavy metal accumulating willows. *Plant and Soil*, *304*(1–2), 35–44. https://doi.org/10.1007/s11104-007-9517-9

Kuiper, I., Lagendijk, E. L., Bloemberg, G. V, & Lugtenberg, B. J. J. (2004). Rhizoremediation : A Beneficial Plant-Microbe Interaction. *Molecular Plant-Microbe Interactions*, *17*(1), 6–15.

Kumata, H., Masuda, K., Yamada, J., & Takada, H. (2000). Water-particle distribution of hydrophobic micro pollutants in storm water runoff. *Polycyclic Aromatic Compounds*, *20*(1–4), 39–54. https://doi.org/10.1080/10406630008034774

Lashford, C., Charlesworth, S., Warwick, F., & Blackett, M. (2014). Deconstructing the Sustainable Drainage Management Train in Terms of Water Quantity - Preliminary Results for Coventry, UK. *CLEAN - Soil, Air, Water*, *42*(2), 187–192. https://doi.org/10.1002/clen.201300161

Lee, H., Lau, S.-L., Kayhanian, M., & Stenstrom, M. K. (2004). Seasonal first flush phenomenon of urban stormwater discharges. *Water Research*, *38*(19), 4153–4163. https://doi.org/10.1016/j.watres.2004.07.012

Lee, J., & Bang, K. . (2000). Characterization of urban stormwater runoff. *Water Research*, *34*(6), 1773–1780. https://doi.org/10.1016/S0043-1354(99)00325-5

Leroy, M. C., Legras, M., Marcotte, S., Moncond'huy, V., Machour, N., Le Derf, F., & Portet-Koltalo, F. (2015). Assessment of PAH dissipation processes in large-scale outdoor mesocosms simulating vegetated road-side swales. *Science of the Total Environment*, *520*, 146–153. https://doi.org/10.1016/j.scitotenv.2015.03.020

Leroy, M., Portet-Koltalo, F., Legras, M., Lederf, F., Moncond'huy, V., Polaert, I., & Marcotte, S. (2016). Performance of vegetated swales for improving road runoff quality in a moderate traffic urban area. *Science of The Total Environment*, *566*–

567, 113–121. https://doi.org/http://dx.doi.org/10.1016/j.scitotenv.2016.05.027

Li, X., Li, P., Lin, X., Zhang, C., Li, Q., & Gong, Z. (2008). Biodegradation of aged polycyclic aromatic hydrocarbons (PAHs) by microbial consortia in soil and slurry phases. *Journal of Hazardous Materials*. https://doi.org/10.1016/j.jhazmat.2007.04.040

Lin, Z.-Q. (2018). Ecological Processes: Volatilization ☆. In *Reference Module in Earth Systems and Environmental Sciences* (2nd ed.). https://doi.org/10.1016/B978-0-12-409548-9.11183-2

Liu, H., Meng, F., Tong, Y., & Chi, J. (2014). Effect of plant density on phytoremediation of polycyclic aromatic hydrocarbons contaminated sediments with Vallisneria spiralis. *Ecological Engineering*, *73*, 380–385. https://doi.org/10.1016/j.ecoleng.2014.09.084

Liu, Y., Ahiablame, L. M., Bralts, V. F., & Engel, B. a. (2015). Enhancing a rainfall-runoff model to assess the impacts of BMPs and LID practices on storm runoff. *Journal of Environmental Management*, *147*, 12–23. https://doi.org/10.1016/j.jenvman.2014.09.005

Lors, C., Damidot, D., Ponge, J. F., & Périé, F. (2012). Comparison of a bioremediation process of PAHs in a PAH-contaminated soil at field and laboratory scales. *Environmental Pollution*, *165*, 11–17. https://doi.org/10.1016/j.envpol.2012.02.004

Lucke, T., Mohamed, M. A. K., & Tindale, N. (2014). Pollutant removal and Hydraulic reduction performance of field grassed swales during runoff simulation experiments. *Water (Switzerland)*, *6*, 1887–1904. https://doi.org/10.3390/w6071887

Lundy, L., Ellis, J. B., & Revitt, D. M. (2012). Risk prioritisation of stormwater pollutant sources. *Water Research*, *46*(20), 6589–6600. https://doi.org/10.1016/j.watres.2011.10.039

Manoli, E., & Samara, C. (1999). Polycyclic aromatic hydrocarbons in natural waters:

sources, occurrence and analysis. *TrAC Trends in Analytical Chemistry*, *18*(6), 417–428. https://doi.org/10.1016/S0165-9936(99)00111-9

Marquès, M., Mari, M., Audí-Miró, C., Sierra, J., Soler, A., Nadal, M., & Domingo, J. L. (2016). Climate change impact on the PAH photodegradation in soils: Characterization and metabolites identification. *Environment International*, *89–90*, 155–165. https://doi.org/10.1016/j.envint.2016.01.019

Marquès, M., Mari, M., Sierra, J., Nadal, M., & Domingo, J. L. (2017). Solar radiation as a swift pathway for PAH photodegradation: A field study. *Science of the Total Environment*, *581–582*, 530–540. https://doi.org/10.1016/j.scitotenv.2016.12.161

Melville-Shreeve, P., Cotterill, S., Grant, L., Arahuetes, A., Stovin, V., Farmani, R., & Butler, D. (2018). State of SuDS delivery in the United Kingdom. *Water and Environment Journal*, *32*(1), 9–16. https://doi.org/10.1111/wej.12283

Messias, J. M., da Costa, B. Z., de Lima, V. M. G., Dekker, R. F. H., Rezende, M. I., Krieger, N., & Barbosa, A. M. (2009). Screening Botryosphaeria species for lipases: Production of lipase by Botryosphaeria ribis EC-01 grown on soybean oil and other carbon sources. *Enzyme and Microbial Technology*. https://doi.org/10.1016/j.enzmictec.2009.08.013

Ministry of Housing, C. and local G. (2015). Drainage and waste disposal - Part H. In *Building Regulations 2010*.

Morbidelli, R., Saltalippi, C., Flammini, A., Cifrodelli, M., Picciafuoco, T., Corradini, C., & Govindaraju, R. S. (2016). Laboratory investigation on the role of slope on infiltration over grassy soils. *Journal of Hydrology*. https://doi.org/10.1016/j.jhydrol.2016.10.024

Mueller, K. E., & Shann, J. R. (2006). PAH dissipation in spiked soil: Impacts of bioavailability, microbial activity, and trees. *Chemosphere*, *64*(6), 1006–1014. https://doi.org/10.1016/j.chemosphere.2005.12.051

Muthukrishnan, S. (2010). Treatment Of Heavy Metals In Stormwater Runoff Using Wet

Pond And Wetland Mesocosms. … *on Soils, Sediments, Water and Energy*, *11*(2006). Retrieved from http://scholarworks.umass.edu/soilsproceedings/vol11/iss1/9/

Napier, F., Jefferies, C., Heal, K. V., Fogg, P., Arcy, B. J. D., & Clarke, R. (2009). Evidence of traffic-related pollutant control in soil-based Sustainable Urban Drainage Systems (SUDS). *Water Science and Technology*, *60*, 221–230. https://doi.org/10.2166/wst.2009.326

Napier, Fiona, D'Arcy, B., & Jefferies, C. (2008). A review of vehicle related metals and polycyclic aromatic hydrocarbons in the UK environment. *Desalination*, *226*(1–3), 143–150. https://doi.org/10.1016/j.desal.2007.02.104

Padmavathiamma, P. K., & Li, L. Y. (2007). Phytoremediation Technology: Hyper-accumulation Metals in Plants. *Water, Air, and Soil Pollution*, *184*(1–4), 105–126. https://doi.org/10.1007/s11270-007-9401-5

Park, K., Sims, C., Dupont, R. R., Doucette, J., & Matthews, E. (1990). Fate of Pah Compounds in Two Soil Types : *Environmenral Toxicology and Chemistry*, *9*(c), 187–195.

Ping, L., Guo, Q., Chen, X., Yuan, X., Zhang, C., & Zhao, H. (2017). Biodegradation of pyrene and benzo[a]pyrene in the liquid matrix and soil by a newly identified Raoultella planticola strain. *3 Biotech*, *7*(1), 1–10. https://doi.org/10.1007/s13205-017-0704-y

Prabhukumar, G., & Program, E. E. (2011). Polycyclic Aromatic Hydrocarbons in Urban Runoff – Sources , Sinks and Treatment : A Review. *Review Literature And Arts Of The Americas*.

Raskin, I., Smith, R. D., & Salt, D. E. (1997). Phytoremediation of metals: using plants to remove pollutants from the environment. *Current Opinion in Biotechnology*, *8*(2), 221–226. https://doi.org/10.1016/S0958-1669(97)80106-1

Rehmann, K., Noll, H. P., Steinberg, C. E. W., & Kettrup, A. A. (1998). Pyrene degradation by Mycobacterium sp. strain KR2. *Chemosphere*. https://doi.org/10.1016/S0045-

6535(97)10240-5

Revitt, D. Michael, Ellis, J. B., & Lundy, L. (2017). Assessing the impact of swales on receiving water quality. *Urban Water Journal*, *9006*(January), 1–7. https://doi.org/10.1080/1573062X.2017.1279187

Revitt, D M, Shutes, R. B. E., Jones, R. H., Forshaw, M., & Winter, B. (2004). The performances of vegetative treatment systems for highway runoff during dry and wet conditions. *The Science of the Total Environment*, *334–335*, 261–270. https://doi.org/10.1016/j.scitotenv.2004.04.046

Revitt, D Michael, Ellis, J. B., & Lundy, L. (2017). Assessing the impact of swales on receiving water quality. *Urban Water Journal*, *14*(8), 839–845. https://doi.org/10.1080/1573062X.2017.1279187

Revitt, D Michael, Lundy, L., Coulon, F., & Fairley, M. (2014). The sources, impact and management of car park runoff pollution: A review. *Journal of Environmental Management*, *146C*, 552–567. https://doi.org/10.1016/j.jenvman.2014.05.041

Rocha, a. C. S., Almeida, C. M. R., Basto, M. C. P., & Vasconcelos, M. T. S. D. (2015). Influence of season and salinity on the exudation of aliphatic low molecular weight organic acids (ALMWOAs) by Phragmites australis and Halimione portulacoides roots. *Journal of Sea Research*, *95*, 180–187. https://doi.org/10.1016/j.seares.2014.07.001

Rockne, K. J., Shor, L. M., Young, L. Y., Taghon, G. L., & Kosson, D. S. (2002). Distributed sequestration and release of PAHs in weathered sediment: The role of sediment structure and organic carbon properties. *Environmental Science and Technology*, *36*(12), 2636–2644. https://doi.org/10.1021/es015652h

Roinas, G. (2015). *Sources , Occurrence and Fate of Hydrocarbon Pollutants in Sustainable Drainage Systems*.

Roinas, G., Mant, C., & Williams, J. B. (2014a). Fate of hydrocarbon pollutants in source and non-source control sustainable drainage systems. *Water Science and*

Technology : A Journal of the International Association on Water Pollution Research, *69*(4), 703–709. https://doi.org/10.2166/wst.2013.747

Roinas, G., Mant, C., & Williams, J. B. (2014b). Fate of hydrocarbon pollutants in source and non-source control sustainable drainage systems. *Water Science and Technology*, *69*(4), 703–709. https://doi.org/10.2166/wst.2013.747

Roinas, G., Tsavdaris, A., Williams, J. B., & Mant, C. (2014). Fate and Behavior of Pollutants in a Vegetated Pond System for Road Runoff. *CLEAN - Soil, Air, Water*, *42*(2), 169–177. https://doi.org/10.1002/clen.201300159

Roslund, M. I., Grönroos, M., Rantalainen, A.-L., Jumpponen, A., Romantschuk, M., Parajuli, A., … Sinkkonen, A. (2018). Half-lives of PAHs and temporal microbiota changes in commonly used urban landscaping materials. *PeerJ*, *6*, e4508. https://doi.org/10.7717/peerj.4508

Rubio-Clemente, A., Torres-Palma, R. A., & Peñuela, G. A. (2014). Removal of polycyclic aromatic hydrocarbons in aqueous environment by chemical treatments: A review. *Science of the Total Environment*, *478*, 201–225. https://doi.org/10.1016/j.scitotenv.2013.12.126

Rujner, H., Leonhardt, G., Marsalek, J., Perttu, A. M., & Viklander, M. (2018). The effects of initial soil moisture conditions on swale flow hydrographs. *Hydrological Processes*, *32*(5), 644–654. https://doi.org/10.1002/hyp.11446

Sansalone, J. J., & Cristina, C. M. (2004). First Flush Concepts for Suspended and Dissolved Solids in Small Impervious Watersheds. *Journal of Environmental Engineering*, *130*(11), 1301–1314. https://doi.org/10.1061/(ASCE)0733-9372(2004)130:11(1301)

Schiff, K. C., Tiefenthaler, L. L., Bay, S. M., & Greenstein, D. J. (2016). Effects of rainfall intensity and duration on the first flush from parking lots. *Water (Switzerland)*, *8*(8). https://doi.org/10.3390/w8080320

Schirmer, M., Leschik, S., & Musolff, A. (2013). Current research in urban hydrogeology

– A review. *Advances in Water Resources*, *51*, 280–291. https://doi.org/10.1016/j.advwatres.2012.06.015

Scholes, L., Revitt, D. M., & Ellis, J. B. (2008). A systematic approach for the comparative assessment of stormwater pollutant removal potentials. *Journal of Environmental Management*, *88*(3), 467–478. https://doi.org/10.1016/j.jenvman.2007.03.003

Seo, J.-S., Keum, Y.-S., & Li, Q. X. (2009). Bacterial degradation of aromatic compounds. In *International journal of environmental research and public health* (Vol. 6). https://doi.org/10.3390/ijerph6010278

Serrano, A., Gallego, M., González, J. L., & Tejada, M. (2008). Natural attenuation of diesel aliphatic hydrocarbons in contaminated agricultural soil. *Environmental Pollution*, *151*, 494–502. https://doi.org/10.1016/j.envpol.2007.04.015

Shafique, M., Kim, R., & Kyung-Ho, K. (2018). Evaluating the capability of grass swale for the rainfall runoff reduction from an Urban parking lot, Seoul, Korea. *International Journal of Environmental Research and Public Health*, *15*(3). https://doi.org/10.3390/ijerph15030537

Smith, D. J. T., Edelhauser, E. C., & Harrison, R. M. (1995). Polynuclear aromatic hydrocarbon concentrations in road dust and soil samples collected in the United Kingdom and Pakistan. *Environmental Technology*, *16*(1), 45–53. https://doi.org/10.1080/09593331608616244

Smith, D., & Lynam, K. (2010). GC/MS Analysis of European Union (EU) Priority Polycyclic Aromatic Hydrocarbons (PAHs) using an Agilent J&W DB-EUPAH GC Column with a Column Performance Comparison. *Agilent Technologies*, 1–6.

Sprovieri, M., Feo, M. L., Prevedello, L., Manta, D. S., Sammartino, S., Tamburrino, S., & Marsella, E. (2007). Heavy metals, polycyclic aromatic hydrocarbons and polychlorinated biphenyls in surface sediments of the Naples harbour (southern Italy). *Chemosphere*, *67*(5), 998–1009. https://doi.org/10.1016/j.chemosphere.2006.10.055

Stagge, J. H., Davis, A. P., Jamil, E., & Kim, H. (2012). Performance of grass swales for improving water quality from highway runoff. *Water Research*, *46*(20), 6731–6742. https://doi.org/10.1016/j.watres.2012.02.037

Stogiannidis, E., & Laane, R. (2015). Source Characterization of Polycyclic Aromatic Hydrocarbons by Using Their Molecular Indices: An Overview of Possibilities. In *reviews of environmental contamination and toxicology* (Vol. 234, pp. 49–133). https://doi.org/10.1007/978-3-319-10638-0_2

Sun, Z., Brittain, J. E., Sokolova, E., Thygesen, H., Saltveit, S. J., Rauch, S., & Meland, S. (2018). Aquatic biodiversity in sedimentation ponds receiving road runoff – What are the key drivers? *Science of the Total Environment*, *610–611*, 1527–1535. https://doi.org/10.1016/j.scitotenv.2017.06.080

Susarla, S., Medina, V. F., & McCutcheon, S. C. (2002). Phytoremediation: An ecological solution to organic chemical contamination. *Ecological Engineering*, *18*(5), 647–658. https://doi.org/10.1016/S0925-8574(02)00026-5

Tavera, I., Tames, F., Avelino, J., Ramos, S., Homem, V., Ratola, N., & Carreras, H. (2018). g levels and trends of PAHs and synthetic musks associated with land use in urban environments. *Science of the Total Environment*, *618*, 93–100. https://doi.org/10.1016/j.scitotenv.2017.10.295

Tedoldi, D., Chebbo, G., Pierlot, D., Kovacs, Y., & Gromaire, M. C. (2016). Impact of runoff infiltration on contaminant accumulation and transport in the soil/filter media of Sustainable Urban Drainage Systems: A literature review. *Science of the Total Environment*, Vol. 569–570, pp. 904–926. https://doi.org/10.1016/j.scitotenv.2016.04.215

The Council of the European Union. (1998). Council Directive 98/83/EC of 3 November 1998 on the quality of water intended for human consumption. *Official Journal of the European Communities*, *L330*, 32–54. https://doi.org/2004R0726 - v.7 of 05.06.2013

Trapido, M. (1999). Polycyclic aromatic hydrocarbons in Estonian soil: Contamination

and profiles. *Environmental Pollution*, *105*(1), 67–74. https://doi.org/10.1016/S0269-7491(98)00207-3

Tsavdaris, A. (2014). *An Evaluation of Vegetated SuDS Ponds using Experimental and Numerical Methods*.

United Nations. (2007). World Urbanization Prospects The 2007 Revision Highlights. *Desa*, *ESA/P/WP/2*(4), 883. https://doi.org/10.2307/2808041

US EPA. (2003). *Pahinsoil*.

Van Den Heuvel, H., & Van Noort, P. C. M. (2003). Competition for adsorption between added phenanthrene and in situ PAHs in two sediments. *Chemosphere*, *53*(9), 1097–1103. https://doi.org/10.1016/S0045-6535(03)00596-4

Vane, C. H., Kim, A. W., Beriro, D. J., Cave, M. R., Knights, K., Moss-Hayes, V., & Nathanail, P. C. (2014). Polycyclic aromatic hydrocarbons (PAH) and polychlorinated biphenyls (PCB) in urban soils of Greater London, UK. *Applied Geochemistry*, *51*, 303–314. https://doi.org/10.1016/j.apgeochem.2014.09.013

Vargas-Luna, A., Crosato, A., & Uijttewaal, W. S. J. (2015). Effects of vegetation on flow and sediment transport: Comparative analyses and validation of predicting models. *Earth Surface Processes and Landforms*, *40*(2), 157–176. https://doi.org/10.1002/esp.3633

Venkatesagowda, B., Ponugupaty, E., Barbosa, A. M., & Dekker, R. F. H. (2012). Diversity of plant oil seed-associated fungi isolated from seven oil-bearing seeds and their potential for the production of lipolytic enzymes. *World Journal of Microbiology and Biotechnology*, *28*(1), 71–80. https://doi.org/10.1007/s11274-011-0793-4

Viavattene, C., & Ellis, J. B. (2013). The management of urban surface water flood risks: SUDS performance in flood reduction from extreme events. *Water Science and Technology : A Journal of the International Association on Water Pollution Research*, *67*(1), 99–108. https://doi.org/10.2166/wst.2012.537

Wang, D., Yang, M., Jia, H., Zhou, L., & Li, Y. (2008). Seasonal variation of polycyclic aromatic hydrocarbons in soil and air of Dalian areas, China: An assessment of soil-air exchange. *Journal of Environmental Monitoring*, *10*(9), 1076–1083. https://doi.org/10.1039/b805840g

Wang, X. T., Miao, Y., Zhang, Y., Li, Y. C., Wu, M. H., & Yu, G. (2013). Polycyclic aromatic hydrocarbons (PAHs) in urban soils of the megacity Shanghai: Occurrence, source apportionment and potential human health risk. *Science of the Total Environment*, *447*, 80–89. https://doi.org/10.1016/j.scitotenv.2012.12.086

Wang, Y.-J., Chen, C.-F., & Lin, J.-Y. (2013). The measurement of dry deposition and surface runoff to quantify urban road pollution in Taipei, Taiwan. *International Journal of Environmental Research and Public Health*, *10*(10), 5130–5145. https://doi.org/10.3390/ijerph10105130

Wang, Z., Liu, Z., Xu, K., Mayer, L. M., Zhang, Z., Kolker, A. S., & Wu, W. (2014). Concentrations and sources of polycyclic aromatic hydrocarbons in surface coastal sediments of the northern Gulf of Mexico. *Geochemical Transactions*, *15*(1), 1–12. https://doi.org/10.1186/1467-4866-15-2

Water UK. (2018). *Sewers for Adoption - 8th edition*. Retrieved from http://sfa.wrcplc.co.uk/Data/Sites/4/GalleryImages/WebImages/pdfs/SFA7smalldev_sep2013.pdf

Weiss, P. T., Gulliver, J. S., & Erickson, A. J. (2010). *The Performance of Grassed Swales as Infiltration and Pollution Prevention Practices A LITERATURE REVIEW*. (November).

Wenzel, W. W. (2009). Rhizosphere processes and management in plant-assisted bioremediation (phytoremediation) of soils. *Plant and Soil*, *321*, 385–408. https://doi.org/10.1007/s11104-008-9686-1

Wenzl, T., Simon, R., Anklam, E., & Kleiner, J. (2006). Analytical methods for polycyclic aromatic hydrocarbons (PAHs) in food and the environment needed for new food legislation in the European Union. *TrAC - Trends in Analytical Chemistry*, *25*(7), 716–

725. https://doi.org/10.1016/j.trac.2006.05.010

Wilcke, W. (2000). SYNOPSIS Polycyclic Aromatic Hydrocarbons (PAHs) in Soil — a Review. *Journal of Plant Nutrition and Soil Science*, *163*(1988), 229–248. https://doi.org/10.1002/1522-2624(200006)163:3<229::aid-jpln229>3.0.co;2-6

Wild, S. R., & Jones, K. C. (1995). Polynuclear aromatic hydrocarbons in the United Kingdom environment: a preliminary source inventory and budget. *Environmental Pollution (Barking, Essex : 1987)*, *88*, 91–108. https://doi.org/10.1016/0269-7491(95)91052-M

Williams, J. B., Jose, R., Moobela, C., Hutchinson, D. J., Wise, R., & Gaterell, M. (2019). Residents' perceptions of sustainable drainage systems as highly functional blue green infrastructure. *Landscape and Urban Planning*, *190*(November 2018), 103610. https://doi.org/10.1016/j.landurbplan.2019.103610

Wong, T. H. F., Duncan, H. P., Fletcher, T. D., Jenkins, G. A., & Coleman, J. R. (2001). A unified approach to modelling urban stormwater treatment. *Proceedings of the 2nd South Pacific Stormwater Conference*, (June), 27–29.

Woods Ballard, B., Kellagher, R., Martin, P., Jefferies, C., Bray, R., Shaffer, P., … Agency, E. (2015). The SUDS manual. In *Ciria, …*. https://doi.org/London C697

Xing, W., Luo, Y., Wu, L., Song, J., & Christie, P. (2006). Accumulation and phytoavailability of benzo[a]pyrene in an acid sandy soil. *Environmental Geochemistry and Health*, *28*(1–2), 153–158. https://doi.org/10.1007/s10653-005-9026-9

Yang, Y., Ratté, D., Smets, B. F., Pignatello, J. J., & Grasso, D. (2001). Mobilization of soil organic matter by complexing agents and implications for polycyclic aromatic hydrocarbon desorption. *Chemosphere*, *43*(8), 1013–1021. https://doi.org/10.1016/S0045-6535(00)00498-7

Yang, Z., Wang, L., & Niu, J. (2011a). Sorption mechanisms of coexisting PAHs on sediment organic fractions. *Environmental Toxicology and Chemistry*, *30*(3), 576–

581. https://doi.org/10.1002/etc.426

Yang, Z., Wang, L., & Niu, J. (2011b). Sorption mechanisms of coexisting PAHs on sediment organic fractions. *Environmental Toxicology and Chemistry*, *30*(3), 576–581. https://doi.org/10.1002/etc.426

Yu, S. L., Kuo, J.-T., Fassman, E., & Pan, H. (2001). Field Test of Grassed -Swale Performance. *Journal of Water Resources Planning and Management*, (June), 168–171.

Yuan, S. Y., Shiung, L. C., & Chang, B. V. (2002). Biodegradation of polycyclic aromatic hydrocarbons by inoculated microorganisms in soil. *Bulletin of Environmental Contamination and Toxicology*, *69*(1), 66–73. https://doi.org/10.1007/s00128-002-0011-z

Zehetner, F., Rosenfellner, U., Mentler, A., & Gerzabek, M. H. (2009). Distribution of road salt residues, heavy metals and polycyclic aromatic hydrocarbons across a highway-forest interface. *Water, Air, and Soil Pollution*, *198*(1–4), 125–132. https://doi.org/10.1007/s11270-008-9831-8

Zeng, J., Lin, X., Zhang, J., & Li, X. (2010). Isolation of polycyclic aromatic hydrocarbons (PAHs)-degrading Mycobacterium spp. and the degradation in soil. *Journal of Hazardous Materials*, *183*(1–3), 718–723. https://doi.org/10.1016/j.jhazmat.2010.07.085

Zerrouki, D., Maatoug, M., Amirat, M., Chaker, I., Kharytonov, M., & Agrarian, S. (2017). *POLLUTION OF AGRICULTURAL LAND by Naphthalene of road side origin*. *18*(2), 181–190.

Zhang, M., Chen, H., Wang, J., & Pan, G. (2010). Rainwater utilization and storm pollution control based on urban runoff characterization. *Journal of Environmental Sciences*, *22*(1), 40–46. https://doi.org/10.1016/S1001-0742(09)60072-3

ZHANG, X.-X., CHENG, S.-P., ZHU, C.-J., & SUN, S.-L. (2006). Microbial PAH-Degradation in Soil: Degradation Pathways and Contributing Factors. *Pedosphere*, *16*(2001),

555–565. https://doi.org/10.1016/S1002-0160(06)60088-X

Zhou, Q. (2014). A Review of Sustainable Urban Drainage Systems Considering the Climate Change and Urbanization Impacts. *Water*, *6*(4), 976–992. https://doi.org/10.3390/w6040976

Zhou, X., Zhou, J., Xiang, X., Cébron, A., Béguiristain, T., & Leyval, C. (2013). *Impact of Four Plant Species and Arbuscular Mycorrhizal (AM) Fungi on Polycyclic Aromatic Hydrocarbon (PAH) Dissipation in Spiked Soil*. *22*(4), 1239–1245.

10 Appendix

10.1 Method protocols

10.1.1 Water PAH extraction method

EPA Method 550.1, (2011) using application note 54 from SUPERLCO (Sigma Aldrich) for C18 discs.

Sample preparation:

- If not analysing straight away, adjust PH to <2 with 6N Hydrochloric acid (HCl).
- Add 5ml of methanol to sample.
- Rinse all filtration apparatus with acetone (filter to waste).
- Place C18 disc in filtration unit.

Disc preparation:

- Disc washing – *Collect in waste vial, place in the solid phase extractor (SPE), to ensure DCM does not enter the water table.*
    - Add 10ml dichloromethane (DCM).
    - Vacuum through.
    - Leave vacuum running for an extra minute to dry disc.
    - Remove waste vial, and dispose of in correct waste bottle.
- Disc conditioning
    - Add 10ml methanol (CH_4O).
    - Vacuum a small amount through and turn off pump.
    - Leave to soak disc for one minute.
    - Vacuum through CH_4O, leaving enough liquid to cover the disc surface to prevent drying.
    - Add 30ml distilled water (DW) and vacuum through, leave enough liquid to cover surface of disc to prevent drying.

(DO NOT ALLOW DISC TO BECOME DRY, IF THIS HAPPENS REPEAT DISC CONDITIONING)

Sample filtration:

- Add sample (1lt) to filtration device.
- Vacuum through to waste.
- Rinse sample bottle with DW and add to filtration unit.
- When all sample has filtered through, leave vacuum on for no longer than five minutes to dry the disc.
- Place collection vial into SPE filtration unit (all filtered liquid will now be collected).

Extraction:

- Add 10ml DCM to sample flask to rinse it out.
- Add this to filter assembly, rinsing down the sides.
- Turn on vacuum briefly to allow a few drops through.
- Wait two minutes, then turn vacuum on and draw remaining DCM through (into collection vial).
- Add 10ml DCM, rinsing down the sides.
- Turn on vacuum briefly to allow a few drops through.
- Wait two minutes, then turn vacuum on to pull liquid through.
- Leave pump on for five minutes to dry disc.
- Remove collection vial, wrap in tin foil and store in dark conditions until next stage, if not being used immediately.

Eluting PAH:

- Set up a sodium sulphate drying tube, with a new collection vial underneath.
- Using Pasteur pipette transfer sample into a sodium sulphate ($NaSO_4$) column (Bond Elute). This is to remove any remaining water.
- Rinse out empty collection vial with a few millilitres of DCM and add this into the $NaSO_4$ drying tube.
- Once all liquid filtered through, add o.o5ml (50µl) of Nonane to the sample in collection vial (this stays on the surface of the sample to prevent the loss of any chemicals during evaporation/concentration phase).
- Wrap sample vial in tin foil (to prevent PAH degradation by light).

Sample blow-down:

- In GC room, set up all samples for blow down in a heating block at 40^{o}C, using a constant stream of nitrogen (N). This temperature is below the flash point for all chemicals used.
- Blow down until sample is 1ml or whatever volume chosen.
- Measure the amount of sample present, add extra Hexane to make sample up to desired volume (e.g. 1ml). Rinse out the collection vial with the Hexane before adding to sample.
- Transfer to a GC vial ready for analysis on GCMS and store in freezer until ready for analysis.

10.2 Waterlooville study

Table 10-1 Results of PAH concentrations (ng/g) for each monthly sample of the Waterlooville swale study site.

date	Location	Sample	NAP ng/g	FLU ng/g	FLAN ng/g	PYR ng/g	CHR ng/g	B(a)P ng/g
Mar-15	outlet	A2	1,430	279	948	993	822	1,221
	60 m	A3	1,351	285	1,346	1,572	1,078	1,331
	40 m	A4	1,275	0	981	1,040	842	1,051
	20 m	A5	1,410	282	1,882	2,452	1,439	1,630
	inlet	A6	1,498	303	1,544	1,716	1,224	1,534
	Control	A7	1,532	0	0	0	0	0
Apr-15	outlet	A9	1,229	0	1,698	1,599	1,295	1,654
	60 m	A10	1,240	0	1,391	1,584	1,264	1,788
	40 m	A11	1,029	0	1,095	1,201	954	1,228
	20 m	A12	1,050	0	1,297	1,372	1,085	1,362
	inlet	A13	1,125	0	950	1,008	826	1,052
	Control	A14	717	0	252	234	0	0
May-15	outlet	A16	670	0	475	454	418	0
	60 m	A17	1,035	0	978	1,025	902	1,180
	40 m	A18	821	0	688	723	662	928
	20 m	A19	1,137	0	0	0	0	0
	inlet	A20	1,072	0	1,411	1,753	1,181	1,474
	Control	A21	710	0	242	225	0	0
Jun-15	outlet	A23	1,142	0	758	746	538	930
	60 m	A24	1,150	0	1,131	1,126	806	1,359
	40 m	A25	1,214	0	1,079	1,085	751	1,104
	20 m	A26	1,239	0	1,548	1,567	1,037	1,474
	inlet	A27	1,306	0	1,231	1,210	802	1,243
	Control	A28	786	0	278	249	0	0
Jul-15	Outlet	A29	1,745	144	967	976	668	1,000
	60 m	A30	1,269	123	1,047	1,076	716	1,010

	40 m	A31a	1,237	113	889	903	481	650
	20 m	A32	1,470	128	1,240	1,307	851	1,059
	inlet	A33	1,104	0	782	820	558	809
	Control	A34	938	0	265	247	190	369
Aug-15	outlet	A35	1,968	167	1,070	1,089	808	1,164
	60 m	A36	5,506	147	876	912	699	1,033
	40 m	A37	1,419	139	880	950	735	1,133
	20 m	A38	1,642	141	979	1,047	807	1,179
	inlet	A39	0	0	0	0	0	0
	Control	A40	864	0	179	160	81	0
Sep-15	outlet	A41	2,390	52	739	750	478	562
	60 m	A42	2,907	106	920	965	581	692
	40 m	A43	569	0	504	515	337	466
	20 m	A44	2,597	92	905	961	604	724
	inlet	A45	2,666	103	941	997	578	719
	Control	A46	1,908	0	213	188	97	0
Oct-15	outlet	A47	4,529	95	581	588	390	517
	60 m	A48	2,660	46	180	165	78	0
	40 m	A49	5,622	128	841	912	624	805
	20 m	A50	4,403	70	658	688	467	619
	inlet	A51	3,462	52	344	294	149	152
	Control	A52	2,871	38	173	171	104	138
Nov-15	outlet	A53	1,663	0	320	328	232	294
	60 m	A54	1,729	90	644	665	488	752
	40 m	A55	1,565	60	652	695	490	660
	20 m	A56	1,964	85	915	964	693	979
	inlet	A57	1,225	0	544	556	406	655
	Control	A58	879	0	100	91	52	0
Dec-15	outlet	A59	3,051	156	789	794	476	477
	60 m	A60	3,709	181	1,071	1,104	718	779
	40 m	A61	2,968	174	992	1,056	633	662
	20 m	A62	4,135	191	898	911	585	636
	inlet	A63	2,873	156	502	505	308	332

	Control	A64	2,618	137	378	330	173	205
Jan-16	outlet	A65	7,873	301	1,040	1,067	660	741
	60 m	A66	5,308	211	847	882	580	706
	40 m	A67	5,924	289	1,000	1,072	712	908
	20 m	A68	5,063	252	1,189	1,261	840	1,043
	inlet	A69	4,909	191	1,122	1,138	738	1,082
	Control	A70	3,644	122	190	170	99	0
Feb-16	outlet	A71	3,161	177	314	315	207	291
	60 m	A72	3,181	141	203	201	141	196
	40 m	A73	2,484	193	662	764	458	587
	20 m	A74	3,995	278	914	928	638	841
	inlet	A75	3,183	148	130	107	0	0
	Control	A76	2,418	136	0	0	0	0
Mar-16	outlet	A80	2,658	169	303	295	243	361
	60 m	A81	4,047	258	636	694	519	678
	40 m	A82	3,586	256	542	583	441	638
	20 m	A83	2,722	200	459	463	398	570
	inlet	A84	3,593	230	436	436	344	526
	Control	A85	1,545	114	157	146	137	242
Apr-16	outlet	A86	0	0	0	0	0	0
	60 m	A87	3,480	201	475	492	389	574
	40 m	A88	4,413	246	586	606	494	706
	20 m	A89	4,436	244	605	623	485	723
	inlet	A90	5,019	241	291	283	288	440
	Control	A91	2,659	142	172	160	145	263
May-16	outlet	A92	2,347	221	551	565	441	634
	60 m	A93	3,257	238	750	800	616	914
	40 m	A94	2,893	219	828	1,015	643	920
	20 m	A95	2,636	204	632	671	528	796
	inlet	A96	3,621	248	476	477	414	648
	Control	A97	2,030	139	302	280	197	369

Table 10-2 Spearman rho correlations for PAHs in Waterlooville swale.

PAH		*NAP (ng/g)*	*FLU (ng/g)*	*FLAN (ng/g)*	*PYR (ng/g)*	*CHR (ng/g)*	*B(a)P (ng/g)*
NAP (ng/g)	*Spearman rho*	*0.654*					
	P-value	*0.000*					
FLU (ng/g)	*Spearman rho*	*0.562*	*0.737*				
	P-value	*0.000*	*0.000*				
FLAN (ng/g)	*Spearman rho*	*-0.403*	*0.019*	*0.168*			
	P-value	*0.000*	*0.862*	*0.113*			
PYR (ng/g)	*Spearman rho*	*-0.384*	*0.028*	*0.185*	*0.997*		
	P-value	*0.000*	*0.795*	*0.081*	*0.000*		
CHR (ng/g)	*Spearman rho*	*-0.385*	*0.003*	*0.183*	*0.968*	*0.970*	
	P-value	*0.000*	*0.979*	*0.085*	*0.000*	*0.000*	
B(a)P (ng/g)	*Spearman rho*	*-0.364*	*-0.032*	*0.164*	*0.931*	*0.935*	*0.973*
	P-value	*0.000*	*0.765*	*0.122*	*0.000*	*0.000*	*0.000*

10.3 Water statistical analysis

Table 10-3 Kruskal-Wallis comparisons of water quality variables across ten trial runs

Variable	Between runs			Between location		
	H	DF	P	H	DF	P
COD	18.81	9	0.027	50.59	7	0.000
EC	18.3	9	0.032	17.42	7	0.015
pH	8.53	9	0.482	37.19	7	0.000

Table 10-4 Kruskal-Wallis analysis of PAHs between trial runs.

PAH	*H*	*DF*	*P*
NAP	*9.51*	*9*	*0.301*
FLU	*18.83*	*9*	*0.027*
FLAN	*12.32*	*9*	*0.196*
PYR	*12.43*	*9*	*0.190*
CHR	*22.00*	*9*	*0.009*
BaP	*26.23*	*9*	*0.002*

Table 10-5 Spearman rho correlation analysis of Swale inflow and outflow variables. Strong correlations are seen between PAHs

	Air temp	*EC*	*COD*	*NAP*	*FLU*	*FLAN*	*PYR*	*CHR*
EC	*-0.384*							
	0.000							
COD	*0.078*	*0.417*						
	0.494	*0.000*						
NAP	*-0.053*	*-0.455*	*-0.216*					
	0.664	*0.000*	*0.074*					
FLU	*0.080*	*-0.546*	*-0.19*	*0.845*				
	0.485	*0.000*	*0.095*	*0.000*				
FLAN	*-0.105*	*-0.513*	*-0.303*	*0.721*	*0.801*			
	0.359	*0.000*	*0.007*	*0.000*	*0.000*			
PYR	*-0.114*	*-0.46*	*-0.246*	*0.748*	*0.792*	*0.96*		
	0.312	*0.000*	*0.028*	*0.000*	*0.000*	*0.000*		
CHR	*-0.145*	*-0.197*	*0.024*	*0.591*	*0.555*	*0.523*	*0.556*	
	0.250	*0.115*	*0.852*	*0.000*	*0.000*	*0.000*	*0.000*	
BaP	*0.308*	*-0.317*	*0.188*	*0.216*	*0.381*	*0.268*	*0.300*	*0.264*
	0.005	*0.004*	*0.095*	*0.075*	*0.001*	*0.018*	*0.007*	*0.033*

10.4 Descriptive Statistics Soil PAHs for all runs, locations and layers.

Table 10-6 Descriptive statistics for Run 1, 0 – 5 cm

Variable	Location	N	N*	Mean	SE Mean	StDev	Minimum	Q1	Median	Q3	Maximum
Naphthalene (ng/g)	1	3	0	601	114	197	448	448	533	823	823
	2	3	0	484	126	218	246	246	531	675	675
	3	3	0	243	155	268	0	0	199	531	531
	5	3	0	264	150	259	0	0	274	518	518
	8	3	0	349	122	211	176	176	287	584	584
Fluorene (ng/g)	1	3	0	1344	643	1114	161	161	1497	2373	2373
	2	3	0	276	153	266	112	112	134	583	583
	3	3	0	104.8	61.1	105.8	39.6	39.6	48	226.9	226.9
	5	3	0	351	296	512	53	53	57	942	942
	8	3	0	24.07	8.72	15.11	6.75	6.75	30.89	34.56	34.56
Fluoranthene (ng/g)	1	2	1	3807	3779	5344	28	*	3807	*	7585
	2	3	0	781	353	612	124	124	885	1335	1335
	3	3	0	218	218	378	0	0	0	655	655
	5	3	0	1256	1227	2126	0	0	58	3711	3711
	8	3	0	0	0	0	0	0	0	0	0
Pyrene (ng/g)	1	2	1	4150	509	720	3641	*	4150	*	4659
	2	3	0	945	479	829	257	257	712	1865	1865
	3	3	0	271	176	305	51	51	142	619	619
	5	3	0	814	687	1189	77	77	179	2186	2186
	8	3	0	112	12.8	22.1	86.5	86.5	124.4	125.1	125.1
Chrysene (ng/g)	1	3	0	2669	1409	2441	0	0	3218	4788	4788
	2	3	0	0	0	0	0	0	0	0	0
	3	3	0	0	0	0	0	0	0	0	0
	5	3	0	398	398	689	0	0	0	1194	1194
	8	3	0	0	0	0	0	0	0	0	0
Benzo(a)pyrene (ng/g)	1	3	0	74.1	45.9	79.6	0	0	64.1	158.2	158.2
	2	3	0	167.1	27.6	47.8	133.7	133.7	145.7	221.8	221.8
	3	3	0	134.9	55.6	96.4	33.6	33.6	145.6	225.4	225.4
	5	3	0	64.9	10.6	18.4	52.5	52.5	56.2	86.1	86.1
	8	3	0	50.5	14.2	24.6	29.7	29.7	44	77.7	77.7

Table 10-7 Descriptive statistics for Run 1, 5 – 10 cm.

Variable	*Location*	*N*	*N**	*Mean*	*SE Mean*	*StDev*	*Minimum*	*Q1*	*Median*	*Q3*	*Maximum*
Naphthalene (ng/g)	*1*	*3*	*0*	*115.6*	*36.1*	*62.5*	*45*	*45*	*138.2*	*163.7*	*163.7*
	2	*3*	*0*	*126.7*	*18*	*31.1*	*93.4*	*93.4*	*131.8*	*155*	*155*
	3	*3*	*0*	*69.7*	*32.5*	*56.3*	*8.9*	*8.9*	*80*	*120.1*	*120.1*
	5	*3*	*0*	*105.3*	*12.1*	*20.9*	*90.1*	*90.1*	*96.6*	*129.1*	*129.1*
	8	*3*	*0*	*0*	*0*	*0*	*0*	*0*	*0*	*0*	*0*
Fluorene (ng/g)	*1*	*3*	*0*	*0*	*0*	*0*	*0*	*0*	*0*	*0*	*0*
	2	*3*	*0*	*0*	*0*	*0*	*0*	*0*	*0*	*0*	*0*
	3	*3*	*0*	*0*	*0*	*0*	*0*	*0*	*0*	*0*	*0*
	5	*3*	*0*	*0*	*0*	*0*	*0*	*0*	*0*	*0*	*0*
	8	*3*	*0*	*0*	*0*	*0*	*0*	*0*	*0*	*0*	*0*
Fluoranthene (ng/g)	*1*	*3*	*0*	*0*	*0*	*0*	*0*	*0*	*0*	*0*	*0*
	2	*3*	*0*	*0*	*0*	*0*	*0*	*0*	*0*	*0*	*0*
	3	*3*	*0*	*0*	*0*	*0*	*0*	*0*	*0*	*0*	*0*
	5	*3*	*0*	*0*	*0*	*0*	*0*	*0*	*0*	*0*	*0*
	8	*3*	*0*	*0*	*0*	*0*	*0*	*0*	*0*	*0*	*0*
Pyrene (ng/g)	*1*	*3*	*0*	*0*	*0*	*0*	*0*	*0*	*0*	*0*	*0*
	2	*3*	*0*	*0*	*0*	*0*	*0*	*0*	*0*	*0*	*0*
	3	*3*	*0*	*0*	*0*	*0*	*0*	*0*	*0*	*0*	*0*
	5	*3*	*0*	*0*	*0*	*0*	*0*	*0*	*0*	*0*	*0*
	8	*3*	*0*	*0*	*0*	*0*	*0*	*0*	*0*	*0*	*0*
Chrysene (ng/g)	*1*	*3*	*0*	*0*	*0*	*0*	*0*	*0*	*0*	*0*	*0*
	2	*3*	*0*	*0*	*0*	*0*	*0*	*0*	*0*	*0*	*0*
	3	*3*	*0*	*0*	*0*	*0*	*0*	*0*	*0*	*0*	*0*
	5	*3*	*0*	*0*	*0*	*0*	*0*	*0*	*0*	*0*	*0*
	8	*3*	*0*	*0*	*0*	*0*	*0*	*0*	*0*	*0*	*0*
Benzo(a)pyrene (ng/g)	*1*	*3*	*0*	*0*	*0*	*0*	*0*	*0*	*0*	*0*	*0*
	2	*3*	*0*	*0*	*0*	*0*	*0*	*0*	*0*	*0*	*0*
	3	*3*	*0*	*0*	*0*	*0*	*0*	*0*	*0*	*0*	*0*
	5	*3*	*0*	*0*	*0*	*0*	*0*	*0*	*0*	*0*	*0*
	8	*3*	*0*	*0*	*0*	*0*	*0*	*0*	*0*	*0*	*0*

Table 10-8 Descriptive statistics for run 2, 0 – 5 cm.

Variable	Location	N	N*	Mean	SE Mean	StDev	Minimum	Q1	Median	Q3	Maximum
Naphthalene (ng/g)	1	3	0	0	0	0	0	0	0	0	0
	2	3	0	216	108	187	0	0	317	332	332
	3	3	0	365.8	12.8	22.1	341.5	341.5	371.2	384.8	384.8
	5	3	0	299.3	19.4	33.7	260.8	260.8	313.7	323.3	323.3
	8	3	0	296.5	15.5	26.9	267.7	267.7	301	321	321
Fluorene (ng/g)	1	3	0	265	100	173	87	87	276	433	433
	2	3	0	193	141	244	0	0	111	467	467
	3	3	0	243.4	66.2	114.6	134.3	134.3	232.9	362.9	362.9
	5	3	0	152.4	74	128.2	73.5	73.5	83.4	300.3	300.3
	8	3	0	86.3	10.4	18	65.6	65.6	95.7	97.6	97.6
Fluoranthene (ng/g)	1	3	0	1205	513	888	275	275	1294	2044	2044
	2	3	0	752	636	1101	4	4	236	2017	2017
	3	3	0	614	248	429	291	291	450	1101	1101
	5	3	0	553	512	886	10	10	74	1576	1576
	8	3	0	203.5	96.4	166.9	14	14	267.6	328.8	328.8
Pyrene (ng/g)	1	3	0	766	301	521	223	223	813	1261	1261
	2	3	0	545	376	651	81	81	265	1290	1290
	3	3	0	486	155	268	295	295	371	793	793
	5	3	0	427	317	549	80	80	141	1060	1060
	8	3	0	235.5	74.8	129.6	86.2	86.2	301.8	318.5	318.5
Chrysene (ng/g)	1	3	0	106.6	42.7	74	38.4	38.4	96	185.3	185.3
	2	3	0	323	117	203	91	91	407	471	471
	3	3	0	369.4	13.1	22.7	352	352	361	395.1	395.1
	5	3	0	271.7	73.5	127.2	125.2	125.2	335.3	354.6	354.6
	8	3	0	258.5	65.2	112.9	152.8	152.8	245.4	377.4	377.4
Benzo(a)pyrene (ng/g)	1	3	0	167.5	75.8	131.3	40.6	40.6	159.3	302.7	302.7
	2	3	0	350	149	258	95	95	347	610	610
	3	3	0	353	29.4	50.9	294.5	294.5	378.2	386.4	386.4
	5	3	0	173.4	38.4	66.5	105.8	105.8	175.6	238.7	238.7
	8	3	0	282	111	193	110	110	245	491	491

Table 10-9 Descriptive statistics for Run 2, 5 – 10 cm.

Variable	*Location*	*N*	*N**	*Mean*	*SE Mean*	*StDev*	*Minimum*	*Q1*	*Median*	*Q3*	*Maximum*
Naphthalene (ng/g)	*1*	*2*	*1*	*1145*	*105*	*149*	*1040*	*	*1145*	*	*1250*
	2	*3*	*0*	*997*	*134*	*232*	*846*	*846*	*883*	*1264*	*1264*
	3	*3*	*0*	*1103*	*183*	*317*	*783*	*783*	*1109*	*1417*	*1417*
	5	*3*	*0*	*795*	*203*	*352*	*388*	*388*	*993*	*1003*	*1003*
	8	*3*	*0*	*1017.1*	*21.2*	*36.7*	*976.8*	*976.8*	*1025.7*	*1048.7*	*1048.7*
Fluorene (ng/g)	*1*	*2*	*1*	*80.56*	*3.51*	*4.96*	*77.06*	*	*80.56*	*	*84.07*
	2	*2*	*1*	*0*	*0*	*0*	*0*	*	*0*	*	*0*
	3	*2*	*1*	*30.84*	*6.85*	*9.69*	*23.99*	*	*30.84*	*	*37.69*
	5	*3*	*0*	*0*	*0*	*0*	*0*	*0*	*0*	*0*	*0*
	8	*3*	*0*	*0*	*0*	*0*	*0*	*0*	*0*	*0*	*0*
Fluoranthene (ng/g)	*1*	*3*	*0*	*480*	*180*	*311*	*132*	*132*	*577*	*732*	*732*
	2	*2*	*1*	*0*	*0*	*0*	*0*	*	*0*	*	*0*
	3	*2*	*1*	*37.1*	*37.1*	*52.4*	*0*	*	*37.1*	*	*74.1*
	5	*3*	*0*	*0.508*	*0.508*	*0.881*	*0*	*0*	*0*	*1.525*	*1.525*
	8	*3*	*0*	*0*	*0*	*0*	*0*	*0*	*0*	*0*	*0*
Pyrene (ng/g)	*1*	*3*	*0*	*464*	*110*	*191*	*248*	*248*	*537*	*608*	*608*
	2	*2*	*1*	*105.43*	*2.79*	*3.94*	*102.64*	*	*105.43*	*	*108.21*
	3	*3*	*0*	*343*	*184*	*318*	*118*	*118*	*202*	*707*	*707*
	5	*3*	*0*	*71.6*	*37.5*	*64.9*	*33.3*	*33.3*	*34.8*	*146.5*	*146.5*
	8	*3*	*0*	*89*	*38.7*	*67*	*22.6*	*22.6*	*87.9*	*156.6*	*156.6*
Chrysene (ng/g)	*1*	*3*	*0*	*554.2*	*75.7*	*131.2*	*434.3*	*434.3*	*533.8*	*694.3*	*694.3*
	2	*3*	*0*	*310.2*	*55.2*	*95.6*	*204.6*	*204.6*	*335*	*390.9*	*390.9*
	3	*3*	*0*	*317.5*	*57.3*	*99.3*	*240.5*	*240.5*	*282.5*	*429.5*	*429.5*
	5	*3*	*0*	*212.5*	*35.5*	*61.5*	*158.2*	*158.2*	*200.1*	*279.3*	*279.3*
	8	*3*	*0*	*214.6*	*64.5*	*111.7*	*138.3*	*138.3*	*162.7*	*342.8*	*342.8*
Benzo(a)pyrene (ng/g)	*1*	*3*	*0*	*835*	*132*	*229*	*680*	*680*	*728*	*1098*	*1098*
	2	*3*	*0*	*374.6*	*85.4*	*148*	*240.2*	*240.2*	*350.5*	*533.2*	*533.2*
	3	*3*	*0*	*384.8*	*38.6*	*66.8*	*315.9*	*315.9*	*389.4*	*449.3*	*449.3*
	5	*3*	*0*	*259.5*	*50.3*	*87*	*201.5*	*201.5*	*217.5*	*359.6*	*359.6*
	8	*3*	*0*	*243*	*102*	*177*	*120*	*120*	*163*	*447*	*447*

Table 10-10 Descriptive statistics for Run 3, 0 – 5 cm.

Variable	Location	N	N*	Mean	SE Mean	StDev	Minimum	Q1	Median	Q3	Maximum
Naphthalene (ng/g)	1	3	0	459	68.2	118.1	380	380	402.1	594.8	594.8
	2	3	0	723.3	87.1	150.8	566.4	566.4	736.5	867.1	867.1
	3	3	0	740	108	187	568	568	712	939	939
	5	3	0	862.3	92.1	159.6	696.7	696.7	875	1015.2	1015.2
	8	3	0	684	135	234	414	414	807	830	830
Fluorene (ng/g)	1	3	0	1718	753	1304	858	858	1078	3218	3218
	2	3	0	1813	435	753	1177	1177	1618	2644	2644
	3	3	0	1149	156	271	932	932	1062	1452	1452
	5	3	0	2536	1174	2034	906	906	1886	4815	4815
	8	3	0	1414	819	1419	516	516	677	3050	3050
Fluoranthene (ng/g)	1	2	1	7391	2381	3367	5010	*	7391	*	9772
	2	3	0	12974	5067	8776	7467	7467	8360	23094	23094
	3	3	0	6297	717	1242	5025	5025	6356	7508	7508
	5	2	1	7795	4852	6862	2943	*	7795	*	12647
	8	3	0	10113	4416	7649	5511	5511	5887	18943	18943
Pyrene (ng/g)	1	3	0	535388	232945	403472	185154	185154	444437	976573	976573
	2	3	0	510488	146736	254155	317437	317437	415588	798437	798437
	3	3	0	315878	30961	53625	276622	276622	294034	376977	376977
	5	2	1	417939	235995	333747	181944	*	417939	*	653934
	8	3	0	498796	238051	412317	219465	219465	304567	972357	972357
Chrysene (ng/g)	1	3	0	19168	3050	5282	14044	14044	18865	24595	24595
	2	3	0	16451	5438	9420	10244	10244	11818	27289	27289
	3	3	0	28122	8296	14370	14460	14460	26798	43108	43108
	5	2	1	38937	5680	8033	33258	*	38937	*	44617
	8	3	0	22017	9379	16244	8359	8359	17711	39980	39980
Benzo(a)pyrene (ng/g)	1	3	0	3190	1416	2452	1754	1754	1794	6022	6022
	2	3	0	3832	628	1088	2577	2577	4404	4513	4513
	3	3	0	4586	923	1599	3153	3153	4295	6310	6310
	5	2	1	2762	504	713	2259	*	2762	*	3266
	8	3	0	1731	390	676	981	981	1920	2293	2293

Table 10-11 Descriptive statistics for Run 3, 5 – 10 cm.

Variable	*Location*	*N*	*N**	*Mean*	*SE Mean*	*StDev*	*Minimum*	*Q1*	*Median*	*Q3*	*Maximum*
Naphthalene (ng/g)	*1*	*3*	*0*	*1184*	*217*	*376*	*946*	*946*	*989*	*1618*	*1618*
	2	*3*	*0*	*1157*	*579*	*1002*	*0*	*0*	*1734*	*1737*	*1737*
	3	*3*	*0*	*1344*	*188*	*325*	*1002*	*1002*	*1380*	*1649*	*1649*
	5	*3*	*0*	*1529*	*445*	*771*	*873*	*873*	*1335*	*2379*	*2379*
	8	*3*	*0*	*1174.1*	*70.7*	*122.4*	*1071.1*	*1071.1*	*1141.9*	*1309.4*	*1309.4*
Fluorene (ng/g)	*1*	*3*	*0*	*41.1*	*41.1*	*71.2*	*0*	*0*	*0*	*123.2*	*123.2*
	2	*3*	*0*	*2.03*	*2.03*	*3.52*	*0*	*0*	*0*	*6.1*	*6.1*
	3	*2*	*1*	*9.98*	*0.833*	*1.178*	*9.147*	***	*9.98*	***	*10.813*
	5	*3*	*0*	*16.9*	*16.9*	*29.3*	*0*	*0*	*0*	*50.8*	*50.8*
	8	*3*	*0*	*0*	*0*	*0*	*0*	*0*	*0*	*0*	*0*
Fluoranthene (ng/g)	*1*	*2*	*1*	*229*	*229*	*324*	*0*	***	*229*	***	*459*
	2	*3*	*0*	*0*	*0*	*0*	*0*	*0*	*0*	*0*	*0*
	3	*2*	*1*	*0*	*0*	*0*	*0*	***	*0*	***	*0*
	5	*3*	*0*	*0*	*0*	*0*	*0*	*0*	*0*	*0*	*0*
	8	*3*	*0*	*21.7*	*21.7*	*37.5*	*0*	*0*	*0*	*65*	*65*
Pyrene (ng/g)	*1*	*3*	*0*	*525*	*233*	*404*	*146*	*146*	*478*	*951*	*951*
	2	*3*	*0*	*75.2*	*40.9*	*70.8*	*0*	*0*	*84.9*	*140.6*	*140.6*
	3	*2*	*1*	*113.7*	*10.9*	*15.4*	*102.8*	***	*113.7*	***	*124.6*
	5	*3*	*0*	*47.6*	*24.1*	*41.8*	*19.2*	*19.2*	*27.9*	*95.6*	*95.6*
	8	*3*	*0*	*87.6*	*71.2*	*123.4*	*0*	*0*	*34.1*	*228.7*	*228.7*
Chrysene (ng/g)	*1*	*2*	*1*	*426.8*	*65.2*	*92.1*	*361.7*	***	*426.8*	***	*492*
	2	*3*	*0*	*227*	*117*	*202*	*0*	*0*	*294*	*387*	*387*
	3	*2*	*1*	*211.2*	*34.7*	*49.1*	*176.5*	***	*211.2*	***	*245.9*
	5	*3*	*0*	*226*	*49.4*	*85.5*	*153.4*	*153.4*	*204.4*	*320.2*	*320.2*
	8	*3*	*0*	*225.2*	*91.7*	*158.8*	*115.8*	*115.8*	*152.6*	*407.4*	*407.4*
Benzo(a)pyrene (ng/g)	*1*	*2*	*1*	*483*	*111*	*157*	*372*	***	*483*	***	*594*
	2	*3*	*0*	*334*	*168*	*291*	*0*	*0*	*474*	*529*	*529*
	3	*2*	*1*	*292.9*	*52.9*	*74.9*	*240*	***	*292.9*	***	*345.8*
	5	*3*	*0*	*307.9*	*75.9*	*131.5*	*190.8*	*190.8*	*282.9*	*450.1*	*450.1*
	8	*3*	*0*	*293*	*152*	*263*	*116*	*116*	*169*	*595*	*595*

Table 10-12 Descriptive statistics for Run 4, 0 – 5 cm

Variable	Location	N	N*	Mean	SE Mean	StDev	Minimum	Q1	Median	Q3	Maximum
Naphthalene (ng/g)	1	3	0	60.1	42.1	73	0	0	39.1	141.3	141.3
	2	3	0	145	115	198	0	0	65	372	372
	3	3	0	0	0	0	0	0	0	0	0
	5	3	0	1.44	1.44	2.5	0	0	0	4.33	4.33
	8	3	0	141.5	30.6	53	94.6	94.6	130.9	199.1	199.1
Fluorene (ng/g)	1	3	0	3585	1582	2740	1953	1953	2055	6748	6748
	2	3	0	2235	1033	1789	697	697	1810	4198	4198
	3	3	0	328.7	81.1	140.4	176.3	176.3	356.9	452.9	452.9
	5	3	0	731	543	941	141	141	237	1817	1817
	8	3	0	130.9	22	38.1	87.6	87.6	146	159.1	159.1
Fluoranthene (ng/g)	1	2	1	17713	5353	7570	12360	*	17713	*	23066
	2	3	0	15644	6887	11928	5065	5065	13294	28572	28572
	3	3	0	2926	803	1392	1421	1421	3190	4166	4166
	5	3	0	6861	4885	8462	1080	1080	2929	16573	16573
	8	3	0	1373	401	695	606	606	1553	1961	1961
Pyrene (ng/g)	1	2	1	12402	3957	5596	8445	*	12402	*	16359
	2	3	0	11515	5093	8821	3657	3657	9830	21057	21057
	3	3	0	1437	560	970	614	614	1190	2506	2506
	5	3	0	5175	3449	5973	942	942	2577	12008	12008
	8	3	0	956	191	330	694	694	847	1327	1327
Chrysene (ng/g)	1	2	1	3096366	1403727	1985170	1692638	*	3096366	*	4500093
	2	2	1	368769	368769	521518	0	*	368769	*	737538
	3	3	0	3778	829	1435	2920	2920	2978	5435	5435
	5	2	1	899958	56801	80329	843157	*	899958	*	956759
	8	3	0	967	667	1156	0	0	655	2247	2247
Benzo(a)pyrene (ng/g)	1	2	1	3309	914	1293	2395	*	3309	*	4223
	2	3	0	5607	1580	2736	3946	3946	4111	8766	8766
	3	3	0	1735	335	581	1221	1221	1618	2364	2364
	5	3	0	2116	1007	1744	517	517	1856	3975	3975
	8	3	0	3074	2307	3995	588	588	951	7683	7683

Table 10-13 Descriptive statistics for Run 4, 5 – 10 cm.

Variable	*Location*	*N*	*N**	*Mean*	*SE Mean*	*StDev*	*Minimum*	*Q1*	*Median*	*Q3*	*Maximum*
Naphthalene (ng/g)	*1*	*3*	*0*	*2.09*	*2.09*	*3.63*	*0*	*0*	*0*	*6.28*	*6.28*
	2	*3*	*0*	*5.13*	*5.13*	*8.89*	*0*	*0*	*0*	*15.39*	*15.39*
	3	*3*	*0*	*0*	*0*	*0*	*0*	*0*	*0*	*0*	*0*
	5	*3*	*0*	*0*	*0*	*0*	*0*	*0*	*0*	*0*	*0*
	8	*3*	*0*	*1.58*	*1.58*	*2.73*	*0*	*0*	*0*	*4.74*	*4.74*
Fluorene (ng/g)	*1*	*3*	*0*	*5.46*	*5.46*	*9.45*	*0*	*0*	*0*	*16.37*	*16.37*
	2	*3*	*0*	*0*	*0*	*0*	*0*	*0*	*0*	*0*	*0*
	3	*3*	*0*	*0*	*0*	*0*	*0*	*0*	*0*	*0*	*0*
	5	*3*	*0*	*0*	*0*	*0*	*0*	*0*	*0*	*0*	*0*
	8	*3*	*0*	*0*	*0*	*0*	*0*	*0*	*0*	*0*	*0*
Fluoranthene (ng/g)	*1*	*2*	*1*	*260*	*175*	*247*	*86*	***	*260*	***	*435*
	2	*3*	*0*	*235*	*119*	*206*	*4*	*4*	*302*	*399*	*399*
	3	*3*	*0*	*52.3*	*16.8*	*29.2*	*26.6*	*26.6*	*46.4*	*84*	*84*
	5	*3*	*0*	*57.8*	*57.8*	*100.1*	*0*	*0*	*0*	*173.4*	*173.4*
	8	*2*	*1*	*13.5*	*13.5*	*19.1*	*0*	***	*13.5*	***	*27*
Pyrene (ng/g)	*1*	*3*	*0*	*527*	*174*	*302*	*244*	*244*	*492*	*844*	*844*
	2	*3*	*0*	*304.3*	*79.3*	*137.3*	*164.6*	*164.6*	*309*	*439.2*	*439.2*
	3	*3*	*0*	*207.3*	*17.6*	*30.5*	*172.1*	*172.1*	*222.5*	*227.1*	*227.1*
	5	*3*	*0*	*195*	*99.2*	*171.8*	*41*	*41*	*163.8*	*380.3*	*380.3*
	8	*3*	*0*	*333*	*130*	*224*	*145*	*145*	*272*	*581*	*581*
Chrysene (ng/g)	*1*	*3*	*0*	*251.6*	*58.5*	*101.3*	*149.4*	*149.4*	*253.4*	*352.1*	*352.1*
	2	*3*	*0*	*228.3*	*93.7*	*162.2*	*131.4*	*131.4*	*137.9*	*415.6*	*415.6*
	3	*3*	*0*	*214.5*	*21.9*	*37.9*	*189.5*	*189.5*	*195.9*	*258.2*	*258.2*
	5	*3*	*0*	*249*	*92.7*	*160.5*	*99.6*	*99.6*	*228.5*	*418.8*	*418.8*
	8	*3*	*0*	*459*	*107*	*185*	*277*	*277*	*454*	*646*	*646*
Benzo(a)pyrene (ng/g)	*1*	*3*	*0*	*0*	*0*	*0*	*0*	*0*	*0*	*0*	*0*
	2	*3*	*0*	*0*	*0*	*0*	*0*	*0*	*0*	*0*	*0*
	3	*3*	*0*	*0*	*0*	*0*	*0*	*0*	*0*	*0*	*0*
	5	*3*	*0*	*0*	*0*	*0*	*0*	*0*	*0*	*0*	*0*
	8	*3*	*0*	*0*	*0*	*0*	*0*	*0*	*0*	*0*	*0*

Table 10-14 Descriptive statistics for Run 5, 0 – 5 cm.

Variable	*Location*	*N*	*N**	*Mean*	*SE Mean*	*StDev*	*Minimum*	*Q1*	*Median*	*Q3*	*Maximum*
Naphthalene (ng/g)	*1*	*3*	*0*	*0*	*0*	*0*	*0*	*0*	*0*	*0*	*0*
	2	*3*	*0*	*0*	*0*	*0*	*0*	*0*	*0*	*0*	*0*
	3	*3*	*0*	*8.18*	*4.2*	*7.27*	*0*	*0*	*10.66*	*13.89*	*13.89*
	5	*3*	*0*	*26.2*	*24.7*	*42.7*	*0*	*0*	*3.1*	*75.5*	*75.5*
	8	*3*	*0*	*16.1*	*16.1*	*28*	*0*	*0*	*0*	*48.4*	*48.4*
Fluorene (ng/g)	*1*	*3*	*0*	*1583*	*306*	*530*	*1163*	*1163*	*1407*	*2178*	*2178*
	2	*3*	*0*	*715*	*489*	*846*	*218*	*218*	*234*	*1692*	*1692*
	3	*3*	*0*	*1485*	*254*	*440*	*1122*	*1122*	*1359*	*1975*	*1975*
	5	*3*	*0*	*253*	*118*	*204*	*109*	*109*	*163*	*486*	*486*
	8	*3*	*0*	*512*	*387*	*671*	*17*	*17*	*244*	*1275*	*1275*
Fluoranthene (ng/g)	*1*	*2*	*1*	*37560*	*1087*	*1538*	*36472*	***	*37560*	***	*38647*
	2	*2*	*1*	*2118*	*230*	*326*	*1888*	***	*2118*	***	*2349*
	3	*2*	*1*	*7107*	*1695*	*2398*	*5412*	***	*7107*	***	*8803*
	5	*3*	*0*	*2314*	*577*	*1000*	*1643*	*1643*	*1836*	*3463*	*3463*
	8	*3*	*0*	*4512*	*1465*	*2538*	*1582*	*1582*	*5926*	*6027*	*6027*
Pyrene (ng/g)	*1*	*3*	*0*	*19012*	*3482*	*6031*	*12246*	*12246*	*20967*	*23823*	*23823*
	2	*3*	*0*	*5566*	*4054*	*7021*	*1334*	*1334*	*1692*	*13671*	*13671*
	3	*3*	*0*	*7605*	*2430*	*4209*	*3904*	*3904*	*6728*	*12183*	*12183*
	5	*3*	*0*	*2033*	*452*	*783*	*1563*	*1563*	*1599*	*2937*	*2937*
	8	*3*	*0*	*3626*	*1164*	*2015*	*1336*	*1336*	*4409*	*5132*	*5132*
Chrysene (ng/g)	*1*	*3*	*0*	*0*	*0*	*0*	*0*	*0*	*0*	*0*	*0*
	2	*3*	*0*	*0*	*0*	*0*	*0*	*0*	*0*	*0*	*0*
	3	*3*	*0*	*0*	*0*	*0*	*0*	*0*	*0*	*0*	*0*
	5	*3*	*0*	*0*	*0*	*0*	*0*	*0*	*0*	*0*	*0*
	8	*3*	*0*	*0*	*0*	*0*	*0*	*0*	*0*	*0*	*0*
Benzo(a)pyrene (ng/g)	*1*	*3*	*0*	*372*	*122*	*211*	*128*	*128*	*482*	*506*	*506*
	2	*3*	*0*	*618*	*108*	*187*	*495*	*495*	*527*	*833*	*833*
	3	*3*	*0*	*621*	*134*	*232*	*423*	*423*	*562*	*876*	*876*
	5	*3*	*0*	*833*	*195*	*338*	*450*	*450*	*960*	*1089*	*1089*
	8	*3*	*0*	*607.5*	*53.9*	*93.3*	*532.7*	*532.7*	*577.7*	*712*	*712*

Table 10-15 Descriptive statistics for Run 5, 5 – 10 cm.

Variable	*Location*	*N*	*N**	*Mean*	*SE Mean*	*StDev*	*Minimum*	*Q1*	*Median*	*Q3*	*Maximum*
Naphthalene (ng/g)	*1*	*3*	*0*	*26.5*	*26.5*	*46*	*0*	*0*	*0*	*79.6*	*79.6*
	2	*3*	*0*	*80.8*	*66.7*	*115.6*	*0*	*0*	*29.1*	*213.2*	*213.2*
	3	*3*	*0*	*130.5*	*66.9*	*115.8*	*0*	*0*	*170.3*	*221.2*	*221.2*
	5	*3*	*0*	*110.3*	*17.1*	*29.7*	*82.6*	*82.6*	*106.7*	*141.6*	*141.6*
	8	*3*	*0*	*100.1*	*30.3*	*52.5*	*39.8*	*39.8*	*125.4*	*135.1*	*135.1*
Fluorene (ng/g)	*1*	*3*	*0*	*0*	*0*	*0*	*0*	*0*	*0*	*0*	*0*
	2	*3*	*0*	*0*	*0*	*0*	*0*	*0*	*0*	*0*	*0*
	3	*3*	*0*	*0*	*0*	*0*	*0*	*0*	*0*	*0*	*0*
	5	*3*	*0*	*0*	*0*	*0*	*0*	*0*	*0*	*0*	*0*
	8	*3*	*0*	*0*	*0*	*0*	*0*	*0*	*0*	*0*	*0*
Fluoranthene (ng/g)	*1*	*3*	*0*	*543*	*152*	*264*	*271*	*271*	*559*	*798*	*798*
	2	*3*	*0*	*215.2*	*74.2*	*128.6*	*139.4*	*139.4*	*142.6*	*363.6*	*363.6*
	3	*3*	*0*	*129.5*	*86.8*	*150.3*	*0*	*0*	*94.1*	*294.2*	*294.2*
	5	*2*	*1*	*0*	*0*	*0*	*0*	***	*0*	***	*0*
	8	*3*	*0*	*0*	*0*	*0*	*0*	*0*	*0*	*0*	*0*
Pyrene (ng/g)	*1*	*3*	*0*	*539*	*111*	*192*	*341*	*341*	*551*	*724*	*724*
	2	*3*	*0*	*261.1*	*64.8*	*112.2*	*157.8*	*157.8*	*245.1*	*380.5*	*380.5*
	3	*3*	*0*	*261*	*101*	*175*	*108*	*108*	*223*	*451*	*451*
	5	*2*	*1*	*123*	*24.7*	*34.9*	*98.3*	***	*123*	***	*147.6*
	8	*3*	*0*	*108.3*	*17.6*	*30.5*	*86*	*86*	*95.7*	*143.1*	*143.1*
Chrysene (ng/g)	*1*	*3*	*0*	*238*	*101*	*175*	*99*	*99*	*180*	*435*	*435*
	2	*3*	*0*	*171.1*	*42.5*	*73.6*	*87.3*	*87.3*	*201*	*225.1*	*225.1*
	3	*3*	*0*	*339*	*138*	*239*	*184*	*184*	*218*	*614*	*614*
	5	*3*	*0*	*306*	*115*	*199*	*172*	*172*	*210*	*535*	*535*
	8	*3*	*0*	*150.94*	*8.93*	*15.48*	*135.87*	*135.87*	*150.16*	*166.79*	*166.79*
Benzo(a)pyrene (ng/g)	*1*	*3*	*0*	*309*	*169*	*293*	*82*	*82*	*205*	*640*	*640*
	2	*3*	*0*	*228.1*	*63.4*	*109.8*	*103.3*	*103.3*	*271.3*	*309.7*	*309.7*
	3	*3*	*0*	*478*	*122*	*212*	*351*	*351*	*360*	*722*	*722*
	5	*3*	*0*	*500*	*231*	*400*	*233*	*233*	*307*	*960*	*960*
	8	*3*	*0*	*194.6*	*21.7*	*37.7*	*161*	*161*	*187.4*	*235.3*	*235.3*

Table 10-16 Descriptive statistics for Run 6, 0 – 5 cm.

Variable	Location	N	N*	Mean	SE Mean	StDev	Minimum	Q1	Median	Q3	Maximum
Naphthalene (ng/g)	1	3	0	95.6	63.5	109.9	0	0	71	215.7	215.7
	2	3	0	48.7	18.3	31.7	14	14	55.8	76.2	76.2
	3	3	0	49.6	24	41.6	1.5	1.5	72.8	74.5	74.5
	5	3	0	8.06	4.04	6.99	0	0	11.66	12.52	12.52
	8	3	0	9.06	9.06	15.7	0	0	0	27.18	27.18
Fluorene (ng/g)	1	2	1	4327.3	44	62.2	4283.3	*	4327.3	*	4371.2
	2	3	0	3907	1003	1737	2057	2057	4161	5502	5502
	3	3	0	2852	1871	3240	56	56	2097	6403	6403
	5	3	0	147.5	87.3	151.3	39.3	39.3	82.9	320.4	320.4
	8	3	0	77.1	42.6	73.8	0	0	84.1	147.1	147.1
Fluoranthene (ng/g)	1	1	2	47497	*	*	47497	*	47497	*	47497
	2	3	0	74018	16344	28308	42600	42600	81915	97539	97539
	3	3	0	23893	15098	26150	1404	1404	17687	52588	52588
	5	3	0	13005	11905	20620	789	789	1414	36812	36812
	8	3	0	5902	2888	5003	2183	2183	3934	11590	11590
Pyrene (ng/g)	1	2	1	96504	62948	89022	33556	*	96504	*	159452
	2	3	0	47421	10642	18432	26872	26872	52895	62496	62496
	3	3	0	15652	9532	16510	1150	1150	12187	33619	33619
	5	3	0	9040	8125	14073	639	639	1193	25287	25287
	8	3	0	4489	2001	3466	1771	1771	3304	8392	8392
Chrysene (ng/g)	1	2	1	92143	32149	45465	59994	*	92143	*	124292
	2	3	0	54531	9301	16110	40121	40121	51549	71924	71924
	3	2	1	29826	10421	14737	19405	*	29826	*	40246
	5	3	0	55630	17075	29574	23196	23196	62591	81103	81103
	8	2	1	28330	15630	22105	12700	*	28330	*	43960
Benzo(a)pyrene (ng/g)	1	2	1	2522	313	443	2209	*	2522	*	2835
	2	3	0	1687	194	336	1493	1493	1494	2075	2075
	3	3	0	2158	1301	2254	814	814	901	4760	4760
	5	3	0	973	441	763	264	264	873	1781	1781
	8	3	0	748.8	49.8	86.3	686.8	686.8	712.2	847.4	847.4

Table 10-17 Descriptive statistics for Run 6, 5 – 10 cm.

Variable	*Location*	*N*	*N**	*Mean*	*SE Mean*	*StDev*	*Minimum*	*Q1*	*Median*	*Q3*	*Maximum*
Naphthalene (ng/g)	*1*	*3*	*0*	*0*	*0*	*0*	*0*	*0*	*0*	*0*	*0*
	2	*3*	*0*	*0*	*0*	*0*	*0*	*0*	*0*	*0*	*0*
	3	*3*	*0*	*0*	*0*	*0*	*0*	*0*	*0*	*0*	*0*
	5	*3*	*0*	*0*	*0*	*0*	*0*	*0*	*0*	*0*	*0*
	8	*3*	*0*	*0*	*0*	*0*	*0*	*0*	*0*	*0*	*0*
Fluorene (ng/g)	*1*	*3*	*0*	*2.71*	*2.71*	*4.69*	*0*	*0*	*0*	*8.12*	*8.12*
	2	*2*	*1*	*24.6*	*24.6*	*34.9*	*0*	***	*24.6*	***	*49.3*
	3	*3*	*0*	*0*	*0*	*0*	*0*	*0*	*0*	*0*	*0*
	5	*3*	*0*	*0*	*0*	*0*	*0*	*0*	*0*	*0*	*0*
	8	*3*	*0*	*0*	*0*	*0*	*0*	*0*	*0*	*0*	*0*
Fluoranthene (ng/g)	*1*	*3*	*0*	*815*	*139*	*241*	*570*	*570*	*822*	*1052*	*1052*
	2	*1*	*2*	*561.77*	***	***	*561.77*	***	*561.77*	***	*561.77*
	3	*3*	*0*	*75.2*	*75.2*	*130.3*	*0*	*0*	*0*	*225.7*	*225.7*
	5	*3*	*0*	*0*	*0*	*0*	*0*	*0*	*0*	*0*	*0*
	8	*3*	*0*	*0*	*0*	*0*	*0*	*0*	*0*	*0*	*0*
Pyrene (ng/g)	*1*	*3*	*0*	*730*	*108*	*186*	*542*	*542*	*733*	*915*	*915*
	2	*2*	*1*	*845*	*357*	*504*	*488*	***	*845*	***	*1202*
	3	*3*	*0*	*179.5*	*51.7*	*89.5*	*103.3*	*103.3*	*157.1*	*278.1*	*278.1*
	5	*3*	*0*	*98.8*	*36.5*	*63.2*	*59.8*	*59.8*	*64.9*	*171.7*	*171.7*
	8	*3*	*0*	*89*	*22.6*	*39.2*	*43.8*	*43.8*	*109.8*	*113.4*	*113.4*
Chrysene (ng/g)	*1*	*3*	*0*	*382.8*	*64*	*110.9*	*306.5*	*306.5*	*331.8*	*510*	*510*
	2	*3*	*0*	*397*	*120*	*207*	*212*	*212*	*357*	*621*	*621*
	3	*3*	*0*	*142.9*	*19.7*	*34*	*103.6*	*103.6*	*161.5*	*163.6*	*163.6*
	5	*3*	*0*	*162.2*	*30.7*	*53.1*	*119.5*	*119.5*	*145.4*	*221.7*	*221.7*
	8	*3*	*0*	*181.6*	*28*	*48.4*	*125.7*	*125.7*	*207.6*	*211.5*	*211.5*
Benzo(a)pyrene (ng/g)	*1*	*3*	*0*	*496.7*	*85.6*	*148.2*	*362.6*	*362.6*	*471.7*	*655.9*	*655.9*
	2	*3*	*0*	*260.1*	*55.2*	*95.6*	*197.2*	*197.2*	*212.9*	*370.1*	*370.1*
	3	*3*	*0*	*168*	*27.5*	*47.6*	*113.1*	*113.1*	*195.2*	*195.8*	*195.8*
	5	*3*	*0*	*237.3*	*65.9*	*114.2*	*141*	*141*	*207.5*	*363.5*	*363.5*
	8	*3*	*0*	*244.5*	*48.4*	*83.8*	*151.8*	*151*	*266.9*	*314.9*	*314.9*

Table 10-18 Descriptive statistics for Run 7, 0 – 5 cm.

Variable	*Location*	*N*	*N**	*Mean*	*SE Mean*	*StDev*	*Minimum*	*Q1*	*Median*	*Q3*	*Maximum*
Naphthalene (ng/g)	*1*	*3*	*0*	*55.9*	*17.6*	*30.5*	*25.1*	*25.1*	*56.5*	*86*	*86*
	2	*3*	*0*	*57.5*	*23.4*	*40.5*	*28.8*	*28.8*	*39.7*	*103.8*	*103.8*
	3	*3*	*0*	*20.1*	*14.2*	*24.6*	*0*	*0*	*12.7*	*47.5*	*47.5*
	5	*3*	*0*	*79.8*	*12*	*20.8*	*66.9*	*66.9*	*68.7*	*103.7*	*103.7*
	8	*3*	*0*	*101.13*	*7.52*	*13.02*	*87.6*	*87.6*	*102.21*	*113.57*	*113.57*
Fluorene (ng/g)	*1*	*3*	*0*	*462*	*325*	*563*	*111*	*111*	*163*	*1111*	*1111*
	2	*3*	*0*	*501*	*401*	*694*	*0*	*0*	*210*	*1294*	*1294*
	3	*3*	*0*	*50.2*	*32.1*	*55.6*	*0*	*0*	*40.7*	*109.9*	*109.9*
	5	*3*	*0*	*220*	*182*	*315*	*2*	*2*	*76*	*581*	*581*
	8	*2*	*1*	*1263*	*966*	*1366*	*297*	***	*1263*	***	*2229*
Fluoranthene (ng/g)	*1*	*2*	*1*	*17429*	*9352*	*13226*	*8077*	***	*17429*	***	*26781*
	2	*3*	*0*	*12201*	*7334*	*12704*	*3041*	*3041*	*6860*	*26704*	*26704*
	3	*3*	*0*	*3228*	*312*	*540*	*2605*	*2605*	*3540*	*3541*	*3541*
	5	*3*	*0*	*3733*	*1396*	*2419*	*1409*	*1409*	*3553*	*6237*	*6237*
	8	*2*	*1*	*32127*	*7409*	*10477*	*24719*	***	*32127*	***	*39536*
Pyrene (ng/g)	*1*	*3*	*0*	*0*	*0*	*0*	*0*	*0*	*0*	*0*	*0*
	2	*3*	*0*	*0*	*0*	*0*	*0*	*0*	*0*	*0*	*0*
	3	*3*	*0*	*0*	*0*	*0*	*0*	*0*	*0*	*0*	*0*
	5	*3*	*0*	*0*	*0*	*0*	*0*	*0*	*0*	*0*	*0*
	8	*3*	*0*	*0*	*0*	*0*	*0*	*0*	*0*	*0*	*0*
Chrysene (ng/g)	*1*	*2*	*1*	*6580*	*208*	*294*	*6372*	***	*6580*	***	*6788*
	2	*3*	*0*	*6234*	*1875*	*3248*	*4201*	*4201*	*4520*	*9980*	*9980*
	3	*3*	*0*	*3909*	*655*	*1134*	*2705*	*2705*	*4064*	*4958*	*4958*
	5	*3*	*0*	*3168*	*288*	*499*	*2780*	*2780*	*2993*	*3731*	*3731*
	8	*2*	*1*	*7540*	*1054*	*1490*	*6486*	***	*7540*	***	*8594*
Benzo(a)pyrene (ng/g)	*1*	*3*	*0*	*3090*	*1611*	*2790*	*1387*	*1387*	*1573*	*6309*	*6309*
	2	*2*	*1*	*502.1*	*46.3*	*65.5*	*455.8*	***	*502.1*	***	*548.4*
	3	*3*	*0*	*648*	*173*	*300*	*315*	*315*	*732*	*896*	*896*
	5	*3*	*0*	*1925*	*668*	*1157*	*682*	*682*	*2122*	*2970*	*2970*
	8	*3*	*0*	*761*	*232*	*401*	*341*	*341*	*800*	*1141*	*1141*

Table 10-19 Descriptive statistics for Run 7, 5 – 10 cm.

Variable	*Location*	*N*	*N**	*Mean*	*SE Mean*	*StDev*	*Minimum*	*Q1*	*Median*	*Q3*	*Maximum*
Naphthalene (ng/g)	*1*	*3*	*0*	*0*	*0*	*0*	*0*	*0*	*0*	*0*	*0*
	2	*3*	*0*	*0*	*0*	*0*	*0*	*0*	*0*	*0*	*0*
	3	*3*	*0*	*0*	*0*	*0*	*0*	*0*	*0*	*0*	*0*
	5	*3*	*0*	*0*	*0*	*0*	*0*	*0*	*0*	*0*	*0*
	8	*3*	*0*	*0*	*0*	*0*	*0*	*0*	*0*	*0*	*0*
Fluorene (ng/g)	*1*	*3*	*0*	*4.49*	*4.49*	*7.77*	*0*	*0*	*0*	*13.46*	*13.46*
	2	*3*	*0*	*59.3*	*59.3*	*102.6*	*0*	*0*	*0*	*177.8*	*177.8*
	3	*3*	*0*	*0*	*0*	*0*	*0*	*0*	*0*	*0*	*0*
	5	*3*	*0*	*0*	*0*	*0*	*0*	*0*	*0*	*0*	*0*
	8	*3*	*0*	*0*	*0*	*0*	*0*	*0*	*0*	*0*	*0*
Fluoranthene (ng/g)	*1*	*2*	*1*	*3196*	*203*	*287*	*2992*	***	*3196*	***	*3399*
	2	*2*	*1*	*1322*	*137*	*193*	*1185*	***	*1322*	***	*1459*
	3	*3*	*0*	*235.1*	*83.7*	*144.9*	*77.2*	*77.2*	*265.9*	*362.1*	*362.1*
	5	*3*	*0*	*27.9*	*27.9*	*48.3*	*0*	*0*	*0*	*83.6*	*83.6*
	8	*2*	*1*	*209*	*209*	*295*	*0*	***	*209*	***	*417*
Pyrene (ng/g)	*1*	*3*	*0*	*0*	*0*	*0*	*0*	*0*	*0*	*0*	*0*
	2	*3*	*0*	*0*	*0*	*0*	*0*	*0*	*0*	*0*	*0*
	3	*3*	*0*	*0*	*0*	*0*	*0*	*0*	*0*	*0*	*0*
	5	*3*	*0*	*0*	*0*	*0*	*0*	*0*	*0*	*0*	*0*
	8	*3*	*0*	*0*	*0*	*0*	*0*	*0*	*0*	*0*	*0*
Chrysene (ng/g)	*1*	*2*	*1*	*312*	*312*	*442*	*0*	***	*312*	***	*625*
	2	*3*	*0*	*291*	*51.5*	*89.2*	*199*	*199*	*296.9*	*377.1*	*377.1*
	3	*3*	*0*	*261.7*	*42.9*	*74.2*	*194.3*	*194.3*	*249.6*	*341.2*	*341.2*
	5	*3*	*0*	*228*	*24.9*	*43.1*	*191.9*	*191.9*	*216.5*	*275.7*	*275.7*
	8	*2*	*1*	*369*	*128*	*181*	*241*	***	*369*	***	*497*
Benzo(a)pyrene (ng/g)	*1*	*2*	*1*	*266*	*266*	*377*	*0*	***	*266*	***	*533*
	2	*3*	*0*	*307.9*	*53.2*	*92.2*	*239.7*	*239.7*	*271.4*	*412.8*	*412.8*
	3	*3*	*0*	*348.4*	*70.3*	*121.8*	*263.6*	*263.6*	*293.6*	*488*	*488*
	5	*3*	*0*	*362.3*	*44.9*	*77.8*	*293.1*	*293.1*	*347.2*	*446.5*	*446.5*
	8	*2*	*1*	*563*	*246*	*347*	*317*	***	*563*	***	*808*

Table 10-20 Descriptive statistics for Run 8, 0 – 5 cm.

Variable	Location	N	N*	Mean	SE Mean	StDev	Minimum	Q1	Median	Q3	Maximum
Naphthalene (ng/g)	1	3	0	46.05	1.85	3.21	42.85	42.85	46.05	49.27	49.27
	2	3	0	32.5	21.2	36.7	0	0	25.2	72.2	72.2
	3	3	0	49.3	28.7	49.6	0	0	48.7	99.3	99.3
	5	3	0	77.7	22.1	38.3	52.5	52.5	58.9	121.8	121.8
	8	3	0	115.16	5.3	9.18	105.75	105.75	115.64	124.09	124.09
Fluorene (ng/g)	1	3	0	221	57.2	99	141.7	141.7	189.3	332	332
	2	3	0	65.5	51.9	89.9	0	0	28.4	167.9	167.9
	3	3	0	793	664	1150	0	0	267	2111	2111
	5	3	0	590	342	593	12	12	561	1197	1197
	8	3	0	279	119	205	79	79	269	489	489
Fluoranthene (ng/g)	1	3	0	13745	4255	7369	5862	5862	14910	20462	20462
	2	2	1	1547	1547	2187	0	*	1547	*	3094
	3	2	1	2944	2944	4164	0	*	2944	*	5888
	5	3	0	8368	4756	8237	1217	1217	6512	17375	17375
	8	3	0	4034	891	1543	2261	2261	4771	5069	5069
Pyrene (ng/g)	1	3	0	624484	198329	343515	237280	237280	743536	892636	892636
	2	2	1	85954	85954	121557	0	*	85954	*	171908
	3	2	1	196195	196195	277461	0	*	196195	*	392389
	5	2	1	335477	103866	146889	231610	*	335477	*	439343
	8	3	0	285852	64561	111822	158541	158541	330849	368166	368166
Chrysene (ng/g)	1	3	0	0	0	0	0	0	0	0	0
	2	3	0	0	0	0	0	0	0	0	0
	3	3	0	0	0	0	0	0	0	0	0
	5	3	0	0	0	0	0	0	0	0	0
	8	3	0	0	0	0	0	0	0	0	0
Benzo(a)pyrene (ng/g)	1	3	0	744	105	182	614	614	667	951	951
	2	3	0	605	324	561	0	0	705	1109	1109
	3	3	0	1813	915	1584	0	0	2510	2930	2930
	5	3	0	1710	817	1415	751	751	1044	3335	3335
	8	3	0	1323	697	1207	452	452	816	2701	2701

Table 10-21 Descriptive statistics for Run 8, 5 – 10 cm.

Variable	*Location*	*N*	*N**	*Mean*	*SE Mean*	*StDev*	*Minimum*	*Q1*	*Median*	*Q3*	*Maximum*
Naphthalene (ng/g)	*1*	*3*	*0*	*0*	*0*	*0*	*0*	*0*	*0*	*0*	*0*
	2	*3*	*0*	*0*	*0*	*0*	*0*	*0*	*0*	*0*	*0*
	3	*3*	*0*	*0*	*0*	*0*	*0*	*0*	*0*	*0*	*0*
	5	*3*	*0*	*0*	*0*	*0*	*0*	*0*	*0*	*0*	*0*
	8	*3*	*0*	*0*	*0*	*0*	*0*	*0*	*0*	*0*	*0*
Fluorene (ng/g)	*1*	*3*	*0*	*12.6*	*12.6*	*21.8*	*0*	*0*	*0*	*37.8*	*37.8*
	2	*3*	*0*	*0*	*0*	*0*	*0*	*0*	*0*	*0*	*0*
	3	*3*	*0*	*0*	*0*	*0*	*0*	*0*	*0*	*0*	*0*
	5	*3*	*0*	*0*	*0*	*0*	*0*	*0*	*0*	*0*	*0*
	8	*3*	*0*	*0*	*0*	*0*	*0*	*0*	*0*	*0*	*0*
Fluoranthene (ng/g)	*1*	*2*	*1*	*410*	*410*	*579*	*0*	***	*410*	***	*820*
	2	*2*	*1*	*480*	*240*	*340*	*240*	***	*480*	***	*721*
	3	*3*	*0*	*161.3*	*65.5*	*113.5*	*32.4*	*32.4*	*204.9*	*246.5*	*246.5*
	5	*3*	*0*	*38*	*38*	*65.9*	*0*	*0*	*0*	*114.1*	*114.1*
	8	*3*	*0*	*0*	*0*	*0*	*0*	*0*	*0*	*0*	*0*
Pyrene (ng/g)	*1*	*2*	*1*	*389*	*389*	*551*	*0*	***	*389*	***	*779*
	2	*2*	*1*	*489*	*174*	*247*	*315*	***	*489*	***	*663*
	3	*3*	*0*	*278.6*	*37.1*	*64.3*	*228.8*	*228.8*	*255.7*	*351.3*	*351.3*
	5	*3*	*0*	*160.2*	*23.3*	*40.3*	*129*	*129*	*145.8*	*205.7*	*205.7*
	8	*3*	*0*	*136.3*	*31.7*	*54.9*	*86.4*	*86.4*	*127.3*	*195.2*	*195.2*
Chrysene (ng/g)	*1*	*2*	*1*	*286*	*273*	*386*	*13*	***	*286*	***	*560*
	2	*3*	*0*	*549*	*101*	*174*	*348*	*348*	*639*	*659*	*659*
	3	*3*	*0*	*457.2*	*88.6*	*153.4*	*284.2*	*284.2*	*510.8*	*576.6*	*576.6*
	5	*3*	*0*	*421.4*	*31.3*	*54.2*	*386.4*	*386.4*	*393.9*	*483.7*	*483.7*
	8	*3*	*0*	*396.3*	*69.4*	*120.2*	*284.3*	*284.3*	*381.5*	*523.2*	*523.2*
Benzo(a)pyrene (ng/g)	*1*	*2*	*1*	*258*	*258*	*365*	*0*	***	*258*	***	*517*
	2	*3*	*0*	*672.8*	*92.7*	*160.5*	*488.9*	*488.9*	*744.8*	*784.7*	*784.7*
	3	*3*	*0*	*693*	*167*	*289*	*366*	*366*	*801*	*912*	*912*
	5	*3*	*0*	*632.9*	*43.1*	*74.6*	*588.1*	*588.1*	*591.5*	*719*	*719*
	8	*3*	*0*	*515.9*	*95.6*	*165.7*	*350.2*	*350.2*	*516*	*681.5*	*681.5*

Table 10-22 Descriptive statistics for Run 8, 10 – 15 cm.

Variable	*Location*	*N*	*N**	*Mean*	*SE Mean*	*StDev*	*Minimum*	*Q1*	*Median*	*Q3*	*Maximum*
Naphthalene (ng/g)	*1*	*3*	*0*	*0*	*0*	*0*	*0*	*0*	*0*	*0*	*0*
	2	*3*	*0*	*0*	*0*	*0*	*0*	*0*	*0*	*0*	*0*
	3	*3*	*0*	*0*	*0*	*0*	*0*	*0*	*0*	*0*	*0*
	5	*3*	*0*	*0*	*0*	*0*	*0*	*0*	*0*	*0*	*0*
	8	*3*	*0*	*0*	*0*	*0*	*0*	*0*	*0*	*0*	*0*
Fluorene (ng/g)	*1*	*3*	*0*	*12*	*12*	*20.8*	*0*	*0*	*0*	*36*	*36*
	2	*3*	*0*	*9.5*	*9.5*	*16.46*	*0*	*0*	*0*	*28.51*	*28.51*
	3	*3*	*0*	*0*	*0*	*0*	*0*	*0*	*0*	*0*	*0*
	5	*3*	*0*	*0*	*0*	*0*	*0*	*0*	*0*	*0*	*0*
	8	*3*	*0*	*0*	*0*	*0*	*0*	*0*	*0*	*0*	*0*
Fluoranthene (ng/g)	*1*	*3*	*0*	*1142*	*1142*	*1978*	*0*	*0*	*0*	*3425*	*3425*
	2	*3*	*0*	*610*	*394*	*683*	*0*	*0*	*482*	*1347*	*1347*
	3	*3*	*0*	*15.8*	*15.8*	*27.3*	*0*	*0*	*0*	*47.4*	*47.4*
	5	*3*	*0*	*2305*	*2305*	*3993*	*0*	*0*	*0*	*6916*	*6916*
	8	*3*	*0*	*58.1*	*45.8*	*79.3*	*0*	*0*	*25.8*	*148.5*	*148.5*
Pyrene (ng/g)	*1*	*3*	*0*	*1015*	*870*	*1507*	*109*	*109*	*181*	*2754*	*2754*
	2	*3*	*0*	*575*	*269*	*466*	*145*	*145*	*511*	*1069*	*1069*
	3	*3*	*0*	*149.8*	*18.7*	*32.4*	*124.6*	*124.6*	*138.5*	*186.4*	*186.4*
	5	*3*	*0*	*1686*	*1617*	*2801*	*0*	*0*	*139*	*4919*	*4919*
	8	*3*	*0*	*233.5*	*70.3*	*121.8*	*98.6*	*98.6*	*266.5*	*335.4*	*335.4*
Chrysene (ng/g)	*1*	*3*	*0*	*657*	*650*	*1126*	*0*	*0*	*13*	*1957*	*1957*
	2	*3*	*0*	*718*	*718*	*1244*	*0*	*0*	*0*	*2155*	*2155*
	3	*3*	*0*	*0*	*0*	*0*	*0*	*0*	*0*	*0*	*0*
	5	*3*	*0*	*3326*	*3316*	*5744*	*0*	*0*	*20*	*9958*	*9958*
	8	*3*	*0*	*403*	*381*	*660*	*0*	*0*	*44*	*1164*	*1164*
Benzo(a)pyrene (ng/g)	*1*	*3*	*0*	*770*	*329*	*570*	*344*	*344*	*548*	*1417*	*1417*
	2	*3*	*0*	*632*	*255*	*441*	*337*	*337*	*419*	*1140*	*1140*
	3	*3*	*0*	*414.7*	*43*	*74.4*	*346.5*	*346.5*	*403.5*	*494.1*	*494.1*
	5	*3*	*0*	*426*	*224*	*388*	*0*	*0*	*517*	*760*	*760*
	8	*3*	*0*	*543*	*249*	*431*	*46*	*46*	*790*	*794*	*794*

Table 10-23 Descriptive statistics for Run 9, 0 – 5 cm.

Variable	*Location*	*N*	*N**	*Mean*	*SE Mean*	*StDev*	*Minimum*	*Q1*	*Median*	*Q3*	*Maximum*
Naphthalene (ng/g)	*1*	*3*	*0*	*127.6*	*45.7*	*79.2*	*73.1*	*73.1*	*91.3*	*218.4*	*218.4*
	2	*3*	*0*	*97.8*	*34.9*	*60.4*	*32.8*	*32.8*	*108.6*	*152.1*	*152.1*
	3	*3*	*0*	*91.7*	*15.5*	*26.9*	*70.2*	*70.2*	*83*	*121.9*	*121.9*
	5	*3*	*0*	*70.2*	*15.8*	*27.4*	*38.6*	*38.6*	*84.3*	*87.7*	*87.7*
	8	*3*	*0*	*113.3*	*21.6*	*37.4*	*89.4*	*89.4*	*94.2*	*156.3*	*156.3*
Fluorene (ng/g)	*1*	*3*	*0*	*170*	*111*	*192*	*2*	*2*	*128*	*379*	*379*
	2	*3*	*0*	*191*	*158*	*274*	*20*	*20*	*47*	*507*	*507*
	3	*3*	*0*	*96.6*	*96.6*	*167.3*	*0*	*0*	*0*	*289.7*	*289.7*
	5	*3*	*0*	*4.28*	*4.28*	*7.41*	*0*	*0*	*0*	*12.83*	*12.83*
	8	*3*	*0*	*3*	*3*	*5*	*0*	*0*	*0*	*10*	*10*
Fluoranthene (ng/g)	*1*	*2*	*1*	*11786*	*256*	*362*	*11530*	***	*11786*	***	*12042*
	2	*3*	*0*	*3250*	*1727*	*2992*	*1354*	*1354*	*1697*	*6700*	*6700*
	3	*3*	*0*	*740*	*634*	*1098*	*0*	*0*	*218*	*2001*	*2001*
	5	*3*	*0*	*34*	*25*	*43*	*0*	*0*	*19*	*81*	*81*
	8	*3*	*0*	*32*	*32*	*55*	*0*	*0*	*0*	*95*	*95*
Pyrene (ng/g)	*1*	*3*	*0*	*3874*	*2799*	*4848*	*967*	*967*	*1184*	*9470*	*9470*
	2	*3*	*0*	*2421*	*1280*	*2218*	*1022*	*1022*	*1264*	*4978*	*4978*
	3	*3*	*0*	*902*	*313*	*541*	*285*	*285*	*1126*	*1296*	*1296*
	5	*3*	*0*	*142*	*32*	*55*	*78*	*78*	*173*	*176*	*176*
	8	*3*	*0*	*134*	*25*	*43*	*94*	*94*	*128*	*180*	*180*
Chrysene (ng/g)	*1*	*3*	*0*	*789*	*325*	*563*	*178*	*178*	*905*	*1285*	*1285*
	2	*3*	*0*	*713*	*529*	*917*	*179*	*179*	*189*	*1772*	*1772*
	3	*3*	*0*	*150*	*31*	*54*	*111*	*111*	*127*	*211*	*211*
	5	*3*	*0*	*71*	*18*	*32*	*45*	*45*	*61*	*106*	*106*
	8	*3*	*0*	*84.7*	*13.5*	*23.4*	*61.3*	*61.3*	*84.9*	*108*	*108*
Benzo(a)pyrene (ng/g)	*1*	*3*	*0*	*163*	*131*	*227*	*0*	*0*	*68*	*422*	*422*
	2	*3*	*0*	*497*	*464*	*804*	*0*	*0*	*66*	*1425*	*1425*
	3	*3*	*0*	*10*	*10*	*17*	*0*	*0*	*0*	*29*	*29*
	5	*3*	*0*	*27*	*14*	*24*	*7*	*7*	*21*	*53*	*53*
	8	*3*	*0*	*9*	*9*	*15*	*0*	*0*	*0*	*26*	*26*

Table 10-24 Descriptive statistics for Run 9, 5 – 10 cm.

Variable	Location	N	N*	Mean	SE Mean	StDev	Minimum	Q1	Median	Q3	Maximum
Naphthalene (ng/g)	1	3	0	0	0	0	0	0	0	0	0
	2	2	1	0	0	0	0	*	0	*	0
	3	3	0	0	0	0	0	0	0	0	0
	5	3	0	0	0	0	0	0	0	0	0
	8	3	0	0	0	0	0	0	0	0	0
Fluorene (ng/g)	1	3	0	15.8	15.8	27.3	0	0	0	47.3	47.3
	2	3	0	2.33	2.33	4.03	0	0	0	6.98	6.98
	3	3	0	0	0	0	0	0	0	0	0
	5	2	1	0	0	0	0	*	0	*	0
	8	3	0	0	0	0	0	0	0	0	0
Fluoranthene (ng/g)	1	3	0	1281	353	611	732	732	1170	1940	1940
	2	3	0	5348	1152	1996	3826	3826	4610	7608	7608
	3	3	0	724	199	345	415	415	660	1095	1095
	5	2	1	390	41	58	349	*	390	*	431
	8	3	0	1081	391	678	368	368	1161	1716	1716
Pyrene (ng/g)	1	3	0	1211	348	602	738	738	1006	1889	1889
	2	2	1	3032	263	371	2769	*	3032	*	3294
	3	3	0	781	175	303	518	518	713	1112	1112
	5	2	1	527	8	11	519	*	527	*	535
	8	3	0	1106	342	592	509	509	1117	1692	1692
Chrysene (ng/g)	1	3	0	1767	257	445	1307	1307	1797	2197	2197
	2	3	0	4523	951	1646	3405	3405	3752	6414	6414
	3	3	0	3039	492	852	2422	2422	2684	4010	4010
	5	2	1	2764	101	142	2664	*	2764	*	2865
	8	2	1	2933	967	1367	1966	*	2933	*	3900
Benzo(a)pyrene (ng/g)	1	3	0	2069	277	480	1708	1708	1885	2613	2613
	2	3	0	5561	950	1646	4481	4481	4747	7456	7456
	3	3	0	5407	970	1681	3991	3991	4967	7265	7265
	5	2	1	4919	15.3	21	4904	*	4919	*	4935
	8	2	1	4111	1649	2332	2462	*	4111	*	5760

Table 10-25 Descriptive statistics for Run 9, 10 – 15 cm.

Variable	*Location*	*N*	*N**	*Mean*	*SE Mean*	*StDev*	*Minimum*	*Q1*	*Median*	*Q3*	*Maximum*
Naphthalene (ng/g)	*1*	*3*	*0*	*0*	*0*	*0*	*0*	*0*	*0*	*0*	*0*
	2	*3*	*0*	*0*	*0*	*0*	*0*	*0*	*0*	*0*	*0*
	3	*3*	*0*	*0*	*0*	*0*	*0*	*0*	*0*	*0*	*0*
	5	*3*	*0*	*0*	*0*	*0*	*0*	*0*	*0*	*0*	*0*
	8	*3*	*0*	*0*	*0*	*0*	*0*	*0*	*0*	*0*	*0*
Fluorene (ng/g)	*1*	*3*	*0*	*0*	*0*	*0*	*0*	*0*	*0*	*0*	*0*
	2	*3*	*0*	*0*	*0*	*0*	*0*	*0*	*0*	*0*	*0*
	3	*3*	*0*	*0*	*0*	*0*	*0*	*0*	*0*	*0*	*0*
	5	*3*	*0*	*0*	*0*	*0*	*0*	*0*	*0*	*0*	*0*
	8	*3*	*0*	*0*	*0*	*0*	*0*	*0*	*0*	*0*	*0*
Fluoranthene (ng/g)	*1*	*3*	*0*	*99.1*	*42.8*	*74.2*	*23.9*	*23.9*	*101*	*172.3*	*172.3*
	2	*3*	*0*	*1053*	*536*	*928*	*0*	*0*	*1410*	*1750*	*1750*
	3	*3*	*0*	*230*	*230*	*398*	*0*	*0*	*0*	*690*	*690*
	5	*3*	*0*	*93.2*	*77.3*	*133.8*	*0*	*0*	*33*	*246.5*	*246.5*
	8	*3*	*0*	*44.4*	*44.4*	*76.9*	*0*	*0*	*0*	*133.2*	*133.2*
Pyrene (ng/g)	*1*	*3*	*0*	*269.7*	*35.5*	*61.5*	*223.1*	*223.1*	*246.7*	*339.4*	*339.4*
	2	*3*	*0*	*985*	*439*	*761*	*133*	*133*	*1224*	*1597*	*1597*
	3	*3*	*0*	*289*	*225*	*389*	*30*	*30*	*101*	*737*	*737*
	5	*3*	*0*	*241.2*	*60*	*103.9*	*143.7*	*143.7*	*229.5*	*350.4*	*350.4*
	8	*3*	*0*	*200*	*138*	*239*	*47*	*47*	*77*	*475*	*475*
Chrysene (ng/g)	*1*	*3*	*0*	*7.32*	*7.32*	*12.68*	*0*	*0*	*0*	*21.97*	*21.97*
	2	*3*	*0*	*1076*	*708*	*1227*	*0*	*0*	*815*	*2412*	*2412*
	3	*3*	*0*	*562*	*559*	*968*	*0*	*0*	*7*	*1680*	*1680*
	5	*3*	*0*	*4.9*	*2.48*	*4.29*	*0.67*	*0.67*	*4.77*	*9.25*	*9.25*
	8	*3*	*0*	*5.19*	*5.19*	*8.99*	*0*	*0*	*0*	*15.57*	*15.57*
Benzo(a)pyrene (ng/g)	*1*	*3*	*0*	*396.8*	*89.1*	*154.2*	*218.7*	*218.7*	*485.1*	*486.7*	*486.7*
	2	*3*	*0*	*1589*	*1333*	*2310*	*238*	*238*	*274*	*4256*	*4256*
	3	*3*	*0*	*785*	*429*	*743*	*174*	*174*	*570*	*1612*	*1612*
	5	*3*	*0*	*543.2*	*46.2*	*80.1*	*451.9*	*451.9*	*576.7*	*601.1*	*601.1*
	8	*3*	*0*	*362*	*110*	*191*	*188*	*188*	*332*	*566*	*566*

Table 10-26 Descriptive statistics for Run 10, 0 – 5 cm.

Variable	Location	N	N*	Mean	SE Mean	StDev	Minimum	Q1	Median	Q3	Maximum
Naphthalene (ng/g)	1	3	0	81.5	15.8	27.3	50.6	50.6	91.9	102.2	102.2
	2	3	0	201.4	62.8	108.7	78.4	78.4	241.4	284.4	284.4
	3	3	0	91.4	38.5	66.6	18.1	18.1	107.8	148.3	148.3
	5	3	0	68.2	23.5	40.7	25.7	25.7	72.1	106.9	106.9
	8	3	0	63.4	37.3	64.6	22.7	22.7	29.6	137.9	137.9
Fluorene (ng/g)	1	3	0	33.2	25.7	44.5	0	0	15.9	83.8	83.8
	2	3	0	6.41	6.41	11.11	0	0	0	19.24	19.24
	3	3	0	0	0	0	0	0	0	0	0
	5	3	0	0	0	0	0	0	0	0	0
	8	3	0	0	0	0	0	0	0	0	0
Fluoranthene (ng/g)	1	2	1	2976	1648	2330	1328	*	2976	*	4623
	2	2	1	488.3	63.4	89.7	424.9	*	488.3	*	551.7
	3	3	0	47.7	47.7	82.6	0	0	0	143.1	143.1
	5	3	0	94.4	94.4	163.6	0	0	0	283.3	283.3
	8	3	0	0	0	0	0	0	0	0	0
Pyrene (ng/g)	1	3	0	5417	2529	4380	1298	1298	4936	10018	10018
	2	3	0	2246	1585	2745	619	619	703	5416	5416
	3	3	0	149.7	59.7	103.4	51.8	51.8	139.4	257.9	257.9
	5	3	0	192.5	84.9	147	85.7	85.7	131.6	360.2	360.2
	8	3	0	34.7	22.9	39.7	0	0	26.2	77.9	77.9
Chrysene (ng/g)	1	3	0	1940	869	1506	564	564	1707	3549	3549
	2	3	0	1161	709	1228	434	434	470	2579	2579
	3	3	0	361	100	174	169	169	405	508	508
	5	3	0	367	106	183	235	235	290	577	577
	8	3	0	153.3	52.6	91	97.4	97.4	104.1	258.3	258.3
Benzo(a)pyrene (ng/g)	1	3	0	618.1	84.6	146.6	523.3	523.3	544	786.9	786.9
	2	3	0	757	163	282	473	473	760	1037	1037
	3	3	0	578	132	229	314	314	704	717	717
	5	3	0	682	135	234	515	515	581	949	949
	8	3	0	280	116	201	128	128	203	508	508

Table 10-27 Descriptive statistics for Run 10, 5 – 10 cm.

Variable	Location	N	N*	Mean	SE Mean	StDev	Minimum	Q1	Median	Q3	Maximum
Naphthalene (ng/g)	1	3	0	0	0	0	0	0	0	0	0
	2	3	0	0	0	0	0	0	0	0	0
	3	3	0	0	0	0	0	0	0	0	0
	5	3	0	0	0	0	0	0	0	0	0
	8	3	0	0	0	0	0	0	0	0	0
Fluorene (ng/g)	1	3	0	208.7	32.9	56.9	144.6	144.6	228.2	253.3	253.3
	2	3	0	0	0	0	0	0	0	0	0
	3	3	0	0	0	0	0	0	0	0	0
	5	3	0	0	0	0	0	0	0	0	0
	8	3	0	0	0	0	0	0	0	0	0
Fluoranthene (ng/g)	1	3	0	9212	1585	2746	6043	6043	10723	10870	10870
	2	3	0	1037	358	620	346	346	1221	1545	1545
	3	2	1	447	133	188	314	*	447	*	580
	5	2	1	863	410	580	452	*	863	*	1273
	8	3	0	394.5	92.8	160.7	243.6	243.6	376.5	563.5	563.5
Pyrene (ng/g)	1	3	0	7119	1151	1994	5258	5258	6875	9224	9224
	2	3	0	1011	295	511	449	449	1138	1447	1447
	3	2	1	534.7	94.5	133.6	440.2	*	534.7	*	629.1
	5	3	0	1518	665	1151	557	557	1202	2794	2794
	8	3	0	519.3	82.7	143.3	387	387	499.3	671.5	671.5
Chrysene (ng/g)	1	2	1	6844.2	67.9	96.1	6776.3	*	6844.2	*	6912.1
	2	3	0	2014	1389	2407	526	526	725	4790	4790
	3	2	1	2736	303	429	2433	*	2736	*	3039
	5	2	1	3792	745	1054	3047	*	3792	*	4537
	8	3	0	2689	581	1006	1829	1829	2442	3796	3796
Benzo(a)pyrene (ng/g)	1	2	1	5216	1450	2051	3765	*	5216	*	6666
	2	3	0	2625	1750	3031	701	701	1056	6119	6119
	3	2	1	3268	525	742	2743	*	3268	*	3793
	5	2	1	3969.3	89.4	126.4	3880	*	3969.3	*	4058.7
	8	3	0	2700	595	1031	1963	1963	2257	3879	3879

Table 10-28 Descriptive statistics for Run 10, 10 – 15 cm.

Variable	*Location*	*N*	*N**	*Mean*	*SE Mean*	*StDev*	*Minimum*	*Q1*	*Median*	*Q3*	*Maximum*
Naphthalene (ng/g)	*1*	*3*	*0*	*0*	*0*	*0*	*0*	*0*	*0*	*0*	*0*
	2	*3*	*0*	*0*	*0*	*0*	*0*	*0*	*0*	*0*	*0*
	3	*3*	*0*	*0*	*0*	*0*	*0*	*0*	*0*	*0*	*0*
	5	*3*	*0*	*0*	*0*	*0*	*0*	*0*	*0*	*0*	*0*
	8	*3*	*0*	*0*	*0*	*0*	*0*	*0*	*0*	*0*	*0*
Fluorene (ng/g)	*1*	*3*	*0*	*0*	*0*	*0*	*0*	*0*	*0*	*0*	*0*
	2	*3*	*0*	*0*	*0*	*0*	*0*	*0*	*0*	*0*	*0*
	3	*3*	*0*	*0*	*0*	*0*	*0*	*0*	*0*	*0*	*0*
	5	*3*	*0*	*0*	*0*	*0*	*0*	*0*	*0*	*0*	*0*
	8	*3*	*0*	*0*	*0*	*0*	*0*	*0*	*0*	*0*	*0*
Fluoranthene (ng/g)	*1*	*3*	*0*	*20.6*	*20.6*	*35.7*	*0*	*0*	*0*	*61.9*	*61.9*
	2	*3*	*0*	*149.8*	*97.2*	*168.3*	*0*	*0*	*117.5*	*331.9*	*331.9*
	3	*3*	*0*	*137*	*137*	*238*	*0*	*0*	*0*	*412*	*412*
	5	*3*	*0*	*398*	*398*	*689*	*0*	*0*	*0*	*1194*	*1194*
	8	*3*	*0*	*2.9*	*2.9*	*5.03*	*0*	*0*	*0*	*8.71*	*8.71*
Pyrene (ng/g)	*1*	*3*	*0*	*190.9*	*20.9*	*36.2*	*161.7*	*161.7*	*179.8*	*231.4*	*231.4*
	2	*3*	*0*	*310.5*	*82.4*	*142.7*	*173.1*	*173.1*	*300.3*	*458*	*458*
	3	*3*	*0*	*246*	*154*	*266*	*74*	*74*	*112*	*553*	*553*
	5	*3*	*0*	*477*	*353*	*611*	*104*	*104*	*144*	*1182*	*1182*
	8	*3*	*0*	*121.3*	*51.2*	*88.7*	*40.8*	*40.8*	*106.7*	*216.4*	*216.4*
Chrysene (ng/g)	*1*	*3*	*0*	*175*	*157*	*273*	*15*	*15*	*22*	*490*	*490*
	2	*3*	*0*	*529.2*	*79.8*	*138.3*	*431.2*	*431.2*	*469*	*687.4*	*687.4*
	3	*3*	*0*	*381*	*368*	*637*	*3*	*3*	*22*	*1116*	*1116*
	5	*3*	*0*	*468*	*77.3*	*133.9*	*347.3*	*347.3*	*444.7*	*612.1*	*612.1*
	8	*3*	*0*	*294*	*161*	*279*	*2*	*2*	*321*	*559*	*559*
Benzo(a)pyrene (ng/g)	*1*	*3*	*0*	*409*	*108*	*187*	*238*	*238*	*379*	*609*	*609*
	2	*3*	*0*	*505*	*128*	*222*	*363*	*363*	*392*	*761*	*761*
	3	*3*	*0*	*573*	*267*	*463*	*243*	*243*	*375*	*1103*	*1103*
	5	*3*	*0*	*3757*	*3283*	*5686*	*446*	*446*	*502*	*10322*	*10322*
	8	*3*	*0*	*333*	*126*	*219*	*134*	*134*	*297*	*567*	*567*

Table 10-29 Correlations between PAHs in swale soil.

Variable		*NAP (ng/g)*	*FLU (ng/g)*	*FLAN (ng/g)*	*PYR (ng/g)*	*CHR (ng/g)*
FLU (ng/g)	*Spearman rho*	*0.378*				
	P-value	*0.000*				
FLAN (ng/g)	*Spearman rho*	*0.040*	*0.716*			
	P-value	*0.484*	*0.000*			
PYR (ng/g)	*Spearman rho*	*0.049*	*0.566*	*0.729*		
	P-value	*0.374*	*0.000*	*0.000*		
CHR (ng/g)	*Spearman rho*	*0.069*	*0.210*	*0.501*	*0.334*	
	P-value	*0.219*	*0.000*	*0.000*	*0.000*	
BaP (ng/g)	*Spearman rho*	*-0.032*	*0.371*	*0.627*	*0.552*	*0.583*
	P-value	*0.563*	*0.000*	*0.000*	*0.000*	*0.000*

Table 10-30 Correlations between PAHs in 0 – 5 cm soil.

Variable		*NAP (ng/g)*	*FLU (ng/g)*	*FLAN(ng/g)*	*PYR (ng/g)*	*CHR (ng/g)*
FLU (ng/g)	*Spearman rho*	*0.129*				
	P-value	*0.118*				
FLAN ng/g)	*Spearman rho*	*-0.05*	*0.794*			
	P-value	*0.567*	*0.000*			
PYR (ng/g)	*Spearman rho*	*0.12*	*0.623*	*0.617*		
	P-value	*0.153*	*0.000*	*0.000*		
CHR (ng/g)	*Spearman rho*	*0.181*	*0.303*	*0.421*	*0.138*	
	P-value	*0.031*	*0.000*	*0.000*	*0.109*	
BaP (ng/g)	*Spearman rho*	*0.028*	*0.536*	*0.655*	*0.52*	*0.466*
	P-value	*0.734*	*0.000*	*0.000*	*0.000*	*0.000*

Table 10-31 Correlations between PAHs in 5 - 10 cm soil layer.

Variable		*NAP (ng/g)*	*FLU (ng/g)*	*FLAN (ng/g)*	*PYR (ng/g)*	*CHR (ng/g)*
FLU (ng/g)	*Spearman rho*	*0.197*				
	P-value	*0.019*				
FLAN (ng/g)	*Spearman rho*	*-0.453*	*0.245*			
	P-value	*0.000*	*0.005*			
PYR (ng/g)	*Spearman rho*	*-0.252*	*0.181*	*0.731*		
	P-value	*0.003*	*0.033*	*0.000*		
CHR (ng/g)	*Spearman rho*	*-0.27*	*0.225*	*0.723*	*0.749*	
	P-value	*0.001*	*0.008*	*0.000*	*0.000*	
BaP (ng/g)	*Spearman rho*	*-0.174*	*0.202*	*0.618*	*0.593*	*0.869*
	P-value	*0.041*	*0.019*	*0.000*	*0.000*	*0.000*

Table 10-32 Correlation between PAHs and soil moisture and air temperature.

Variable		*Soil moisture*	*Air Temp*
NAP (ng/g)	*Spearman rho*	*0.189*	*-0.267*
	P-value	*0.000*	*0.000*
FLU (ng/g)	*Spearman rho*	*0.390*	*-0.304*
	P-value	*0.000*	*0.000*
FLAN (ng/g)	*Spearman rho*	*0.235*	*-0.040*
	P-value	*0.036*	*0.484*
PYR (ng/g)	*Spearman rho*	*0.116*	*-0.221*
	P-value	*0.036*	*0.000*
CHR (ng/g)	*Spearman rho*	*-0.009*	*0.153*
	P-value	*0.866*	*0.006*
BaP (ng/g)	*Spearman rho*	*0.031*	*0.172*
	P-value	*0.570*	*0.002*

Table 10-33 Certificate of Ethics Review

University of Portsmouth

Certificate of Ethics Review

Project Title:	Role of Plants in the uptake of pollutants in Sustainable Drainage Systems
User ID:	636903
Name:	Janine Louise Robinson
Application Date:	22/09/2015 11:46:34

You must download your referral certificate, print a copy and keep it as a record of this review.

The FEC representatives for the School of Civil Engineering & Surveying are Tim Whitehead and John Williams

It is your responsibility to follow the University Code of Practice on Ethical Standards and any Department/School or professional guidelines in the conduct of your study including relevant guidelines regarding health and safety of researchers including the following:

- University Policy
- Safety on Geological Fieldwork

It is also your responsibility to follow University guidance on Data Protection Policy:

- General guidance for all data protection issues
- University Data Protection Policy

SchoolOrDepartment: SCES
PrimaryRole: PostgraduateStudent
SupervisorName: John Williams
HumanParticipants: No
PhysicalEcologicalDamage: No
HistoricalOrCulturalDamage: No
HarmToAnimal: No
HarmfulToThirdParties: No
OutputsPotentiallyAdaptedAndMisused: No
Confirmation-ConsideredDataUse: Confirmed
Confirmation-ConsideredImpactAndMitigationOfPontentialMisuse: Confirmed
Confirmation-ActingEthicallyAndHonestly: Confirmed

Certificate Code: 0AD7-F3D1-4AF7-BE90-3AEE-1AAD-0594-E30D Page 1